ISSN 0031 - 9465

PHYTOPATHOLOGIA MEDITERRANEA

Plant health and food safety

Volume 60 • No. 1 • April 2021

The international journal of the
Mediterranean Phytopathological Union

FIRENZE UNIVERSITY PRESS

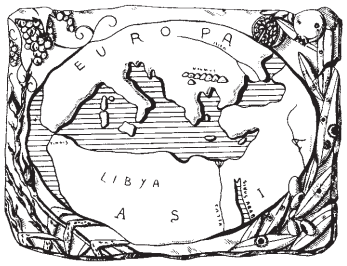

PHYTOPATHOLOGIA MEDITERRANEA

Plant health and food safety

The international journal edited by the Mediterranean Phytopathological Union
founded by A. Ciccarone and G. Goidànich

Phytopathologia Mediterranea is an international journal edited by the Mediterranean Phytopathological Union The journal's mission is the promotion of plant health for Mediterranean crops, climate and regions, safe food production, and the transfer of knowledge on diseases and their sustainable management.
The journal deals with all areas of plant pathology, including epidemiology, disease control, biochemical and physiological aspects, and utilization of molecular technologies. All types of plant pathogens are covered, including fungi, nematodes, protozoa, bacteria, phytoplasmas, viruses, and viroids. Papers on mycotoxins, biological and integrated management of plant diseases, and the use of natural substances in disease and weed control are also strongly encouraged. The journal focuses on pathology of Mediterranean crops grown throughout the world.
The journal includes three issues each year, publishing Reviews, Original research papers, Short notes, New or unusual disease reports, News and opinion, Current topics, Commentaries, and Letters to the Editor.

PHYTOPATHOLOGIA MEDITERRANEA

The international journal of the Mediterranean Phytopathological Union

Volume 60, April, 2021

Firenze University Press

***Phytopathologia Mediterranea*. The international journal of the Mediterranean Phytopathological Union**
Published by
Firenze University Press – University of Florence, Italy
Via Cittadella, 7–50144 Florence–Italy
http://www.fupress.com/pm
Direttore Responsabile: **Giuseppe Surico**, University of Florence, Italy

Phytopathologia Mediterranea
The international journal of the
Mediterranean Phytopathological Union

Firenze University Press
www.fupress.com/pm

Research Papers

Mating type distribution, genetic diversity and population structure of *Ascochyta rabiei*, the cause of Ascochyta blight of chickpea in western Iran

Somayeh FARAHANI[1], Reza TALEBI[2,*], Mojdeh MALEKI[1,*], Rahim MEHRABI[3], Homayoun KANOUNI[4]

[1] *Department of Plant Protection, Varamin-Pishva Branch, Islamic Azad University, Varamin, Iran*
[2] *Department of Agronomy & Plant Breeding, Sanandaj Branch, Islamic Azad University, Sanandaj, Iran*
[3] *Department of Biotechnology, College of Agriculture, Isfahan University of Technology, Isfahan, Iran*
[4] *Kordestan Agricultural and Natural Resources Research and Education Center, Agricultural Research, Education and Extension Organization (AREEO), Sanandaj, Iran*
*Corresponding author. E-mail: srtalebi@yahoo.com, mojdehmaleki@yahoo.com

Summary. Ascochyta blight (caused by *Ascochyta rabiei*) is an important disease of chickpea. Mating type distribution, genetic diversity and population structure *A. rabiei* isolates from western Iran, using specific matting type primers, and ISSR and SSR molecular markers. Two mating types were identified, with the 57% of isolates belonging to MAT1-1. Ten ISSR markers produced 78 polymorphic bands with an average polymorphism information content (PIC) value of 0.33. Seven SSR markers showed high allelic variation (four to seven alleles) with the average PIC value of 0.61. The generated dendrogram using neighbor joining approach with ISSR and SSR marker data grouped isolates in three clusters. Combined dendrogram and model-based population structure analysis divided the isolates into two distinct populations. No significant correlation was found between geographical origins of isolates and their genetic diversity patterns, although the isolates from North Kermanshah and Kurdistan were closely grouped, and most of isolates from Lorestan and Kermanshah were clustered in a separate group. This relative spatial correlation between geographical locations and *A. rabiei* grouping indicated high genetic diversity within populations and no significant gene flow between distinctly geographical regions. This suggests the nece0ssity of continuous monitoring of *A. rabiei* populations in order to design effective chickpea breeding strategies to control the disease.

Keywords. ISSR, SSR, population structure, Ascochyta blight, sexual reproduction.

OPEN ACCESS

Citation: S. Farahani, R. Talebi, Mojdeh Maleki, R. Mehrabi, H. Kanouni (2021) Mating type distribution, genetic diversity and population structure of *Ascochyta rabiei*, the cause of Ascochyta blight of chickpea in western Iran. *Phytopathologia Mediterranea* 60(1): 3-11. doi: 10.36253/phyto-11616

Accepted: August 12, 2020

Published: May 15, 2021

Data Availability Statement: All relevant data are within the paper and its Supporting Information files.

Competing Interests: The Author(s) declare(s) no conflict of interest.

Editor: Diego Rubiales, Institute for Sustainable Agriculture, (CSIC), Cordoba, Spain.

INTRODUCTION

Chickpea (*Cicer arietinum* L.) is the third most important food legume, which provides human feed as a stable, rich and cheap source of vegetar-

ian protein (Varshney *et al.*, 2013). Chickpea originated from Middle-East, North Africa and Central Asia (van der Maesen, 1987; Talebi *et al.*, 2008). Chickpea is produced in over 50 countries and India is the most important producer, with average yields of approx. 900 kg ha^{-1}. Iran ranks ninth in the world for chickpea production, with 2% of world production (Merga *et al.* 2019).

International chickpea seed yields are less than potential yield due to the narrow genetic base of most improved cultivars and uniform reaction to different abiotic and biotic stresses (Ghaffari *et al.,* 2014). Ascochyta blight (AB), caused by *Ascochyta rabiei* (Pass.) Lab. (syn: *Didymella rabiei* Kov.), is one of the most important fungal diseases of chickpea. The disease may cause yield losses up to 100% under favourable cool and humid conditions (Ahmad *et al.,* 2014; Farahani *et al.,* 2019). In Western Iran (Kermanshah, Kurdistan and Ilam provinces) AB is a serious damaging disease of chickpea, and in spring seasons (April to May), the disease is often severe (Nourollahi *et al.* 2011; Azizpour and Rouhrazi, 2017). Integrated strategies have to be applied to reduce AB, including agronomic practices (crop rotation and adjusting sowing date), application of fungicides and use of durably resistant chickpea cultivars (Kimurto *et al.,* 2013; Vafaei *et al.,* 2016; Farahani *et al.,* 2019). Employment of resistant varieties has been considered the most effective, economic and environmentally-friendly strategy to manage the disease (Singh and Reddy, 1996; Varshney *et al.,* 2009).

Both asexual and sexual reproduction has been reported for *A. rabiei*. The asexual stage occurs during the host growing season and the sexual stage develops on infected seed and crop residues during the winter (Trapero-Casas and Kaiser, 1992; Nourollahi *et al.,* 2011). Sexual reproduction plays an important role in genetic diversity of fungal pathogens, which enable them to rapidly overcome host resistance genes as a response to selection pressure imposed by resistant cultivars (Chen and McDonald, 1996; Aghamiri *et al.,* 2015). This variability of the pathogen led to breakdown of resistance in chickpea germplasm. Knowledge of pathogen diversity and mating type systems is fundamental for effective diseases management and breeding programmes (Varshney *et al.,* 2009; Mehrabi *et al.,* 2015; Baite and Dubey, 2018). However, field assessment of the genetic structure in *A. rabiei* populations may be not reliable due to lack of powerful discriminating tools and variable environmental condition. Measuring pathogen genetic diversity based on molecular markers at the DNA level can provide unbiased estimates of genetic variation which is independent of culture conditions (Nourollahi *et al.,* 2011).

Different molecular methods, including SSR (Geistlinger *et al.,* 2000; Phan *et al.,* 2003b), AFLP (Varshney *et al.,* 2009), RAPD (Santra *et al.,* 2001), and mating-type specific markers (Phan *et al.,* 2003a; Ozer *et al.,* 2012), have been developed and utilized for genetic diversity assessment in *A. rabiei* populations from different countries, including Turkey (Bayraktar *et al.,* 2007), Pakistan (Ali *et al.,* 2012), India (Varshney *et al.,* 2009) and other chickpea growing areas (reviewed by Pande *et al.,* 2005). High levels of genetic and pathogenic diversity have also been reported in Iranian *A. rabiei* populations (Nourollahi *et al.,* 2011; Azizpour and Rouhrazi, 2017). Biased mating type distribution has been reported in populations of this fungus collected from west and north-west Iran, that was dominated by the Mat1-1 mating type (Nourollahi *et al.,* 2011; Azizpour and Rouhrazi, 2017). In Turkey and Tunisia, Mat1-2 has been reported as the dominant mating type (Rhaiem *et al.,* 2007; Taylor and Ford, 2007). Previous studies on pathogenicity, genetic diversity using SSRs and Specific mating type DNA markers among Iranian isolates of *A. rabiei* have not been comprehensively described, and most previous Iranian studies were focused on a province or small geographical region (Younessi *et al.,* 2004; Vafaei *et al.,* 2016; Nourollahi *et al.,* 2011; Azizpour and Rouhrazi, 2017).

The present study was undertaken to: (i) assess pathogenicity *A. rabiei* isolates collected from the west of Iran; (ii) assess genetic diversity of these isolates using SSR and ISSR markers; and (iii) characterize mating type distribution of Iranian *A. rabiei* isolates from different provinces using MAT-specific primers.

MATERIALS AND METHODS

Ascochyta rabiei *sampling and isolation*

Seventy-five *A. rabiei* isolates were collected from infected chickpea fields of western Iran provinces (20 isolates from Kurdistan, 46 from Kermanshah and nine from Lorestan) during the 2017 and 2018 growing seasons (Table 1). These provinces are geographically juxtaposed, but due to substantial mountains between them, their climatic conditions are different. Kurdistan has cold winters with mild summers and greater annual precipitation than the other two provinces. Samples were collected from 15 locations with minimum distance between the locations of 10–15 km. At each location, samples were chosen every 20 m along a row from three to five parts of each infected field. Infected leaves were removed to a laboratory, were surface sterilized with sodium hypochlorite (0.5%) for 2 min, and washed twice

Table 1. Numbers and mating types of 75 *Ascochyta rabiei* isolates collected from western Iran.

Province	No. of isolates	Mat1-1	Mat1-2	X^{2*}	*P*
Kermanshah	46	30	16	4.26	0.039
Kurdistan	20	9	11	0.20	0.655
Lorestan	9	4	5	0.11	0.739
Total	75	43	32	1.61	0.204

*Chi-square values were calculated under the null hypothesis of a 1:1 ratio of equal proportions of *Mat1-1* and *Mat1-2.*

with sterilized distilled water. Samples were then plated onto CSMDA (40 g of chickpea seed meal, 20 g dextrose and 18 g agar in 1 L sterilized distilled water). Plates were incubated for 7 to 10 d at 20/22°C. Single pycnidium isolates were obtained from the isolation plates, and were stored on CSMDA for pathogenicity tests.

Pathogenicity tests

Pathogenicity test for all isolates was carried out on the two susceptible chickpea cultivars 'Bivanij' (Iranian landrace susceptible check) and ILC1929 (International susceptible check) (Farahani *et al.* 2019). Purified single pycnidium *A. rabiae* isolates were grown in potato dextrose broth (PDB). The inoculum of each isolate was prepared in a water solution containing 0.20% of Tween 20, and was adjusted to 6×10^5 conidia mL^{-1}.

Two-week-old chickpea seedlings of the susceptible cultivars were inoculated with each isolate, and inoculated plants were kept in the dark under plastic bags for 24 h. The plants were then transferred to a controlled greenhouse where environmental conditions were maintained at 23/18°C day/night, a 16 h photoperiod, and ≥85% relative humidity (Farahani *et al.,* 2019). After 2 weeks, disease reactions on both cultivars were assessed using a 0–9 scale (Pande *et al.,* 2011; Farahani et al. 2019). Plants that showed disease scores greater than 5 were considered susceptible to *A. rabiae* (Farahani *et al.,* 2019).

DNA extraction from isolates

Single pycnidium *A. rabiae* isolates grown on CSMDA were each used to inoculate 50 mL PDB and then incubated at 20/22°C on an orbital shaker (100 rpm) for 5 d. Fungal biomass was harvested from each culture by filtration through Miracloth, was rinsed with distilled water, and then finely ground in liquid nitrogen. These preparations were then subjected to DNA extraction using the CTAB method (Weising *et al.,* 1991).

Mating type assay

Mating types of all 75 *A. rabiei* isolates was determined using the multiplex MAT-specific PCR assay (Barve et al., 2003). Primer combinations of SP21, Tail5 and Com1 were used in a single PCR reaction carried out in 20 µL reaction volume, containing 1× PCR buffer, 25 ng sample DNA, 2 µM primer, 200 µM of each dNTPs, 2.5 mM $MgCl_2$ and 1.5 units of Taq DNA polymerase (Cinnagene). PCR amplifications were carried out in an Eppendorf thermocycler (Ali *et al.,* 2012) as follows: initial denaturation at 95°C for 3 min followed by 35 cycles of 94°C for 20 s, 58°C for 20 s, 72°C for 40 s, and a final extension at 72°C for 10 min. PCR products were separated on 1.5% agarose gels, stained with ethidium bromide and visualized under UV light using a gel documentation system (Bio-Rad).

ISSR analyses

A set of 10 primers (UBC set, University of British Columbia, Canada) were used to determine genetic diversity of the *A. rabiei* isolates (Table 2). PCR reactions were each performed in 20 µL reaction volume containing 1× PCR buffer, 30 ng sample DNA, 2.5 µM primer, 200 µM of each dNTPs, 2.5 mM $MgCl_2$ and 1.5 units of Taq DNA polymerase (Cinnagene). PCR amplifications were carried out in an Eppendorf thermocycler (Germany), as follows: initial denaturation at 95°C for 2 min, followed by 32 cycles of denaturation at 94°C for 30 s, annealing at optimum *Ta* for 60s, and extension at 72°C for 90 s. A final extension cycle at 72°C for 10 min followed. PCR products were separated on 1.5% agarose gels, stained with ethidium bromide and visualized under UV light using a gel documentation system (Bio-Rad).

SSR analysis

A set of seven SSR markers (Supplementary Table S1), previously described by Geistlinger *et al.* (2000) and Hayden *et al.* (2008), was used to determine the genetic diversity of the 75 *A. rabiei* isolates. PCR reactions were each performed in 20 µL reaction volume containing 1× PCR buffer, 15 ng sample DNA, 2 µM primer, 200 µM of each dNTP, 2.5 mM $MgCl_2$ and 1.5 units of Taq DNA polymerase (Cinnagene). PCR amplifications were carried out using an Eppendorf thermo cycler (Varshney

et al., 2009) as follows: initial denaturation at 95°C for 2 min, followed by 35 cycles of 94°C for 20 s, 53°C for 30 s, 67°C for 30 s. PCR products were separated on 3% metaphor agarose gels, stained with ethidium bromide and visualized under UV light using a gel documentation system (Bio-Rad).

Data analyses

DNA bands obtained with ISSR primers were scored visually for the presence (1) or absence (0) of bands for all the *A. rabiei* isolates. Frequencies of incidence of all polymorphic alleles for each SSR marker were calculated and used for determining statistical parameters. Each band identified as an allele and scored as 'a', 'b', etc., from largest to smallest sized band. Number of alleles (Na), effective number of alleles (Ne), heterozygosity (μe), Shannon-index (I) and polymorphism information content (PIC) were calculated for ISSR and SSR markers using GENALEX 6.1 software (Peakall and Smouse 2006). Marker indices (MI) were obtained by multiplying the average PIC with the effective multiplex ratio. Cluster analysis was conducted on the basis of a neighbor joining (NJ) tree using dissimilarity matrix using DARwin 5.0.128 (Perrier *et al.,* 2003). For the analysis of population structure, a Bayesian model-based analysis was performed using STRUCTURE 2.1 software (Pritchard *et al.,* 2000). A Monte Carlo Markov chain method was used to estimate allele frequencies in each of the K populations and the degree of admixture for each individual plant. The number of clusters was inferred using five independent simultaneous runs with 10,000 replications, using the admixture model and correlated allele frequencies with the K value ranging from 1 to 10.

RESULTS

Pathogenicity tests and mating type distribution

Initially, the pathogenicity of 75 *A. rabiei* isolates was confirmed on two susceptible genotypes. Prominent morphological differences were not seen between isolates. Both chickpea genotypes showed high susceptibility to all the isolates. Symptoms of Ascochyta blight appeared on the Iranian susceptible landrace, Bivanij 2–4 d earlier than on ILC1929 (Supplementary Table S2).

The multiplex PCR using the mating type primers amplified two amplicons (490 bp for Mat1-2 and 700 bp for Mat1-1), across the 75 *A. rabiei* isolates collected from three major chickpea growing provinces (Table 1; Supplementary Figure 1). Both mating types were found in isolates collected from different provinces. Isolates from Kurdistan and Lorestan showed equal distribution for both mating types, while isolates from Kermanshah had different proportions ($P = 0.039$) of the two mating types. This may have resulted from the low number of collected isolates from the other provinces or the geographical differences of the collection sites. Overall, 57% of the isolates were the MAT1-1 mating type and 43% were Mat1-2, but the mating type ratio was not significantly different ($P = 0.204$) from 50:50 (Table 1).

ISSR markers diversity analysis

The ISSR markers revealed clear and scorable bands per primer for all the studied isolates (Supplementary Figure 1). Ten ISSR markers amplified 78 polymorphic bands with an average of 7.8 bands per primer (Table 2). The maximum number of polymorphic bands was obtained using UBC807 (ten bands) and the minimum

Table 2. Numbers of polymorphic bands (NPB), heterozygosity (μe), Shannon indices, polymorphism information content (PIC), and marker indices (MI) of ISSR markers used for defining genetic diversity of 75 *Ascochyta rabiei* isolates.

Primer	Sequence	NPB	μe	Shannon Index (I)	PIC	MI
UBC807	AGAGAGAGAGAGAGAGT	10	0.48	0.58	0.42	4.2
UBC815	CTCTCTCTCTCTCTCTG	8	0.38	0.47	0.38	3.04
UBC818	CACACACACACACACAG	8	0.36	0.46	0.37	2.96
UBC857	ACACACACACACACACYG	7	0.33	0.43	0.34	2.72
UBC822	TCTCTCTCTCTCTCTCA	9	0.42	0.51	0.32	2.88
UBC860	TGTGTGTGTGTGTGTGRA	8	0.31	0.49	0.31	2.48
UBC864	ATG ATG ATG ATG ATG ATG	6	0.29	0.37	0.29	1.74
UBC880	GGAGAGGAGAGGAGA	7	0.30	0.39	0.29	2.03
UBC895	AGAGTTGGTAGCTCT TGA TC	8	0.28	0.42	0.32	2.56
UBC899	CAT GGT GTT GGT CAT TGT TCC A	7	0.28	0.34	0.28	1.96
Mean		7.8	0.34	0.44	0.33	2.65

number using UBC864 (six bands). The PIC values for the ISSR primers ranged from 0.28 to 0.42, with an average of 0.33 per primer. The marker index (MI) of the primers ranged from 1.74 (UBC864) to 4.2 (UBC807) (Table 2). At the population level the average of Shannon-index was 0.44 and heterozygosity (μe) was 0.34. Cluster analysis using ISSR markers grouped the *A. rabiei* isolates into three distinct clusters (Supplementary Figure 2). Cluster I consisted of nine isolates, all collected from Kermanshah. Cluster II comprised 30 isolates that divided into two sub-clusters, and all isolates from Lorestan province grouped closely along with a few isolates from Kermanshah grouped in first sub-cluster. Cluster III contained 36 isolates and divided into two sub-clusters. All isolates in Cluster III originated from Kermanshah and Kurdistan provinces, while all isolates from Kurdistan grouped in a second sub-cluster (Supplementary Figure 2).

SSR markers diversity analysis

Seven SSR loci were used for genetic diversity analysis in the 75 *A. rabiei* isolates, and these showed clear and scorable amplicons (Supplementary Figure 1). The SSR loci analyzed produced 38 alleles with an average of 5.42 alleles per marker. The numbers of alleles ranged from 4 to 7, where the maximum number of alleles was observed in ArH05T and ArH06T (Table 3). The numbers of effective alleles ranged from 4.28 (ArH06T) to 1.97 (ArR01T) with an average value of 3. PIC ranged from 0.48 (ArR01T) to 0.76 (ArH06T) with an average of 0.61. The Shannon's information index (I) ranged from 1.06 (ArA06D) to 2.17 (ArH06T) (Table 3). Gene diversity (μe) ranged from 0.56 to 0.84 with a mean of 0.69. Genetic relationships between the *A. rabiei* isolates based on polymorphic bands from seven SSR markers grouped the isolates into three major clusters (Supplementary Figure 3). Cluster I contained seven isolates that all originated from Kermanshah province. Cluster II comprised 39 isolates divided into two sub-clusters. One sub-cluster contained seven isolates from Kurdistan and the other contained isolates from different regions. Cluster III comprised 29 isolates in two sub-clusters. In this cluster, isolates from Kurdistan and Kermanshah showed distinct patterns from isolates collected from Lorestan province.

Table 3. Numbers of alleles (Na) and effective alleles (Ne), heterozygosity (μe), Shannon indices, polymorphism information content (PIC), and marker indices (MI) of SSR markers used for determining genetic diversity of 75 *Ascochyta rabiei* isolates.

SSR locus	Na	Ne	μe	Shannon index (I)	PIC	MI
ArH02T	6	3.07	0.72	1.68	0.63	3.78
ArH05T	7	4.17	0.81	2.11	0.73	5.11
ArH06T	7	4.28	0.84	2.17	0.76	5.32
ArR12D	5	2.79	0.69	1.47	0.59	2.95
ArA03T	5	2.68	0.63	1.39	0.56	2.80
ArR01T	4	1.97	0.56	1.11	0.48	1.92
ArA06D	4	2.10	0.59	1.06	0.52	2.08
Mean	5.43	3.01	0.69	1.57	0.61	3.42

Genetic structure of Ascochyta rabiei *isolates*

The general dendrogram (Figure 1) that was constructed using the combined data of all molecular markers (ISSRs and SSRs) grouped the *A. rabiei* isolates in two major clusters. Cluster I comprised isolates mostly collected from Kurdistan, and few isolates from north Kermanshah and Lorestan. Cluster II divided into two sub-clusters, one with all isolates originating in Kermanshah, and the other with isolates from Kermanshah, Lorestan and three from Kurdistan. The NJ-cluster analysis showed no relationships with geographical origin, but most isolates in cluster I were from closely associated regions (Kurdistan and North Kermanshah), except for two isolates from Lorestan.

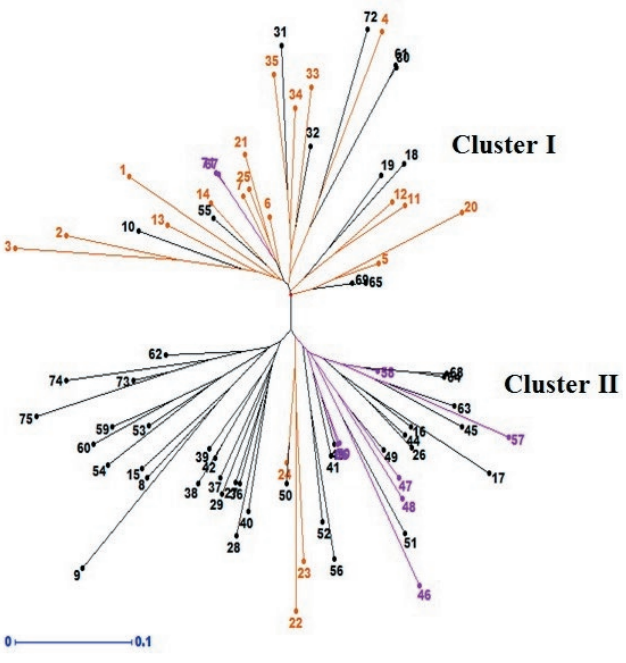

Figure 1. Neighbor joining (NJ) phylogenetic tree from pooled ISSR and SSR molecular data for 75 *Ascochyta rabiei* isolates collected from the western Iran provinces of Kermanshah (black), Kurdistan (red) and Lorestan (blue).

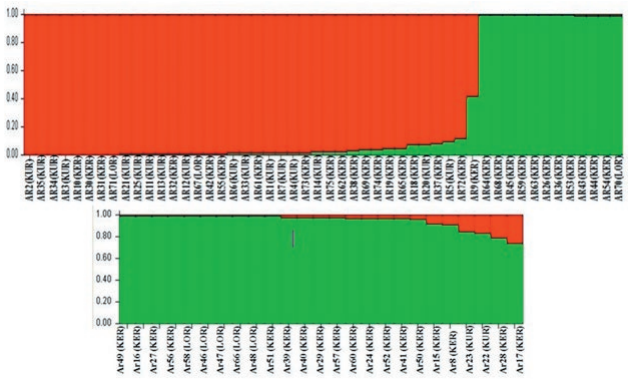

Figure 2. Membership coefficients estimated for *Ascochyta rabiei* isolates, determined from the greatest *a posteriori* likelihood using analysis with STRUCTURE and based on SSR and ISSR markers. The different isolates are represented by individual vertical bars divided into two colored segments (red and green) corresponding to the fraction of membership determined in Populations 1 and 2. The isolates are classified by province; Kermanshah (KER), Kurdistan (KUR) or Lorestan (LOR).

The genetic structure of the 75 *A. rabiei* isolates was further explored using the Bayesian clustering model implemented with the STRUCTURE software. This showed the greatest K value of 2, indicating the presence of two major clusters (Figure 2). The first population (Figure 2, indicated in red) comprised isolates from Kermanshah and Kurdistan, and two isolates (Ar67 and Ar71) from Lorestan. The second population (Figure 2, in green) included isolates from Kermanshah and Lorestan, and some isolates from Kurdistan. These results match those obtained from the NJ analysis (above), without significant correlation of isolate origin and population grouping.

DISCUSSION

Chickpea as cool season crops is mainly cultivated in many semi-arid areas, and seed yields and quality are reduced by major abiotic and biotic stresses (Kanouni *et al.,* 2011; Karami *et al.,* 2015). Ascochyta blight, caused by *A. rabiei*, is one of the most important fungal diseases of chickpea causing yield losses up to 100% in favourable cool and humid climates (Ahmad *et al.,* 2014; Farahani *et al.,* 2019). Variable pathogenicity and genetic structure in Iranian *A. rabiei* populations has been reported previously (Nourollahi *et al.,* 2011; Azizpour and Rouhrazi, 2017; Farahani *et al.,* 2019). Different factors, including sexual recombination, mutation, gene flow, migration, and selection pressure play important roles in population diversity of fungal pathogens (McDonald, 1997; Aghamiri *et al.,* 2015). This can lead to breakdown of host resistance in commercial cultivars (McDonald and Linde, 2002; Rhaiem *et al.,* 2007; Peever *et al.,* 2004; Ali *et al.,* 2012). Characterization of genetic diversity and population structure of fungal populations in disease epidemic areas is fundamentally important for effective disease management, farming practices and design of crop breeding strategies (Azizpour and Rouhrazi, 2017).

The present study was conducted to the define population structure of Iranian *A. rabiei* isolates, through outline of aggressiveness patterns, mating types and molecular marker diversity in isolates of this pathogen collected from three major chickpea growing areas of western Iran. All the assessed isolates showed high aggressiveness in pathogenicity tests. Two identified mating types had similar distributions, except for isolates those collected from Kermanshah province, where Mat1-1 was dominant. Nourollahi *et al.* (2011) showed that majorities (64%) of Iranian isolates collected from two provinces in western Iran were of Mat1-1, but within populations the proportions of each mating type were close to 50%.

Previous studies have showed biased distribution for *A. rabiei* mating types Mat1-1 in Tunisia and MAT1-2 in Turkey (Taylor and Ford, 2007; Rhaiem *et al.,* 2007). Fungi can reproduce in different ways through sexual, asexual or mixed mating systems (McDonald and Linde, 2002). Mixed mating types provide greater capability for overcoming resistance genes in crop resources (McDonald and Linde, 2002; Rhaiem *et al.,* 2007). In fungi, different mating types may be related to pathogenicity and fitness (Zhan *et al.,* 2002; Phan *et al.,* 2003a). However this is remains a question for Iranian populations of the pathogen, as the present study did not show relationship between aggressiveness and mating types in the *A. rabiei* population examined. These results indicate random sexual propagation of *A. rabiei* populations in Iran, has been reported in neighboring countries such as Turkey and Syria (Turkkan and Dolar, 2009; Atik *et al.,* 2011).

Genetic diversity and population structure of 75 *A. rabiei* isolates were analyzed using ten ISSR and seven SSR markers. Both marker types showed high genetic diversity in the *A. rabiei* isolates. The polymorphism of SSR markers showed 4 to 7 alleles with an average 5.42 alleles per locus. In contrast, Nourollahi *et al.* (2011) and Barve *et al.* (2004) reported greater allelic variation in *A. rabiei* populations, which was likely due to the greater number and geographic diversity of isolates used in their studies. The average PIC values in the present study for ISSR markers was 0.33, and for SSR markers was 0.61. The high Shannon diversity index (I) and heterozygo-

sity (gene diversity) of SSR markers also indicated the diverse nature of the collected *A. rabiei* isolates.

NJ-cluster analysis using ISSR and SSR markers grouped *A. rabiei* isolates into three distinct clusters. The molecular data of ISSRs and SSRs were combined, to give the best interpretation of genetic diversity of the isolates examined, which grouped the isolates in two distinct clusters. The Kurdistan climate is Mediterranean, with cold winters, where most chickpea crops are sown in spring (February to March). These contrasts with south Kermanshah and Lorestan, which have a relatively warm climate with moderate winters, and where chickpea crops are mostly sown in autumn (November to December). These differences in chickpea growth conditions may influence the nature of *A. rabiei* isolates and their evolutionary processes. All *A. rabiei* isolates in this study showed high levels of pathogenicity and no significant relationships were detected between pathogenicity of isolates and collection sites.

Knowledge about pathogen genetic diversity and pathogenicity in different geographical areas can help plant breeders, to assist characterization of susceptible/resistant host germplasm against important diseases in chickpea, and for Ascochyta blight in particular (Farahani *et al.,* 2019; Montakhabi *et al.,* 2020). Results from the present study showed no correlation between *A. rabiei* isolate origin and genetic diversity pattern, although most of isolates collected from north Kermanshah and Kurdistan closely grouped in one cluster, and those collected from Lorestan and south Kermanshah grouped in another. This spatial relationship between geographical diversity and *A. rabiei* grouping indicated high genetic diversity within populations and no significant gene flow between distinctly geographical regions. Previous reports have indicated that some *A. rabiei* isolates from distinct continents grouped together, reflecting possible intercontinental migration by movement of pathogens through infected plants carried by seed exchange or agricultural vehicles (Kaiser, 1997; Nourollahi *et al.,* 2011). Iran, Turkey and India are the main centres of origins for chickpea domestication and their fungal pathogens (van der Maesen, 1987; Talebi *et al.,* 2008). The high genetic diversity of *A. rabiei* isolates detected in the present study supports the hypothesis that during long domestication and evolution of chickpea and *A. rabiei* in this area, genetic drift probably occurred. Distinct *A. rabiei* populations from Iran, Turkey and India indicate that pathogen migration rarely occurred, from closely-associated regions (Varsheny *et al.,* 2009; Nourollahi *et al.,* 2011). Abundance of asexual over sexual reproduction occurs in local populations (Morjane *et al.,* 1994; Keller *et al.,* 1997; Aghamiri *et al.,* 2015). Although, limited numbers of *A. rabiei* isolates were analyzed in this study, the present results showed high genetic diversity in isolates collected from different provinces. This study has given a basis for future strategies for breeding programmes and farming practices. Genetic variability and sexual recombination within populations may both increase the risks of increasingly diverse isolates that may overcome resistance in Iranian chickpea germplasm, and also enhance fungicide resistance in *A. rabiei* populations (McDonald and Linde, 2002; Varshney *et al.,* 2009).

In conclusion, the present results have shown interesting aspects of *A. rabiei* populations co-evolved with chickpea in their domestication origins or more probably linked to climate condition associated with differences in cropping seasons. In addition, the necessity of designing appropriate breeding strategies for chickpea improvement in each region is emphasized, due to the host and pathogen genetic differences within specific populations.

ACKNOWLEDGEMENT

The authors thank Dr Mohammad Kazem Montakhabi (Iranian Plant Pathology Institute) for assistance with field sampling and for providing isolates for this study.

LITERATURE CITED

Aghamiri A., Mehrabi R., Talebi R., 2015. Genetic diversity of *Pyrenophera tritici-repentis* isolates, the causal agent of wheat tan spot disease from Northern Iran. *Iranian Journal of Biotechnology* 13(2): e1118.

Ahmad S., Khan M.A., Sahi S.T., Ahmad R., 2014. Identification of resistant sources in chickpea against chickpea blight disease. *Archive of Phytopathology and Plant Protection* 47(15): 1885–1892.

Ali H., Alam S.S., Attanayake R.N., Rahman M., Chen W., 2012. Population structure and mating type distribution of the chickpea blight pathogen *Ascochyta rabiei* from Pakistan and the United states. *Journal of Plant Pathology* 94: 99–108.

Atik O., Baum M., El-Ahmed S., Ahmed M.M., Abang M.M., …Hamwieh A., 2011. Chickpea Ascochyta blight: Disease status and pathogen mating type distribution in Syria. *Journal of Phytopathology* 159: 43–449.

Azizpour N., Rouhrazi K., 2017. Assessment of genetic diversity of Iranian *Ascochyta rabiei* isolates using

rep-PCR markers. *Journal of Phytopathology* 165 (7-8): 508–514.

Baite M.S., Dubey S.C., 2018. Pathogenic variability of *Ascochyta rabiei* causing blight of chickpea in India. *Physiological and Molecular Plant Pathology* 102: 122–127.

Barve M. P., Arie T., Salimath S.S., Muehlbauer F.J., Peever T.L., 2003. Cloning and characterization of the mating type (MAT) locus from *Ascochyta rabiei* (teleomorph: *Didymella rabiei*) and a MAT phylogeny of legume-associated *Ascochyta* spp. *Fungal Genetics and Biology* 39: 151–167.

Barve M.P., Santra D.K., Ranjekar P.K., Gupta V.S., 2004. Genetic diversity analysis of a world-wide collection of *Ascochyta rabiei* isolates using sequence tagged microsatellite markers. *World Journal of Microbiology & Biotechnology* 20: 735–741.

Bayraktar H., Dolar F.S., Tor M., 2007. Determination of genetic diversity within Ascochyta rabiei (Pass.) Labr., the cause of Ascochyta blight of chickpea in Turkey. *Journal of Plant Pathology* 89: 341–347.

Chen R.S., McDonald B.A., 1996. Sexual reproduction plays a major role in the genetic structure of populations of the fungus *Mycosphaerella graminicola*. *Genetics* 142(4): 1119–1127.

Farahani S., Talebi R., Maleki M., Mehrabi R., Kanouni H., 2019. Pathogenic diversity of Ascochyta rabiei isolates and identification of resistance sources in core collection of chickpea germplasm. *Plant Pathology Journal* 35(4): 321–329.

Geistlinger J., Weising K., Winte, P., Kahl G., 2000. Locus specific microsatellite markers for the fungal chickpea pathogen *Didymella rabiei* (anamorph) *Ascochyta rabiei*. *Molecular Ecology* 9: 1939–1941.

Ghaffari P., Talebi R., Keshavarzi F., 2014. Genetic diversity and geographical differentiation of Iranian landrace, cultivars, and exotic chickpea lines as revealed by morphological and microsatellite markers. *Physiology and Molecular Biology of Plants* 20(2): 225–233.

Hayden M., Nguyen T., Waterman A., Chalmers K., 2008. Multiplex-Ready PCR: A new method for multiplexed SSR and SNP genotyping. *BMC Genomics* 9: 80.

Kaiser W.J., 1997. Inter- and international spread of Ascochyta pathogens of chickpea, faba bean, and lentil. *Canadian Journal of Plant Pathology* 19: 215–224.

Kanouni H., Taleei A., Okhovat M., 2011. Ascochyta blight (Ascochyta rabiei (Pass.) Lab.) of chickpea (Cicer arietinum L.): Breeding strategies for resistance. *International Journal of Plant Breeding & Genetics* 5(1): 1–22.

Karami E., Talebi R., Kharkesh M., Saidi A., 2015. A linkage map of chickpea (*Cicer arietinum* L.) based on population from ilc3279×ilc588 crosses: location of genes for time to flowering, seed size and plant height. *Genetika* 47: 253–263.

Keller S.M., McDermott J.M., Pettway R.E., Wolfe M.S., McDonald B.A., 1997. Gene flow and sexual reproduction in the wheat glume blotch pathogen *Phaeosphaeria nodorum* (anamorph: *Stagonospora nodorum*). *Phytopathology* 87: 353–358.

Kimurto P. K., Towett B. K., Mulwa R. S., Njogu N., Jeptanui L. J., Rao G. N., Silim S., Kaloki P., Korir P., Macharia J. K., 2013. Evaluation of chickpea genotypes for resistance to ascochyta blight (*Ascochyta rabiei*) disease in the dry highlands of Kenya. *Phytopathologia Mediterranea* 52: 212–221.

McDonald B. A., Linde C., 2002. Pathogen population genetics, evolutionary potential and durable resistance. *Annual Review of Phytopathology* 40: 349–379.

McDonald B.A., 1997. The population genetics of fungi: Tools and techniques. *Phytopathology* 87: 448–453.

Mehrabi R., Makhdoomi A., Jafar-Aghaie M., 2015. Identification of new sources of resistance to septoria tritici blotch caused by *Zymoseptoria tritici*. *Journal of Phytopathology* 163(2): 84–90.

Merga B., Haji J., Fatih Y., 2019. Economic importance of chickpea: Production, value, and world trade. *Cogent Food & Agriculture* 5(1): 1615718.

Montakhabi M.K., Shahidi Bonjar G.H., Talebi R., 2020. mating type profiling and SSR-based genetic diversity analysis of Iranian *Fusarium oxysporum* f. sp. *ciceris* causing wilt in chickpea. *International Journal of Agriculture & Biology* 23: 1101-1106.

Morjane H., Geistlinger J., Harrabi M., Weising K., Kahl G., 1994. Oligonucleotide fingerprinting detects genetic diversity among *Ascochyta rabiei* isolates from a single chickpea field in Tunisia. *Current Genetics* 26: 191–197.

Nourollahi K., Javannikkhah M., Naghavi M. R., Lichtenzveig J., Okhovat M., … Ellwood S. R., 2011. Genetic diversity and population structure of *Ascochyta rabiei* from the western Iranian Ilam and Kermanshah provinces using MAT and SSR markers. *Mycological progress* 10: 1–7.

Ozer G., Bayraktar H., Dolar F.S., 2012. Genetic diversity and mating-type distribution within populations of *Ascochyta rabiei* in Turkey. *Indian Journal of Agricultural Sciences* 82(1): 3–7.

Peakall R., Smouse P.E., 2006. GenAlEx 6: genetic analysis in Excel. Population genetic software for teaching and research. *Molecular Ecology Notes* 6: 288–295.

Pande S., Sharma M., Gaur P.M., Tripathi S., Kaur L., …Siddique K.H.M., 2011. Development of screening techniques and identification of new sources of

resistance to Ascochyta blight disease of chickpea. *Australian Plant Pathology* 40(2): 149–156.

Pande S., Siddique K.H.M., Kishore G.K., Baaya B., Gaur P.M., …Crouch J.H., 2005. Ascochyta blight of chickpea (*Cicer arietinum* L.): a review of biology, pathogenicity, and disease management. *Australian Journal of Agricultural Research* 56: 317–332.

Peever T. L., Salimath S., Su G., Kaiser W. J., Muehlbauer F. J., 2004. Historical and contemporary multilocus population structure of *Ascochyta rabiei* (teleomorph: *Didymella rabiei*) in the Pacific Northwest of the United States. *Molecular Ecology* 13: 291–309.

Perrier X., Flori A., Bonnot F., 2003. Data analysis methods. In: Hamon P., Seguin M., Perrier X., Glaszmann J.C., Ed., Genetic diversity of cultivated tropical plants. Enfield, Science Publishers, Montpellier, pp 43–76.

Phan H.T.T., Ford R., Taylor P.W.J., 2003a. Mapping the mating type locus of *Ascochyta rabiei*, the causal agent of Ascochyta blight of chickpea. *Molecular Plant Pathology* 4: 373–381.

Phan H.T.T., Ford R., Taylor P.W.J., 2003b. Population structure of Ascochyta rabiei in Australia based on STMS fingerprints. *Fungal Diversity* 13: 111–129.

Pritchard J.K., Stephens M., Donnelly P., 2000. Inference of population structure using multilocus genotype data. *Genetics* 155: 945–959.

Rhaiem A., Cherif M., Dyer P. S., Peever T. L., 2007. Distribution of mating types and genetic diversity of Ascochyta rabiei populations in Tunisia revealed by mating-type- specific PCR and random amplified polymorphic DNA markers. *Journal of Phytopathology* 155: 596–605.

Santra D. K., Singh G., Kaiser W. J., Gupta V. S., Ranjekar P. K., Muehlbauer F. J., 2001. Molecular analysis of *Ascochyta rabiei* (Pass.) Labr., the pathogen of ascochyta blight in chickpea. *Theoretical and Applied Genetics* 102: 676–682.

Singh K.B., Reddy M.V., 1996. Improving chickpea yield by incorporating resistance to *ascochyta blight*. *Theoretical and Applied Genetics* 92: 509–515.

Talebi R., Naji A.M., Fayaz F., 2008. Geographical patterns of genetic diversity in cultivated chickpea (*Cicer arietinum* L.) characterized by amplified fragment length polymorphism. *Plant Soil Environment* 54(10): 447–452.

Taylor P. W. J., Ford R., 2007. Diagnostics, genetic diversity and pathogenic variation of ascochyta blight of cool season food and feed legumes. *European Journal of Plant Pathology* 119: 127–133.

Trapero-Casas A., Kaiser W.J., 1992. Development of *Didymella rabiei*, the teleomorph of *Ascochyta rabiei*, on chickpea straw. *Phytopathology* 82: 1261–1266

Turkkan M., Dolar F.S., 2009. Determination of pathogenic variability of *Didymella rabiei*, the agent of ascochyta blight of chickpea in Turkey. *Turkish Journal of Agriculture & Forestry* 33: 585–591

Vafaei S.H., Rezaee S., Moghadam A., Zamanizadeh H.R., 2016. Virulence diversity of Ascochyta rabiei the causal agent of Ascochyta blight of chickpea in the western provinces of Iran. *Archive of Phytopathology and Plant Protection* 48: 921–930.

VanDer Maesen L.J.G., 1987. Origin, history and taxonomy of chickpea. In: *The chickpea*. Saxena, M.C. and Singh, K.B. (eds). CAB International Publications, Oxford, UK, 11–34.

Varshney R., Pande S., Kannan S., Mahendar T., Sharma M., …Hoisington D., 2009. Assessment and comparison of AFLP and SSR based molecular genetic diversity in Indian isolates of *Ascochyta rabiei*, a causal agent of ascochyta blight in chickpea (*Cicer arietinum* L.). *Mycological Progress* 8: 87–97

Varshney R.K., Song C., Saxena R.K., Azam S., Yu S., Sharpe A.G., 2013. Draft genome sequence of chickpea (*Cicer arietinum*) provides a resource for trait improvement. *Nature Biotechnology* 31: 240–246.

Weising K., Kaemmer D., Epplen J. T., Weigand F., Saxena M., Kahl, G., 1991. DNA fingerprinting of *Ascochyta rabiei* with synthetic oligodeoxynucleotides. *Current Genetics* 19: 483–489.

Younessi H., Okhovat S. M., Hejaroud G. A., Zad S. J., Taleei A. R., Zamani, M. R., 2004. Virulence variability of *Ascochyta rabiei* isolates on chickpea cultivars in Kermanshah province. *Iranian Journal of Plant Pathology* 39: 213–228.

Zhan J., Kema G.H., Waalwijk C., McDonald B.A., 2002. Distribution of mating type alleles in the wheat pathogen *Mycosphaerella graminicola* over spatial scales from lesions to continents. *Fungal Genetics and Biology* 36: 128–136.

Phytopathologia Mediterranea
The international journal of the
Mediterranean Phytopathological Union

Firenze University Press
www.fupress.com/pm

Short Notes

Characterization of two *Cucumber mosaic virus* isolates infecting *Allium cepa* in Turkey

Adyatma I. SANTOSA*, Filiz ERTUNC

Department of Plant Protection, Faculty of Agriculture, Ankara University, 06110 Diskapi, Ankara, Turkey
*Corresponding author. E-mail: adyatma_santosa@yahoo.com

Summary. *Cucumber mosaic virus* (CMV) is polyphagous, infecting plants in several families. CMV has occurred as a minor pathogen in *Allium* crops in several Mediterranean countries, but little was known of the virus naturally infecting *Allium* spp. This study completed molecular and biological characterization of CMV-14.3Po and CMV-15.5Po, two newly identified CMV isolates infecting onion (*Allium cepa* L.) in Turkey. Phylogenetic, and nucleotide and amino acid sequence identity analyses of partial RNA2 and RNA3 of the two isolates showed that they were very similar to other CMV isolates from Mediterranean, European, and East Asian countries. Phylogenetic analysis of the partial sequence of RNA3 also showed that the onion isolates belong to subgroup IA. Onion isolates were mechanically transmissible, and caused mild leaf malformation on onion, severe leaf malformation and stunting on garlic (*Allium sativus* L.), and mosaic and mottle on cucumber (*Cucumis sativus* L.) and melon (*Cucumis melo* L.).

Keywords. Onion, phylogenetic analysis, host indexing.

Citation: A. I. Santosa, F. Ertunc (2021) Characterization of two *Cucumber mosaic virus* isolates infecting *Allium cepa* in Turkey. *Phytopathologia Mediterranea* 60(1): 13-21. doi: 10.36253/phyto-11840

Accepted: September 22, 2020

Published: May 15, 2021

Data Availability Statement: All relevant data are within the paper and its Supporting Information files.

Competing Interests: The Author(s) declare(s) no conflict of interest.

Editor: Anna Maria D'Onghia, CIHEAM/Mediterranean Agronomic Institute of Bari, Italy.

INTRODUCTION

Allium crops, including onion (*Allium cepa* L.), garlic (*Allium sativus* L.), and leek (*Allium ampeloprasum* L.), have been reported to be infected by viruses belonging to *Potyvirus*, *Carlavirus*, *Tospovirus*, and *Allexivirus* (Shahraeen *et al*., 2008; Tomassoli *et al*., 2009; Parrano *et al*., 2012). Several of these viruses, including *Leek yellow stripe virus* (LYSV), *Onion yellow dwarf virus* (OYDV), *Iris yellow spot virus* (IYSV), *Shallot latent virus* (SLV), and *Garlic common latent virus* (GarCLV), are frequently found in *Allium* crops (Dovas and Volvas, 2003; Ward *et al*., 2009; Sevik and Akcura, 2013; Bag *et al*., 2015; Abraham *et al*., 2019). Other viruses, including *Turnip mosaic virus* (TuMV), *Shallot yellow stripe virus* (SYSV), and *Groundnut bud necrosis virus* (GBNV), have been considered as minor pathogens that occasionally infect *Allium* spp. only in particular regions (Gera *et al*., 1997; Chen *et al*., 2005; Sujitha *et al*., 2012).

Cucumber mosaic virus (CMV) (*Cucumovirus*, *Bromoviridae*) has a very broad host range. It usually causes diseases on plant in *Cucurbitaceae*, *Sola-*

naceae, *Brassicaceae*, and *Fabaceae*, and typically induces mild to severe systemic mosaic symptoms on these plants (Brunt *et al*., 1996). More than 80 aphid species have been recorded to non-persistently non-circulatively transmit CMV (Palukaitis and Garcia-Arenal, 2003). CMV is a tripartite virus, with the genome in three single-stranded plus-sense RNAs (RNA1-3). RNA1 encodes 1a protein and RNA2 encodes 2a protein, which are both involved in the replicase complex (Hayes and Buck, 1990). A small 2b protein involved in cell-to-cell movement, suppression of post-transcriptional gene silencing, and symptom induction, is also expressed in RNA2 (Bujarski *et al*., 2019). RNA3 encodes 3a protein (movement protein (MP)) and coat protein (CP), which are important in viral movement processes (Boccard and Baulcombe, 1993).

CMV was probably first recorded infecting *Allium* when it was serologically detected in a single garlic sample in Zagreb, Croatia (formerly Yugoslavia) (Stefanac, 1980). A large survey on *Allium* viruses in the East Mediterranean region of Turkey identified CMV as a minor virus infecting garlic in the area (Fidan, 2010). The CMV-ALC1 isolate was detected in leek in Alicante, Spain, and its nucleotide sequence was registered in NCBI GenBank with accession no. JN806091 (Alfaro-Fernandez *et al*., unpublished). These findings showed presence of CMV isolates naturally infecting *Allium* crops in different Mediterranean regions.

Recently, two onion samples from Ankara province in Turkey tested positive for CMV and negative for LYSV, OYDV, GarCLV, and SLV infections. The two CMV isolates were subsequently named CMV-14.3Po and CMV-15.5Po, and the partial nucleotide (nt) sequence of their RNA2 were deposited in NCBI GenBank (accession no. MN070136-37). Initial phylogenetic analysis showed that the isolates were similar to isolates from Iran, Serbia, Hungary, Poland, Germany, Japan, China, and South Korea, which indicated very wide distribution of CMV isolates genetically similar to onion isolates (Santosa and Ertunc, 2020).

The relationship between CMV and *Allium* spp. still requires investigation, because CMV is prevalent and many *Allium* spp. are economically important crops. Wide phylogenetic analyses of partial nt sequences of RNA2 and RNA3, and host indexing of CMV-14.3Po and CMV-15.5Po, are presented in this study, to provide further knowledge about CMV infection in onion and other *Allium* spp.

MATERIALS AND METHODS

Nucleotide sequences of RNA2 of onion isolates

The previously reported partial nt sequences of RNA2 were 521 bp long (Santosa and Ertunc, 2020), covering 27 bp of 5' UTR and 494 bp of partial 2a protein gene (1-494 position), for reference isolate accession no. D10538. These are the only nt sequences of CMV isolates naturally infecting onion that are currently available in NCBI GenBank. Therefore, a portion of their RNA3 was also sequenced in the present study to provide more information about their genetic makeup.

RT-PCR and sequencing of partial RNA3

Total nucleic acid was extracted from onion samples using tris-EDTA buffer (100 mM tris, 50 mM EDTA, 500 mM NaCl, 10 mM 2-mercaptoethanol, pH 8.0) (Presting *et al*., 1995). RT-PCR was performed in two stages (Santosa and Ertunc, 2020). A primer pair F-GTAGACATCTGTGACGCGA and R-GCGC-GAAACAAGCTTCTTATC was used in the PCR to amplify 540 bp of RNA3 (De Blas *et al*., 1994).

PCR cycles were carried out using a thermocycler (Biometra, Germany). Each cycle consisted of initial denaturation at 94°C for 5 min; 35 cycles of denaturation at 94°C for 60 s, annealing at 54°C for 60 s, elongation at 72°C for 60 s, and a final extension at 72°C for 10 min. Products were visualized on a 1% (w/v) tris-acetate agarose gel stained with ethidium bromide. Successfully amplified RT-PCR products were sent to BM Lab. Ltd. (Ankara, Turkey) for purification and Sanger sequencing. The obtained nt sequences were then submitted to NCBI GenBank.

Neighbor-joining tree construction, and nucleotide and amino acid sequences identity percentage calculation

Genes that were homologous to Turkish onion isolates were determined using the BLAST program from the the NCBI website. The Turkish onion isolates were then compared with reference CMV isolates from GenBank. The selected CMV isolates were mostly those which each had both RNA2 and RNA3 sequences available in GenBank. All sequences were aligned using ClustalW version 1.6, with default parameters in MEGA7 software (megasoftware.net). MEGA7 then applied a Neighbor-joining algorithm with both transition and transversion substitutions, and uniform rates, to construct two phylogenetic trees for RNA2 and RNA3

comparisons (Hall, 2013). Statistical significance of isolate clusters were tested using 1000 bootstrap replicates in the Tamura 3 parameter model (Tamura, 1992). Nucleotide (nt) and amino acid (aa) similarity percentages among tested isolates were estimated using Sequence Demarcation Tool (SDT) v1.2 software (Muhire *et al*., 2014).

Host indexing

Each onion isolate of CMV was mechanically inoculated to four onion, garlic, cucumber (*Cucumis sativus* L.), and melon (*Cucumis melo* L.) plants, to determine host responses. Prior to inoculation, plants were tested to be CMV-free by RT-PCR. Onion and garlic plants were also tested to be free from LYSV, SLV, GarCLV, and OYDV infections using RT-PCR and specific primers for each virus (Fajardo *et al*., 2001; Majumder *et al*., 2008; Parrano *et al*., 2012; Nam *et al*., 2015).

Plant sap was prepared by grinding 1 g of naturally infected onion leaf samples in 5 mL of 0.01 M potassium phosphate buffer (pH 7) using a mortar and pestle. Leaves of treated plants were dusted with abrasive-celite, then plant sap was manually rubbed on the leaves. Four onion, garlic, cucumber, and melon plants were each dusted with abrasive-celite then rubbed with potassium phosphate buffer as controls. Ten minutes after treatment, inoculated and control plants were rinsed with distilled water. The plants were then kept in a greenhouse at 24–28°C, and any symptoms were recorded during the following 2 to 5 weeks (Hill, 1984; Ohno *et al*., 1997; Hull, 2009). At 5 weeks after inoculation, a composite sample of leaves of the inoculated plants of the each species were collected for RT-PCR. This allowed onion isolates infection on each plant species to be confirmed by a small number of RT-PCRs, but infection rates were unknown. A primer pair of F-GTTTATTTACAAGAGCGTACGG and R-GGTTCGAA(AG)(AG)(AT)ATAACCGGG, to amplify 650 bp of RNA2, was used in the PCR (Finetti Sialer *et al*., 1999).

RESULTS

Sequencing of RNA3

The obtained partial nt sequences of RNA3 were 540 bp long, covering 216 bp of 5' UTR and 324 bp of the partial CP gene (1–324 position) for reference isolate accession no. D10538. NCBI GenBank accession no. MN864792-93 were acquired for them.

Phylogenetic analysis and nucleotide and amino acid sequences identity percentage

The phylogenetic tree constructed based on the partial RNA2 comparison was divided into four groups (1–4). The two onion isolates clustered with 21 other isolates in Group 1. The tree constructed based on the partial RNA3 comparison was also divided into four groups (1–4). However, the onion isolates only clustered in Group 1 with 15 other CMV isolates, which showed that not all isolates used in this study had high identities to the onion isolates in their RNA2 and RNA3 sequences (Figure 1).

CMV-14.3Po and CMV-15.5Po shared very high nt and aa sequence similarities in both RNA2 and RNA3. All the compared CMV isolates showed high nt (91.2–99.4%) and aa (89–100%) in partial RNA2 to onion isolates. The compared CMV isolates showed relatively lower nt (86.7–99.8%) and aa (81.8–100%) sequences to the onion isolates in comparison of partial RNA3 (Table 1).

TUR84, TUR86, I17F, PV0187, Ns, Rs, Gd, Ri-8, CMV21, NND454J and Can isolates had very high nt and aa similarities in both RNA2 and RNA3 sequences to the onion isolates, and also were clustered in the same group with onion isolates in both phylogenetic trees. The outcome showed that these isolates were genetically more similar to CMV Turkish onion isolates than the other virus isolates compared in this study.

Host indexing

Both of the onion isolates caused mild leaf malformations on all the inoculated onion plants, which was difficult to differentiate from the controls. Severe leaf malformations and stunting were observed on all inoculated garlic plants. Mottle symptoms appeared on leaves of most of the cucumber and melon plants inoculated with both onion isolates. Only one cucumber and one melon plant produced clear mosaic symptoms after inoculation with isolate CMV-14.3Po (Table 2; Figure 2). Infections on all the tested plant species were confirmed by RT-PCR (Figure 3**).**

DISCUSSION

Based on partial RNA2 and RNA3 sequence comparisons, the two onion isolates (CMV-14.3Po and CMV-15.5Po) had high similarities to at least 11 other CMV isolates. Some of these other isolates were also originally from Turkey, while some were from geographically close countries (Iran, Hungary, Germany, Austria,

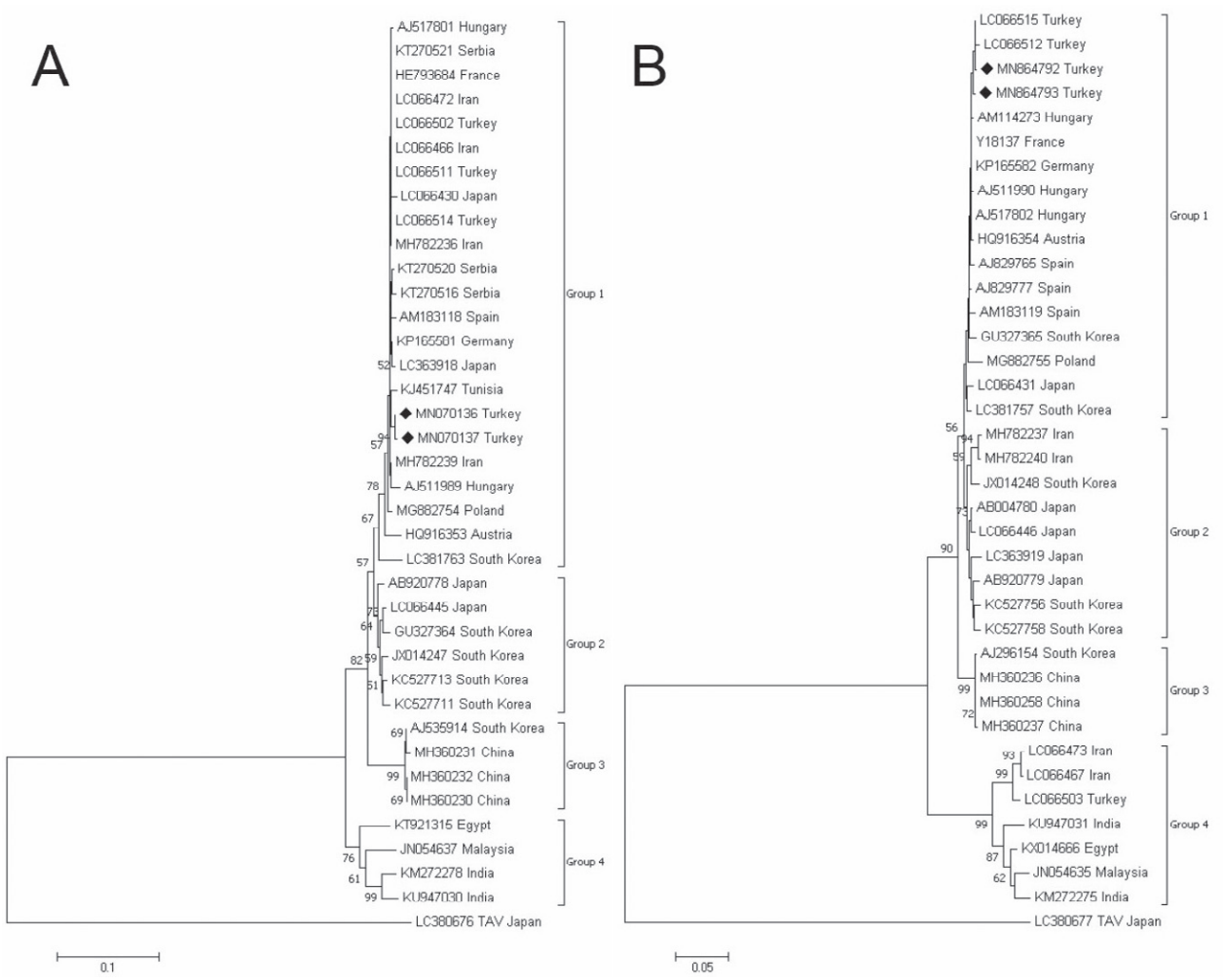

Figure 1. A. Phylogenetic tree based on nucleotide sequence comparisons of partial RNA2 of two onion isolates (MN070136-37) and 35 other CMV isolates. B. Phylogenetic tree based on nucleotide sequence comparisons of partial RNA3 of two onion isolates (MN864792-93) and 35 other CMV isolates. Bootstrap values on each branch were supported by 1000 replicates, and only values greater than 50% are shown. An isolate of *Tomato aspermy virus* (TAV Japan) was used as out-group.

France, Spain, and Poland), and some others were from East Asian countries (South Korea and Japan). The two onion isolates were also similar to three Serbian isolates (650-07, 581-11, and 473-12) and one Tunisian isolate (89-2012) only in the RNA2 sequence comparisons, since these isolates have no information on their RNA3 sequences available in NCBI GenBank. In only the RNA3 sequence comparisons, the two onion isolates were highly homologous to one Hungarian isolate (Le02) and two Spanish isolates (MAD01/2 and BAR96/1).

There is no sequence of CMV isolates from Croatia available in NCBI GenBank to be compared to onion isolates examined in the present study, but the onion isolates were very similar to isolates from Serbia, Hungary, and Austria, which are direct neighbours of Croatia. Thus, there was possibility that the CMV garlic isolate (CMV-G) that was reported in Croatia (Stefanac, 1980) also had high nt sequence similarities to CMV-14.3Po and CMV-15.5Po.

Two Iranian CMV isolates (IRN-REY4 and IRN-REY10) and one Turkish isolate (TUR54) all from radish (*Raphanus sativus* L.) were very similar in RNA2 sequences, but were divergent in RNA3 sequences, in comparison to the two onion isolates. These isolates clustered together with onion isolates in Group 1 of the phylogenetic tree of RNA2, but clustered in Group 4 of the tree of RNA3, which was very distant to the onion isolates. The RNA3 of CMV was known to be little conserved, as was also shown by the sequences iden-

Tabel 1. CMV isolates used in this study. The partial RNA2 and RNA3 nucleotide and amino acid sequence percentages to onion isolates are indicated.

No.	Isolate name[a]	Origin	Host	RNA2 comparison				RNA3 comparison			
				Accession No.	Phylo group	nt identity (%)	aa identity (%)	Accession No.	Phylo group	nt identity (%)	aa identity (%)
1.	**14.3Po**[b]	Turkey	*Allium cepa*	MN070136	1	100	100	MN864792	1	100	100
2.	**15.5Po**[b]	Turkey	*Allium cepa*	MN070137	1	100	100	MN864793	1	100	100
3.	**Rs**	Hungary	*Raphanus sativus*	AJ517801	1	99.0-99.2	99.4	AJ517802	1	99.4-99.6	100
4.	**IRN-REY4**	Iran	*Raphanus sativus*	LC066466	1	99.2-99.4	100	LC066467	4	87.8-88.3	83.5
5.	**TUR86**	Turkey	*Rapistrum rugosum*	LC066514	1	99.2-99.4	100	LC066515	1	99.6-99.8	100
6.	**TUR84**	Turkey	*Rapistrum rugosum*	LC066511	1	99.2-99.4	100	LC066512	1	99.3-99.4	99.4
7.	**TUR54**	Turkey	*Raphanus sativus*	LC066502	1	99.2-99.4	100	LC066503	4	87.8-88	81.8
8.	**MeEs**	Iran	*Cucumis melo*	MH782236	1	99.2-99.4	100	MH782237	2	97.0-97.2	98.9
9.	**IRN-REY10**	Iran	*Raphanus sativus*	LC066472	1	99.2-99.4	100	LC066473	4	87.6-88.1	83
10.	**NND454J**	Japan	*Raphanus sativus*	LC066430	1	98.7-98.8	100	LC066431	1	98.5-98.7	98.3
11.	**I17F**	France	*Solanum lycopersicum*	HE793684	1	99.2-99.4	100	Y18137	1	99.4-99.6	100
12.	**Ri-8**	Spain	*Solanum lycopersicum*	AM183118	1	98.7-98.8	100	AM183119	1	98.7-98.9	98.9
13.	**PV0187**	Germany	-	KP165581	1	99.0-99.2	100	KP165582	1	99.4-99.6	100
14.	**Co-46**	Japan	*Corchorus olitorius*	LC363918	1	98.7-98.8	100	LC363919	2	97.0-97.2	98.3
15.	**SqSh**	Iran	*Cucurbita pepo*	MH782239	1	99.0-99.2	100	MH782240	2	97.2-97.4	98.9
16.	**Ns**	Hungary	*Nicotiana glutinosa*	AJ511989	1	98.5-98.7	99.4	AJ511990	1	99.3-99.4	100
17.	**CMV21**	Poland	*Cucurbita pepo*	MG882754	1	98.5-98.7	100	MG882755	1	97.8-98	96.6
18.	**Gd**	Austria	*Cucurbita pepo*	HQ916353	1	97.1-97.3	97.1	HQ916354	1	99.3-99.4	100
19.	**Can**	S. Korea	*Canna generalis*	LC381763	1	96.5-96.7	97.7	LC381757	1	98.5-98.7	98.9
20.	650-07	Serbia	*Nicotiana tabacum*	KT270521	1	99.2-99.4	100	-	-	-	-
21.	581-11	Serbia	*Capsicum annuum*	KT270520	1	98.9-99	99.4	-	-	-	-
22.	473-12	Serbia	*Citrullus lanatus*	KT270516	1	98.7-98.8	99.4	-	-	-	-
23.	89-2012	Tunisia	*Cynara scolymus*	KJ451747	1	98.9-99	98.8	-	-	-	-
24.	Le02	Hungary	*Lycopersicon esculentum*	-	-	-	-	AM114273	1	99.4-99.6	100
25.	MAD01/2	Spain	*Diplotaxis erucoides*	-	-	-	-	AJ829765	1	99.1-99.3	99.4
26.	BAR96/1	Spain	*Cucumis melo*	-	-	-	-	AJ829777	1	99.1-99.3	99.4
27.	KM	Japan	*Cucumis melo*	-	-	-	-	AB004780	2	98.0-98.5	98.3
28.	**m1**	Japan	*Nicotiana tabacum*	AB920778	2	96.5-96.7	97.7	AB920779	2	97.2-97.4	98.3
29.	**TKD766J**	Japan	*Raphanus sativus*	LC066445	2	96.4-96.5	97.1	LC066446	2	97.6-98.1	98.3
30.	**Rb**	S. Korea	*Rudbeckia hirta*	GU327364	2	96.4-96.5	95.4	GU327365	1	98.5-98.7	99.4
31.	**Va**	S. Korea	*Vigna angularis*	JX014247	2	96.5-96.7	96.5	JX014248	2	97.2-97.8	98.3
32.	**RP30**	S. Korea	*Capsicum annuum*	KC527713	2	96.5-96.7	97.1	KC527758	2	97.0-97.2	97.2
33.	**RP28**	S. Korea	*Capsicum annuum*	KC527711	2	96.4-96.5	95.9	KC527756	2	97.0-97.2	97.7
34.	**Ly2**	S. Korea	*Lilium longiflorum*	AJ535914	3	93.7-93.9	94.2	AJ296154	3	96.5-96.7	94.3
35.	**C4**	China	*Lilium* spp.	MH360231	3	93.3-93.5	93.6	MH360236	3	96.7-96.9	94.9
36.	**C6**	China	*Lilium* spp.	MH360232	3	93.7-93.9	93.6	MH360237	3	96.5-96.7	94.3
37.	**C2**	China	*Lilium longiflorum*	MH360230	3	93.7-93.9	93.6	MH360258	3	96.7-96.9	94.9
38.	**HM3**	Egypt	*Solanum lycopersicum*	KT921315	4	93.1-93.2	91.3	KX014666	4	87.8-88.3	83
39.	**CLW2**	Malaysia	*Cucumis sativus*	JN054637	4	92.7-92.9	89.6	JN054635	4	87.0-87.6	83
40	**KO**	India	*Capsicum annuum*	KM272278	4	91.7-91.9	88.4	KM272275	4	86.7-87.2	81.8
41	ICAR-IISR PN25	India	*Piper nigrum*	KU947030	4	91.2-91.3	89	KU947031	4	87.2-87.4	83

[a] Isolates that name typed in bold are those that both RNA2 and RNA3 sequences are available in NCBI GenBank.
[b] CMV onion isolates that were identified in this study.

Table 2. Symptoms caused from inoculations with two CMV isolates on different inoculated test plants.

Isolate	Plant species	Symptoms on inoculated plant number[a]			
		1	2	3	4
CMV-14.3Po	Onion	Mild leaf malformation	Mild leaf malformation	Mild leaf malformation	Mild leaf malformation
	Garlic	Severe leaf malformation and stunting	Severe leaf malformation and stunting	Severe leaf malformation and stunting	Severe leaf malformation and stunting
	Cucumber	Mottle	Mottle	Mosaic	Mottle
	Melon	Mottle	Mottle	Mottle	Mosaic and mottle
CMV-15.5Po	Onion	Mild leaf malformation	Mild leaf malformation	Mild leaf malformation	Mild leaf malformation
	Garlic	Severe leaf malformation and stunting	Severe leaf malformation and stunting	Severe leaf malformation and stunting	Severe leaf malformation and stunting
	Cucumber	Mottle	Mottle	Mottle	Mottle
	Melon	Mottle	Mottle	Mottle	Mottle

[a] Mottle was considered mild, while mosaic was considered as a more severe symptom.

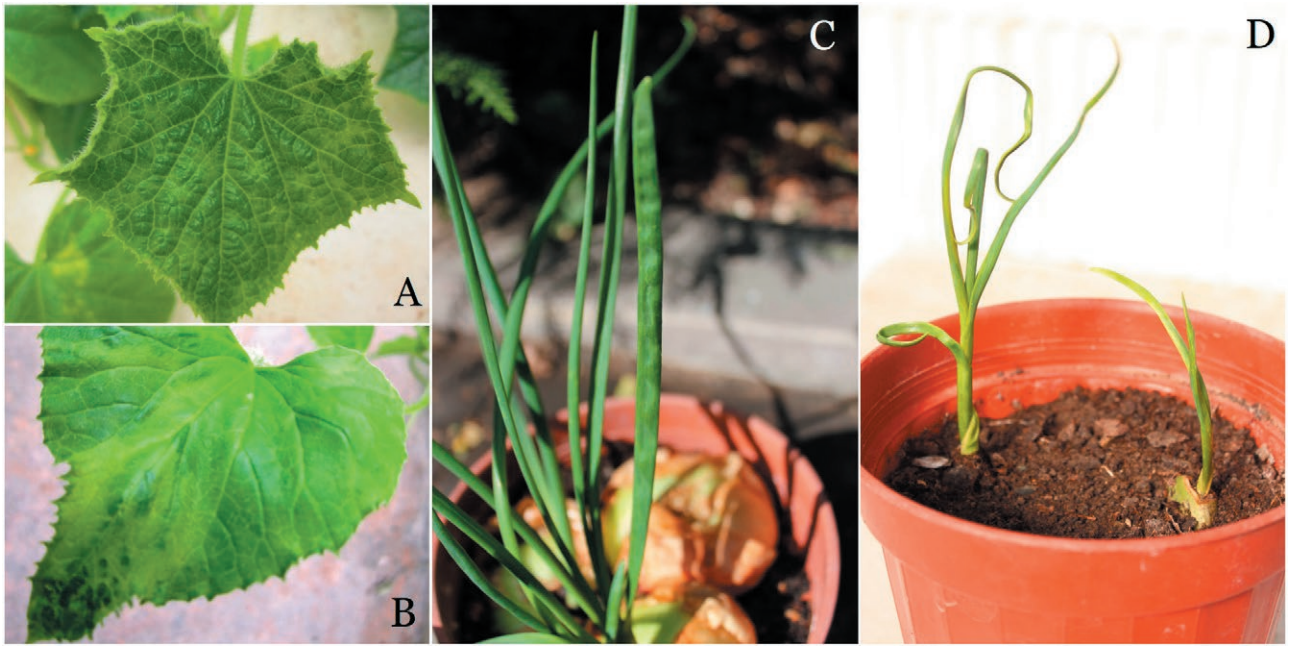

Figure 2. Symptoms on plants mechanically inoculated with two CMV isolates from onion. A. Mosaic on cucumber inoculated with CMV-14.3Po, B. Mosaic and mottle on melon inoculated with CMV-14.3Po, C. Mild leaf malformation on onion inoculated with CMV-15.5Po, D. Severe leaf malformation and stunting on garlic inoculated with CMV-15.5Po.

tity analyses of this study. Phylogenetic analyses on this region were useful for classification of CMV isolates into subgroups IA, IB, and II (Roossinck *et al.*, 1999). The two onion isolates belonged to subgroups IA according to phylogenetic analysis in the present study.

Isolates that have high genomic similarities to CMV-14.3Po and CMV-15.5Po were identified from different plant species from several families. As comparison, four isolates in Group 3 (Ly2-CMV, C2, C4, and C6) were all identified from *Lilium* spp. Results from phylogenetic and similarity analyses also showed that CMV isolates with genome signature similar to CMV-14.3Po and CMV-15.5Po naturally had wide host ranges, and had been found in a broad geographic area, comprising Mediterranean, European, and East Asian countries. CMV should therefore be included in future virus surveys of *Allium* conducted in these regions, especially where CMV was known to be prevalent.

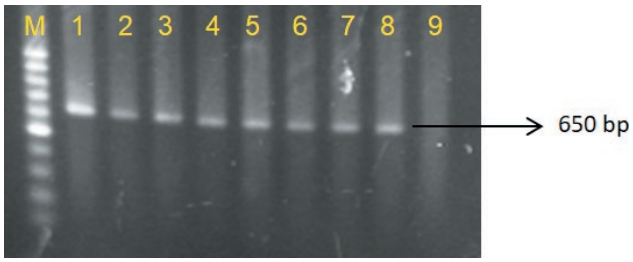

Figure 3. Gel from extracts of onion, garlic, cucumber, and melon plants mechanically inoculated with two onion isolates of CMV in the host indexing study gave positive results in RT-PCR to amplify partial RNA2 of CMV (650 bp). Isolate CMV-14.3Po in lane 1. onion, lane 2. garlic, lane 3. cucumber, and lane 4. Melon. Isolate CMV-15.5Po in lane 5. onion, lane 6. garlic, lane 7. cucumber, lane 8. Melon. Lane 9. negative control (uninoculated onion). Lane M = 100 bp DNA ladder marker (Thermo Fisher Scientific).

Partial RNA3 sequences of CMV-14.3Po and CMV-15.5Po shared high similarities to two other Turkish CMV isolates (TUR84 and TUR86) identified from *Rapistrum rugosum* (Oshima *et al*., 2016). This provided more evidence to the previous suggestion based on phylogenetic analyses of partial RNA2, that onion isolates were probably transmitted from *R. rugosum*, or other weed species, in onion fields. During the survey that was conducted in Ankara province, only two of 210 onion samples tested positive for CMV infections. This low infection rate may have been due to absence of aphid vectors (Santosa and Ertunc, 2020). The two onion isolates were found in two different fields close to each other during a survey that covered a wide area. The isolates were therefore likely to only spread locally, because natural mechanical transmission in onion was difficult.

CMV-14.3Po and CMV-15.5Po were shown to be mechanically transmissible to onion, garlic, cucumber, and melon, based on host indexing results. CMV-G was also reported to be transmitted to onion and cucumber by mechanical inoculation. Similar to CMV-14.3Po and CMV-15.5Po, CMV-G produced severe symptoms on garlic (Stefanac, 1980). CMV-G caused severe symptom (necrotic streaks) on onion, contrary to CMV-14.3Po and CMV-15.5Po that only produced mild leaf malformation on onion. These results probably showed response of different onion varieties to CMV isolates. The mild leaf malformation on inoculated onions was consistent with symptoms on inoculum sources (samples that were naturally infected by CMV-14.3Po and CMV-15.5Po) (Santosa and Ertunc, 2020). Onion isolates mostly only caused mild symptom (mottle) on inoculated cucumber and melon, with only one of each cucumber and melon plants developing severe symptoms (mosaic).

Based on low infection rate and mild symptom severity, it can be shown that CMV is a minor virus that does not pose serious threats to onion production. CMV could be a threat for garlic cultivation, since it caused severe damage to garlic plants, and garlic vegetative propagation would easily transmit viruses to next generations. However, CMV infection on garlic was determined to be rare in a survey (Fidan, 2010). Severe symptoms on garlic which could eliminate the possibility for infected plants to become planting material, and the difficulty to transmit CMV-G by aphids, were thought to be the reasons for rare CMV infection on garlic (Stefanac and Milicic, 1992).

Phylogenetic and similarity analyses and host indexing that were performed on CMV-14.3Po and CMV-15.5Po revealed knowledge of CMV isolates that naturally infect onion, which was lacking prior to this study. However, information on distribution, transmission, economic importance and genomic diversity of CMV in onion and other *Allium* spp. is still needed to be further investigated.

ACKNOWLEDGEMENT

This research was funded by the Scientific Research Projects Coordinator of Ankara University (Project No. 18H0447001, “Detection of Viral Infection Sources on Onion Production Areas”).

LITERATURE CITED

Abraham A.D., Kidanemariam D.B., Holton T.A., 2019. Molecular identification, incidence and phylogenetic analysis of seven viruses infecting garlic in Ethiopia. *European Journal of Plant Pathology* 55: 181–191. https://doi.org/10.1007/s10658-019-01760-9

Alfaro-Fernandez A., Villaescusa F.J., Hermoso de Mendoza A., Ferrandiz J.C., Sanjuan S., Font San Ambrosio M.I., Unpublished. First report of aster yellows and stolbur phytoplasma infecting commercial leek (*Allium porrum* L.) in Spain.

Bag S., Schwartz H.F., Cramer C.S., Havey M.J., Pappu H.R., 2015. *Iris yellow spot virus* (*Tospovirus*: *Bunyaviridae*): From obscurity to research priority. *Molecular Plant Pathology* 16(3): 224–237. https://doi.org/10.1111/mpp.12177

Boccard F., Baulcombe D., 1993. Mutational analysis of cis acting sequences and gene function in RNA3 of *Cucumber mosaic virus*. *Virology* 193: 563–578. https://doi.org/10.1006/viro.1993.1165

Brunt A.A., Crabtree K., Dallwitz M.J., Gibbs A.J., Watson L., 1996. Plant Viruses Online: Description and Lists from the VIDE Database. Cucumber mosaic *cucumovirus*. Available at: http://bio-mirror.im.ac.cn/mirrors/pvo/vide/descr267.htm. Accessed January 31, 2020.

Bujarski J., Gallitelli D., García-Arenal F., Pallás V.B., Palukaitis P., ... ICTV Report Consortium., 2019. ICTV Virus Taxonomy Profile: Bromoviridae. *Journal of General Virology* 100: 1206–1207. https://doi.org/10.1099/jgv.0.001282

Chen J., Wei C.B., Zheng H.Y., Shi Y.H., Adams M.J., ... Chen J.P., 2005. Characterisation of the welsh onion isolate of *Shallot yellow stripe virus* from China. *Archives of Virology* 150: 2091–2099. https://doi.org/10.1007/s00705-005-0580-3

De Blas C., Borja M.J., Saiz M., Romero J., 1994. Broad spectrum detection of *Cucumber mosaic virus* (CMV) using the Polymerase Chain Reaction. *Journal of Phytopathology* 141(3): 323–329. https://doi.org/10.1111/j.1439-0434.1994.tb01476.x

Dovas C.I., Volvas C., 2003. Viruses infecting *Allium* spp. in Southern Italy. *Journal of Plant Pathology* 85(2): 135. http://dx.doi.org/10.4454/jpp.v85i2.1022

Fajardo T.V.M., Nishijima M., Buso J.A., Torres A.C., Ávila A.C., Resende R.O., 2001. Garlic viral complex: identification of potyviruses and carlavirus in central Brazil. *Fitopatologia Brasileira* 26: 619–626. https://doi.org/10.1590/S0100-41582001000300007

Fidan H., 2010. *Sarımsak, soğan ve pırasadaki virüs hastalıklarını saptanması ve Taşköprü 56 sarımsak tipinin en yaygın virüse karşı reaksiyonunun belirlenmesi*. PhD Thesis, Cukurova University, Adana, Turkey, 163 pp (in Turkish).

Finetti Sialer M.M., Cillo F., Barbarossa L., Gallitelli D., 1999. Differentiation of *Cucumber mosaic virus* subgroups by RT-PCR RFLP. *Journal of Plant Pathology* 81(2): 145–148. http://dx.doi.org/10.4454/jpp.v81i2.1059

Gera A., Lesemann D.E., Cohen J., Franck A., Levy S., Salomo R., 1997. The natural occurrence of Turnip Mosaic Potyvirus in *Allium ampeloprasum*. *Journal of Phytopathology* 145(7): 289–293. https://doi.org/10.1111/j.1439-0434.1997.tb00403.x

Hall B.G., 2013. Building phylogenetic trees from molecular data with MEGA. *Molecular Biology and Evolution* 30(5): 1229–1235. https://doi.org/10.1093/molbev/mst012

Hayes R.J., Buck K.W., 1990. Complete replication of a eukaryotic virus RNA *in vitro* by a purified RNA-dependent RNA Polymerase. *Cell* 63(2): 363–368. https://doi.org/10.1016/0092-8674(90)90169-f

Hill S.A., 1984. *Methods in Plant Virology*. Blackwell Scientific Publications, Oxford, United Kingdom, 167 pp.

Hull R., 2009. Mechanical inoculation of plant viruses. *Current Protocols in Microbiology* 13: 16B.6.1–16B.6.4. https://doi.org/10.1002/9780471729259.mc16b06s13

Majumder S., Baranwal V.K,. Joshi S., 2008. Simultaneous detection of *Onion yellow dwarf virus* and *Shallot latent virus* in infected leaves and cloves of garlic by Duplex RT-PCR. *Journal of Plant Pathology* 90(2): 371–374. https://doi.org/10.1007/s13337-010-0008-x

Muhire B.M., Varsani A., Martin D.P., 2014. SDT: A virus classification tool based on pairwise sequence alignment and identity calculation. *PloS One* 9(9): e108277. https://doi.org/10.1371/journal.pone.0108277

Nam M., Lee Y., Park C.H., Lee M., Bae Y., ... Lee S., 2015. Development of multiplex RT-PCR for simultaneous detection of garlic viruses and the incidence of garlic viral disease in garlic genetic resources. *The Plant Pathology Journal* 31(1): 90–96. https://doi.org/10.5423/PPJ.NT.10.2014.0114

Ohno H., Hase S., Ehar, Y., 1997. Analysis of the pH effect on infectivity of *Cucumber mosaic virus*-A possible role of Ribonuclease. *Annals of the Phytopathological Society of Japan* 63: 445–449.

Ohshima K., Matsumoto K., Yasaka R., Nishiyama M., Soejima K., ... Takeshita M., 2016. Temporal analysis of reassortment and molecular evolution of *Cucumber mosaic virus*: Extra clues from its segmented genome. *Virology* 487: 188–197. https://doi.org/10.1016/j.virol.2015.09.024

Palukaitis P., Garcia-Arenal F., 2003. Cucumoviruses. *Advances in Virus Research* 62: 241–323. https://doi.org/10.1016/s0065-3527(03)62005-1

Parrano L., Afunian M., Pagliaccia D., Douhan G., Vidalakis G., 2012. Characterization of viruses associated with garlic plants propagated from different reproductive tissues from Italy and other geographic regions. *Phytopathologia Mediterranea* 51(3): 549–565. https://doi.org/10.14601/Phytopathol_Mediterr-10479

Presting G.G., Smith O.P., Brown C.R., 1995. Resistance to *Potato leafroll virus* in Potato plants transformed with the Coat protein gene or with vector control constructs. *Phytopathology* 85: 436–442. https://doi.org/10.1094/Phyto-85-436

Roossinck M.J., Zhang L., Hellwald K.H., 1999. Rearrangements in the 5' nontranslated region and phylogenetic analyses of *Cucumber mosaic virus* RNA 3 indicate radial evolution of three subgroups. *Journal*

of Virology 73(8): 6752–6758. http://www.ncbi.nlm.nih.gov/pmc/articles/pmc112760/

Santosa A.I., Ertunc F., 2020. Identification, molecular detection and phylogenetic analysis of four viruses infecting *Allium cepa* in Ankara province, Turkey. *Journal of Plant Diseases and Protection* 127(4): 561–569. https://doi.org/10.1007/s41348-020-00347-5

Sevik M.A., Akcura C., 2013. Viruses occurring in onion crop in Amasya province, the major onion producing region in Turkey. *Indian Journal of Virology* 24(1): 78–81. https://doi.org/10.1007/s13337-012-0114-z

Shahraeen N., Lesemann D.E., Ghotbi T., 2008. Survey for viruses infecting onion, garlic and leek crops in Iran. *Bulletin OEPP/EPPO Bulletin* 38: 131–135. https://doi.org/10.1111/j.1365-2338.2008.01198.x

Stefanac Z., 1980. *Cucumber mosaic virus* in Garlic. *Acta Botanica Croatica* 39: 21–26.

Stefanac Z., Milicic D., 1992. Observations on infection of garlic (*Allium sativum* L.) with *Cucumber mosaic virus*. *Acta Botanica Croatica* 51: 1–5.

Sujitha A., Bhaskara Reddy B.V., Sivaprasad Y., Usha R., Sai Gopal D.V.R., 2012. First report of *Groundnut bud necrosis virus* infecting onion (*Allium cepa*). *Australasian Plant Disease Notes* 7: 183–187. https://doi.org/10.1007/s13314-012-0080-8

Tamura K., 1992. Estimation of the number of nucleotide substitutions when there are strong Transition-Transversion and G+C-content biases. *Molecular Biology and Evolution* 9(4): 678–687. https://doi.org/10.1093/oxfordjournals.molbev.a040752

Tomassoli L., Tiberini A., Masenga V., Vicchi V., Turina M., 2009. Characterızatıon of *Iris yellow spot virus* isolates from onion crops in Northern Italy. *Journal of Plant Pathology* 91(3): 733–739.

Ward L.I., Perez-Egusquiza Z., Fletcher J.D., Clover G.R.G., 2009. A survey of viral diseases of *Allium* crops in New Zealand. *Australasian Plant Pathology* 38: 533–539. https://doi.org/10.1071/AP09039

Phytopathologia Mediterranea
The international journal of the
Mediterranean Phytopathological Union

Firenze University Press
www.fupress.com/pm

Research Papers

Antibacterial activity of tannins towards *Pseudomonas syringae* pv. *tomato*, and their potential as biostimulants on tomato plants

Paolo CANZONIERE[1], Sara FRANCESCONI[1], Samuele GIOVANDO[2], Giorgio M. BALESTRA[1,*]

[1] *Dipartimento di Scienze Agrarie e Forestali (DAFNE), Università degli Studi della Tuscia, Via San Camillo de Lellis, 01100, Viterbo, Italy*
[2] *Centro Ricerche per la Chimica Fine Srl, Via Torre, 7, 12080, San Michele di Mondovì (CN), Italy*
*Corresponding author. E-mail: balestra@unitus.it

Summary. *Pseudomonas syringae* pv. *tomato* (Pst), the causal agent of bacterial speck of tomato, is a significant cause of economic losses in tomato crops. This disease is mainly controlled with preventive use of cupric salt formulations. Antibacterial activity of the tannins U1, U2, U3 and U4, applied alone at 1% w/v concentration or in combination with half (0.045% w/v) of standard of copper hydroxide treatments, was assayed for effects on Pst. *In vitro*, the four tannins completely inhibited Pst colony formation after 24 h, but U2 (quebracho tannins) + ½ $Cu(OH)_2$ allowed Pst growth after 48 h of incubation, indicating that, since U2 is composed of high molecular condensed tannins it is likely that their structures have chelated the copper hydroxide much more then hydrolysable ones, thus inactivating copper hydroxide and tannins. In fact, this activity of the tannins was equivalent to that for 0.045% w/v of copper hydroxide. Effects of tannins on tomato plant growth were also assessed. On seedlings, long-term U1 treatments increased dry weight of shoots compared to copper hydroxide, but not to water treatment. The U4 treatment increased the NBI values compared to copper treatment but did not show significant differences compared to the water treatment. Inhibitory activity of tannin treatments reduced disease by 37–62%, and 60% after copper treatment, while disease severity was reduced by 33–54% after treating plants with tannins and 36% after copper treatment. On mature plants treated once, the disease reduction was 27–39% after tannin treatments and 44% after copper treatment, while severity was reduced by 50–60% from tannin treatments, and 47% by copper. In seedlings and mature plants, these reductions were similar ($P > 0.05$) for the tannins and copper treatments. This study indicates a novel crop protection strategy using natural products as alternatives to xenobiotic compounds.

Keywords. Bacterial speck, antibacterial activity, plant growth promotion, eco-friendly strategies.

OPEN ACCESS

Citation: P. Canzoniere, S. Francesconi, S. Giovando, G. M. Balestra (2021) Antibacterial activity of tannins towards *Pseudomonas syringae* pv. *tomato*, and their potential as biostimulants on tomato plants. *Phytopathologia Mediterranea* 60(1): 23-36. doi: 10.36253/phyto-11732

Accepted: October 10, 2020

Published: May 15, 2021

Data Availability Statement: All relevant data are within the paper and its Supporting Information files.

Competing Interests: The Author(s) declare(s) no conflict of interest.

Editor: Roberto Buonaurio, University of Perugia, Italy.

INTRODUCTION

Pseudomonas syringae pv. *tomato* (Okabe) Alstatt (Pst) is the causal agent of bacterial speck on tomato plants (*Solanum lycopersicum* L.), and is capa-

ble of causing considerable economic losses from tomato crops. The pathogen survives as an epiphyte on weeds and on symptomless tomato transplants, as well as in the soil and in host seeds (Devash *et al.,* 1980; McCarter *et al.,* 1983), utilizing molecules released from leaves and organic matter carried by the wind (Schneider and Grogan, 1976). Bacterial speck symptoms can affect various plant organs. On leaflets, where the pathogen penetrates into depressions between epidermal cells, substomatal chambers and around trichomes, speck symptoms appear as black spots, usually surrounded by yellow halos. Lesions on tomato fruit are small raised black spots, often surrounded by green halos (Varvaro *et al.,* 1993). Fruit developed on defoliated plants are small, thus reducing the quality of fresh and processed tomatoes (Gruda, 2005; Pietrarelli *et al.,* 2006).

Control of bacterial diseases is mainly based on appropriate agronomic practices, including use of healthy seeds, balanced fertilisation, crop rotation, and design of irrigation systems, to limit the spread of the pathogens (Quattrucci *et al.,* 2013). As regards chemical control, Cupric salts are important pesticide components for management of phytopathogenic bacteria in conventional and organic agriculture (La Torre *et al.,* 2018). Due to European restrictions on the use of copper, Pst control strategies based on low environmental impact and substitution of copper compounds are urgently required (Quattrucci and Balestra, 2009). This approach is already obtaining positive results for control of pathogens that cause parenchymatic and vascular diseases in tomatoes (Quattrucci and Balestra, 2009; Baka and Rashad, 2016; Kalleli *et al.,* 2020). Nevertheless, Marrone (2019) stated, "there is still a relatively low percentage of naturally derived pesticides relative to the number of pharmaceuticals derived from natural sources". Effective pest management is a major challenge in modern agriculture, where control efficacy, cost affordability, environmental safety, toxicity towards non-target organisms, and sustainability of the production system are important factors (Vurro *et al.,* 2019).

Tannins are polyphenolic secondary metabolites abundant in vascular plants, commonly occurring at 5-10% dry weight of plant biomass (Haslam *et al.,* 1988; Lochab, 2014). They are the third most abundant components extracted from biomass, after cellulose, hemicelluloses and lignin (Arbenz and Avérous, 2016). Furthermore, they are mainly involved in plant protection through mechanisms of direct action on microbial pathogens, insects and herbivorous animals (Barbehenn and Constabel, 2011). The conventional extract process for tannins is based on plentiful water, which is partly recycled based mainly on solid/liquid extraction. Other extraction techniques, including extractions based on supercritical fluid, pressurized water, microwaves, or ultrasound, are applied for laboratory studies (De Hoyos-Martínez *et al.,* 2019). Due to the heterogeneous nature of tannins, a universal method can be used for their extraction (Bacelo *et al.,* 2016).

Two of the most important classes of tannins are the hydrolysable and condensed varieties. Hydrolysable tannins are multiple esters of gallic acid with glucose and products of their oxidative reactions, and these have molecular weights from 500 to 3,000 Da. Condensed tannins (syn. proanthocyanidins) are derivatives of catechin and esters of gallic acid with quinic acid, and these compounds have molecular weights from 1,000 to 20,000 Da (Hümmer and Schreier, 2008; Quideau *et al.*, 2011; Aroso *et al.*, 2017). Hydrolysable tannins include gallotannins and ellagitannins. Upon hydrolysis by acids, bases or certain enzymes, gallotannins yield glucose and gallic acid, while ellagitannins produce the hydroxydiphenoyl residue; the latter undergoes lactonization to produce ellagic acid, which is not easily hydrolyzed because of the further C–C coupling of the polyphenolic residue with the polyol unit. So it should be mentioned that ellagitannins are not hydrolysable but are nevertheless for historical reasons classified as hydrolysable tannins. (Hernes and Hedges, 2004). Condensed tannins are polymers of flavonoids and their building block includes catechin and epicatechin. Condensed tannins can have different degrees of polymerization (between 3 and 11), depending on the linkage between the elementary units, which can be C-C or occasionally C-O-C. Their condensation occurs through an oxidative reaction between the C_4 carbon of the heterocycle and C_6 or C_8 carbons (Venter *et al.*, 2012).

Many industrial tannins with agri-food applications are extracted from different plant species. In the present study tannins from three different sources were assayed: from sweet chestnut, tara pods or quebracho. Chemical characteristic of the tannins used have been reported in the Materials and Methods section. For agricultural uses of condensed tannins, their efficacy in plant protection has assessed against the gram-negative phytopathogenic bacterium *Pseudomonas savastanoi* pv. *neri*, where some extracts showed inhibitory activity on the Type Three Secretion System (TTSS) and in Quorum Sensing (QS). Grapeseed polyphenolic extracts consisted of several catechins and epicatechins, with molecular weights ranging from 290 to 1,170 Da, and of free gallic acid (0.004 mg g^{-1}), while the phytocompounds in green tea extracts were epigallocatechin gallate (839 mg g^{-1}) and epicatechin gallate (32 mg g^{-1}) (Biancalani *et al.*, 2016).

Hydrolysable tannins are mainly extracted from sweet chestnut, and several studies have assessed how these compounds counteract plant pathogens. Tests on potato plants inoculated with *Meloidogyne javanica* (Treub) Chitwood showed reductions of nematode egg numbers *in vitro* and reproduction rates *in vivo* (Renčo *et al*., 2012). A crude methanol extract of *Sapium baccatum* (Roxb) has been shown to be highly active against *Ralstonia solanacearum* (Smith) with *in vitro* and *in vivo* tests (Vu *et al*., 2017). The antibacterial effect of tannins on watermelon seeds has been demonstrated, with reduction of symptoms caused by *Acidovorax citrulli* from inoculated seeds and increased germination, following treatments with a product (AGRITAN®, Silvateam S.p.A.) containing plant polyphenol extracts based on tannins. The hypothesis that tannins could also induce host resistance has been advanced (Giovanardi *et al*., 2015). A raw sweet chestnut hydrolysable extract has found application as a biostimulant in transplanted tobacco crops, as a starter treatment boosting early root growth through phosphate uptake, making plants resistant to pathogens including nematodes, and thus allowing reduced usage of xenobiotic products (Bargiacchi *et al*,. 2013, 2017). In agriculture, hydrolysable tannins are also used as organic acidifying solutions and iron fertilizers. Iron fertilization occurs due to the metal chelation proprieties of tannins (Bargiacchi *et al*., 2004). Although studies have evaluated the biostimulant activities of tannins applied to plant roots and seeds, none have focused on the biostimulant activity of tannins nebulised on leaves.

The present study evaluated tannins antibacterial activity towards Pst, and potential biostimulant activity towards host plants. Three tannins from different plant sources were used to prepare four formulations (U1, U2, U3, and U4). Tannins were assessed for applications of these products onto tomato plant leaves at different stages of plant growth.

MATERIALS AND METHODS

Tannin chemical characteristics

Tannin formulations

Tannin components in the different formulations were: U1, sweet chestnut (*Castanea sativa*) hydrolysable tannins water extract; U2, sulfited quebracho (*Schinopsis lorentzii*) condensed tannins water extract; U3, a mixture (1:9) of tara (*Casealpina spinosa*) pods solvent extract of hydrolysable tannins and sweet chestnut hydrolysable tannins water extract; and U4, a mixture (1:1) of sweet chestnut hydrolysable tannins water extract and sulfited quebracho condensed tannins water extract. Each product assayed was a liquid formulation, containing 40% tannins and 60% water, and was provided by Silvateam S.p.A. (San Michele Mondovì, Italy).

The chemical structures of the tannins assayed in this study were previously characterized by Pizzi *et al.* (2009), Giovando *et al.* (2013), Radebe *et al.* (2013). Turkey gall, and chestnut woods were analyzed and compared using matrix-assisted laser desorption/ionization time-of-flight (MALDI-TOF and Molino *et al.* (2018).

In vitro *effects of tannins on* Pseudomonas syringae *pv.* tomato

Bacterium culture

Pseudomonas syringae pv. *tomato* isolate CFBP-1323 from the French Bacterial Collection was used in this study. The isolate was stored at -80°C, and was grown according to King *et al.* (1954) at 25 ± 1°C for 24 h for the preparation of inoculum. Bacterium suspensions were prepared in 0.01 M $MgSO_4$, and adjusted to 1×10^6 CFU mL^{-1} at OD_{600}.

Bacterium inhibition and growth on tannin-containing media

The minimum inhibitory concentrations (MICs) of the tannins were assayed by testing five concentrations of each, at 0.2, 0.5, 1, 1.5, or 2% (w/v), following the protocol reported in Francesconi *et al.* (2020). The tannins were dissolved in sterile distilled water at these concentrations, and the solutions were then filtered using a sterile syringe filter (0.2 µm pore size). The filtered solutions were then pipetted into the microtiter plates, and bacterium suspension was added to each well to obtain final concentration of 1×10^4 CFU mL^{-1}. The plates were then incubated at 27°C in the dark for 24 h. Ten µL of each bacterium/tannin suspension were transferred into a new microtiter plate containing Nutrient Broth (NB), and incubated at 27°C in the dark for 48 h. Absorbance from the resulting bacteria was measured at OD_{600}, using a DR-200B Microplate reader (Diatek Instruments). Mock (untreated bacterium suspension cultured on NB) and blank (NB only) controls were also included.

The tannin formulations were incorporated into KB medium at 1% (w/v). Copper hydroxide (standard) was used at 0.09% (w/v), on the basis of average concentrations of cupric salts in many commercial formulations. Suspensions of tannins (at 10% w/v) and copper hydrox-

ide (at 0.9% w/v) were each prepared in 100 mL of sterile deionised water. To obtain the final concentrations, 1 mL of each suspension was sterilised with 0.22 µm pore size filters and added to 100 mL of the medium. The plates were inoculated with 100 µL of Pst suspension (10^4 CFU mL^{-1}) and incubated at 27°C for 48 h. Three independent replicates were performed with three plates for each experimental group, and the CFU were determined after 24 and 48 h.

In vivo *effects of tannin treatments*

Bacterium inoculations

Three hours before bacterium inoculation, the relative humidity where test plants were growing (see below) was increased to 95% to favour the opening of the leaf stomata. Inoculation were carried out by spraying each plant with 30 mL of bacterium suspension containing 1 × 10^6 CFU mL^{-1}, which was obtained by serial 1:10 dilutions (Katagiri *et al.,* 2002).

Host plant material, growth conditions and experimental design

In the autumn of 2018, experiments were conducted in a glass greenhouse at the Tuscia University experimental farm (Viterbo, central Italy, 42°25'N, 12°08'E). Tomato seedlings (*Solanum lycopersicum* L. cv. San Marzano; susceptible to Pst) were acquired from an organic nursery. The experimental design was a randomized complete-block design consisting of three independent experiments, each containing ten plants for each experimental group. The plants were kept in controlled conditions at 28±2°C and 70 to 80% relative humidity. Seedlings at the cotyledon stage were transplanted into pots (15 cm diam.) containing a sterilised soil/sand/peat mix (2:1:1 volume), and were watered daily using drip irrigation. A mineral solution (N, P, K, 20:20:20 plus B, Cu, Fe, Mn, Mo, Zn, 1:5:30:10:10:10), at 2 g L was administered to the pots once each week, to maintain optimum nutritional conditions.

The seedling experiments commenced 15 d before inoculation, in which the tannin treatments were applied three times at 5, 10 and 15 d. The mature plants were treated 1 d before inoculation with tannin formulations. Each experiment spanned 21 d from inoculation to final assessments.

To determine if there were phytotoxic effects of the tannin formulations used, the tannins were infiltrated into the mesophylls of tobacco leaves. No unspecific phytotoxicity was observed (data not shown). Tomato plants were also visually evaluated for phytotoxicity during each rating period.

The tannin treatments were applied to the seedlings and the mature plants with a CO_2-pressurised handheld sprayer equipped with a large orifice nozzle (TeeJet 8004), operating at 2.8 g cm^{-1}, to produce large spray droplets to runoff. The treatments applied were: 1% tan-

Table 1. Descriptions of treatments used in this study. tannins = hydrolysable and condensed tannins (U1 to U4).

Treatment designation	Plant sources	Extraction mode	Description
Ts (U1)	Sweet chestnut	Water	Tannin formulations provided by Silvateam used at 1% (w/v).
Ts (U2)	Quebracho	Water	
Ts (U3)	Sweet chestnut + Tara pods (9:1)	Water	
		Solvent	
Ts (U4)	Sweet chestnut + quebracho (1:1)	Water	
Ts (U1) + ½ $Cu(OH)_2$			Tannin formulations at 1% (w/v) mixed with 0.045% (w/v), halved dose of the standard of copper hydroxide.
Ts (U2) + ½ $Cu(OH)_2$			
Ts (U3) + ½ $Cu(OH)_2$			
Ts (U4) + ½ $Cu(OH)_2$			
Pst (negative control)			Inoculated and untreated plants.
$Cu(OH)_2$ (standard)			0.09% (w/v) concentration (average concentration of cupric salts in commercial formulations).
½ $Cu(OH)_2$			0.045% (w/v) concentration (halved dose of the standard of copper hydroxide)
TPE			Biostimulant commercial formulate at 0.2% (w/v).
H_2O (blank control)			Water treatments used as no-biostimulant control treatment.

nins only; 1% tannins mixed with half of the standard dose (0.045%) of copper hydroxide; full standard dose (0.09%) of copper hydroxide; negative control (inoculated plants with no chemical treatments); or tropical plants extract (TPE) based, for biostimulant activity at 0.2% (w/v) (Auxym®, Italpollina S.p.A.); or blank control (water-treated plants). All combinations of these treatments are listed in Table 1.

Effects of treatments on epiphytic survival of *Pseudomonas syringae* pv. *tomato*

The *in vivo* antibacterial activity of tannins was evaluated by assessing epiphytic survival of Pst at 1, 7, 14, and 21 days post inoculation (dpi). For each experimental group, three independent replicates, each comprising nine plants, were evaluated. From each plant, one young leaflet from the latest treated apical meristem and one mature leaflet were sampled. The leaflets were transferred into a sterile plastic bag and washed with 10 mL of sterile distilled water at 180 rpm for 10 sec, using a Stomacher® 400 Circulator. The washing water (100 µL) was then plated on the KB medium and incubated at 27°C for 24 h (Balestra and Varvaro, 1998). The numbers of CFUs were counted and were related to the surface areas of the sampled leaves, using APS Asses software. This procedure was used for each experimental group.

Effects of tannins on disease incidence, severity and disease reduction

Disease severity (% DS) was assessed at 7, 14 and 21 dpi, and was scored using a 0-4 scale where, 0 = no symptoms; 1 = one leaf with at least one necrosis; 2 = two or three leaves with at least one necrosis; 3 = four or five leaves with at least one necrosis; and 4 = more than five leaves with at least one necrosis. Severity was calculated by the following equation:

$$DS\ (\%) = \frac{\Sigma \mathrm{dn}}{DN} \times 100$$

where, d = severity score; n = number of diseased plants with the same severity score; N = total number of the examined plants, and D = the greatest severity score (He *et al.,* 1983; Mekam *et al.,* 2019). Proportional disease reduction (% DR) was calculated using the following formula:

$$DR\ (\%) = \frac{S - s}{S} \times 100$$

where, S = disease severity on tomato inoculated with Pst, and s = disease severity on tomato treated with different formulations then inoculated with Pst.

Disease incidence (DI) was also calculated as a percentage of the symptomatic plants per experimental group (Steel *et al.,* 1997).

DS, DR and DI were calculated from three independent experiments, each one consisting of ten plants.

Biostimulation of seedlings

Since the seedlings were treated three times, the biostimulant activity of tannins was assessed by measuring the average leaf surface area, nitrogen balance index (NBI) relating to the ratio of chlorophyll and the flavonoids, and the biomass development expressed as the ratio of shoot to root dry weights. The TPE-based biostimulant was used as positive control (Caruso *et al.,* 2019), water-treated plants were considered as mock control, and copper-treated plants were the negative control. For each experimental group, three independent replicates were evaluated, each comprising nine plants. For each independent experiment, the plants were divided into three groups of three plants. For each group, six leaflets were harvested as follows: three young leaflets from the latest apical treated meristem and three mature leaflets. The measurements were obtained using APS Asses software, relating the total area of the leaflets and the number of leaflets sampled. For the evaluation of NBI, the measurements were performed 21 d after the treatments with tannins were applied. Data were collected between the midrib and margin of each leaf, and the NBI meter was shielded from direct sunlight. The measurements were obtained randomly from three independent experiments, each consisting of ten plants for each experimental group. Plant root and shoot dry biomass was determined by weighing the plant tissues before and after drying in a forced air oven at 80°C for 72 h (Colla *et al.,* 2015). Three independent experiments were performed and for each experiment three plants were randomly sampled.

Statistical analyses

All the data were subjected to variance analyses (ANOVA) using DSAASTAT software. Two levels of significance ($P < 0.05$, $P < 0.01$) were considered to assess the significance of the F values. When significant F values were calculated, pairwise analyses were carried out using the Tukey Honestly Significant Difference test (Tukey's test) at 0.95 or 0.99 confidence levels.

RESULTS

In vitro *effects of tannins on* Pseudomonas syringae *pv.* tomato

MIC values of chestnut, tara and quebracho extracts, and their antibacterial activities in media

All the tannin formulations reduced Pst growth, and were bactericidal to the bacterium. At the concentration used, pH was in the range of within 6 to 7, so pH did not influence the antibacterial activity. Tannins U1, U3 and U4 were the most effective forwards Pst, giving MIC values of 0.5%, while the MIC for U2 was 1%. Following these results, the concentration of 1% for tannins was used for further investigations. Table 2 shows the *in vitro* results after incorporating the tannins into KB medium at 1%. After 24 h incubation, no Pst colonies were visible under the stereomicroscope on the media containing the tannin formulations, either where the four tannins were used alone or in mixture. This indicated that their antimicrobial activity at 24 h was comparable to that of a field dose of copper hydroxide. On KB plates containing the halved dose of copper hydroxide, 8.17E + 02 CFU mL^{-1} were counted. After 48 h incubation, three of the tannin formulations (U1, U3 and U4) used alone or mixed gave complete Pst inhibition. The exception was U2 + ½ $Cu(OH)_2$ (1.06E + 03 CFU mL^{-1}), which gave antimicrobial activity comparable to the halved dose of copper hydroxide (8.17E + 02 CFU mL^{-1}). Both these experimental groups significantly reduced Pst growth compared to the negative control (6.01E + 03 CFU mL^{-1}).

Table 2. Mean numbers (n = 10) ± mean of the standard errors (SEM) of three independent replicates for each experimental group of colony forming units (CFU mL^{-1}) of *Pseudomonas syringae* pv. *tomato* from different treatments containing tannin formulations, either alone or in mixtures with half (0.045% w/v) of standard of copper hydroxide, at 24 or 48 h after inoculation in KB plates containing the substances listed in Table 1.

Treatment	log CFU mL^{-1}	
	24h	48h
Ts (U1)	TID	TID
Ts (U2)	TID	TID
Ts (U3)	TID	TID
Ts (U4)	TID	TID
Ts (U1) + ½ $Cu(OH)_2$	TID	TID
Ts (U2) + ½ $Cu(OH)_2$	TID	1.06E+03 b
Ts (U3) + ½ $Cu(OH)_2$	TID	TID
Ts (U4) + ½ $Cu(OH)_2$	TID	TID
Pst (negative control)	6.01E+03 a	6.01E+03 a
$Cu(OH)_2$ (standard)	TID	TID
½ $Cu(OH)_2$	8.17E+02 b	8.17E+02 b
(SEM)	2.34E+01	3.04E+01

TID = total inhibition determined. Different letters within the same column indicate significant differences ($P < 0.01$) according to the Tukey HSD test.

In vivo *effects of tannin treatments*

Epiphytic survival of *Pseudomonas syringae* pv. *tomato*

All of the tannin treatments were antibacterial, with activity at 1 dpi similar to that from copper hydroxide (Table 3). The tannins U4 applied alone (8.58E + 03 CFU cm^{-2}), U2 + ½ $Cu(OH)_2$ (4.65E + 03 CFU cm^{-2}) and U3 + ½ $Cu(OH)_2$ (1.02E + 04 CFU cm^{-2}), all had similar antibacterial activity. At 7 dpi, all the tannin treatments, with the exception of U2 (2.86E + 04 CFU cm^{-2}) markedly reduced epiphytic survival of Pst compared to the negative control (Pst) (4.05E + 05 CFU cm^{-2}) and their antibacterial activity was similar to that of copper hydroxide (1.32E + 05 CFU cm^{-2}). At 14 dpi, U1 applied alone (8.22E + 03 CFU cm^{-2}), U3 + ½ $Cu(OH)_2$ (2.04E + 04 CFU cm^{-2}) and U3 + ½ $Cu(OH)_2$ (1.10E + 04 CFU cm^{-2}), all reduced epiphytic survival of Pst compared to that in the negative control plants (8.41E + 04 CFU cm^{-2}), and showed antibacterial effects similar to that of copper hydroxide (4.04E + 04 CFU cm^{-2}). Tannin U2 (1.31E + 05 CFU cm^{-2}) was not effective in reducing Pst epiphytic survival. At 21 dpi, all the tannins, either alone or in mixtures, reduced Pst growth on tomato leaves compared to the negative control plants (Pst). Furthermore, U1 (6.16E + 03 CFU cm^{-2}), U2 (5.06E + 03 CFU cm^{-2}), U4 (2.33E + 03 CFU cm^{-2}), U1 + ½ $Cu(OH)_2$ (8.39E + 03 CFU cm^{-2}) and U3 + ½ $Cu(OH)_2$ (8.31E + 02 CFU cm^{-2}), all reduced the epiphytic survival of Pst much more than the standard copper hydroxide treatment (4.72E + 04 CFU cm^{-2}), while U3 used alone showed intermediate values (8.31E + 02 CFU cm^{-2}).

On mature tomato plants (Table 3) at 1 dpi, all the tannin treatments (except U2 and U3 used alone) decreased epiphytic Pst populations, and gave populations similar to that from copper hydroxide. Tannin U1 and all the mixtures with tannins and copper reduced Pst populations similarly to copper hydroxide, and more than U2 and U3 used alone. At 7 dpi, no Pst colonies were recorded after copper hydroxide treatment, and this antibacterial effect was greater than from the tannin formulations. Tannins U1 (1.80E + 04 CFU cm^{-2}), U3 (2.58E + 04 CFU cm^{-2}), U1 + ½ $Cu(OH)_2$ (4.06E + 03 CFU cm^{-2}), U3 + ½ $Cu(OH)_2$ (1.18E + 04 CFU cm^{-2}) and U4 + ½ $Cu(OH)_2$ (1.23E + 04 CFU cm^{-2}) were statistically similar among them. At 14 dpi, all the tannin treat-

Table 3. Mean numbers (n = 10) ± mean of the standard errors (SEM) of three independent replicates for each experimental group of colony forming units (Log CFU cm^{-2}) of *Pseudomonas syringae* pv. *tomato* (Pst) from different treatments containing tannins, either alone or in mixtures with half (0.045% w/v) of standard of copper hydroxide, at 1, 7, 14 and 21 d post inoculation (dpi) in tomato plants.

Treatment	Epiphytic survival (Log CFU cm^{-2})			
	1 dpi	7 dpi	14 dpi	21 dpi
Seedlings				
Ts (U1)	2.7E+04 bc	5.23E+04 c	8.22E+03 c	6.16E+03 de
Ts (U2)	2.86E+04 bc	6.25E+05 a	1.31E+05 a	5.06E+03 de
Ts (U3)	4.95E+04 bc	2.12E+04 c	2.04E+04 c	2.65E+04 cd
Ts (U4)	8.58E+03 c	1.60E+05 c	2.81E+04 bc	2.33E+03 e
Ts (U1) + ½ $Cu(OH)_2$	9.80E+04 b	9.30E+04 c	2.96E+04 bc	8.39E+03 de
Ts (U2) + ½ $Cu(OH)_2$	4.65E+03 c	2.44E+04 c	5.26E+04 bc	4.96E+04 b
Ts (U3) + ½ $Cu(OH)_2$	1.02E+04 c	6.76E+04 c	1.10E+04 c	8.31E+02 e
Ts (U4) + ½ $Cu(OH)_2$	4.43E+04 bc	5.49E+04 c	4.42E+04 bc	3.69E+04 bc
Pst (negative control)	1.79E+05 a	4.05E+05 b	8.41E+04 ab	8.95E+04 a
$Cu(OH)_2$ (standard)	3.85E+04 bc	1.32E+05 c	4.04E+04 bc	4.72E+04 bc
(S.E.M.)	1.50E+04	3.56E+02	1.19E+02	4.48E+01
P value	$P < 0.01$	$P < 0.01$	$P < 0.01$	$P < 0.01$
Mature plants				
Ts (U1)	2.50E+04 c	1.80E+04 c	1.74E+04 ab	1.93E+04 b
Ts (U2)	9.50E+04 b	1.02E+05 ab	7.63E+03 bc	8.32E+02 b
Ts (U3)	9.07E+04 b	2.58E+04 c	1.30E+03 c	3.61E+04 b
Ts (U4)	4.87E+04 bc	5.14E+04 bc	8.11E+03 bc	3.66E+02 b
Ts (U1) + ½ $Cu(OH)_2$	1.38E+04 c	4.06E+03 c	755E+02 c	5.84E+04 b
Ts (U2) + ½ $Cu(OH)_2$	1.73E+03 c	4.41E+04 bc	5.14E+02 c	1.75E+04 b
Ts (U3) + ½ $Cu(OH)_2$	2.55E+04 c	1.18E+04 c	6.78E+02 c	1.70E+03 b
Ts (U4) + ½ $Cu(OH)_2$	1.47E+04 c	1.23E+04 c	5.45E+02 c	5.33E+03 b
Pst (negative control)	2.03E+05 a	1.26E+05 a	2.36E+04 a	1.45E+05 a
$Cu(OH)_2$ (standard)	8.73E+01 c	0.00E+00 d	5.37E+02 c	1.17E+02 b
(S.E.M.)	1.13E+04	1.16E+04	1.95E+02	1.26E+03
P value	$P < 0.01$	$P < 0.01$	$P < 0.01$	$P < 0.01$

Seedlings were treated 5, 10 and 15 d before inoculation, and mature plants were treated once at 24 h before inoculation. Treatments were with substances listed in Table 1. The mean values in each column followed by different letters are significantly different ($P < 0.01$) according to the Tukey HSD test.

ments, with the exception of U1 (1.74E + 04 CFU cm^{-2}), promptly contained Pst multiplication compared to that in the negative control plants (Pst) and showed antibacterial effects similar to that from copper hydroxide. Tannins U2 and U4 applied alone showed intermediate values and were similar among them. At 21 dpi, all the tannin treatments pointed out an antibacterial activity statistically similar to that in the positive control (1.17E + 02 CFU cm^{-2}).

Disease severity and reduction

Table 4 presents data of the progress of bacterial speck as mean proportions (%) of disease severity (DS) and disease reduction (DR). On seedlings, at 7 dpi, the tannins U1 (mean DS = 16.7%), U2 (20.8%), U4 (15.8%), U1 + ½ $Cu(OH)_2$ (24.2%) and U3 + ½ $Cu(OH)_2$ (12.5%), all reduced the DS compared to that in the negative control (53.3%). At 14 and 21 dpi all the tannin treatments reduced mean DS values (25-40% at 14 dpi and 32-50% at 21 dpi) compared to the negative controls (75% at 14 dpi and 87% at 21 dpi). The tannin treatments generally reduced the mean DR values, similarly to that from copper hydroxide. The exceptions were the U4 + ½ $Cu(OH)_2$ and U2 + ½ $Cu(OH)_2$ treatments, which gave mean DRs of 47.4% at 7 dpi and 37.3% at 21 dpi, when the DR values were significantly less than from copper hydroxide (77.9% at 7 dpi and 59.0% at 21 dpi).

On mature plants (Table 4), at 7 dpi, all the tannin treatments gave similar mean DS values (20 to 36%),

Table 4. Mean numbers (n = 10) ± mean of the standard errors (SEM) of three independent replicates for each experimental group of bacterial speck disease severity (DS) and reduction (DR) after different treatments containing tannins, either alone or in mixtures with half (0.045% w/v) of standard of copper hydroxide, at 7, 14 and 21 d post inoculation (dpi) in tomato plants.

Treatment	7 dpi		14 dpi		21 dpi	
	DS (%)	DR (%)	DS (%)	DR (%)	DS (%)	DR (%)
Seedlings						
Ts (U1)	16.67 b	70.58 ab	27.50 b	63.59 ab	40.00 b	54.06 ab
Ts (U2)	20.83 b	61.34 ab	36.67 b	51.19 ab	47.50 b	45.27 ab
Ts (U3)	26.67 ab	51.42 ab	39.17 b	48.31 ab	49.17 b	43.44 ab
Ts (U4)	15.83 b	70.92 ab	25.00 b	66.94 a	32.50 b	62.65 a
Ts (U1) + ½ $Cu(OH)_2$	24.17 b	54.79 ab	31.67 b	63.59 ab	35.83 b	58.64 a
Ts (U2) + ½ $Cu(OH)_2$	25.83 ab	53.64 ab	40.83 b	45.70 b	54.17 b	37.27 b
Ts (U3) + ½ $Cu(OH)_2$	12.50 b	53.64 a	27.50 b	63.25 ab	35.83 b	58.69 a
Ts (U4) + ½ $Cu(OH)_2$	28.33 ab	47.44 b	40.83 b	45.81 b	50.00 b	42.57 ab
Pst (negative control)	53.33 a	…	75.00 a	…	86.67 a	…
$Cu(OH)_2$ (standard)	12.50 b	77.94 a	20.83 b	65.75 ab	35.83 b	59.00 a
(S.E.M.)	5.75	7.15	4.54	5.41	4.98	5.45
P value	*P* < 0.01	*P* < 0.05	*P* < 0.01	*P* < 0.05	*P* < 0.01	*P* < 0.05
Mature plants						
Ts (U1)	20.83 bc	62.85 ab	42.50 b	39.51	58.33 b	29.49
Ts (U2)	36.67 b	34.84 c	49.17 b	29.63	60.00 b	27.05
Ts (U3)	24.17 bc	56.68 abc	39.17 b	44.20	52.50 b	36.43
Ts (U4)	29.17 bc	47.89 bc	43.33 b	38.02	51.67 b	37.56
Ts (U1) + ½ $Cu(OH)_2$	23.33 bc	58.50 abc	35.00 b	50.00	50.83 b	38.51
Ts (U2) + ½ $Cu(OH)_2$	34.17 b	38.72 c	47.50 b	32.10	59.17 b	28.27
Ts (U3) + ½ $Cu(OH)_2$	23.33 bc	58.35 abc	41.67 b	40.74	54.17 b	34.61
Ts (U4) + ½ $Cu(OH)_2$	24.17 bc	56.90 abc	37.50 b	46.54	55.83 b	32.44
Pst (negative control)	55.83 a	…	70.00 a	…	82.50 a	…
$Cu(OH)_2$ (standard)	13.33 c	76.21 a	35.00 b	50.37	46.67 b	43.72
(S.E.M.)	3.60	5.38	3.94	4.98	4.66	4.85
P value	*P* < 0.01	*P* < 0 *P* < 0.05	*P* < 0.01	*P* < 0.05	*P* < 0.01	*P* < 0.05

Seedlings were treated 5, 10 and 15 d before inoculation, and mature plants were treated once at 24 h before inoculation. Treatments were with substances listed in Table 1. DS was calculated by using the following formula: DS (%) = 100 × [(number of plants in class 1 × 1) + (number of plants in class 2 × 2) + (number of plants in class 3 × 3) + (number of plants in class 4 × 4)] / (total number of plants in the treatment × 4). DR was calculated using the following formula: DR (%) = 100 × (DS of control – DS of treatment) / DS of control. The mean values in each column followed by different letters are significantly different ($P < 0.01$ and $P < 0.05$) according to the Tukey HSD test.

which were significantly less than the negative control (mean = 55.8%). The tannins U1 (mean DS = 20.8%), U3 (24.2%), U4 (29.2%), U1 + ½ $Cu(OH)_2$ (23.3%), U3 + ½ $Cu(OH)_2$ (23.3%) and U4 + ½ $Cu(OH)_2$ (24.2%), all reduced mean DS percentages in a manner similar to copper hydroxide (Mean DS = 13.3%). U2 (mean DS = 36.7%) and U2 + ½ $Cu(OH)_2$ (34.2%) did not protect the plants as much as copper hydroxide (13.3%). At 14 and 21 dpi, all the tannin treatments (mean DS 35 to 49% at 14 dpi and 50 to 60 % at 21 dpi) gave similar DS to copper hydroxide (mean DS = 35.0% at 7 dpi and 46.7 at 14 dpi). These treatments reduced DS compared to negative controls, which gave mean DS of 70% at 14 dpi and 86% at 21 dpi. Mean DR proportions at 7 dpi from the tannin formulations (56 to 62%) were similar to those from copper hydroxide (mean = 76.2 ± 5.4%), with the exception of U2 (34.8%), U4 (47.9%) and U2 + ½ $Cu(OH)_2$ (38.7%). No statistically significant differences in mean DR proportions were detected at 14 and 21 dpi.

Disease incidence

Table 5 shows the incidence of the disease in seedlings and mature plants.

On seedlings at 7 dpi, U1 (Mean DI = 53.3%), U4 (53.3%) and U3 + ½ $Cu(OH)_2$ (33.3%), were able to

Table 5. Mean numbers (n = 10) ± mean of the standard errors (SEM) of three independent replicates for each experimental group of bacterial speck disease incidence (DI) after different treatments containing tannins, either alone or in mixtures with half (0.045% w/v) of standard of copper hydroxide, at 7, 14 and 21 d post inoculation (dpi) in tomato plants.

Treatment	Disease Incidence (%)					
	7 dpi		14 dpi		21 dpi	
	Seedlings	Mature plants	Seedlings	Mature plants	Seedlings	Mature plants
Ts (U1)	53.33 bc	80.00 ab	80.00 ab	96.67 ab	83.33 ab	96.67 ab
Ts (U2)	73.33 abc	100 a	90.00 ab	100.00 a	90.00 ab	100.00 a
Ts (U3)	63.33 abc	80.00 ab	76.67 ab	100.00 a	86.67 ab	100.00 a
Ts (U4)	53.33 bc	96.67 a	66.67 b	100.00 a	70.00 b	100.00 a
Ts (U1) + ½ $Cu(OH)_2$	73.33 abc	83.33 ab	80.00 ab	100.00 a	83.33 ab	100.00 a
Ts (U2) + ½ $Cu(OH)_2$	60.00 abc	96.67 a	90.00 ab	100.00 a	90.00 ab	100.00 a
Ts (U3) + ½ $Cu(OH)_2$	33.33 cd	80.00 ab	63.33 b	96.67 ab	83.33 ab	100.00 a
Ts (U4) + ½ $Cu(OH)_2$	76.67 ab	80.00 ab	86.67 ab	96.67 ab	90.00 ab	96.67 ab
Pst (negative control)	100.00 a	100.00 a	100.00 a	100.00 a	100.00 a	100.00 a
$Cu(OH)_2$ (standard)	36.66 bc	53.33 b	63.33 b	80.00 b	70.00 b	86.67 b
(S.E.M.)	8.88E-02	6.41E-02	5.68E-02	3.65E-02	5.87E-02	2.58E-02
P value	$P < 0.01$	$P < 0.01$	$P < 0.01$	$P < 0.05$	$P < 0.05$	$P < 0.05$

Seedlings were treated 5, 10 and 15 d before inoculation, and mature plants were treated once 24 h before inoculation. Treatments were with substances listed in Table 1. dpi = days post inoculation; DI was calculated as the percentage of plants with at least one symptom /10 (total number of plants per experimental group). Different letters within the same column indicate significant differences ($P < 0.01$ and $P < 0.05$) according to the Tukey HSD test.

reduce mean disease incidence compared to the negative control (Pst). At 14 dpi, U4 (66.7%) and U3 + ½ $Cu(OH)_2$ (63.3%) reduced the disease incidence compared to negative control (Pst), while all the tannin treatments did not show significant reduction compared to the negative control and the standard (mean DI = 63.3%). At 21 dpi, only U4 used alone (Mean DI = 70.0%) reduced disease incidence compared to the negative control (Pst), while all the tannin treatments (83 to 90%) did not give significant reductions compared to the negative control and the standard (Mean DI = 70.0%).

On mature plants, at 7, 14 and 21 dpi, none of the tannin treatments reduce disease incidence compared to the negative control (Pst).

Biostimulant effects of tannins on seedling tomato plants

Leaf development

Table 6 shows the effects of the different treatments on seedling tomato plants, expressed as average leaf surface area (cm^2). After treatment with tannins, the sampled tomato leaves showed no symptoms of burning or bleaching. Nevertheless, the average leaf areas recorded for plants receiving the tannin formulations were less compared to the water controls. At 1 dpi, no significant differences were recorded, but at 7 and 14 dpi all the tannin and copper hydroxide treatments gave significantly less mean leaf areas than the TPE (the positive control) and water treatments. At 21 dpi, U1 applied alone (mean leaf area = 15.8 cm^2) increased the leaf area surface compared to copper hydroxide (11.8 cm^2) and the negative control (11.3 cm^2), but not compared to water control (13.5 cm^2). At 7, 14 and 21 dpi, TPE gave a biostimulant effect on aerial biomass development of the plants.

Nitrogen Balance Indices (NBI)

Table 7 presents the mean NBI values after treatments of plants, as general indices of their state of health. All the tannin formulations (mean NBI = 19.5 to 24.3) did not increase the NBI values compared to water treatment (22.0), but the mean NBI index of plants treated with tannin formulations increased only compared to the negative control (8.4).

Shoots development

Table 7 shows the results for biostimulant effects of the different treatments on plant biomass expressed as mean shoot dry weights (g) at 21 dpi. The dry weight of

Table 6. Mean leaf surface areas (n = 10) ± mean of the standard errors (SEM) of three independent replicates for each experimental group after different treatments containing tannins, either alone or in mixtures with half (0.045% w/v) of standard of copper hydroxide, at 1, 7, 14 and 21 d post inoculation (dpi) in seedling tomato plants.

Treatment	Average leaf surface area (cm^2)			
	1 dpi	7 dpi	14 dpi	21 dpi
Ts (U1)	11.51	14.97 c	13.09 c	15.84 b
Ts (U2)	14.14	12.98 c	12.62 c	14.50 bc
Ts (U3)	10.99	13.89 c	11.66 c	14.37 bc
Ts (U4)	9.07	11.83 c	12.73 c	11.05 c
Ts (U1) + ½ $Cu(OH)_2$	10.44	13.15 c	12.85 c	12.88 bc
Ts (U2) + ½ $Cu(OH)_2$	8.68	11.47 c	13.99 c	14.76 bc
Ts (U3) + ½ $Cu(OH)_2$	8.12	10.40 c	11.57 c	13.25 bc
Ts (U4) + ½ $Cu(OH)_2$	9.62	13.15 c	12.10 c	11.60 c
Pst (negative control)	8.93	12.41 c	12.11 c	11.27 c
$Cu(OH)_2$ (standard)	9.19	12.60 c	12.23 c	11.78 c
TPE (positive control)	14.33	26.31 a	25.15 a	18.72 a
H_2O (blank control)	10.44	21.01 b	20.01 b	13.51 bc
(S.E.M.)	1.347	1.212	1.148	0.811
P value	$P < 0.01$	$P < 0.01$	$P < 0.01$	$P < 0.01$

Table 7. Mean values of Nitrogen Balance Indices (n = 40) and dry weight of shoots (n = 10) ± mean of the standard errors (SEM) of three independent replicates for each experimental group after different treatments containing tannins, either alone or in mixtures with half (0.045% w/v) of standard of copper hydroxide, at 21 d post inoculation (dpi) in seedling tomato plants.

Treatment	NBI (DUALEX)	Dry weight of shoots (g)
Ts (U1)	19.54 c	1.130 b
Ts (U2)	19.60 c	0.913 bc
Ts (U3)	20.31 c	0.837 bc
Ts (U4)	24.28 b	0.952 bc
Ts (U1) + ½ $Cu(OH)_2$	21.74 bc	1.020 bc
Ts (U2) + ½ $Cu(OH)_2$	20.68 c	0.913 bc
Ts (U3) + ½ $Cu(OH)_2$	21.79 bc	0.978 bc
Ts (U4) + ½ $Cu(OH)_2$	21.65 bc	0.912 bc
Pst (negative control)	8.39 d	0.516 c
$Cu(OH)_2$ (standard)	20.51 c	0.597 c
TPE (positive control)	26.25 a	1.560 a
H_2O (blank control)	21.98 bc	0.907 bc
(S.E.M.)	0.703	0.078
P value	$P < 0.01$	$P < 0.01$

Seedlings were treated three times 5, 10 and 15 d before inoculation. Treatments were with substances listed in Table 1. Different letters within each column indicate significant differences ($P < 0.01$) according to the Tukey HSD test.

shoots of U1 treated plants (mean = 1.13 g) was similar to the water control (0.91 g), but greater than for copper hydroxide treated plants (0.60 g) and the negative control plants (0.52 g), while the rest tannin treatments (means = 0.84 to 1.02 g) did not show significant differences compared to water, copper and negative control plants. The TPE treatment increased the shoot dry weight. Statistically significant differences in mean root dry weights were not detected (data not shown).

DISCUSSION

This study has demonstrated that condensed and hydrolysable tannins exhibited antimicrobial activity against Pst, as shown by their *in vitro* effectiveness to completely inhibit Pst growth 24 h after inoculation. The chestnut, tara, and quebracho tannins prevented *in vitro* growth of Pst. Several studies have evaluated the antibacterial activity of hydrolysable and condensed tannins towards different bacteria. Gallotannins (hydrolysable) obtained from tara pod extracts and their hydrolysis product have been assessed for activity against gram-positive and gram-negative bacteria (including *Staphylococcus aureus* and *Pseudomonas fluorescens*) (Aguilar-Galvez *et al.*, 2014)antioxidant activity, antimicrobial activity (AA. Previous research has shown that crude tannin extracts more effectively inhibited pathogenic bacteria than pure molecules (Akhtar *et al.*, 2015). For this reason, the present study concentrated on four tannin formulations instead of their components. Few evaluations of crude tannin extracts from chestnut, quebracho and tara plant matrices against phytopathogenic bacteria have been carried out, but many studies have assessed anti-bacterial activity of these tannins. Elizondo *et al.* (2010) tested quebracho and chestnut tannins, applied alone or mixed, for activity against toxinotypes of *Clostridium perfringens*. In the present study, the highest MIC values for the quebracho tannins was 0.12%, while the lowest one (0.015%) was observed for chestnut tannins. In our study we also obtained a similar trend, observing MIC values of 1% for U2 (quebracho tannins) and 0,5% for U1 (chestnut tannins), while the MIC values of the chestnut and quebracho tannins were 0.5% for both the U3 (90:10) and U4 (50:50). It is likely that the greater MIC values resulted from the use of the tannin extracts towards a gram-negative bacterium. This bacterium could be resistant to tannins because it possesses a lipopolysaccharide cell membrane which provides strength and prevents the cell penetration of bioactive compounds (Puupponen-Pimiä *et al.*, 2005). Elizondo *et al.* (2010) demonstrated that chestnut tannins

extract was more efficient than quebracho. Our study results are similar, since U1 and U3, chestnut-based tannins, were more effective in controlling Pst than U2. Elizondo *et al.* (2010) observed that the antibacterial effects of quebracho tannins increased by up to 20 times after adding 25% of chestnut tannins, and by up to 85 times with 75% of chestnut tannins. They concluded that the antibacterial activity of the mixed products was approx. 50 times greater than quebracho tannins applied alone. Results from the our study were similar, since U4, a mixture of 50% quebracho tannins and 50% of chestnut tannins, showed similar antibacterial activity to U1. During the *in vitro* assay by incorporating the tannins into the KB medium, we observed that no Pst growth was recorded at 24 and 48 h after incubation, except for U2 mixed with the 50% dose of copper hydroxide, where Pst CFUs were present after 48 h incubation. Our hypothesis is that this may be related to copper precipitation, because of the chelation activity of tannins. Some studies have reported that chelation ability is strongly related to the molecular weight of condensed tannins (Yoneda and Nakatsubo, 1998; Karamać, 2009). Since U2 is composed of condensed tannins, it is likely that their structures chelated copper hydroxide, thus inactivating copper hydroxide and tannins, allowing Pst growth.

For the antibacterial *in vivo* trials, tannin treatments reduced Pst epiphytic survival and disease severity (DS) compared to negative control treatments (Pst), while the disease incidence (DI) was not influenced by the tannin applications. Karamanoli *et al.* (2011) reducing its bioavailability to plant-associated bacteria. In response to limited iron levels, most bacteria produce siderophores to acquire needed iron quantities. The amount of phenolic compounds detected in methanolic washings of leaves of different plant species varied greatly, being nearly sevenfold higher in *Viburnum tinus* than in *Phaseolus vulgaris*. In species with high levels of total phenolics (e.g. *Pelargonium hortorum* suggested that the antibacterial activity of tannins was due to their ability to chelate iron, reducing its bioavailability to phytopathogenic bacteria. Although the biological role of tannins is mainly attributed to their ability to bind proteins (Smith *et al.*, 2005), Karamanoli *et al.* (2011) concluded that iron sequestration by tannins was a dominant factor inhibiting bacterial growth on host plant leaves. This iron chelating ability has been also supported by Engels *et al.* (2009). We therefore conclude that the antibacterial activity of tannins towards Pst could be an indirect effect from their capacity to prevent the pathogen from taking up some essential nutrients, such as metal ions.

Other studies have evaluated tannins extract for effects on plant pathogenic bacteria. For example, Vu *et al.* (2013) evaluated the effects of diluted tannins from *Sedum takesimense* corresponding to concentrations of 1 and 0.5%, on *R. solanacearum*. At 14 dpi they observed dose-dependent disease reductions, of 78% from 1% and 54% from 0.5%. Vu *et al.* (2017) tested tannins extract from *S. baccatum* towards *R. solanacearum* at concentrations of 0.1% and 0.2%, demonstrating disease reduction of 63% from 0.1% and 83% from 0.2%, at 14 dpi. In the present study, disease reductions of 45 to 63% in seedlings and 30 to 50% in mature plants were also recorded at 14 dpi. Despite the fact that in this study, and in those cited above, tannins have been shown to have antimicrobial activity, it is highly reductive, to make comparisons between active tannin concentrations. Firstly, tannin concentrations in crude extracts change depending on genetic and environmental factors applying to different tannin-producing plant species. Secondly, these concentrations can also vary depending on the methods of extraction and fractioning used to obtain the pure molecules (Nader *et al.,* 2010).

Although tannins have been studied as biostimulators of plant roots (Bargiacchi *et al.*, 2013), in the present study biostimulant effects on tomato plants were not detected, as the data obtained were similar to those from water-treated plants. Nevertheless, it is important to determine if the tannin treatments were not toxic to tomato plants.

CONCLUSIONS

The results obtained in this research have highlighted the possibility of using natural compounds (tannins) for reducing Pst populations on tomato plants, as a "green" strategy that is similarly efficacious as cupric salts for the control of tomato bacterial speck. Further research is required, including evaluation of possible induction of defensive genes and defence metabolites (e.g. salicylic acid) in tomato plants, and the production of reactive oxygen species (ROS).

This research has highlighted innovative crop protection strategies aimed assess the use of natural products for management of bacterial plant diseases. This will assist reduction of the use of cupric salts in agricultural disease and pest control programmes, minimising potential impacts of these materials on human and environmental health.

LITERATURE CITED

Aguilar-Galvez A., Noratto G., Chambi F., Debaste F., Campos D., 2014. Potential of tara (*Caesalpinia spi-*

nosa) gallotannins and hydrolysates as natural antibacterial compounds. *Food Chemistry* 156: 301–304.

Akhtar S., Ismail T., Fraternale D., Sestili P., 2015. Pomegranate peel and peel extracts: chemistry and food features. *Food Chemistry* 174: 417–425.

Arbenz A., Avérous L., 2016. Tannins: a resource to elaborate aromatic and biobased polymers. *Biodegradable and Biobased Polymers for Environmental and Biomedical Applications*: 97–148.

Aroso I.M., Araújo A.R., Pires R.A., Reis R.L., 2017. Cork: current technological developments and future perspectives for this natural, renewable, and sustainable material. *ACS Sustainable Chemistry and Engineering* 5: 11130–11146.

Bacelo H.A.M., Santos S.C.R., Botelho C.M.S., 2016. Tannin-based biosorbents for environmental applications - A review. *Chemical Engineering Journal* 303: 575–587.

Baka Z., Rashad Y., 2016. Alternative control of early blight disease of tomato using the plant extracts of *Acacia nilotica*, *Achillea fragrantissima* and *Calotropis procera*. *Phytopathologia Mediterranea* 55: 121–129.

Balestra G.M., Varvaro L., 1998. Seasonal fluctuations in kiwifruit phylloshere. *Journal of Plant Pathology* 80: 151–156.

Barbehenn R., Constabel C., 2011. Tannins in plant-herbivore interactions. *Phytochemistry* 72: 1551–1565.

Bargiacchi E., Costa G., Della Croce C., Foschi L., Pampana S., … Rizzi G., 2004. Method for obtaining organic acidifying solutions and fertilizers using organic extracts from aqueous wood leaching processes Eur. Pat. EP1464635, 24-03-2010, priority: IT2003MI00640 2003-03-31. : 1–12.

Bargiacchi E., Miele S., Romani A., Campo M., 2013. Biostimulant activity of hydrolyzable tannins from sweet chestnut (*Castanea sativa* Mill.). *Acta Horticulturae* 1009: 111–116.

Bargiacchi E., Campo M., Romani A., Milli G., Miele S., 2017. Hydrolysable tannins from sweet chestnut (*Castanea sativa* Mill.) to improve tobacco and food/feed quality. Note 1: fraction characterization, and tobacco biostimulant effect for gall-nematode resistance. *AIMS Agriculture and Food* 2: 324–338.

Biancalani C., Cerboneschi M., Tadini-Buoninsegni F., Campo M., Scardigli A., … Tegli S., 2016. Global analysis of type three secretion system and quorum sensing inhibition of *Pseudomonas savastanoi* by polyphenols extracts from vegetable residues. *PLoS ONE* 11: 1–21.

Caruso G., De-Pascale S., Cozzolino E., Cuciniello A., Cenvinzo V., … Rouphael Y., 2019. Yield and nutritional quality of vesuvian piennolo tomato PDO as affected by farming system and biostimulant application. *Agronomy* 9: 505–517.

Colla G., Rouphael Y., Di-Mattia E., El-Nakhel C., Cardarelli M., 2015. Co-inoculation of *Glomus intraradices* and *Trichoderma atroviride* acts as a biostimulant to promote growth, yield and nutrient uptake of vegetable crops. *Journal of the Science of Food and Agriculture* 95: 1706–1715.

De Hoyos-Martínez P.L., Merle J., Labidi J., Charrier-El Bouhtoury F., 2019. Tannins extraction: a key point for their valorization and cleaner production. *Journal of Cleaner Production* 206: 1138–1155

Devash Y., Okon Y., Henis Y., 1980. Survival of *Pseudomonas* tomato in soil and seeds. *Journal of Phytopathology* 99: 175–185.

Elizondo A.M., Mercado E.C., Rabinovitz B.C., Fernandez-Miyakawa M.E., 2010. Effect of tannins on the *in vitro* growth of *Clostridium perfringens*. *Veterinary Microbiology* 145: 308–314.

Engels C., Knödler M., Zhao Y.Y., Carle R., Gänzle M.G., Schieber A., 2009. Antimicrobial activity of gallotannins isolated from mango (*Mangifera indica* L.) kernels. *Journal of Agricultural and Food Chemistry* 57: 7712–7718.

Francesconi S., Steiner B., Buerstmayr H., Lemmens M., Sulyok M., Balestra G.M., 2020. Chitosan hydrochloride decreases *Fusarium graminearum* growth and virulence and boosts growth, development and systemic acquired resistance in two durum wheat genotypes. *Molecules* 25: 4752. doi:10.3390/molecules25204752.

Giovanardi D., Ferrari M., Stefani E., 2015. Seed trasmission of *Acidovorax citrulli*: implementazion of detection in watermelon seeds and development of disinfection methods. *Proceedings of the 7th Congress on Plant Protection. Plant Protection Society of Serbia*, 71–75.

Giovando S., Pizzi A., Pasch H., Pretorius N., 2013. Structure and oligomers distribution of commercial tara (*Caesalpina spinosa*) hydrolysable tannin. *Pro Ligno* 9: 22–31.

Gruda N., 2005. Impact of environmental factors on product quality of greenhouse vegetables for fresh consumption. *Critical Reviews in Plant Sciences* 24: 227–247.

Haslam E., Lilley T.H., Cai Y., Martin R., Magnolato D., 1988. Traditional herbal medicines. *Planta Medica* 55: 1–8.

He L., Sequeira L., Kelman A., 1983. Characteristics of strains of *Pseudomonas solanacearum* from China. *Plant Disease* 67: 1357–1361.

Hernes P.J., Hedges J.I., 2004. Tannin signatures of barks, needles, leaves, cones, and wood at the molecular

level. *Geochimica et Cosmochimica Acta* 68: 1293–1307.

Hümmer W., Schreier P., 2008. Analysis of proanthocyanidins. *Molecular Nutrition and Food Research* 52: 1381–1398.

Kalleli F., Abid G., Salem I. Ben, Boughalleb-M'Hamdi N., M'Hamdi M., 2020. Essential oil from fennel seeds (*Foeniculum vulgare*) reduces fusarium wilt of tomato (*Solanum lycopersicon*). *Phytopathologia Mediterranea* 59: 63–76.

Karamać M., 2009. Chelation of Cu(II), Zn(II), and Fe(II) by tannin constituents of selected edible nuts. *International Journal of Molecular Sciences* 10: 5485–5497.

Karamanoli K., Bouligaraki P., Constantinidou H.I.A., Lindow S.E., 2011. Polyphenolic compounds on leaves limit iron availability and affect growth of epiphytic bacteria. *Annals of Applied Biology* 159: 99–108.

Katagiri F., Thilmony R., He S.Y., 2002. The *Arabidopsis thaliana-Pseudomonas syringae* Interaction. *The Arabidopsis Book* 1: e0039.

King E.O., Ward M.K., Raney D.E., 1954. Two simple media for the demonstration of pyocyanin and fluorescin. *The Journal of Laboratory and Clinical Medicine* 44: 301–307.

La Torre A., Iovino V., Caradonia F., 2018. Copper in plant protection: current situation and prospects. *Phytopathologia Mediterranea* 57: 201–236.

Lochab B., 2014. Naturally occurring phenolic sources: monomers and polymers. *RSC Advances* 4: 21712-21753. doi:10.103.

Marrone P.G., 2019. Pesticidal natural products – status and future potential. *Pest Management Science* 75: 2325–2340.

McCarter S.M., Jones J.B., Gitaitis R.D., Smitley D.R., 1983. Survival of *Pseudomonas syringae* pv. *tomato* in association with tomato seed, soil, host tissue, and epiphytic weed hosts in Georgia. *Phytopathology* 73: 1393–1398.

Mekam P.N., Martini S., Nguefack J., Tagliazucchi D., Mangoumou G.N., Stefani E., 2019. Activity of extracts from three tropical plants towards fungi pathogenic to tomato (*Solanum lycopersicum*). *Phytopathologia Mediterranea* 58: 573–586.

Molino S., Fernández-Miyakawa M., Giovando S., Rufián-Henares J.Á., 2018. Study of antioxidant capacity and metabolization of quebracho and chestnut tannins through *in vitro* gastrointestinal digestion-fermentation. *Journal of Functional Foods* 49: 188–195.

Nader T., Coppede J., Amaral L., Facchin A., Pereira A., Ferreira L., 2010. Avaliação *in vitro* da eficácia de extratos de plantas medicinais do cerrado frente *Staphylococcus aureus* isolado de diferentes fontes de propriedades leiteiras. *Arquivod do Instituto Biològico* 77: 429-433.

Pietrarelli L., Balestra G.M., Varvaro L., 2006. Effects of simulated rain on *Pseudomonas syringae* pv. *tomato* populations on tomato plants. *Journal of Plant Pathology* 88: 245–251.

Pizzi A., Pasch H., Rode K., Giovando S., 2009. Polymer structure of commercial hydrolyzable tannins by matrix-assisted laser desorption/ionization-time-of-flight mass spectrometry. *Journal of Applied Polymer Science* 113: 3847–3859.

Puupponen-Pimiä R., Nohynek L., Hartmann-Schmidlin S., Kähkönen M., Heinonen M., … Oksman-Caldentey K.-M., 2005. Berry phenolics selectively inhibit the growth of intestinal pathogens. *Journal of Applied Microbiology* 98: 991–1000.

Quattrucci A., Balestra G.M., 2009. Antibacterial activity of natural extracts in *Pseudomonas syringae* pv. *tomato* control. *Acta Horticulturae* 808: 339–341.

Quattrucci A., Ovidi E., Tiezzi A., Vinciguerra V., Balestra G.M., 2013. Biological control of tomato bacterial speck using *Punica granatum* fruit peel extract. *Crop Protection* 46: 18–22.

Quideau S., Deffieux D., Douat-Casassus C., Pouységu L., 2011. Plant polyphenols: chemical properties, biological activities, and synthesis. *Angewandte Chemie - International Edition* 50: 586–621.

Radebe N., Rode K., Pizzi A., Giovando S., Pasch H., 2013. MALDI-TOF-CID for the microstructure elucidation of polymeric hydrolysable tannins. *Journal of Applied Polymer Science* 128: 97–107.

Renčo M., Sasanelli N., Papajová I., Maistrello L., 2012. Nematicidal effect of chestnut tannin solutions on the potato cyst nematode *Globodera rostochiensis* (Woll.) Barhens. *Helminthologia* 49: 108–114.

Schneider R.W., Grogan R.G., 1976. Bacterial speck of tomato: sources of inoculum and establishment of a resident population. *Phytopathology* 67: 388–394.

Smith A.H., Zoetendal E., Mackie R.I., 2005. Bacterial mechanisms to overcome inhibitory effects of dietary tannins. *Microbial Ecology* 50: 197–205.

Steel R.G.D., Dickey D.A., Torrie J.H., 1997. *Principles and procedures of statistics: a biometrical approach*. New York : McGraw-Hill, New York, 666 pp.

Varvaro L., Fanigliulo R., Babelegoto N.M., 1993. Transmission electron microscopy of susceptible and resistant tomato leaves following infection with *Pseudomonas syringae* pv. *tomato*. *Journal of Phytopathology* 138: 265–273.

Venter P.B., Senekal N.D., Amra-Jordaan M., Bonnet S.L., Westhuizen J.H. Van der., 2012. Analysis of commer-

cial proanthocyanidins. Part 2: An electrospray mass spectrometry investigation into the chemical composition of sulfited quebracho (*Schinopsis lorentzii* and *Schinopsis balansae*) heartwood extract. *Phytochemistry* 78: 156–169.

Vu T.T., Kim J.C., Choi Y.H., Choi G.J., Jang K.S., … Lee S.W., 2013. Effect of gallotannins derived from *Sedum takesimense* on tomato bacterial wilt. *Plant Disease* 97: 1593–1598.

Vu T.T., Kim H., Tran V.K., Vu H.D., Hoang T.X., … Kim J.C., 2017. Antibacterial activity of tannins isolated from *Sapium baccatum* extract and use for control of tomato bacterial wilt. *PLoS ONE* 12: 1–12.

Vurro M., Miguel-Rojas C., Pérez-de-Luque A., 2019. Safe nanotechnologies for increasing the effectiveness of environmentally friendly natural agrochemicals. *Pest Management Science* 75: 2403–2412.

Yoneda S., Nakatsubo F., 1998. Effects of the hydroxylation patterns and degrees of polymerization of condensed tannins on their metal-chelating capacity. *Journal of Wood Chemistry and Technology* 18: 193–205.

Phytopathologia Mediterranea
The international journal of the
Mediterranean Phytopathological Union

Firenze University Press
www.fupress.com/pm

Research Papers

Infection of papaya (*Carica papaya*) by four powdery mildew fungi

Diána SERESS[1], Gábor M. KOVÁCS[1,2], Orsolya MOLNÁR[1], Márk Z. NÉMETH[1,*]

[1] *Plant Protection Institute, Centre for Agricultural Research, Eötvös Loránd Research Network (ELKH), 1525 Budapest, P.O. Box 102, Hungary*
[2] *Eötvös Loránd University, Institute of Biology, Department of Plant Anatomy, Budapest, Hungary*
*Corresponding author. E-mail: nemeth.mark@atk.hu

Summary. Papaya (*Carica papaya* L.) is an important fruit crop in many tropical and subtropical countries. Powdery mildew commonly affects this host, causing premature leaf loss, reduced yields and poor fruit quality. At least fifteen different fungi have been identified as the causal agents of papaya powdery mildew. Powdery mildew symptoms were detected on potted papaya plants growing in two locations in Hungary. This study aimed to identify the causal agents. Morphology of powdery mildew samples was examined, and sequences of two loci were used for molecular taxonomic identifications. Only anamophs were detected in all samples, and four morphological types were distinguished. Most samples had *Pseudoidium* anamorphs, while some were of the *Fibroidium* anamorph. Based on morphology and molecular taxonomy, the *Fibroidium* anamorph was identified as *Podosphaera xanthii*. The *Pseudoidium* anamorphs corresponded to three different *Erysiphe* species: *E. cruciferarum*, *E. necator* and an unidentified *Erysiphe* sp., for which molecular phylogenetic analyses showed it belonged to an unresolved species complex of *E. malvae*, *E. heraclei* and *E. betae*. Infectivity of *P. xanthii* and *E. necator* on papaya was verified with cross inoculations. A review of previous records of powdery mildew fungi infecting papaya is also provided. *Podosphaera xanthii* was known to infect, and *E. cruciferarum* was suspected to infect *Carica papaya*, while *E. necator* was recorded on this host only once previously. No powdery mildew fungus belonging to the *E. malvae*/*E. heraclei*/*E. betae* species complex is known to infect papaya or any other plants in the Caricaceae, so the unidentified *Erysiphe* sp. is a new record on papaya and the Caricaceae. This study indicates host range expansion of this powdery mildew fungus onto papaya.

Keywords. *Carica*, *Erysiphales*, *Erysiphe necator,* host range expansion, phylogenetic analysis, *Pseudoidium*.

OPEN ACCESS

Citation: D. Seress, G. M. Kovács, O. Molnár, M. Z. Németh (2021) Infection of papaya (*Carica papaya*) by four powdery mildew fungi. *Phytopathologia Mediterranea* 60(1): 37-49. doi: 10.14601/Phyto-11976

Accepted: September 21, 2020

Published: May 15, 2021

Data Availability Statement: All relevant data are within the paper and its Supporting Information files.

Competing Interests: The Author(s) declare(s) no conflict of interest.

Editor: Thomas A. Evans, University of Delaware, Newark, DE, United States.

INTRODUCTION

Papaya (*Carica papaya* L.) is a tree native to Central America (Carvalho, 2013) that is cultivated for its fruit in many tropical and subtropical countries. In Europe, Spain is the largest papaya producer, with plants grown on

the Canary Islands and the southern regions of mainland Spain (Honoré *et al*., 2020). The most economically important papaya products are edible fruits and the papain enzyme extracted from the fruits (Carvalho, 2013; Carvalho *et al*., 2015). Papain is widely used in beer production, medicines, as a meat tenderizer and for softening textiles and leather (Carvalho, 2013). Additionally, papaya trees are planted for their ornamental value.

Papaya is very susceptible to several diseases (Rawal, 2010). Most of these, such as root and foot rot, damping off, different types of leaf spots, powdery mildew, anthracnose and stem end rot, are caused by fungi or oomycetous pathogens (Ventura *et al*., 2004; Rawal, 2010). Among these, anthracnose and other postharvest diseases are considered the most important, but the significance of these diseases varies with the growing region (Ventura *et al*., 2004). Powdery mildew on papaya is generally regarded as a disease of minor importance, but it has been reported to be severe in some regions (Liberato *et al*., 2004; Ventura *et al*., 2004; Rawal, 2010; Cunningham and Nelson, 2012). Powdery mildew on papaya causes premature leaf drop, reduced yields, poor fruit quality (Cunningham and Nelson, 2012), and may also kill seedlings (Ventura *et al*., 2004). Identification of the causal species of powdery mildews is complicated because the vegetative stages of these fungi are often morphologically similar or indistinguishable (Braun *et al*., 2017).

Braun *et al*. (2017) settled some taxonomic questions concerning powdery mildew fungi infecting papaya, described two new species, and provided a key for identification of the pathogens. At least four *Erysiphe* species commonly occur on papaya (Braun *et al*., 2017). *Erysiphe caricae* was described from Switzerland after it was detected on greenhouse-grown plants of babaco (mountain papaya, *Vasconcellea* × *heilbornii*) (Bolay, 2005). Other *Erysiphe* species infecting papaya include *E. caricae-papayae* (in Thailand and Taiwan), which is newly described, *E. diffusa* (in Brazil, Taiwan and possibly several other countries) and *E. fallax*, also newly described (in the United States of America and Mexico) (Braun *et al*., 2017). In addition, *E. necator* was detected from a sample originating from Hawaii, which was attributed to "accidental infection" (Braun *et al*., 2017). Two *Podosphaera* species were reported on papaya, *P. caricicola* (in Thailand, Taiwan, in the United States of America, and probably also in Australia and Java) (Braun *et al*., 2017), and *P. xanthii* (in Taiwan and Korea) (Tsay *et al*., 2011; Joa *et al*., 2013). Four *Phyllactinia* species are also known to occur on papaya, including *Ph. caricae, Ph. caricicola, Ph. papayae* and *Ph. caricifolia* (Takamatsu *et al*., 2016). Tsay *et al*. (2011) listed three powdery mildew fungi responsible for the disease on papaya. In addition to *E. diffusa* and *P. xanthii, Pseudoidium neolycopersici*, the pathogen associated with tomato powdery mildew (Kiss *et al*., 2001) was found to be widespread in papaya plantations in Taiwan (Tsay *et al*., 2011). *Pseudoidium neolycopersici* was also reported from China, and its identification was verified with cross inoculations onto tomato (Mukhtar and van Peer, 2018). Other species, such as *E. cruciferarum*, *P. macularis*, *Golovinomyces orontii* and *Leveillula* sp. are also listed as powdery mildew fungi infecting papaya, although the status of these species on papaya is lesser known, or the identifications are doubtful (Liberato *et al*., 2004; Braun *et al*., 2017). Altogether, about fifteen different powdery mildew species (including insufficiently known taxa) are thought to infect papaya, based on the data currently available (Table 1). In Europe, *Erysiphe diffusa* was recently reported from papaya plants in Spain (Vielba-Fernández *et al*., 2019), the main papaya producing country on that continent. Three other powdery mildew fungi, *Oidium papayae* (now thought to represent *E. diffusa*) (Liberato *et al*., 2004; Braun *et al*., 2017), *Sphaerotheca caricae-papayae* (now *P. xanthii*) (Braun *et al*., 2017), and *Leveillula taurica*, were reported from Portugal (Sequeira, 1992). Additional reports from Europe include samples identified as *E. caricae* from Switzerland (Bolay, 2005), Ukraine (Takamatsu *et al*., 2015) and Germany (Braun *et al*., 2017).

We have detected powdery mildew symptoms on papaya plants at two locations in Hungary. The aim of the present study was to characterize and identify the causal agents of powdery mildew on the infected plants.

MATERIALS AND METHODS

Samples and morphology

In 2018 and 2019, spontaneous powdery mildew infections were observed on young papaya plants growing in pots as hobby plants in a family yard in Győrújbarát, and in a greenhouse, on plants intended for research purposes in Budapest, Hungary. All these plants were grown from germinated seeds originating from one fruit.

Samples collected during this study are listed in Supplementary Table 1. Fresh powdery mildew colonies were sampled with cellotape and mounted in glycerine on microscope slides. Samples were also prepared using the lactic acid boiling method (Shin and La, 1993). For morphological characterization, a Zeiss Axioskop 2 Plus microscope was used with an AxioCam ICc5 camera. Size, shape and development of conidia (singly or in

Table 1. Powdery mildew species recorded on papaya, with collection data of the corresponding samples. "?" denotes doubtful records because of taxonomic uncertainties and/or lack of molecular-based identifications or other data. Countries where papaya is thought to be indigenous are indicated in *italic* font. Several early reports of '*Erysiphe caricae*' could not be included, as these records cannot be assigned to currently accepted species.

Powdery mildew species	Relevant synonyms or alternative names	Known host plants in Caricaceae	Geographic origin	Form detected on papaya	References
Species reported in this study					
Podosphaera xanthii	*Podosphaera caricae-papayae* *Sphaerotheca caricae-papayae*	*Carica papaya* *Vasconcellea* × *heilbornii* *Vasconcellea pubescens*	Australia, China, Cook Islands, Hungary, India, Japan, New Zealand, Thailand, USA, Portugal(?), Ukraine(?)	anamorph and teleomorph	Miller 1938; Sequeira, 1992; Braun and Cook, 2012; Braun *et al*., 2017 and references therein; this study
Erysiphe sp.		*Carica papaya*	Hungary	anamorph only	this study
Erysiphe cruciferarum		*Carica papaya* *Vasconcellea* × *heilbornii* *Vasconcellea pubescens*	Hungary, New Zealand, South Africa	anamorph only	Boesewinkel, 1982a,b; Gorter, 1993; this study
Erysiphe necator		*Carica papaya*	USA (Hawaii), Hungary	anamorph only	Braun *et al*., 2017; this study
Other species occurring on papaya					
Erysiphe caricae		*Carica papaya* *Vasconcellea* × *heilbornii*	Switzerland, Ukraine, Germany(?), Portugal(?)	anamorph and teleomorph	Bolay, 2005; Takamatsu *et al*., 2015; Braun *et al*., 2017
Erysiphe caricae-papayae		*Carica papaya*	Thailand, Taiwan(?)	anamorph and teleomorph	Tsay *et al*., 2011; Braun *et al*., 2017
Erysiphe diffusa	*Oidium caricae* *Oidium papayae* *Pseudoidium caricae*	*Carica papaya*	*Brazil*, Portugal, Spain, *Venezuela*, Taiwan(?)	anamorph and teleomorph	Liberato *et al*., 2004; Tsay *et al*., 2011; Braun *et al*., 2017; Vielba-Fernández *et al*., 2019
Erysiphe fallax		*Carica papaya*	*Mexico*, USA	anamorph only	Braun *et al*., 2017
Golovinomyces orontii	*Erysiphe cichoracearum*	*Carica papaya*(?) *Vasconcellea* × *heilbornii*(?) *Vasconcellea pubescens*(?)	*Mexico*(?), New Zealand(?), Peru(?)		Boesewinkel, 1982a,b; Braun and Cook, 2012; Braun *et al*., 2017 and references therein
Leveillula taurica s. lat.	*Oidiopsis sicula*	*Carica papaya*	Australia, India, Malawi, Nigeria, Portugal, Zambia, Zimbabwe		Liberato *et al*., 2004 and references therein; Braun *et al*., 2017 and references therein
O. caricae-papayae		*Carica papaya*	India,Taiwan	anamorph only	Braun and Cook, 2012
Phyllactinia caricae	*Ovulariopsis caricae*	*Carica papaya*	Taiwan, Australia(?), India(?)	anamorph only	Braun and Cook, 2012
Phyllactinia caricicola	*Ovulariopsis caricicola* *Streptopodium caricae*	*Carica papaya*	*Brazil*	anamorph only	Liberato *et al*., 2004; Takamatsu *et al*., 2016
Phyllactinia caricifolia	*Phyllactinia caricaefolia*	*Carica papaya*	*Brazil*	anamorph and teleomorph	Liberato *et al*., 2004 and references therein
Phyllactinia papayae	*Ovulariopsis papayae*	*Carica papaya*	Madagascar, Reunion, Rwanda, South Africa, Tanzania	anamorph only	van der Bijl, 1921; Braun and Cook, 2012
Podosphaera caricicola	*Oidium caricicola*	*Carica papaya*	Taiwan, Thailand, USA, Australia(?), Indonesia(?)	anamorph only	Boesewinkel, 1982a; Yen and Wang, 1973; Braun *et al*., 2017

chains), presence of fibrosin bodies in conidia, lengths of conidiophores, size of foot-cells, and morphology of hyphal appressoria were determined. Thirty conidia and all available conidiophores, including foot-cells, were measured from each sample. Type of conidium germination was noted when observed.

Representative herbarium specimens from each morphological type were deposited at the Mycological Collection of the Hungarian Natural History Museum, under accession numbers HNHM-MYC-008079 (111134BP) to HNHM-MYC-008083 (111138BP).

Sequence determinations

Genomic DNA was extracted from powdery mildew material removed from leaf surfaces with cellotape, using the sample boiling method (Pintye *et al.*, 2020), or from powdery mildew-infected leaf fragments using the DNeasy Plant Mini Kit (Qiagen), following the manufacturer's instructions. The internal transcribed spacer (ITS) region of the nuclear ribosomal DNA (nrDNA) was amplified in two fragments (Scholler *et al.*, 2016) using the primer pairs ITS5-PM6 and PM5-ITS4 (Takamatsu and Kano, 2001). A fragment of Minichromosome Maintenance Complex Component 7 encoding gene (*Mcm7*) was amplified with primers Mcm7F2 and Mcm7R8 (Ellingham *et al.*, 2019). For amplifications, Phusion Green Hot Start II High-Fidelity PCR Master Mix (Thermo Fisher Scientific) was used as recommended by the manufacturer, with primer annealing temperatures set to 58°C for ITS and 55°C for *Mcm7* amplifications. The reaction mixture contained 1 µL of template DNA in the ITS and 2 µL in the *Mcm7* amplifications. Amplicons were run on 1% agarose gel, and were sent for sequencing to LGC Genomics GmbH. Sequencing was done with the same primers used for the amplifications. The resulting chromatograms were processed with Staden Program Package (Staden *et al.*, 2000) and CodonCode Aligner version 9.0.1 (CodonCode Corporation). Sequences determined in this study were deposited in GenBank under accession numbers MT658714 to MT658729 and MT755388 to MT755394 (Supplementary Table 1).

Sequence analyses

Three phylogenetic analyses were conducted using ITS sequences (as in Braun *et al.*, 2017): one with sequences of samples belonging to the *Microsphaera* lineage of *Erysiphe* (Takamatsu *et al.*, 2015), the second with *E. necator* sequences, and the third with sequences of *Podosphaera xanthii* and closely related species. These analyses used the determined ITS sequences and sequences from the datasets of Braun *et al.* (2017), supplemented with additional sequences from closely related species obtained from GenBank after a search with Basic Local Alignment Search Tool (BLAST; Altschul *et al.*, 1990). The *E. necator* dataset also contained ITS sequences of isolates originating from non-*Vitaceae* hosts (Fonseca *et al.*, 2019; Pieroni *et al.*, 2020).

ITS alignments were prepared using MAFFT online (Katoh and Standley, 2013) with the E-INS-i algorithm (other settings were used as defaults). Leading and trailing gaps were included as unknown characters.

Mcm7 sequences from fungi of morphological types 2, 3 and 4 determined in this study were aligned with sequences from other *Erysiphe* sp. samples (Ellingham *et al.*, 2019; Shirouzu *et al.*, 2020) with FFT-NS-i algorithm of MAFFT online, and were added to the ITS dataset of the same samples, creating a combined ITS_*Mcm7* alignment.

Two *Cystotheca* species, *E. ornata* and *E. necator* var. *ampelopsidis*, were used as outgroups in the ITS analyses based on the results of Braun *et al.* (2017). For the ITS_*Mcm7* dataset, *Arthrocladiella mougeotii* and *Golovinomyces bolayi* were used as outgroup (Shirouzu *et al.*, 2020).

Phylogenetic analyses were carried out with the maximum likelihood (ML) method using raxmlGUI 1.5 (Silvestro and Michalak, 2012; Stamatakis, 2014). For the analysis of the ITS_*Mcm7* dataset, two partitions were set according to the two loci. Branch supports were calculated from 1000 bootstrap replicates. Phylogenetic trees resulting from analyses were visualized in TreeGraph 2.14.0 (Stöver and Müller, 2010) and were submitted to TreeBASE (study ID 26269).

Cross inoculation experiments

Cross inoculations were conducted with *P. xanthii* and *E. necator*. The two other powdery mildew fungi detected on papaya were not used.

Papaya plants (both infected and healthy) used in these experiments were less than 1 year old, and were 30–50 cm in size. These plants were germinated from the same batch of seeds as the plants originally identified as powdery mildew infected. The seeds were collected from a commercially available papaya fruit of unknown variety, originating from Indonesia. Other plant species used in cross inoculation tests were 1-month-old cucumber plants (*Cucumis sativus* 'Párizsi Fürtös') and 8-month-old grapevine (*Vitis vinifera* 'Chardonnay') plants grown from cuttings in pots.

Table 2. Summary of cross inoculation test results. (+) denotes successful infections and (–) denotes no infection.

Inoculum	To papaya	To cucumber	To grapevine	To *in vitro* grapevine leaves
Podosphaera xanthii ex papaya	–	+		
Podosphaera xanthii ex cucumber	+	+		
Erysiphe necator ex papaya	–		–	+
Erysiphe necator ex grapevine	+		+	+

The first series of experiments were carried out with powdery mildew from *P. xanthii*-infected papaya and cucumber plants onto healthy papaya and cucumber plants, by gently pressing the diseased leaves onto the surfaces of healthy leaves. In the second set of experiments *E. necator*-infected papaya and grapevine plants were used on to similarly inoculate healthy papaya and grapevine plants. All inoculations included two seedlings of each tested plant species to be inoculated, and two plants as positive controls, with the respective powdery mildew-inoculated to the same host plant species. Inoculated seedlings were covered with powdery mildew impermeable transparent plastic foil. Two uninoculated plants from each species were used as negative controls. All experiments were conducted twice.

In addition, transfer of *E. necator* from papaya and grapevine onto grapevine leaves maintained in an *in vitro* system was tested. *In vitro* grapevine plantlets were micropropagated from two-nodal explants grown on Murashige and Skoog (MS) medium (Murashige and Skoog, medium Mod. No. 1B, Duchefa) solidified with 6.5 g L^{-1} phyto agar (Murashige and Skoog, 1962; Aziz *et al.*, 2003). Plants were grown at 22°C with a daily 12 h photoperiod. Grapevine leaves were cut under sterile conditions and cultivated further on the same medium in disposable Petri dishes. Conidia from powdery mildew on papaya were placed on grape leaves using a sterile glass needle under sterile conditions. The Petri dishes were then incubated under the same conditions as the *in vitro* grapevine plantlets.

Inoculated plants and *in vitro* leaves were checked regularly for symptom development. When powdery mildew colonies were observed, the identity of the fungus was verified with microscopic analysis as described above. Cross inoculation experiments are summarized in Table 2.

RESULTS

Small powdery spots, each a few cm^2 in size, were detected on the stems and/or adaxial surfaces of the leaves on all plants investigated (Figure 1). No infection was detected on abaxial leaf surfaces. Some of the infected leaves became necrotic and curled, and later dried and fell off the plants.

According to morphological analysis by light microscopy, infections on some leaves were caused by powdery mildew fungi belonging to the *Fibroidium*, while others belonged to the *Pseudoidium* anamorphs. Four morphological types of powdery mildew fungi occurred in our samples, one *Fibroidium* morphological type and three *Pseudoidium* anamorphs with slightly differing morphology (Figure 2). Chasmothecia were not detected in any sample.

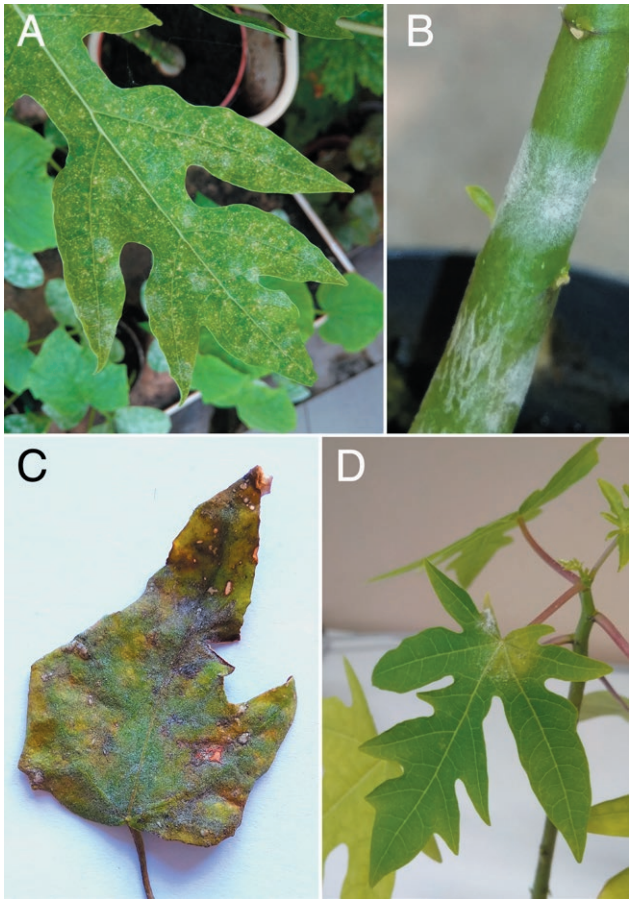

Figure 1. Powdery mildew symptoms on papaya plants. Symptoms caused by: A) *Podosphaera xanthii*, B) *Erysiphe* sp., C) *Erysiphe cruciferarum* and D) *Erysiphe necator.*

Figure 2. Conidiophore morphology of the four different powdery mildew morphological types designated in this study. A) *Podosphaera xanthii,* B) *Erysiphe* sp., C) *E. cruciferarum*, D) *E. necator*. Arrow in D) indicates the twisted conidiophore foot cell, characteristic of *E. necator.* Bars = 20 µm.

Morphological types

Morphological type 1. This type was detected in samples collected only in Budapest (Supplementary Table 1). Infections in most cases caused small, but well visible colonies on adaxial leaf surfaces. The fungus had *Fibroidium* anamorph, characterized by indistinct hyphal appressoria and production of conidia in chains. Conidium chains usually contained four to six conidia. Conidiophores measured up to 356 µm (including conidium chains), averaging 215 µm. Conidiophore foot cells were 57–94 µm × 8–13 µm and were each usually surmounted by 2-3 shorter cells. Foot cells sometimes showed slight constrictions at the basal septae. Conidia were doliiform, 25–40 µm in length, and 13–25 µm in width and contained fibrosin bodies, which were visible when mounting without boiling. Conidium germination was lateral and germ tubes did not have distinct appressoria. Based on morphological characteristics, the fungi in these samples were tentatively identified as *Podosphaera xanthii*.

Morphological types 2, 3 and 4 were identified as *Erysiphe* spp. based on morphology similar to *Pseudoidium* anamorphs (Braun and Cook, 2012).

Morphological type 2. A morphologically different subset of samples collected in Budapest (Supplementary Table 1) had small, distinct colonies, mainly on stems and petioles of affected host plants. Hyphae formed lobed appressoria. Conidiophores measured 97–152 µm, their foot cells were 26–47 µm × 9–12 µm, and these were each surmounted by two shorter cells. Conidia formed singly, were cylindrical or doliiform with lengths of 35–50 µm and widths of 13–23 µm, and lacked fibrosin bodies. Conidia germinated terminally with short germ tubes which formed lobed to multilobed appressoria.

Morphological type 3. A proportion of samples collected in Budapest and Győrújbarát (Supplementary Table 1) was characterized by thin, evanescent to persistent colonies on petioles and on adaxial leaf surfaces of affected hosts. These fungi developed lobed hyphal appressoria. Conidiophores measured 70–121 µm. Conidiophore foot cells were 18–33 µm × 7–12 µm, and were each surmounted by two shorter cells. Conidiophores each produced single cylindrical conidia, with lengths of 28–45 µm and widths of 10–20 µm, without fibrosin bodies. Conidia germinated terminally and formed moderately lobed appressoria.

Morphological type 4. Powdery mildew of other samples from papaya in Budapest and in Győrújbarát (Supplementary Table 1) developed thin or persistent colonies on host plants. Hyphal appressoria were lobed to multilobed. Conidiophores were highly variable in length, from 109 µm to sometimes slightly longer than 300 µm, averaging 205 µm. Conidiophore foot cells measured 73–154 µm × 5 µm. A portion of foot cells was sinuous or spirally twisted. Foot cells were usually surmounted by two shorter cells. Conidia formed singly, and were ellipsoid-ovoid or doliiform, 30–45 µm long and 15–20 µm wide, and did not contain fibrosin bodies. Conidia germinated terminally and formed lobed appressoria, or germination followed longitubus pattern. Based on these characteristics (Nomura *et al.*, 2003; Braun and Cook, 2012), the fungus was tentatively identified as *E. necator.*

Sequence analyses

Molecular taxonomic analyses of the nrDNA ITS region were carried out for 16 samples, representing all four morphological types. The dataset for the phylogenetic analysis of *Podosphaera* species included 46 sequences (including two newly determined sequences) and had a length of 480 characters, while the dataset with *Erysiphe* species in the *Microsphaera* lineage contained 85 sequences (including six newly sequenced) and the alignment consisted of 530 characters. The alignment of *Erysiphe necator* ITS sequences contained 27 sequences (of which eight were determined in the present study) and had 529 characters. The combined dataset of ITS and *Mcm7* sequences contained newly obtained sequences from seven samples, and altogether 62 samples, with an alignment length of 1068 characters, from which the *Mcm7* partition had 468 characters.

The identical ITS sequences determined from two Hungarian samples representing the *P. xanthii* morphotype formed a clade with three other identical *P. xanthii* sequences from powdery mildews originating from

Cucumis, *Helianthus* and *Saintpaulia* (Supplementary Figure 1).

In the phylogenetic analysis of the *Microsphaera* lineage of *Erysiphe* species, ITS sequences from the various samples from papaya were spread across six different clades (Figure 3). The Hungarian isolates (morphological types 2 and 3) were found in two of the clades. The three samples belonging to morphological type 2 had identical ITS sequences. These clustered in a clade containing identical sequences of other powdery mildew fungi identified as *E. malvae*, *E. heraclei* and *E. betae*, infecting five different plant species. ITS of two other samples labelled as *E. heraclei* and *E. betae* differed in one nucleotide position from the former samples (Figure 3). Three sequences from samples of morphological type 3 clustered in a clade formed by sequences of powdery mildews infecting *Brassicaceae* hosts (Figure 3). The ITS sequences of powdery mildew fungi from our papaya samples from Budapest and Győrújbarát, and *Brassica* sp., *Raphanus sativus* and *Sisymbrium officinale*, were identical.

In the combined ITS_*Mcm7* analysis, samples from morphological type 2 similarly clustered together in a well supported clade with samples labelled as *E. malvae*, *E. heraclei* and *E. betae* (Figure 4). However, sequences of our samples differed at least in one nucleotide position from all currently known *Mcm7* sequences.

The phylogenetic analysis of *E. necator* ITS sequences resulted in two groups, and both groups contained samples from papaya as well as from grapevine (Figure 5). Three of our papaya samples collected in Győrújbarát with identical ITS sequences formed a group with eight other identical sequences of powdey mildews from *Vitis* sp. and one from *Caryocar brasiliense*, and two other sequences differing in one position from the Hungarian samples. ITS sequences of *E. necator* infecting cashew differed in three nucleotides, while the ITS of the isolate infecting rubber tree differed in two nucleotides from our sequences belonging to this group.

Five of our papaya samples with identical sequences from Budapest formed a clade with three *E. necator* samples, including one originating from papaya, and two others from *V. vinifera* (Figure 5). These were all characterized by the same nucleotide sequence. In addition, an Australian *E. necator* sample from grapevine differed in one nucleotide from these sequences.

Cross inoculation tests

Results of cross inoculation tests are summarized in Table 2. Cross inoculations from infected papaya plants to healthy papaya plants were unsuccessful in experiments involving *P. xanthii*. However, healthy cucumber plants, regular hosts of *P. xanthii*, could be infected with the powdery mildew originating from papaya. Cucumber plants developed powdery mildew symptoms after 11 d.

Visible powdery mildew patches developed on the inoculated papaya leaves 11 d after inoculations with *P. xanthii* from cucumber, indicating that infection with powdery mildew from cucumber to papaya was successful (Supplementary Figure 2A). The same inoculum also infected healthy cucumber plants inoculated as controls.

Symptomless papaya plants and grapevine plants became infected with *E. necator* from grapevine, but not with *E. necator* from papaya. However, an *E. necator* sample from papaya (PM198) and another *E. necator* sample from grapevine as a control, were successfully used for starting *in vitro* powdery mildew cultures on *V. vinifera* leaves, causing symptoms 10-12 d after inoculations (Supplementary Figure 2B). The powdery mildews have been maintained on *in vitro* grapevine leaves.

DISCUSSION

Carica papaya and other *Carica* species are hosts of numerous powdery mildew species representing many different lineages of Erysiphales (Table 1). Based on morphological and sequence analyses, we detected *Podosphaera xanthii* and three *Erysiphe* spp. occurring on papaya plants in Budapest and Győrújbarát, Hungary.

Podosphaera xanthii, generally known as cause of powdery mildew on cucurbits, has a broad host range (Pérez-García *et al*., 2009; Braun and Cook, 2012) which is expanding as new hosts are reported (eg. Fan *et al*., 2019; Nayak and Babu, 2019; Nemes *et al*., 2019). Previous cross inoculation studies (Miller, 1938; Alcorn, 1968; Munjal and Kapoor, 1973; all cited in Liberato *et al*., 2004) showed that *P. xanthii* was able to infect papaya. Other studies reported spontaneous infections of papaya by the same species in Taiwan and Korea (Tsay *et al*., 2011; Joa *et al*., 2013). This fungus is a widespread colonizer of papaya in different geographic regions of the world, especially as samples identified earlier as *P. caricae-papayae* also represent *P. xanthii* (Braun *et al*., 2017).

The samples of the morphological type 2 formed a clade with powdery mildew fungi identified as *E. malvae*, *E. heraclei* and *E. betae*. Samples of morphological type 2 differed from *E. malvae* by the longer conidia, and the conidiophores of *E. malvae* arise mostly from towards the ends of mother cells (Braun and Cook, 2012), which was not observed in our samples. However, our samples were morphologically indistinguish-

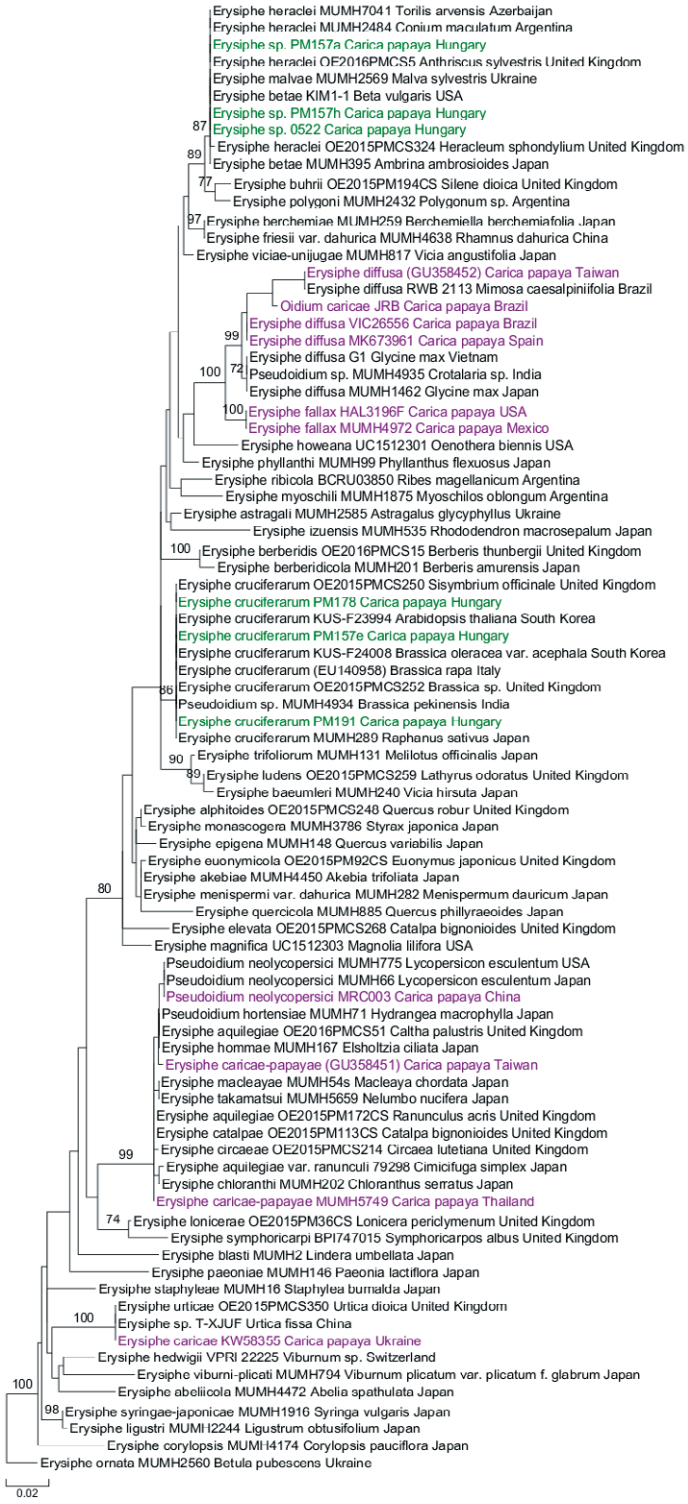

Figure 3. Phylogenetic tree with the greatest likelihood value resulting from the maximum likelihood (ML) analysis of ITS sequences of selected powdery mildew species belonging to the *Microsphaera* lineage of *Erysiphe*. Species names are followed by herbarium accession numbers (or GenBank accession numbers in parentheses if the herbarium accession number is not available), name of host plant, and country of collection. Samples collected in the present study are in green font, while other powdery mildew samples from papaya are in purple. Bootstrap values were calculated from 1000 replicates in the ML analysis (values below 70% and in subclades are not shown). Bar indicates 0.02 expected changes per site per branch.

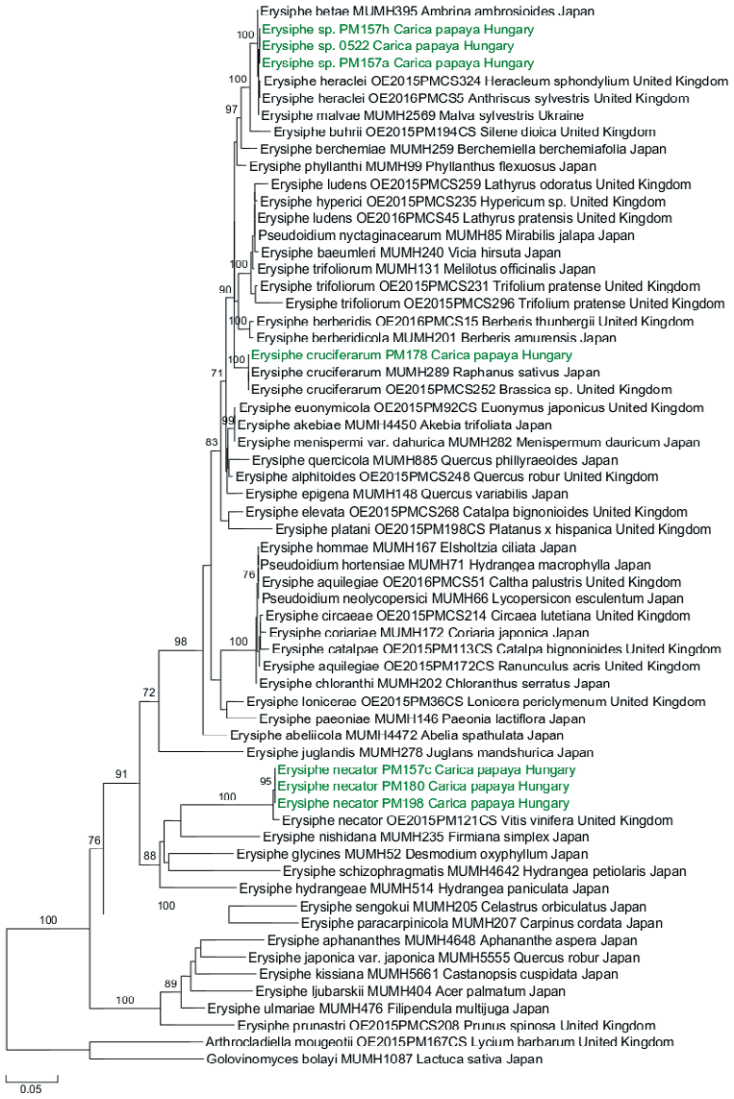

Figure 4. Phylogenetic tree with the greatest likelihood value resulting from the maximum likelihood (ML) analysis of ITS and *mcm7* sequences of selected powdery mildew species belonging to the *Microsphaera* lineage of *Erysiphe*. Species names are followed by herbarium accession numbers (or GenBank accession numbers in parentheses if the herbarium accession number is not available), name of host plant, and country of collection. Samples collected in the present study are in green font. Bootstrap values were calculated from 1000 replicates in ML analysis (values below 70% and in subclades are not shown). Bar indicates 0.05 expected changes per site per branch.

able from *E. betae* and *E. heraclei*. ITS sequences from morphological type 2 belonged to an unresolved complex within the *Microsphaera* lineage (Takamatsu *et al.*, 2015), so this fungus cannot be unambiguously identified to the species level based solely on ITS sequence data. This could be due to the low phylogenetic resolution of nrDNA sequences at the species level for powdery mildew fungi (Takamatsu *et al.*, 2015; Shin *et al.*, 2019). In order to further characterize, and possibly identify, the fungus in this complex, we also determined the sequence of a fragment of *Mcm7*. This locus is known to provide greater resolution than ITS among powdery mildew fungi (Ellingham *et al.*, 2019). This sequence is known to differ between *E. heraclei* and *E. betae*, based on the few sequences obtained to date (Ellingham *et al.*, 2019; Shirouzu *et al.*, 2020). Using *Mcm7* did not give species-level identification of the fungus with morphological type 2, as our sequences differed from both *E. heraclei* and *E. betae*. This indicates that a unique haplotype of an unindentified (or unknown) species infected papaya. Sequencing of additional reference samples could confirm if it belongs to an unknown spe-

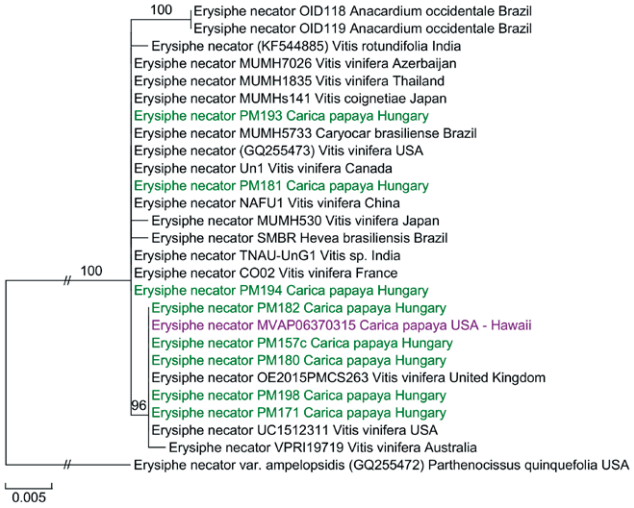

Figure 5. Phylogenetic tree with the greatest likelihood value resulting from the maximum likelihood (ML) analysis of ITS sequences of selected *Erysiphe necator* samples. Species names are followed by herbarium accession numbers (or GenBank accession numbers in parentheses if herbarium accession number is not available), name of host plant, and country of collection. Samples collected in the present study are in green font, while other powdery mildew samples from papaya are in purple. Bootstrap values were calculated from 1000 replicates in ML analysis (values below 70% and in subclades are not shown). Bar indicates 0.005 expected changes per site per branch.

cies. We are not aware of any previous study presenting powdery mildew fungi belonging to this species complex from papaya or any other host plants in the Caricaceae. Our results further indicate that fungi from this lineage infect diverse hosts from different plant families.

The assembly containing morphological type 3 samples can be identified as *E. cruciferarum*. Although this species is found mainly on brassicaceous plants (Braun and Cook, 2012), infectivity of *E. cruciferarum* on papaya is also known from previous results, as the powdery mildew infecting *Brassica napus* was able to cause disease on papaya plants (Boesewinkel 1982a, cited in Braun *et al*., 2007). A checklist of South African powdery mildew fungi also listed papaya as a host of *E. cruciferarum* (Gorter, 1993). Our sequence results provide further evidence of *E. cruciferarum* occurring on papaya. It should be noted that *E. cruciferarum* was detected on papaya leaves collected in the two sampled locations in Hungary, which are more than 100 km apart.

Erysiphe caricae, the first *Erysiphe* species on papaya of which the teleomorph has been detected (Bolay, 2005; Braun *et al*., 2017) is phylogenetically distant from other *Erysiphe* species occurring on papaya (Braun *et al.,* 2017; and see Figure 3). Moreover, as additional sequences were included in our analysis, this showed that *E. caricae* formed a group with two powdery mildew samples from *Urtica* sp., having identical ITS sequences. Further research is required to decipher the relation of *E. caricae* and the fungi causing powdery mildew on *Urtica* sp.

Erysiphe necator is mainly associated with plants in the *Vitaceae* (Braun and Cook, 2012). However, it has been shown recently that this fungus can also infect cashew and rubber tree (Fonseca *et al*., 2019; Pieroni *et al*., 2020). *Erysiphe necator* was also identified from papaya in a single sample from Hawaii (Braun *et al*., 2017). In the present study, infections of papaya were found to be caused by *E. necator* in half of the samples. The fungus was found in two distinct locations in Hungary, and the ITS sequences of samples from the two locations were different, indicating at least two independent occurrences of the fungus on papaya. The two groups differed by a fixed nucleotide difference (T/C at the nucleotide position corresponding to no. 48 of the reference sequence GQ255473), which is known to differ between two genetically differentiated *E. necator* subpopulations (Brewer and Milgroom, 2010). Our results suggest that *E. necator* can readily infect papaya in some circumstances.

Cross inoculations with *E. necator* and *P. xanthii* from papaya onto healthy papaya plants were unsuccessful. On the other hand, *P. xanthii* from papaya infected cucumber, and *E. necator* from papaya infected *in vitro* grapevine leaves. One explanation could be that the powdery mildew growth on papaya is often sparse, providing insufficient inoculum pressure on the healthy plants for successful infections. The respective hosts may also be more susceptible to the corresponding powdery mildew species than papaya. Furthermore, it is also pos-

sible that the growth conditions in our experiments were less conducive to powdery mildew infections on papaya than on the other host plants.

Erysiphe species detected in the present study are different from the species commonly occurring on papaya (see Braun *et al*., 2017). This could be that most of the reports have originated from locations where papaya is widely grown, or commonly found. In Hungary, papaya is present in homes of hobby growers or in greenhouses. Papaya is not native in Europe, but the powdery mildew species detected on papaya are established in Hungary (Sz. Nagy and Kiss, 2006). Fungal pathogens (Thines, 2019), including powdery mildews (Limkaisang *et al*., 2006; Vági *et al*., 2006; Cook *et al*., 2015; Beenken, 2017) have been reported to infect introduced non-local plants. This is considered as host range expansion (Thines, 2019), which is similar to the results from the present study of powdery mildew on papaya.

Our findings and the previous reports show that papaya is a host of several different powdery mildew fungi wherever it is grown. This may indicate that papaya could become a host for locally occurring powdery mildew species when this host is out of its native geographic range. This could lead to repeated occurrences of papaya powdery mildew, as papaya is more widely grown around as a crop or as an ornamental.

ACKNOWLEDGEMENTS

The authors thank Tamás Farkas for providing papaya plants, and for his assistance in sample transport. This research was partly supported by the Széchenyi 2020 Programme, the European Regional Development Fund and the Hungarian Government (GINOP-2.3.2-15-2016-00061), and by the ELTE Institutional Excellence Program by the National Research, Development and Innovation Office (NKFIH-1157-8/2019-DT).

LITERATURE CITED

Alcorn J.L., 1968. Cucurbit powdery mildew on pawpaw. *Queensland Journal of Agricultural and Animal Sciences* 2: 161–164.

Altschul S.F., Gish W., Miller W., Myers E.W., Lipman D.J., 1990. Basic local alignment search tool. *Journal of Molecular Biology* 215: 403–410.

Aziz A., Poinssot B., Daire X., Adrian M., Bézier A., ... Pugin A., 2003. Laminarin elicits defense responses in grapevine and induces protection against *Botrytis cinerea* and *Plasmopara viticola*. *Molecular Plant-Microbe Interactions* 16: 1118–1128. https://doi.org/10.1094/MPMI.2003.16.12.1118

Beenken L., 2017. First records of the powdery mildews *Erysiphe platani* and *E. alphitoides* on *Ailanthus altissima* reveal host jumps independent of host phylogeny. *Mycological Progress* 16: 135–143. https://doi.org/10.1007/s11557-016-1260-2

Boesewinkel H., 1982a. The identity of *Oidium caricae* and the first recording on papaya, mountain papaya and babaco in New Zealand. *Fruits* 37: 473–504.

Boesewinkel H., 1982b. Babaco, mountain papaya and papaya: all are susceptible to powdery mildew. *New Zealand Journal of Agriculture* 45: 28.

Bolay A., 2005. Les Oïdiums de Suisse (Erysiphacées). *Cryptogamica Helvetica* 20: 1–173.

Braun U., Cook R.T.A., 2012. *Taxonomic Manual of the Erysiphales (Powdery Mildews)*. CBS-KNAW Fungal Biodiversity Centre, Utrecht, The Netherlands.

Braun U., Meeboon J., Takamatsu S., Blomquist C., Fernandez Pavia S., ... Macedo D.M. 2017. Powdery mildew species on papaya – a story of confusion and hidden diversity. *Mycosphere* 8: 1403–1423. https://doi.org/10.5943/mycosphere/8/9/7

Brewer M.T., Milgroom M.G., 2010. Phylogeography and population structure of the grape powdery mildew fungus, *Erysiphe necator*, from diverse *Vitis* species. *BMC Evolutionary Biology* 10: 268. https://doi.org/10.1186/1471-2148-10-268

Carvalho F.A., e–Monograph of Caricaceae. Version 1, November 2013 http://herbaria.plants.ox.ac.uk/bol/Caricaceae, Accessed 19 May 2020

Carvalho F.A., Filer D., Renner S.S., 2015. Taxonomy in the electronic age and an e-monograph of the papaya family (Caricaceae) as an example. *Cladistics* 31: 321–329. https://doi.org/10.1111/cla.12095

Cook R.T.A., Denton J.O., Denton G., 2015. Pathology of oak–wisteria powdery mildew. *Fungal Biology* 119: 657–671. https://doi.org/10.1016/j.funbio.2015.02.008

Cunningham B., Nelson S., 2012. Powdery mildew of papaya in Hawai'i. *Colleague of Tropical Agriculture and Human Resources, University of Hawaii at Mānoa, Plant Disease* PD 90: 1–4.

Ellingham O., David J., Culham A., 2019. Enhancing identification accuracy for powdery mildews using previously underexploited DNA loci. *Mycologia* 111: 798–812. https://doi.org/10.1080/00275514.2019.1643644

Fan C., Cui H., Ding Z., Gao P., Luan F., 2019. First report of powdery mildew caused by *Podosphaera xanthii* on okra in China. *Plant Disease* 103: 1027–1027. https://doi.org/10.1094/PDIS-09-18-1543-PDN

Fonseca W., Cardoso J., Ootani M., Brasil S., Assunção F., ... Martins M.V.V., 2019. Morphological, molecular phylogenetic and pathogenic analyses of *Erysiphe* spp. causing powdery mildew on cashew plants in Brazil. *Plant Pathology* 68: 1157–1164. https://doi.org/10.1111/ppa.13032

Gorter G., 1993. A revised list of South African Erysiphaceae (powdery mildews) and their host plants. *South African Journal of Botany* 59: 566–566.

Honoré M.N., Belmonte-Ureña L.J., Navarro-Velasco A., Camacho-Ferre F., 2020. Effects of the size of papaya (*Carica papaya* L.) seedling with early determination of sex on the yield and the quality in a greenhouse cultivation in continental Europe. *Scientia Horticulturae* 265: 109218. https://doi.org/10.1016/j.scienta.2020.109218

Joa J., Chung B., Han K., Cho S., Shin H.-D., 2013. First report of powdery mildew caused by *Podosphaera xanthii* on papaya in Korea. *Plant Disease* 97: 1514–1514. https://doi.org/10.1094/PDIS-06-13-0581-PDN

Katoh K., Standley D.M., 2013. MAFFT multiple sequence alignment software version 7: improvements in performance and usability. *Molecular Biology and Evolution* 30: 772–780. https://doi.org/10.1093/molbev/mst010

Kiss L., Cook R.T.A., Saenz G.S., Cunnington J.H., Takamatsu S., ... Rossman A.Y., 2001. Identification of two powdery mildew fungi, *Oidium neolycopersici* sp. nov. and *O. lycopersici*, infecting tomato in different parts of the world. *Mycological Research* 105: 684–697. https://doi.org/10.1017/S0953756201004105

Liberato J.R., Barreto R.W., Louro R.P., 2004. *Streptopodium caricae* sp. nov., with a discussion of powdery mildews on papaya, and emended descriptions of the genus *Streptopodium* and *Oidium caricae*. *Mycological Research* 108: 1185–1194. https://doi.org/10.1017/s0953756204000991

Limkaisang S., Cunnington J.H., Wui L.K., Salleh B., Sato Y., ... Takamatsu S., 2006. Molecular phylogenetic analyses reveal a close relationship between powdery mildew fungi on some tropical trees and *Erysiphe alphitoides*, an oak powdery mildew. *Mycoscience* 47: 327–335. https://doi.org/10.1007/s10267-006-0311-y

Miller P.A., 1938. Cucurbit powdery mildew on *Carica papaya*. *Phytopathology* 28: 672.

Mukhtar I., van Peer A., 2018. Occurrence of powdery mildew caused by *Pseudoidium neolycopersici* on papaya (*Carica papaya*) in China. *Plant Disease* 102: 2645–2645. https://doi.org/10.1094/PDIS-10-17-1642-PDN

Munjal R.L., Kapoor J.N., 1973. *Carica papaya*: a new host of *Sphaerotheca fuliginea*. *Indian Phytopathology* 26: 366–367.

Murashige T., Skoog F., 1962. A revised medium for rapid growth and bio assays with tobacco tissue cultures. *Physiologia Plantarum* 15: 473–497.

Nayak A.K., Babu B.K., 2019. First report of powdery mildew caused by *Podosphaera fusca* on *Euphorbia hirta* in Odisha state, India. *Journal of Plant Pathology* 101: 191–191. https://doi.org/10.1007/s42161-018-0143-6

Nemes K., Salánki K., Pintye A., 2019. *Punica granatum* (pomegranate) as new host of *Erysiphe platani* and *Podosphaera xanthii*. *Phytopathologia Mediterranea* 58: 707–711. https://doi.org/10.14601/Phyto-10890

Nomura Y., Takamatsu S., Fujioka K., 2003. Teleomorph of *Erysiphe necator* var. *necator* on *Vitis vinifera* and *Ampelopsis brevipedunculata* var. *heterophylla* (Vitaceae) newly found in Japan. *Mycoscience* 44: 157–158. https://doi.org/10.1007/s10267-003-0094-3

Pérez-García A., Romero D., Fernández-Ortuño D., López-ruiz F., De Vicente A., Tores J.A., 2009. The powdery mildew fungus *Podosphaera fusca* (synonym *Podosphaera xanthii*), a constant threat to cucurbits. *Molecular Plant Pathology* 10: 153–160. https://doi.org/10.1111/j.1364-3703.2008.00527.x

Pieroni L.P., Gorayeb E.S., Benso L.A., Kurokawa S.Y.S., Siqueira O.A.P.A., ... Furtado E.L., 2020. First report of *Erysiphe necator* causing powdery mildew to rubber tree (*Hevea brasiliensis*) in Brazil. *Plant Disease* 104: 3078. https://doi.org/10.1094/PDIS-04-20-0848-PDN

Pintye A., Németh M.Z., Molnár O., Horváth Á.N., Spitzmüller Z., ... Kovács G.M., 2020. Improved DNA extraction and quantitative real-time PCR for genotyping *Erysiphe necator* and detecting the DMI fungicide resistance marker A495T, using single ascocarps. *Phytopathologia Mediterranea* 59: 97–106. https://doi.org/10.14601/Phyto-11098

Rawal R.D., 2010. Fungal diseases of papaya and their management. *Acta Horticulturae* 851: 443-446. 10.17660/ActaHortic.2010.851.68

Scholler M., Schmidt A., Siahaan S.A.S., Takamatsu S., Braun U., 2016. A taxonomic and phylogenetic study of the *Golovinomyces biocellatus* complex (Erysiphales, Ascomycota) using asexual state morphology and rDNA sequence data. *Mycological Progress* 15: 56. https://doi.org/10.1007/s11557-016-1197-5

Sequeira M., 1992. Notes on Erysiphaceae. Powdery mildew on Carica papaya. *Garcia de Orta. Série de Estudos Agronómicos* 18: 23–26.

Shin H.-D., La Y.-J., 1993. Morphology of edge lines of chained immature conidia on conidiophores in powdery mildew fungi and their taxonomic significance. *Mycotaxon* 46: 445–451.

Shin H.-D., Meeboon J., Takamatsu S., Adhikari M.K., Braun U., 2019. Phylogeny and taxonomy of *Pseudoidium pedaliacearum*. *Mycological Progress* 18: 237–246. https://doi.org/10.1007/s11557-018-1429-y

Shirouzu T., Takamatsu S., Hashimoto A., Meeboon J., Ohkuma M., 2020. Phylogenetic overview of Erysiphaceae based on nrDNA and *MCM7* sequences. *Mycoscience* 61: 249–258. https://doi.org/10.1016/j.myc.2020.03.006

Silvestro D., Michalak I., 2012. raxmlGUI: a graphical front-end for RAxML. *Organisms Diversity & Evolution* 12: 335–337. https://doi.org/10.1007/s13127-011-0056-0

Staden R., Beal K.F., Bonfield J.K., 2000. The Staden package, 1998. *Methods in Molecular Biology* 132: 115–130. https://doi.org/10.1385/1-59259-192-2:115

Stamatakis A., 2014. RAxML version 8: a tool for phylogenetic analysis and post-analysis of large phylogenies. *Bioinformatics* 30: 1312–1313. https://doi.org/10.1093/bioinformatics/btu033

Stöver B.C., Müller K.F., 2010. TreeGraph 2: Combining and visualizing evidence from different phylogenetic analyses. *BMC Bioinformatics* 11: 7. https://doi.org/10.1186/1471-2105-11-7

Sz. Nagy G., Kiss L., 2006. A check-list of powdery mildew fungi of Hungary. *Acta Phytopathologica et Entomologica Hungarica* 41: 79–91.

Takamatsu S., Kano Y., 2001. PCR primers useful for nucleotide sequencing of rDNA of the powdery mildew fungi. *Mycoscience* 42: 135–139. https://doi.org/10.1007/BF02463987

Takamatsu S., Ito H., Shiroya Y., Kiss L., Heluta V., 2015. First comprehensive phylogenetic analysis of the genus *Erysiphe* (Erysiphales, Erysiphaceae) I. The *Microsphaera* lineage. *Mycologia* 107: 475–489. https://doi.org/10.3852/15-007

Takamatsu S., Siahaan S.A.S., Moreno-Rico O., Cabrera de Álvarez M.G., Braun U., 2016. Early evolution of endoparasitic group in powdery mildews: molecular phylogeny suggests missing link between *Phyllactinia* and *Leveillula*. *Mycologia* 108: 837–850. https://doi.org/10.3852/16-010

Thines M., 2019. An evolutionary framework for host shifts – jumping ships for survival. *New Phytologist* 224: 605–617. https://doi.org/10.1111/nph.16092

Tsay J.-G., Chen R.-S., Wang H.-L., Wang W.-L., Weng B.-C., 2011. First report of powdery mildew caused by *Erysiphe diffusa*, *Oidium neolycopersici*, and *Podosphaera xanthii* on papaya in Taiwan. *Plant Disease* 95: 1188–1188. https://doi.org/10.1094/PDIS-05-11-0362

Vági P., Kovács G.M., Kiss L., 2006. Host range expansion in a powdery mildew fungus (*Golovinomyces* sp.) infecting *Arabidopsis thaliana*: *Torenia fournieri* as a new host. *European Journal of Plant Pathology* 117: 89–93. https://doi.org/10.1007/s10658-006-9072-x

van der Bijl P.A., 1921. On a fungus - *Ovulariopsis papayae*, n. sp. - which causes powdery mildew on the leaves of the pawpaw plant (*Carica papaya*, Linn.). *Transactions of the Royal Society of South Africa* 9: 187–189. 10.1080/00359192109520208

Ventura J.A., Costa H., da Silva Tatagiba J., 2004. Papaya diseases and integrated control. In: *Diseases of Fruits and Vegetables: Volume II* (S. A. M. H. Naqvi ed.), Kluwer Academic Publishers, Dordrecht, The Netherlands, 201–268.

Vielba-Fernández A., de Vicente A., Pérez-García A., Fernández-Ortuño D., 2019. First report of powdery mildew elicited by *Erysiphe diffusa* on papaya (*Carica papaya*) in Spain. *Plant Disease* 103: 2477. https://doi.org/10.1094/PDIS-03-19-0627-PDN

Yen J., Wang C., 1973. Étude sur les champignons parasites du Sud-Est asiatique XXII: Les *Oidium* de Formose (II). *Revue de Mycologie* 37: 125–153.

Phytopathologia Mediterranea
The international journal of the
Mediterranean Phytopathological Union

Firenze University Press
www.fupress.com/pm

Research Papers

Characterization of *Xanthomonas campestris* pv. *campestris* in Algeria

Samia LAALA[1,*], Sophie CESBRON[2], Mohamed KERKOUD[3], Franco VALENTINI[4], Zouaoui BOUZNAD[1], Marie-Agnès JACQUES[2], Charles MANCEAU[5]

[1] *ENSA, Ecole Nationale Supérieure d'Agronomie, 1 Avenue Pasteur, Hassan Badi - 16000 El Harrach - Alger, Algeria*
[2] *INRA, UMR1345 Institut de Recherche en Horticulture et Semences, Beaucouzé, Rue Georges Morel 42, 49071 Beaucouzé, France*
[3] *Diag-Gene, 8 rue Lenôtre, 49066, Angers, France*
[4] *CIHEAM - Istituto Agronomico Mediterraneo di Bari, Via Ceglie, 9, I-70010, Valenzano (BA), Italy*
[5] *ANSES, Agence Nationale de Sécurité Sanitaire de l'alimentation, de l'environnement et du travail. Laboratoire de la santé des végétaux, 7 rue Dixméras, 49044 Angers, France*
*Corresponding author. E-mail: slaala@hotmail.com

Summary. *Xanthomonas campestris* pv. *campestris* (*Xcc*) causes the black rot of cruciferous plants. This seed-borne bacterium is considered as the most destructive disease to cruciferous crops. Although sources of contamination are various, seeds are the main source of transmission. Typical symptoms of black rot were first observed in 2011 on cabbage and cauliflower fields in the main production areas of Algeria. Leaf samples displaying typical symptoms were collected during 2011 to 2014, and 170 strains were isolated from 45 commercial fields. *Xcc* isolates were very homogeneous in morphological, physiological and biochemical characteristics similar to reference strains, and gave positive pathogenicity and molecular test results (multiplex PCR with specific primers). This is the first record of *Xcc* in Algeria. Genetic diversity within the isolates was assessed in comparison with strains isolated elsewhere. A multilocus sequence analysis based on two housekeeping genes (*gyrB* and *rpoD*) was carried out on 77 strains representative isolates. The isolates grouped into 20 haplotypes defined with 68 polymorphic sites. The phylogenetic tree obtained showed that *Xcc* is in two groups, and all Algerian strains clustered in group 1 in three subgroups. No relationships were detected between haplotypes and the origins of the seed lots, the varieties of host cabbage, the years of isolation and agroclimatic regions.

Keywords. *Brassicaceae,* seed-borne bacterium, genetic diversity, multilocus sequence analysis.

OPEN ACCESS

Citation: S. Laala, S. Cesbron, M. Kerkoud, F. Valentini, Z. Bouznad, M.-A. Jacques, C. Manceau (2021) Characterization of *Xanthomonas campestris* pv. *campestris* in Algeria. *Phytopathologia Mediterranea* 60(1): 51-62. doi: 10.36253/phyto-11726

Accepted: December 22, 2020

Published: May 15, 2021

Data Availability Statement: All relevant data are within the paper and its Supporting Information files.

Competing Interests: The Author(s) declare(s) no conflict of interest.

Editor: Joel L. Vanneste, Plant and Food Research, Sandringham, New Zealand.

INTRODUCTION

Black rot caused by *Xanthomonas campestris* pv. *campestris* (*Xcc*), is the most widespread disease of cruciferous crops. It was first reported in the United States of America in 1895 by Pammel (Swing and Civerolo, 1993), and

is considered one of the most destructive bacterial diseases of vegetables (Williams, 1980). Under optimal temperature and humidity conditions, the disease can cause losses up to 100% on sensitive brassica varieties (Mgonja and Swai, 2000; Janse and Wenneker, 2002; Massomo *et al*., 2004). Several *Brassica* species can be infected (cabbage, cauliflower, kale, broccoli, turnip, radish and mustard). Cabbage and cauliflower are the most susceptible (Kocks and Zadoks, 1996). Many weeds can also be infected by the bacterium, and these ensure the conservation of the pathogen throughout the year as inoculum sources (Schaad and White, 1974; Rat and Chauveau, 1985). *Xcc* is a seed-borne pathogen, this being the primary inoculum source (Cook *et al*., 1952; Schaad *et al*., 1980; Schultz and Gabrielson, 1986), but *Xcc* can survive for months in leaves and other plant debris in the soil.

Black rot management is mainly based on prophylactic measures, which include eradication of inoculum reservoirs especially crop debris and cruciferous weeds, and certified pathogen-free seed lots (Janse and Wenneker, 2002). One contaminated seed among 10 000 healthy seeds can initiate a black rot outbreak after planting (Cook *et al*., 1952; Schaad *et al*., 1980; Laala *et al*., 2015).

Xcc has not been previously reported in Algeria. A survey conducted by Emmanouilidis dates back to 1976; but reported the absence of black rot in the Algerian territory. Nevertheless, similar symptoms of black rot were observed in 2011 (Figure 1) in several cabbage and cauliflower producing areas of Algeria. The symptoms observed were yellow V-shaped, chlorotic lesions on host leaf margins and blackening of vascular tissue (Janse and Wennekek, 2002; Tsygankova *et al*., 2004).

Figure 1. Symptoms of black rot in a cauliflower crop (Zéralda, Wilaya of Algeries, Algeria), with yellow V- shaped lesions at margin of a leaf (blue arrow).

The purpose of this study was to collect symptomatic samples, and to identify and characterize pathogen strains isolated in Algeria and to assess the diversity of their populations.One hundred and seventy isolates were identified as *Xcc* and characterized with a range of biochemical, biological and molecular tests. Seventy-seven isolates were selected to study their genetic diversity by Multilocus Sequence Analysis (MLSA), based on two housekeeping genes, the *gyrB* and *ropD* which code, respectively, for a DNA gyrase B and the sigma factor 70.

MATERIALS AND METHODS

Collection of samples

During surveys conducted from 2011 to 2014, three hundred and fifteen samples of Brassica leaves with typical symptoms of black rot were collected. The sampling was carried out in 76 fields, from 35 cabbage crops (*Brassica oleracea* subsp. *capitata)* and 41 of cauliflower crops (*Brassica oleracea* subsp. *botrytis*), located in the Wilaya of Algiers, Boumerdes, Tipaza, Ain Defla, Skikda, Mostaganem and Tizi Ouzou regions of Algeria (Figure 2). During sampling, climatic conditions were 20 to 30°C, and 80% humidity on average.

The leaf samples were labelled, stored in plastic bags and transported to the Phytosanitary laboratory at the Centre National de Contrôle et de Certification des semences et plants (CNCC), El Harach, Alger, and were stored at 4°C until use (1 to 2 d). The samples and their main characteristics are listed in Table 1.

Bacterial isolation and purification

One hundred and seventy isolates were obtained from symptomatic samples, using the protocol of Schaad

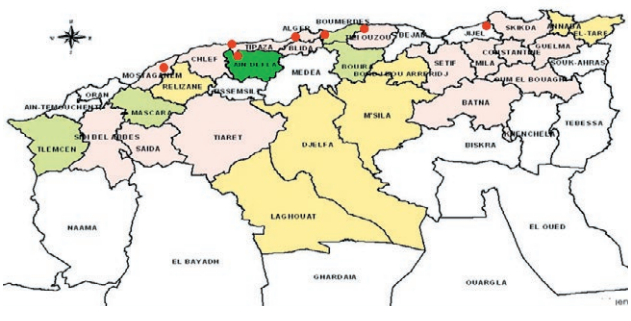

Figure 2. Surveyed and sampled *Brassica*-growing areas (red circles) in Algeria (from 2011-2014).

Table 1. *Xanthomonas campestris* pv. *campestris* isolate designations, their hosts, source regions, and haplotypes formed with concatenated partial sequences, for 77 isolates ontained in Algeria.

Isolate	Host	Host variety	Region of isolation	Field No.	Year of isolation	Conc. haplotype
XccDZ111	*Brassica oleracea* spp. *capitata*	Smilla	Staoueli ITCMI	green house 1	05/10/2011	H1
XccDZ112	*Brassica oleracea* spp. *botrytis*	Yebouze	Staoueli ITCMI	green house 2	05/10/2011	H1
XccDZ112.6	*Brassica oleracea* spp. *botrytis*	Arizona	Rouiba	2	10/10/2011	H1
XccDZ11272	*Brassica oleracea* spp. *botrytis*	Arizona	Rouiba	2	10/10/2011	H1
XccDZ113.1	*Brassica oleracea* spp. *capitata*	Solo	Rouiba	3	10/10/2011	H1
XccDZ113.5	*Brassica oleracea* spp. *capitata*	Solo	Rouiba	3	10/10/2011	H1
XccDZ114.9	*Brassica oleracea* spp. *capitata*	Bitch	Rouiba	4	10/10/2011	H1
XccDZ114.10	*Brassica oleracea* spp. *capitata*	Bitch	Rouiba	4	10/10/2011	H2
XccDZ115.1	*Brassica oleracea* spp. *botrytis*	Arizona	Tipaza	5	27/10/2011	H1
XccDZ116.1	*Brassica oleracea* spp. *botrytis*	Arizona	Tipaza	6	27/10/2011	H3
XccDZ116.2	*Brassica oleracea* spp. *botrytis*	Arizona	Tipaza	6	27/10/2011	H3
XccDZ1230.2	*Brassica oleracea* spp. *capitata*	Chebli	SidiFredj	30	07/01/2012	H4
XccDZ1230.3	*Brassica oleracea* spp. *capitata*	Chebli	SidiFredj	30	07/01/2012	H4
XccDZ1230.4	*Brassica oleracea* spp. *capitata*	Chebli	SidiFredj	30	07/01/2012	H4
XccDZ1230.5	*Brassica oleracea* spp. *capitata*	Chebli	SidiFredj	30	07/01/2012	H1
XccDZ1241.3	*Brassica oleracea* spp. *capitata*	Smilla	Staoueli	41	06/04/2012	H1
XccDZ1242.3	*Brassica oleracea* spp. *capitata*	Chebli	SidiFredj	42	06/04/2012	H5
XccDZ1243.1	*Brassica oleracea* spp. *capitata*	Chebli	Staoueli	43	06/04/2012	H6
XccDZ1243.2	*Brassica oleracea* spp. *capitata*	Chebli	Staoueli	43	06/04/2012	H1
XccDZ1243.3	*Brassica oleracea* spp. *capitata*	Chebli	Staoueli	43	06/04/2012	H1
XccDZ1244.1	*Brassica oleracea* spp. *capitata*	Spacestar	Staoueli	44	06/04/2012	H1
XccDZ1244.2	*Brassica oleracea* spp. *capitata*	Spacestar	Staoueli	44	06/04/2012	H1
XccDZ1244.3	*Brassica oleracea* spp. *capitata*	Spacestar	Staoueli	44	06/04/2012	H7
XccDZ1246.1	*Brassica oleracea* spp. *capitata*	Yerbouze	Staoueli	46	06/04/2012	H1
XccDZ1246.2	*Brassica oleracea* spp. *capitata*	Yerbouze	Staoueli	46	06/04/2012	H1
XccDZ1358	*Brassica oleracea* spp. *capitata*	Standard	Boumerdès	58	21/02/2013	H1
XccDZ1360	*Brassica oleracea* spp. *capitata*	Canapatchi	K. El Khechna	60	18/03/2013	H1
XccDZ1360.1	*Brassica oleracea* spp. *capitata*	Canapatchi	K. El Khechna	60	18/03/2013	H1
XccDZ1375.2	*Brassica oleracea* spp. *capitata*	Yerbouze	Aïn Taya	75	23/06/2013	H1
XccDZ1375.3	*Brassica oleracea* spp. *capitata*	Yerbouze	Aïn Taya	75	23/06/2013	H8
XccDZ1375.6	*Brassica oleracea* spp. *capitata*	Yerbouze	Aïn Taya	75	23/06/2013	H1
XccDZ1376.9	*Brassica oleracea* spp. *capitata*	Yerbouze	Aïn Taya	76	23/06/3013	H9
XccDZ1382.2	*Brassica oleracea* spp. *capitata*	Yerbouze	Ouled Moussa	82	23/06/2013	H1
XccDZ1384.3	*Brassica oleracea* spp. *capitata*	Yerbouze	Ouled Moussa	84	23/06/2013	H1
XccDZ.1388.2	*Brassica oleracea* spp. *capitata*	Arizona	Mostaganem	88	25/03/2013	H20
XccDZ1388.4	*Brassica oleracea* spp. *capitata*	Arizona	Mostaganem	88	23/03/2013	H1
XccDZ1490.43	*Brassica oleracea* spp. *botrytis*	Atlas	Zéralda	90	17/01/2014	H1
XccDZ1490.54	*Brassica oleracea* spp. *botrytis*	Atlas	Zéralda	90	17/01/2014	H1
XccDZ1493.12	*Brassica oleracea* spp. *botrytis*	Spacestar	Zéralda	93	17/01/2014	H10
XccDZ1493.31	*Brassica oleracea* spp. *botrytis*	Spacestar	Zéralda	93	17/01/2014	H1
XccDZ1493.32	*Brassica oleracea* spp. *botrytis*	Spacestar	Zéralda	93	17/01/2014	H9
XccDZ1493.34	*Brassica oleracea* spp. *botrytis*	Spacestar	Zéralda	93	17/01/2014	H1
XccDZ1493.51	*Brassica oleracea* spp. *botrytis*	Spacestar	Zéralda	93	17/01/2014	H1
XccDZ1493.54	*Brassica oleracea* spp. *botrytis*	Spacestar	Zéralda	93	17/01/2014	H1
XccDZ14100.6	*Brassica oleracea* spp. *capitata*	Sakata	Aïn Taya	100	06/05/2014	H1
XccDZ14101.20	*Brassica oleracea* spp. *capitata*	Raissa	Aïn Taya	101	06/05/2014	H1
XccDZ14101.21	*Brassica oleracea* spp. *capitata*	Raissa	Aïn Taya	101	06/05/2014	H1

(Continued)

Table 1. (Continued).

Isolate	Host	Host variety	Region of isolation	Field No.	Year of isolation	Conc. haplotype
XccDZ14101.22	*Brassica oleracea* spp. *capitata*	Raissa	Aïn Taya	101	06/05/2014	H7
XccDZ14101.27	*Brassica oleracea* spp. *capitata*	Raissa	Aïn Taya	101	06/05/2014	H1
XccDZ14102.28	*Brassica oleracea* spp. *botrytis*	Arizona	Aïn Taya	102	06/05/2014	H1
XccDZ14102.29	*Brassica oleracea* spp. *botrytis*	Arizona	Aïn Taya	102	06/05/2014	H1
XccDZ14/102.30	*Brassica oleracea* spp. *botrytis*	Arizona	Aïn Taya	102	06/05/2014	H1
XccDZ14/102.34	*Brassica oleracea* spp. *botrytis*	Arizona	Aïn Taya	102	06/05/2014	H7
XccDZ14/102.38	*Brassica oleracea* spp. *botrytis*	Arizona	Aïn Taya	102	06/05/2014	H1
XccDZ14/104.60	*Brassica oleracea* spp. *botrytis*	Arizona	Tizi Ouzou	104	25/06/2014	H1
XccDZ14/104.61a	*Brassica oleracea* spp. *botrytis*	Arizona	Tizi Ouzou	104	25/06/2014	H11
XccDZ14/104.61b	*Brassica oleracea* spp. *botrytis*	Arizona	Tizi Ouzou	104	25/06/2014	H12
XccDZ14/104.61c	*Brassica oleracea* spp. *botrytis*	Arizona	Tizi Ouzou	104	25/06/2014	H13
XccDZ14/104.64	*Brassica oleracea* spp. *botrytis*	Arizona	Tizi Ouzou	104	25/06/2014	H1
XccDZ14/104.66a	*Brassica oleracea* spp. *botrytis*	Arizona	Tizi Ouzou	104	25/06/2014	H14
XccDZ14/104.66b	*Brassica oleracea* spp. *botrytis*	Arizona	Tizi Ouzou	104	25/06/2014	H1
XccDZ14/104.67	*Brassica oleracea* spp. *botrytis*	Arizona	Tizi Ouzou	104	25/06/2014	H1
XccDZ14/104.68	*Brassica oleracea* spp. *botrytis*	Arizona	Tizi Ouzou	104	25/06/2014	H1
XccDZ14/104.69a	*Brassica oleracea* spp. *botrytis*	Arizona	Tizi Ouzou	104	25/06/2014	H1
XccDZ14/104.69b	*Brassica oleracea* spp. *botrytis*	Arizona	Tizi Ouzou	104	25/06/2014	H1
XccDZ14/104.69c	*Brassica oleracea* spp. *botrytis*	Arizona	Tizi Ouzou	104	25/06/2014	H15
XccDZ14/105.75	*Brassica oleracea* spp. *botrytis*	Solo	Zéralda/Azurplage	105	12/09/2014	H16
XccDZ14/106/126	*Brassica oleracea* spp. *botrytis*	Arizona	Aïn Dafla	106	16/11/2014	H17
XccDZ14/106/127	*Brassica oleracea* spp. *botrytis*	Arizona	Aïn Dafla	106	16/11/2014	H16
XccDZ14/106/129	*Brassica oleracea* spp. *botrytis*	Arizona	Aïn Dafla	106	16/11/2014	H16
XccDZ14/106/130	*Brassica oleracea* spp. *botrytis*	Arizona	Aïn Dafla	106	16/11/2014	H18
XccDZ14/106/131	*Brassica oleracea* spp. *botrytis*	Arizona	Aïn Dafla	106	16/11/2014	H1
XccDZ14/106/132	*Brassica oleracea* spp. *botrytis*	Arizona	Aïn Dafla	106	16/11/2014	H1
XccDZ14/106/134	*Brassica oleracea* spp. *botrytis*	Arizona	Aïn Dafla	106	16/11/2014	H1
XccDZ14/106/135	*Brassica oleracea* spp. *botrytis*	Arizona	Aïn Dafla	106	16/11/2014	H19
XccDZ14/106/136	*Brassica oleracea* spp. *botrytis*	Arizona	Aïn Dafla	106	16/11/2014	H1
XccDZ14/106/137	*Brassica oleracea* spp. *botrytis*	Arizona	Aïn Dafla	106	16/11/2014	H1
CFBP 1121*	*Brassica oleracea* cv. *bullata gemmifera.*	///	France	///	1967	
CFBP 5241 * (ATCC 33915)	*Brassica oleracea* var. *gemmifera*	///	United Kingdom	///	1957	

*Type strain.

et al. (2001). Each sample was rinsed with tap water and then dried. Small sections of affected tissue were taken and crushed using a sterile scalpel and soaked in a small volume (approx. 2 mL) of sterile distilled water for 15-20 min to allow diffusion of bacterial cells.

Aliquots of 50 µL of tenfold dilutions (10^{-1} to 10^{-8}) of the suspension were plated onto YPGACvc medium (yeast extract 7 g L^{-1}, peptone 7 g L^{-1}, glucose 7 g L^{-1}, agar 15 g L^{-1}, pH 7), supplemented with cephalexine 25 mg L^{-1}, vancomycin 0.5 mg L^{-1} and cycloheximide 100 mg L^{-1}). The plates were then incubated for 24 h at 28°C and observed daily for bacterial growth. *Xcc*-like colonies (colour and shape) were purified by repeated subculturing of a single colony on YPGA and on GYCA (yeast extract 5 g L^{-1}, glucose 10 g L^{-1}, $CaCO_3$ 40 g L^{-1} agar 15 g L^{-1}, pH 7) medium (Lelliot and Stead, 1987).

Two reference strains of *Xanthomonas campestris* pv. *campestris* (CFBP 1121 and 5241) were used for this study, obtained from the Collection Française de Bactéries Associées aux Plantes (CFBP), Angers, France (https://www6.inrae.fr/cirm_eng/CFBP-Plant-Associated-Bacteria).

All purified isolates were preserved at -20°C and -80°C in microtubes, containing 1 mL of YP medium (yeast extract 7 g L^{-1}, peptone 7 g L^{-1}) supplemented with 20% glycerol.

Table 2. Primers used for PCR amplification and sequencing of Algerian isolates of *Xanthomonas campestris* pv. *campestris*.

Target gene	Primers names	Annealing temperature	Sequences (5'-3')	Expected fragment size (bp)	References
hrpF	DLH120[a] DLH125[b]	63°C	CCGTAGCACTTAGTGCAATGGCA TTTCCATCGGTCACGATTG	619	Berg *et al.,* 2005
rrs (Universal Primers)	1052–F[a] Bac–R [b]	63°C	GCATGGTTGTCGTCAGCTCGTTA CGGCTACCTTGTTACGACT	441	Eden *et al.,*1991
atpD	P-X-ATPD-F[a] P-X-ATPD-R[b]	62°C	GGGCAAGATCGTTCAGAT GCTCTTGGTCGAGGTGAT	868	Fargier *et al.,* 2011
dnaK	P-X-DNAK-F[a] P-X-DNAK-R[b]	62°C	GGTATTGACCTCGGCACCAC ACCTTCGGCATACGGGTCT	1,034	Fargier *et al.,* 2011
gyrB	emigyrB1F[a] emigyrB4R[b]	63°C	TGCGCGGCAAGATCCTCAAC GCGTTGTCCTCGATGAAGTC	904	Fargier *et al.,* 2011
rpoD	emirpo11F[a] emirpo13R[b]	63°C	ATGGCCAACGAACGTCCTGC AACTTGTAACCGCGACGGTATTCG	1,313	Fargier *et al.,* 2011

[a] Forward primers; [b] reverse primers.

Bacterial characterization

Isolates were tested for cytochrome oxidase activity (Klement *et al.,* 1990), esculine hydrolysis (Lelliot *et al.,* 1987), oxidative and fermentative metabolism of glucose as described previously (Hugh and Leifson, 1953). The hypersensitive host response was monitored in tobacco leaf tissues (*Nicotiana tabacum* Xanthi) after infiltration of 10^8 cfu mL^{-1} bacterial suspensions from 24 h cultures.

Molecular characterization was performed on DNA extracts obtained by boiling bacterial suspensions of 10^6 cfu mL^{-1} for 10 min and subsequently keeping these on ice for 15 min. The suspensions were then centrifuged at 10 000 rpm for 5 min and stored at -20°C. Amplifications were performed by multiplex PCR according to (Laala *et al*., 2015). Each reaction was performed in a final volume of 20 µL containing: 1× Green GoTaq Flexi Buffer (Promega), 1.5 mM of $MgCl_2$, 0.2 mM of dNTP, 0.5 µM of each specific primer DLH 120/LH125 (Berg *et al*., 2005), 0.05 µM of each universal bacterial primer (used to validate the PCR reaction) 1052-F/Bac-R (Eden *et al*., 1991), 0.05 U of GoTaq Flexi DNA polymerase and 3 µL of template DNA. The primer sequences used in this study are presented in Table 2.

PCR reactions were conducted with a C1000 thermocycler (Bio-Rad). The programme consisted of initial denaturation at 95°C for 3 min, followed by 35 cycles of 40 s at 95°C, 40 s at 63°C (touchdown to 58°C over the first six cycles) and 40 s at 72°C. The amplification products were separated on 1.5 % agarose gels in 1× TBE buffer, stained with ethidium bromide, and visualized using UV transilluminator on a Gel Doc 2000 (Bio-Rad).

Pathogenicity tests

Presumptive isolates were tested for their pathogenicity on cauliflower seedlings (cv. Arizona) after seed contamination, according to Laala *et al.* (2015). Symptoms were observed 7 to 14 d after sowing inoculated seeds. A positive control (*Xcc* strain CFBP 5241) and a negative control (sterile distillate water) were included in the assays. Koch's postulates were confirmed by symptomatic leaves onto YPGACvc medium and by PCR characterization of re-isolated bacterial colonies.

Housekeeping gene amplification and sequencing

Sequences from three isolates (Xcc DZ114.10, Xcc DZ113.5 and Xcc DZ1388.2) were selected from the main varieties cultivated in Algeria to be compared with those available in the database with BLASTN (Altschul *et al*., 1990). Fragments of four housekeeping genes were sequenced for each isolate, including gyr*B* (DNA gyrase subunit B), *rpoD* (RNA polymerase sigma-70 factor), *atpD* (ATP synthase beta chain), and DnaK (heat shock protein 70), according to (Fargier *et al.,* 2011) (Table 2). The amplifications were each carried out in a thermocycler (iCycler; Bio-Rad), in a final volume of 20 µL containing 1× green GoTaq Hot Start buffer, 1.5 µL of 25 mM $MgCl_2$, 0.2 mM of dNTP, 0.5 µM of each primer and 1U of GoTaq Hot Start DNA polymerase (Promega) and 3 µL of target DNA. The amplification program consisted of 5 min at 95°C followed by 35 cycles of 30 s at 95°C, 45 s at Tm (Table 2) and 1.30 min at 72°C, and finished with 72°C for 5 min. The PCR products were analysed on 1.5% agarose

gel in 1× TBE buffer. The two strands of the amplicons obtained from the three isolates were sequenced by the GATC Biotech laboratory, Germany. The sequence electropherograms were analysed using the software 4 peaks 1.7.2 (https://nucleobytes.com/4peaks/index.html). The DNA sequences were aligned using the Multalin software (Corpet, 1988: http://multalin.toulouse.inra.fr/multalin/).

Multilocus Sequences Analysis (MLSA) and phylogenetic analysis

The purposes of this approach were to study the genetic diversity of *Xcc* isolated in Algeria in comparison with strains from different countries, based on the diversity of the housekeeping genes, and to identify potential inoculum sources.

Ninety-six isolates were selected for a phylogenetic study from the 170 *Xcc* isolates identified by their microbiological, biochemical and molecular traits. Two housekeeping genes (*gyrB* gene and *rpoD*) were chosen for this study. The *gyrB* gene is a good marker of specificity between species, while the *rpoD* gene is a good marker of discrimination within a species (Fischer-Le Saux, personal communication). The amplification conditions were the same as those defined above. The quality and yield of each amplicon were verified by loading 10 µL of the reaction product onto 1.5% agarose gel in 1× TBE buffer, and also by Nano-Drop ND-2000 (ThermoFisher Scientific). The 96 amplicons were sequenced at the GATC Biotech laboratory, Germany.

DNA sequences were analysed using the software 4 peaks 1.7.2. and were aligned using the Bioedit program (Hall, 1999). Only sequences having average lengths of 500 bp were used for analyses. The sequence data of the two genes were concatenated according to the alphabetical order of the gene, the *gyrB* gene followed by the *rpoD* gene, using the GENEIOUS software Version 4.8.5 (BIOMATTERS).

Phylogenetic analyses were carried out on individual genes as well as on the concatenated sequences using the DNA Sequence polymorphism (DnaSP) software version 5.10 (Rozas *et al.,* 2010). This analysis is based on the Tajima's method (Tajima, 1996), allowing a multiple alignment by determining pairwise nucleotide diversity. The differentiation between the haplotypes is based on the presence of a single nucleotide different per sequence (Wicker *et al.,* 2012; Tancos *et al*., 2015).

The phylogenetic tree was constructed using Mega software version 6.06 (Tamura *et al*., 2013) based on the Maximum likelihood (ML) method (Tamura and Nei, 1993). This software allows quick analysis of a large number of sequences, and evolutionary phylogenetic reconstruction based on statistical bootstrap analysis at 1000 replications. The tree was constructed with the DNA sequences of each gene and with the concatenated sequences. Sequences of *Xcc* strains (Xcc-C168, Xcc-C278, ICMP 6541, strain 0407, strain 0470, ICMP 13, CFBP 5241, 70 genome, ICMP 4013, ATCC 33913, 21080, Xcc-8004), published on the NCBI database were used for comparisons with sequences from the Algerian strains, and the sequence from *X. campestris* pv. *vesicatoria* (*Xcv*) 85-10 (Thieme *et al.,* 2005) was used to root the tree.

RESULTS

Characterization of Xanthomonas campestis *pv.* campestris *isolates*

Out of the 315 symptomatic samples collected between 2011 and 2014, 170 isolates showed typical morphological colonies on the YPGACvc medium. After 24 h incubation, the bacterial colonies were round, yellow, mucoid, convex and shiny.

All these isolates were Gram negative and correspond to the biochemical characteristics as previously described (Schaad, 1980; Lelliott and Stead, 1987). They were glucose oxidative (Hugh and Leifson, 1953). The activity of levansucrase and catalase were positive, and the isolates induced HRs on tobacco leaves. They did not display cytochrome oxidase (strike oxidase strips: Fluka Analytical) and did not reduce nitrates.

The multiplex PCR designed for *Xcc* identification (Laala *et al*., 2015) generated amplicons with expected sizes (619 and 441 pb) for the 170 isolates tested.

Pathogenicity assays

All the plants inoculated with bacterial suspensions (1 10^7 cfu mL^{-1}) of the Algerian *Xcc* isolates and the reference strain (CFBP 5242) showed symptoms of rotting within 7-14 d after sowing. No symptoms were observed in plants inoculated with sterile water. Re-isolations were performed on YPGACvc from germinated seedlings. Resulting bacterial colonies were yellowish, circular, and mucoid, and were identified as *Xcc* by multiplex PCR (Laala *et al*., 2015), confirming the Koch's postulates.

Amplification of housekeeping genes

Sequence amplifications from the three isolates of *Xcc* (Xcc DZ114.10, Xcc DZ113.5 and Xcc DZ1388.2) using four housekeeping genes, gave four bands of

Table 3. Comparison of housekeeping gene DNA sequences of Algerian strains of *Xanthomonas campestris* pv. *campestris* with that of other strains of *Xanthomonas campestris* (*X.c.*).

Algerian strains	Reference strains	Genes			
		*gyr*B	*rpo*D	*atp*D	*dna*k
XccDZ114.10	ATCC 33913/ Xcc-C-168	734/735[a] (99%)[b]	574/577 (99%)	661/667(99%)	778/779 (99%)
	X.c. pv. *vesicatoria* 85-10	639/736 (87%)	539/578 (93%)	630/666 (95%)	736/779 (94%)
XccDZ113.5	ATCC 33913/ Xcc-C-168	734/735 (99%)	577/577(100%)	663/667 (99%)	777/779 (99%)
	X.c. pv. *vesicatoria* 85-10	639/736 (87%)	639/736 (87%)	542/578 (94%)	735/779 (94%)
XccDZ1388.2	ATCC 33913/ Xcc-C-168	734/735 (99%)	576/577(99%)	663/667 (99%)	776/779 (99%)
	X.c. pv. *vesicatoria* 85-10	639/736 (87%)	541/578 (94%)[b]	630/666(95%)	734/779 (94%)

[a] Ratio of identical nucleotides; [b] identity level

Table 4. Genetic diversity of *Xanthomonas campestris* pv. *campestris* isolates assessed by MLSA.

Gene	Fragment size (pb)	No. of sequences selected	No. of haplotypes	No. of polymorphic sites	% of polymorphic sites
gyrB	737	94	6	9	1.22%
rpoD	575	83	20	61	10.6 %
Concatened Sequences	1,312	77	20	68	5.18 %

the expected sizes of 904 bp for the *gyrB* gene, 1313 bp for the *rpoD* gene, 868 bp for the *atpD* gene and 1034 bp for the *dnaK* gene (Fargier *et al.,* 2011). The DNA sequences of the four genes from the three Algerian isolates showed high percentage similarities of 98 to 100%, in comparison with *Xcc* sequences, and less than 96% similarity with other *Xanthomonas* species available in the NCBI database (Table 3). The partial nucleotide sequences of the strains *Xcc* DZ114.10, *Xcc* DZ113.5 and *Xcc* DZ1388.2 were deposited in the NCBI database under the following accession numbers: the *atpD* gene (KU556302 to KU556304), the *DnaK* gene (KU556305 to KU556307), the *gyrB* gene (KU556308 to KU556310) and *rpoD* (KU556311 to KU556312).

The strains were deposited in the CFBP, under the numbers CFBP 8405, CFBP 8406, CFBP 8407.

Phylogenetic analysis of housekeeping genes

Of the 170 of *Xcc* isolates, 96 representatives of all the sampled regions were selected for examination of genetic diversity. Two loci, the *gyrB* and the *rpoD* genes were used. DNA fragments of the two genes were sequenced. Ninety-four sequences of 735 bp for the *gyrB* gene, 83 sequences of 577 bp for the *rpoD* gene and 77 sequences concatenated (1312 bp) were used.

The phylogenetic analysis carried out by the DnaSP (Rozas *et al*., 2010) revealed the presence of polymorphism among the strains. The number of polymorphic nucleotide sites varied from nine to 68 (Table 4).

The *rpoD* locus displayed greatest discriminating power, which corroborates the MLSA studies published by Fargier *et al*. (2011), Lange *et al*. (2016) and Popović *et al*. (2019). Twenty haplotypes were obtained for this gene with a variable site level reaching 10.6%, compared with 1.22% for *gyrB* (Table 4). The concatenation of the two loci grouped the 77 strains into 20 haplotypes with 68 polymorphic sites (Table 4).

Fifty strains were of haplotype H1 and these were isolated from different areas throughout the sampling period (Table 1). Fourteen haplotypes out of 20 (H2 to H20) were each of a single isolate. The phylogenetic tree constructed with the partial sequences of the *gyrB* gene showed strong homology between the Algerian strains and the 33 *Xcc* reference sequences. The *Xcv* was an outgroup, as expected (data not showed). The *rpoD* gene was more polymorphic. The *Xcc* strains clustered in two groups, among which the Algerian strains clustered in group I associated with 13 reference strains isolated from many international locations. No strains isolated in Algeria clustered in group II (Figure 3). The *Xcv* was associated to *Xcc* group II with a high bootstrap value. This could be explained by the presence of a recombination event between *Xcc* and *Xcv* within the *rpoD* gene.

The phylogenetic tree showed that the Algerian isolates were in three subgroups within group I (Figure 3). The first subgroup (Ia) contained the majority of

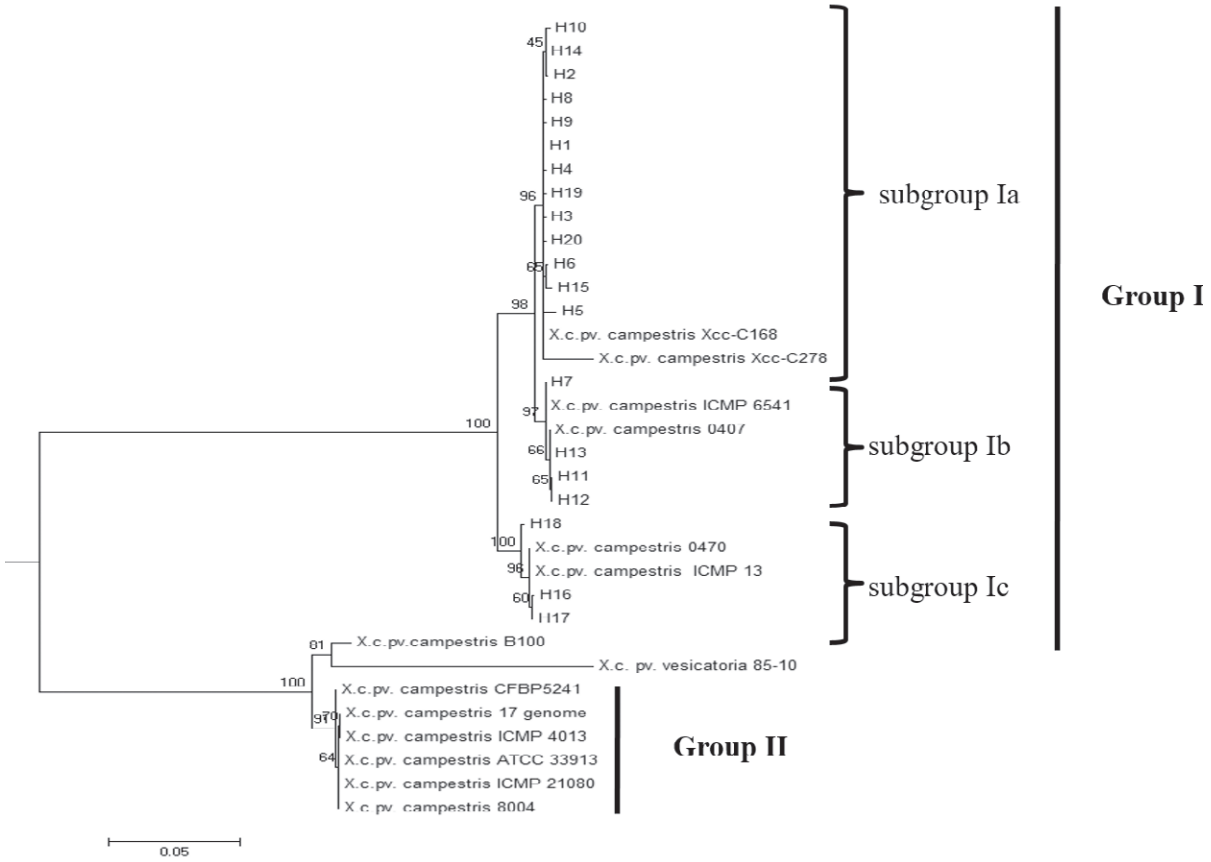

Figure 3. Maximum likelihood tree constructed with concatenated partial sequences of two housekeeping gene (*gyrB* and *rpoD*) of 20 Algerian haplotypes and 13 *Xanthomonas campestris* pv. *campestris* international strains, and rooted with *Xanthomonas campestris* pv. *vesicatoria*. Bootstrap percentages obtained for 1000 replicates are indicated at each node.

Algerian isolates with 13 haplotypes. It also included two strains isolated in India (*Xcc*-C168 and *Xcc*-C278) (Rathaur *et al.,* 2015; Singh *et al.,* 2016). Subgroup Ib contained four Algerian haplotypes and ICMP 6541 isolated in New Zealand, and 0407 isolated in New York State, United States of America. The subgroup Ic included three Algerian haplotypes, and *Xcc* 0470 from New York State and ICMP 13 from the United Kingdom. Furthermore, the strains 0407 and 0470 isolated in New York State were separated in two distinct subgroups, which is in accordance with the study of Lange *et al*. (2016). Results obtained by DnaSP software showed that the 20 haplotypes identified in Algeria displayed homology with strains isolated from many international regions. The Algerian isolates grouped in the haplotype H1 with strong similarity to Xcc-168 strain isolated in India (Rathaur *et al.,* 2015), and haplotype H7 was very similar to strain ICPM 6541 isolated in New Zealand (Young *et al*., 2008) (Figure 3). However, none of the strains isolated in Algeria fitted into the clusters of group 2, which suggests that Algerian population Algeria did not cover all of the recognized diversity of *Xcc*.

DISCUSSION

This study reports for the first time the presence of *Xcc* in Algeria, after the investigation conducted in cabbage and cauliflower fields from 2011 to 2014. A total of 170 *Xcc* isolates was obtained from 45 fields. These isolates were identified as *Xcc* by morphological, physiological and molecular tests. The analysis of four housekeeping genes (*gyrB*, the *rpoD*, the *atpD* and the *dnaK*) performed on partial DNA sequences of three representative Algerian strains showed 98 to 100% similarity with homologous *Xcc* sequences available in the GenBank database (Table 3). Results obtained from this survey indicate the importance of black rot in Algeria, and how widespread the disease is in the main Brassica growing areas of the country. However, the sampling

method used did not allow assessment of how the disease spreads in this country, because each region was not monitored each year.

The MLSA approach was conducted for the genetic studies. This is a powerful tool for study of phylogenetic relationships at the inter- and intraspecies levels, by analyzing sequences of two or more housekeeping genes from a large number of bacterial isolates (Hanage *et al*., 2006; Fargier *et al*., 2011). Genes encoding housekeeping proteins are universally distributed among bacteria, present in single copies and dispersed in the genomes (Hanage *et al*., 2006; Youseif *et al*., 2014). In the present study, the MLSA results in general revealed the existence of genetic diversity within Algerian *Xcc* isolates. A total of 20 haplotypes were obtained displaying 68 polymorphic nucleotide sites (Table 4). However, no correlation was found between haplotypes with species and host variety, year of isolation or geographic origin of host plants. This strongly indicates that inoculum came from seeds that would have been imported and distributed in the country. This also supports the conclusions of previous studies (Zaccardelli *et al*., 2008; Fargier *et al*., 2011; Rathaur *et al.,* 2015; Lange *et al*., 2016; Bella, 2019). Fargier *et al*. (2011) described two groups of *Xcc* from MLSA using genomic sequences of seven housekeeping genes. The present study confirmed the occurrence of two genomic groups within *Xcc*, and showed that all the strains isolated in Algeria belonged to the group *Xcc* I of Fargier *et al*. (2011). Therefore, the MLSA haplotypes of Algerian isolates were not unique, as no distinct clustering was present when Algerian *Xcc* haplotypes were compared with the internationally collected haplotypes.

Haplotype H1 contained approx. 50 strains isolated from several *Brassica* varieties and from 21 fields over all collection periods. It also contained two strains collected from a nursery seedling, strain Xcc DZ11.1 isolated from a cauliflower (cv. Smilla) leaf and strain Xcc DZ11.2 isolated from a cabbage (cv. Yerbouze). It cannot be confirmed that these two isolates derived from a seed lot infected with the same inoculum, because haplotype H1 is widely distributed in Algeria and internationally. Strains Xcc DZ114.9 and Xcc DZ114.10 were collected from one plant but were of different haplotypes, respectively, haplotype H1 and H2. This indicates that these isolates were from different everal sources, either a seed lot contaminated by more than one haplotype, from two different seed lots sowed in the field, or from infected seed and with different environmental origins (Schaad and White,1974; Alvarez and Cho, 1978; Schaad and Dianese 1981; Chun and Alvarez; 1983; Alvarez and Lou 1985).

The phylogenetic tree obtained showed that Algerian *Xcc* isolates were of three subgroups with a high bootstrap values. The majority of *Xcc* isolates clustered in subgroup Ia. This included 13 haplotypes, and the isolates were collected from different conditions over the period 2011-2014, as well as Xcc-C168 isolated from Uttar Pradesh (India) and Xcc-C278 isolated from Delhi (India) (Rathaur *et al.,* 2015, Singh *et al.,* 2016). The subgroup Ib contained haplotypes H7, H11, H12 and H13, as well as ICMP 6541 from New Zealand and 0407 (Fresco) from New York State (Lange *et al*., 2016). Subgroup Ic contained three haplotypes (H16, H17 and H18) were included in subgroup Ic, along with strain 470 (Kaiten) isolated in New York State (Lange *et al.,* 2016) and ICMP 13 (CFBP 2350) isolated in 1957 in the United Kingdom. This suggests that the *Xcc* population isolated in the present study covered the full diversity of group *Xcc* I described by Fargier *et al*. (2011). Previous studies have been conducted to trace the origins of *Xcc* isolates using molecular characterization techniques based on PCR or housekeeping MLSA (Ignatov *et al*., 2007; Zaccardelli *et al*., 2008; Jensen *et al*., 2010; Mulema *et al*., 2011; Lema *et al*., 2012; Rathaur *et al*., 2015; Lange *et al*., 2016; Bella *et al*., 2019), but these methods were not suitable for tracing particular inoculum sources in the Algerian situation described here. This was probably due to the international trading of Brassica seed lots, since the pathogen is a seed-borne bacterium (Cook *et al*., 1952; Weller and Saettler, 1980; Blackeman, 1991). Fields may therefore contain strains from several origins conserved in plant debris (Schaad and Dianese, 1981), or strains may be associated with cruciferous weeds. The preliminary results presented here revealed the existence of diversity within Algerian isolates. However the MLSA approach, using two housekeeping genes, and the type of sampling, were not discriminating enough to trace relationships between genetic diversity within Algerian strains and seed lot origins, varities, years or regions.

New approaches are currently under development, such as multilocus variable number tandem repeat analysis (MLVA) (Vogler *et al.,* 2006; Bui Thi Ngoc *et al.,* 2009). MLVA is widely used to study genetic diversity and deduce patterns of the spread of bacterial pathogens (Achtman, 2008; Cunty *et al*., 2015), and this methodology would allow increased understanding of the structure of Algerian *Xcc* populations. This pathogen is occurring in the main market gardens in the Algiers, Mostaghenem, Ain Defla regions, and in Tipaza in western Algeria and Tizi Ouzou and Boumerdes in the east of the country. It would be useful to extend the survey area in western and eastern parts of Algeria where cabbages are grown. Although first symptoms of black rot were reported in Algeria only at the beginning of this study (2011), the level of diversity of recorded haplo-

types in Algeria indicates that *Xcc* was introduced in the country before that year.

The present study provides a basis to assess the relative roles of host weeds and infected plant debris versus that of contaminated seed lots in the epidemiology of the black rot of cruciferous plants in Algeria. Control of seed-borne pathogens is important for appropriate disease management, and to prevent their introduction and spread. To this aim, research on control and certification of vegetable seeds is currently being promulgated by the Ministry of Agriculture of the Republic of Algeria. This should allow improved management of seed-borne pathogens and improve agricultural production. This is likely to include the use of certified pathogen-free propagative materials (seeds and seedlings) coupled with appropriate agronomic practices such as destruction of crop debris and wild hosts, and seedbed rotation.

ACKNOWLEDGEMENTS

The authors thank Lyes Beninal, of the Centre National de Contrôle et de Certification des Semences et Plants), for her assistance with sampling.

COMPLIANCE WITH ETHICAL STANDARDS

Studies in this article do not involve human participants nor animals.

LITERATURE CITED

Achtman M., 2008. Evolution population structure and phylogeography of genetically monomorphic bacterial pathogens. *Annual Review of Microbiology* 62: 53–70. https://doi.org/10.1146/annurev.micro.62.081307.162832 354

Altschul S., Gish W., Miller W., Myers E., Lipman D., 1990. Basic local alignment search tool. *Journal of Molecular Biology* 215: 403–410. https://doi.org/10.1016/S00222836 (05)80360-2 356

Alvarez A.M., Cho J.J., 1978. Black rot of cabbage in Hawaii: Inoculum source and disease 357 incidence. *Phytopathology* 68: 1456–1459. https://doi.org/10.1094/Phyto-68–1456

Alvarez A.M., Lou K., 1985. Rapid identification of *Xanthomonas campestris* pv. *campestris* by ELISA. *Plant Disease* 69: 1082–1086. https://doi.org/10.1094/PD-69–1082

Bella P., Moretti C., Licciardello G., Strano C.P., Pulvirenti A., … Catara V., 2019. Multilocus sequence typing analysis of Italian *Xanthomonas campestris* pv. *campestris* strains suggests the evolution of local endemic populations of the pathogen and does not correlate with race distribution. *Plant Pathology* 68: 278–87. https://doi.org/10.1111/ppa.12946

Berg T., Tesoriero L., Hailstones D.L., 2005. PCR-based detection of *Xanthomonas campestris* pathovars in Brassica seed. *Plant Pathology* 54: 416–427. https://doi.org/10.1111/j.1365–3059.2005.01186.x

Blackeman J.P, 1991. Foliar bacterial pathogens: epiphytic growth and interactions on leaves. *Journal of Applied Bacteriology*, Symposium Supplement 70: 49S–59S

Bui Thi Ngoc L., Verniere C., Vital K., Guerin F., Gagnevin L., … Pruvost O., 2009. Development of 14 minisatellites markers for the citrus canker bacterium, *Xanthomonas citri* pv. *citri*. *Molecular Ecology Resources* 9: 125–127. https://doi.org/10.1111/j.1755–0998.2008.02242.x

Chun W.W.C., Alvarez A.M., 1983. A starch-methionine medium for isolation of *Xanthomonas campestris* pv. *campestris* from plant debris in soil. *Plant Disease* 67: 632–635. https://doi.org/10.1094/PD-67–632

Cook A.A., Larson R.H., Walker J.C., 1952. Relation of the black rot pathogen to cabbage seed. *Phytopathology* 42: 316–320.

Corpet F., 1988. Multiple sequence alignment with hierarchical clustering. *Nucleic Acids Research* 16 (22): 10881–10890. https://doi.org/10.1093/nar/16.22.10881

Cunty A., Cesbron S., Poliakoff F., Jacques M.A., Manceau C., 2015. The origin of the outbreak in France of *Pseudomonas syringae* pv. *actinidiae* biovar 3, the causal agent of bacterial canker of Kiwifruit, revealed by a Multilocus Variable-number of Tandem Repeat Analysis. *Applied and Environmental Microbiology* 81: 6773–6789. https://doi.org/10.1128/AEM.01688-15

Eden P.A., Schmidt T.M., Blackemore R.P., Pace N.R., 1991. Phylogenetic Analysis of *Aquaspirillum magnetotacticum* using Polymerase Chain Reaction Amplified 16S rRNA specific DNA. *International Journal of Systematic Bacteriology* 41: 324–325. https://doi.org/10.1099/00207713-41-2-324

Fargier E., Fischer-Le Saux M., Manceau C., 2011. A multilocus sequence analysis of *Xanthomonas campestris* reveals a complex structure within crucifer-attacking pathovars of this species. *Systematic and Applied Microbiology* 34: 156–165. https://doi.org/10.1016/j.syapm.2010.09.001

Hall T.A., 1999. BIOEDIT: a user-friendly biological sequence alignment editor and analysis program for Windows 95/98/NT. *Nucleic Acids*. Symposium Series 41, 95–98.

Hanage, W.P., Fraser, C. and Spratt, B. G. 2006. Sequences, sequence clusters and bacterial species. Philosophical Transactions of the Royal Society. *Biological Sciences* 361, 1917–1927. https://doi.org/10.1098/rstb.2006.1917

Hugh R., Leifson E., 1953. The taxonomic significance of fermentative versus oxidative metabolism of carbohydrates of various Gram- bacteria. *Journal of Bacteriology* 66: 24–26. https://doi.org/10.1128/JB.66.1.24-26.1953

Ignatov A.N., Sechler A., Schuenzel E.L., Agarkova L., Oliver B., Vidaver A.K., 2007. Genetic Diversity in Populations of *Xanthomonas campestris* pv. *campestris* in Cruciferous Weeds in Central Coastal California. *Phytopathology* 97: 803–812. https://doi.org/10.1094/PHYTO-97-7-406 0803

Janse J.D., Wenneker M., 2002. Possibilities of avoidance and control of bacterial plant diseases when using pathogen-tested (certified) or treated planting material. *Plant Pathology* 51: 523–536. https://doi.org/10.1046/j.0032-0862.2002.00756.x

Jensen B.D., Vicente J.G., Manandhar H.K., Roberts S.J., 2010. Occurrence and diversity of *Xanthomonas campestris* pv. *campestris* in vegetable Brassica fields in Nepal. *Plant Disease* 94: 298–305. https://doi.org/10.1094/PDIS-94-3-0298

Klement Z., Rudolph K., Sands D.C., 1990. *Methods in Phytobacteriology*. Akademiai Kiadò, Budapest.

Kocks C.G., Zadoks J.C., 1996. Cabbage refuses piles as source of inoculum for black rot epidemics. *Plant Disease* 80: 789–792. https://doi.org/10.1094/PD-80-0789

Laala S., Bouznad Z., Manceau C., 2015. Development of a new technique to detect living cells of *Xanthomonas campestris* pv. *campestris* in crucifers seeds: the seed qPCR. *European Journal of Plant Pathology* 141: 637–646. https://doi.org/10.1007/s10658-014-0532-4 420

Lange H.W., Tancos M.A., Carlson M.O., Smart C.D., 2016. Diversity of *Xanthomonas campestris* isolates from symptomatic crucifers in New York State. *Phytopathology* 106: 113–122. https://doi.org/10.1094/PHYTO-06-15-0134-R

Lelliott R.A., Stead D.E., 1987. *Methods in Plant Pathology*, Vol. 2. Oxford, UK: Blackwell Scientific Publications.

Lema M., Cartea M.E., Sotelo T., Velasco P., Soengas P., 2012. Discrimination of *Xanthomonas campestris* pv. *campestris* races among strains from north western Spain by Brassica spp. genotypes and rep-PCR. *European Journal of Plant Pathology* 133: 159–169. https://doi.org/10.1007/s10658-011-9929-5

Massomo S.M.S., Mortensen C.N., Mabagala R.B., Newman M.A., Hockenhull J., 2004. Biological Control of Black Rot (*Xanthomonas campestris* pv. *campestris*) of Cabbage in Tanzania with *Bacillus* strains. *Journal of Phytopathology* 152: 98–105. https://doi.org/10.1111/j.1439–434 0434.2003.00808.x

Mulema J.M.K., Vicente J.G, Pink D.A.C., Jackson A., Chacha D.O., … Hand P., 2011. Characterization of isolates that cause black rot of crucifers in East Africa. *European Journal of Plant Pathology* 133: 427–438. https://doi.org/10.1007/s10658-011-9916-x

Mgonja A.P., Swai I., 2000. Importance of diseases and insect pests of vegetables in Tanzania and limitations in adopting the control methods. Workshop in vegetable research and development center. In: *Proceedings, Second National Vegetable Research and Development Planning Workshop*, 28–34 (M. L. Chadha, A. P. Mgonja, R. Nono-Womdim & I. S. Swai Ed.), HORTI-Tengeru, 25–26 June 1998. AVRDC-ARP Arusha, Tanzania.

Pammel L.H., 1895. *Bacteriosis of rutabaga* (*Bacillus campestris*. sp.). Bulletin of the Iowa State College Agriculture Experiment Station 27: 130–134.

Popović T., Mitrović P., Jelusić A., Dimkić I., Marjanović-Jeromela A., Nikolić I., Stanković S., 2019. Genetic diversity and virulence of *Xanthomonas campestris* pv. *campestris* isolates from *Brassica napus* and six *Brassica oleracea* crops in Serbia. *Plant Pathology* 68 (2): 1448–1457. https://doi.org/10.1111/ppa.13064

Rat B., Chauveau J. F., 1985. La nervation des crucifères. *Phytoma*, 41–42.

Rathaur P.S., Singh D., Raghuwanshi R., Yadava D. K., 2015. Pathogenic and Genetic Characterization of *Xanthomonas campestris* pv. *campestris* Races Based on Rep-PCR and Multilocus Sequence Analysis. *Journal of Plant Pathology and Microbiology* 6: 1-9. https://doi.org/10.4172/2157-7471.1000317

Rozas J., Librado P., Sánchez-Del Barrio J.C., Messeguer X., Rozas R., 2010. DNA sequence polymorphism. Ver. 5.10.1 Universidad de Barcelona. Available at http://www.ub.edu/dnasp/. Accessed July 20, 2015.

Schaad N.W., 2001. *Laboratory Guide for Identification of Plant Pathogenic Bacteria*. 3rd Edition. ISBN: 0-89054–263-5.

Schaad N.W., White W. C., 1974. Survival of *Xanthomonas campestris* in soil. *Phytopathology* 64: 1518–1520. https://doi.org/10.1094/Phyto-64-1518

Schaad N.W., Dianese J.C., 1981. Cruciferous weeds as source of inoculum of *Xanthomonas campestris* in black rot of crucifers. *Phytopathology* 71: 1215–1220. https://doi.org/10.1094/Phyto- 71–1215

Schaad N.W., Sitterly W.R., Humaydan H., 1980. Relationship of incidence of seedborne *Xanthomonas campestris* to black rot of crucifers. *Plant Disease* 64: 91–92. https://doi.org/10.1094/PD-64-91

Schultz T., Gabrielson R.L., 1986. *Xanthomonas campestris* pv. *campestris* in Western Washington crucifer seed fields: occurrence et survival. *Phytopathology* 76: 1306–1309. https://doi.org/10.1094/Phyto-76-1306

Singh D., Rathaur P.S., Vicente J.G., 2016. Characterization, genetic diversity and distribution of *Xanthomonas campestris* pv. *campestris* races causing black rot disease in cruciferous crops of India. *Plant Pathology* 65: 1411–8. https://doi.org/10.1007/s00284-011-0024-0

Swings J.G., Civerolo E.L., 1993. *Xantomonas*, Chapman and Hall, London, UK. ISBN: 0 412 479 434202.

Tajima F., 1996. The amount of DNA polymorphism maintained in a finite population when the neutral mutation rate varies among sites. *Genetics* 143: 1457–1465.

Tamura K., Nei M., 1993. Estimation of the number of nucleotide substitutions in the control region of mitochondrial DNA in humans and chimpanzees. *Molecular Biology and Evolution* 10: 512–526.

Tamura K., Stecher G., Peterson D., Filipsk A., Kumar S., 2013. MEGA6: Molecular evolutionary genetics analysis version 6.0. *Molecular Biology and Evolution* 30: 2725–2729. https://doi.org/10.1093/molbev/mst197

Tancos M.A., Lange H.W., Smart C.D., 2015. Characterizing the genetic diversity of the New York *Clavibacter michiganensis* subsp. *michiganensis* population. *Phytopathology* 10: 169–179. https://doi.org/10.1094/PHYTO-06-14-0178-R

Thieme F., Koebnik R., Bekel T., Berger C., Boch J., Buttner D., … Kaiser D., 2005. Insights into genome plasticity and pathogenicity of the plant pathogenic bacterium. *Xanthomonas campestris* pv. *vesicatoria* revealed by the complete genome sequence. *Journal of Bacteriology* 187: 7254–66. https://doi.org/10.1128/JB.187.21.7254-7266.2005

Tsygankova S.V., Ignatov A. N., Boulygina E. S., Kuznetsov B. B., and Korotkov E. V., 2004. Genetic relationships among strains of *Xanthomonas campestris* pv. *campestris* revealed by novel rep-PCR primers. *European Journal of Plant Pathology* 110: 845–853. https://doi.org/10.1007/s10658-004-2726-7

Vogler A.J., Keys C., Nemoto Y., Colman R.E., Jay Z., Keim P., 2006. Effect of repeat copy number on variable-number tandem repeat mutations in *Escherichia coli* O157: H7. *Journal of Bacteriology* 188: 4253–4263. https://doi.org/10.1128/JB.00001-06

Weller D.M., Saettler A.W., 1980. Evaluation of seedborne *Xanthomonas phaseoli* and *Xanthomonas phaseoli* var. *fuscans* as primary inocula in bean blights. *Phytopathology* 70: 148–152. https://doi.org/10.1094/Phyto-70-148

Wicker E., Lefeuvre P., De Cambiaire J.C., Lemaire C., Poussier S., Prior P., 2012. Contrasting recombination patterns and demographic histories of the plant pathogen *Ralstonia solanacearum* inferred from MLSA. *ISME Journal Multidisciplinary Journal of Microbial Ecology* 6: 961–974. https://doi.org/10.1038/ismej.2011.160

Williams P.H., 1980. Black rot: A continuing threat to world crucifers. *Plant Disease* 64: 736–742. https://doi.org/10.1094/PD-64-736

Young J.M., Parka D.C., Shearmanb H.M., Fargier E., 2008. A multilocus sequence analysis of the genus Xanthomonas. *Systematic and Applied Microbiology* 31: 366–377. https://doi.org/10.1016/j.syapm.2008.06.004

Youseif S.H., Abd El-Megeed F. H., Ageez A., Cocking E C., Saleh S.A, 2014. Phylogenetic multilocus sequence analysis of native rhizobia nodulating faba bean (*Vicia faba* L.) in Egypt. *Systematic and Applied Microbiology* 37: 560–569. https://doi.org/10.1016/j.syapm.2014.10.001

Zaccardelli M., Campanile F., Moretti C., Buonaurio R., 2008. Characterization of Italian populations of *Xanthomonas campestris* pv. *campestri*s using primers based on DNA repetitive sequences. *Journal of Plant Pathology* 90: 375–381.

Phytopathologia Mediterranea
The international journal of the
Mediterranean Phytopathological Union

Firenze University Press
www.fupress.com/pm

Short Notes

Molecular detection and identification of a '*Candidatus* Phytoplasma solani'-related strain associated with pumpkin witches' broom in Xinjiang, China

Xu WANG[1], Chun-Guang WANG[1,*], Xiao-Yan LI[2], Zheng-Nan LI[2,*]

[1] *College of Mechanical and Electrical Engineering, Inner Mongolia Agricultural University, Hohhot 010018, China*
[2] *College of Horticulture and Plant Protection, Inner Mongolia Agricultural University, Hohhot 010018, China*
*Corresponding authors. E-mail: jdwcg@imau.edu.cn; lizhengnan@imau.edu.cn

Summary. Pumpkin plants showing symptoms of witches' broom (PuWB) were observed in Xinjiang Uyghur autonomous region, China, in September 2018. A phytoplasma was detected in symptomatic plants by PCR amplifying portions of the 16S ribosomal and *tuf* genes. In addition, the phylogeny based on these genes sequencing indicated that the PuWB strain clusters with '*Candidatus* Phytoplasma solani' (subgroup 16SrXII-A). Furthermore, based on *in silico* and *in vitro* restriction fragment length polymorphism analyses, the PuWB phytoplasma was confirmed as a '*Ca.* P. solani'-related strain. This was the first record of the occurrence of phytoplasma presence in pumpkins in China, and the first record of 16SrXII phytoplasma infecting pumpkins in the world.

Keywords. *Cucurbita moschata*, pathogen, phylogeny, RFLP.

Citation: X. Wang, C.-G. Wang, X.-Y. Li, Z.-N. Li (2021) Molecular detection and identification of a '*Candidatus* Phytoplasma solani'-related strain associated with pumpkin witches' broom in Xinjiang, China. *Phytopathologia Mediterranea* 60(1): 63-68. doi: 10.36253/phyto-11066

Accepted: October 21, 2020

Published: May 15, 2021

Data Availability Statement: All relevant data are within the paper and its Supporting Information files.

Competing Interests: The Author(s) declare(s) no conflict of interest.

Editor: Assunta Bertaccini, Alma Mater Studiorum, University of Bologna, Italy.

INTRODUCTION

Phytoplasmas are prokaryotic plant pathogens first discovered in 1967 (Doi *et al.*, 1967). They are wall-less *Mollicutes* phylogenetically related to low G+C Gram-positive bacteria (Weisburg *et al.*, 1989). Phytoplasma presence is associated with host symptoms such as phyllody, virescence, and witches' broom (Hogenhout and Segura, 2010). Due to difficulties in establishing axenic cultures of these organisms (Contaldo *et al.*, 2012; Contaldo *et al.*, 2016; Contaldo and Bertaccini, 2019), the methods routinely used for bacterial diagnosis and taxonomy are not yet applicable to phytoplasmas. These organisms are classified in '*Candidatus* Phytoplasma', according to IRPCM (2004). Based on similarities in restriction fragment length polymorphism (RFLP) patterns of 16S rRNA genes, phytoplasmas are also classified into 16Sr groups and subgroups. For the recognition of a new subgroup, the similarity coefficient among the RFLP patterns should be 0.97 or lower (Wei

et al., 2008); for a new group, the threshold value is 0.85 (Zhao *et al.*, 2009). In addition, for finer differentiation of closely related phytoplasma strains, some other genetic *loci* are used, such as the ribosomal protein (*rp*) genes and the elongation factor Tu (*tuf*) genes (Schneider *et al.*, 1997; Lee *et al.*, 1998). More than 30 16Sr groups (16SrI to 16SrXXXVI) and 43 '*Ca.* Phytoplasma' species have been established to date (Bertaccini and Lee, 2018; Bertaccini, 2019). The 16SrXII group, also known as "stolbur", includes '*Ca.* P. australiense', '*Ca.* P. convolvuli', '*Ca.* P. fragariae', '*Ca.* P. japonicum', and '*Ca.* P. solani' (Zhao and Davis, 2016).

Pumpkins (*Cucurbita moschata*) are grown for various uses. Their fruit has high vitamin, amino acids, polysaccharide, fibre and mineral contents, and are extensively used as vegetables, processed food and stock feed in different parts of the world (Kumar *et al.*, 2018). Pumpkin seeds are low in fat and rich in proteins, providing highly nutritional and health protective value for humans (Quanhong and Caili, 2005; Devi *et al.*, 2018). As one of the leading producers of *Cucurbita* spp., China had total production of 7,789,437 tonnes of pumpkins, squash and gourds in 2016 (http://www.fao.org/faostat/en/#data/QC/visualize).

The present study reports pumpkin disease with witches' broom as the main symptom, which occurred in Xinjiang Uyghur autonomous region of China. In this region, viruses, including *Cucumber mosaic virus* and *Zucchini aphid-borne yellows virus*, have been reported as the main pathogens on *Cucurbita* species (Cheng *et al.*, 2013; Peng *et al.*, 2019).

MATERIALS AND METHODS

Samples collection

In September 2018, during a survey on pumpkin diseases in Urumqi, Xinjiang, China, pumpkins (*C. moschata*) with symptoms indicative of phytoplasma presence were observed at a vegetable plot (ca. 1,300 m^2), with incidence of approx. 1.5%. The infected plants had small leaves, short internodes, growth of multiple leaves at each node, and delayed or no fruit development (Figure 1). The disease was named pumpkin witches' broom (PuWB). Samples were collected from symptomatic and asymptomatic plants for phytoplasma detection.

Amplification and sequencing phytoplasma gene specific regions

To detect phytoplasma presence in affected plants, the region encompassing the 16S rRNA, 16S-23S internal transcribed spacer region and partial 5' end of the 23S rRNA genes, and the partial *tuf* gene of phytoplasmas were amplified using PCR. Fresh leaves of the PuWB samples were collected and total nucleic acid extraction was performed using a cetyltrimethylammonium bromide-based (CTAB) method (Kollar *et al.*, 1990). Leaves of asymptomatic pumpkins were used as a negative control. The extracted nucleic acids were then used as templates in PCR assays. The PCR reactions were carried out using rTaq (TaKaRa). The reaction mixture consisted of 2.5 µL of 10× PCR buffer, 1 µL of each primer (10 µM), 2 µL of dNTPs (2.5 mM each), 0.5 µL of the DNA polymerase (5 U μL^{-1}), and 1 µL of DNA template (20 ng μL^{-1}), with added sterilized distilled water up to a final volume of 25 µL. The primers P1/P7 (Deng and Hiruki, 1991; Schneider *et al.*, 1995) followed by the primers R16F2n/R2 (Gundersen and Lee, 1996), amplifying the partial 16S rRNA gene for RFLP analyses, were used in nested PCR; 1 µL of 1:30 sterilized distilled water diluted PCR products from the first amplification was used as template in the nested PCR reactions. The PCR amplification cycling was set up for P1/P7, as described by Lee *et al.* (1998), and for R16F2n/R2, as described by Nejat *et al.* (2010). The primers fTufu/rTufu (Schneider *et al.*, 1997) were used to amplify the partial *tuf* genes, using 94°C for 3 min, 35 cycles each of 94°C for 30 s, 50°C for 30 s and 72°C for 1 min, and a final extension at 72°C for 10 min.

The PCR products of the expected sizes were purified using a QIAquick gel extraction kit (Qiagen), ligated onto pMD18-T vector (TaKaRa), and competent cells of *Escherichia coli* strain JM109 were transformed. Colonies containing recombinant plasmids were screened

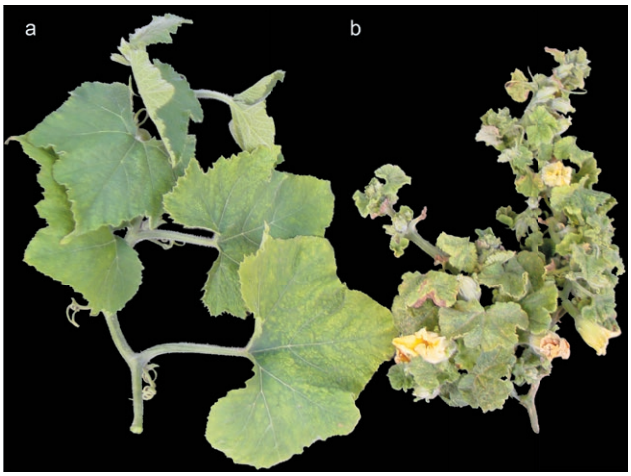

Figure 1. Symptoms on pumpkin. a) a healthy pumpkin vine; b) pumpkin vine exhibiting witches' broom symptom.

using agar plates of LB medium containing ampicillin (100 μg mL^{-1}) and X-Gal. The inserts were sequenced by TaKaRa. The M13 forward primer (-47): CGCCAGGGTTTTCCCAGTCACGAC and M13 reverse primer (-48): AGCGGATAACAATTTCACACAGGA were used for sequencing the inserts from both ends, which gave approx. 1.5 times of coverage for P1/P7 amplicons and 2 times of coverage for the *tuf* gene. For each gene from each sample, the inserts of three colonies were selected for sequencing.

RFLP and phylogenetic analyses

To identify the detected phytoplasma, RFLP patterns of the R16F2n/R2 region were analyzed, and phylogeny was determined based on sequences of partial ribosomal and *tuf* genes. To re-construct the phylogenetic tree, the 16S partial ribosomal sequences of phytoplasmas enclosed in subgroups 16SrXII-A to -K, and in another 11 ribosomal groups, were selected. A total of 15 *tuf* gene sequences from phytoplasmas in group 16SrXII and two from group 16SrI were used to infer the tree of *tuf* genes. Phylogenetic trees were built using the software MEGA7.0, by aligning sequences with ClustalW and using the neighbour-joining method with a bootstrapping of 1000 pseudoreplicates. In virtual RFLP analysis, the sequence of the R16F2n/R2 region of the detected phytoplasma was submitted to the online tool *i*Phyclassifier (https://plantpathology.ba.ars.usda.gov/cgi-bin/resource/iphyclassifier_legacy.cgi) for virtual gel image production and similarity coefficient calculations. The gel purified PCR products of the R16F2n/R2 amplicons were digested with the *Alu*I restriction enzyme according to the manufacturer's instruction (TaKaRa) and separated in a 2% agarose gel.

RESULTS AND DISCUSSION

Using the primers P1/P7, PCR fragments of approx. 1.8 kb were amplified from two PuWB samples (PuWB1 and PuWM2), which were of identical size to the P1/P7 region of phytoplasmas. The subsequent nested PCR used the primers R16F2n/R2 generated fragments of approx. 1.2 kb. PCR products of approx. 0.8 kb were of identical size to the partial *tuf* gene of phytoplasmas and were produced with the primers fTufu/rTufu. After cloning and sequencing, six sequences of the P1/P7 region (three from the PuWB1 and three from the PuWB2) were identical to each other, and were each of size 1,783 bp. The consensus sequence was deposited in GenBank under the accession number MH731275.

Six single colonies (three for PuWB1 and three for PuWB2) of the 0.8 kb fragment were also sequenced. The three sequences from the PuWB1 were identical to each other, and the consensus sequence was deposited under the accession number MK770825. One of the three sequences from the PuWB2 showed two site polymorphisms at nucleotide positions 62 and 758 with the other two, and this was deposited under the accession number MK770826. The consensus sequence for the other two strains was deposited under the accession number MK770827. All the three *tuf* gene sequences were of size 842 bp and had 99.8% similarity (840 bp / 842 bp) to each other. BLASTn searches for homologous gene sequences indicated that the obtained P1/P7 region sequence was homologous to those of phytoplasmas classified in the 16SrXII group, having the greatest nucleotide sequence similarity of 99.5% (1772 nt / 1781 nt) with '*Ca*. P. solani' strain SX-CP from *Salvia miltiorrhiza* from Shanxi Province, China (GenBank accession number KT844648). The *tuf* gene sequences showed the greatest nucleotide sequence similarity 99.6% (840 nt / 843 nt) to that of '*Ca*. P. solani' strain PFY from paper flower from China (GenBank accession number KC481242).

On the phylogenetic tree of the 16S ribosomal gene region, the sequence of the PuWB strain clustered with members classified in subgroups 16SrXII-J (GenBank accession number FJ409897) and 16SrXII-A (GenBank accession number AJ964960) (Figure 2a). On the tree of *tuf* genes, the PuWB strain clustered with '*Ca*. P. solani' strain PFY (GenBank accession number KC481242, 16SrXII-A) (Figure 2b).

Based on the virtual RFLP patterns generated using *i*Phyclassifier, the PuWB strain was different from the described representatives of subgroups 16SrXII-A to 16SrXII-K at the restriction site *Alu*I (Figure 3b). In addition, the phytoplasma had similarity coefficients ranging from 0.74 to 0.96 with the representatives of 16SrXII-A to 16SrXII-K subgroups (Supplementary table 1). These results indicated the possible occurrence of a novel subgroup in the 16SrXII group. Furthermore, the RFLP pattern generated using *Alu*I on the amplicons was identical to the virtual pattern (Figure 3a), confirming the reliability of virtual results. The PuWB phytoplasma is therefore considered a '*Ca*. P. solani'-related strain.

The phytoplasmas in the 16SrXII group are widely distributed, and the identification of the PuWB strain described here expands knowledge their genetic diversity. Phytoplasmas infecting *Cucurbita* spp. have been previously reported in several countries including Brazil, Japan, India, Iran, Egypt, Argentina, and have been

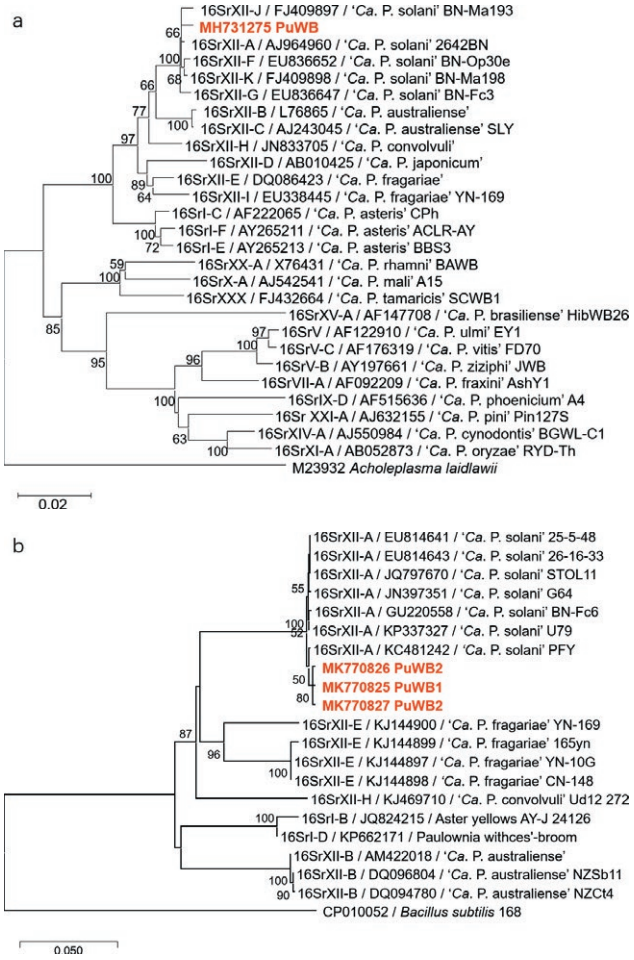

Figure 2. Phylogenies of PuWB phytoplasma strains and other phytoplasmas based on two conserved gene loci. The phylogenetic trees were reconstructed based on, a) the R16F2n/R2 regions, and b) the partial *tuf* genes of phytoplasmas. The sequences obtained in the present study are indicated in red font. Bootstrap values greater than 50% are shown. Bars = number of substitutions per base.

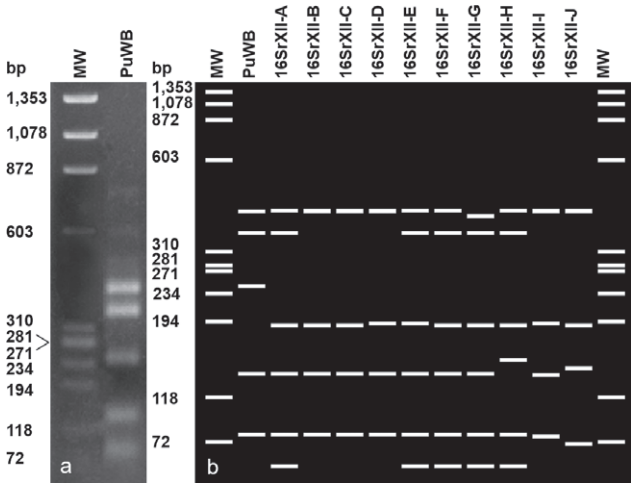

Figure 3. The RFLP patterns of the R16F2n/R2 region of the PuWB phytoplasma. a) PCR products digested using *Alu*I. b) *i*Phyclassifier generated virtual patterns of the PuWB phytoplasma and members of subgroups 16SrXII-A to -K. MW, φX174 DNA digested with *Hae*III.

associated with host symptoms of yellows, virescence, stunting, witches' broom and phyllody. The detected phytoplasmas belong to several ribosomal groups, including 16Sr I, -II and -III (Tanaka *et al.*, 2000; Montano *et al.*, 2006; Omar and Foissac, 2012; Galdeano *et al.*, 2013; Salehi *et al.*, 2015; Rao *et al.*, 2017). Identification of the PuWB strain in pumpkins showing witches' broom symptom in Xinjiang, China is the first record of a phytoplasma disease of pumpkin in China, and a first international record of a 16SrXII phytoplasma infecting pumpkin.

The occurrence of phytoplasmas in group 16SrXII has been reported previously in China, in *Artemisia scoparia* associated with witches' broom (Yu *et al.*, 2016) and *Peonia suffruticosa* associated with yellows symptoms in Shandong (Gao *et al.*, 2013), and *Salvia miltiorrhiza* with red-leaf symptoms in Shaanxi (Yang *et al.*, 2016). In addition, a phytoplasma in group 16SrII was detected in *Senna surattensis* stem fasciation (Wu *et al.*, 2012), and phytoplasmas related to '*Ca*. P. fragariae' were identified in *Solanum tuberosum* showing purplish leaves and aerial tuber formation (Cheng *et al.*, 2012).

The pumpkin plants exhibiting the symptom of witches' broom were mainly observed in Xinjiang, with incidence of approx. 1.5%. It is important, however, to record this disease in China for epidemiological reasons. Although the spread of PuWB was not fully evaluated, it is known that insects in *Auchenorrhyncha* are responsible for the transmission of phytoplasmas. These include members of *Cercopidae*, *Cixiidae*, *Derbidae*, *Delphacidae*, *Cicadellidae* and *Psyllidae* (Weintraub and Beanland, 2006). These insects were reported in Xinjiang, in particular leafhoppers (*Cicadellidae*) and psyllids (*Psyllidae*) (Zhang *et al.*, 2013; Chen *et al.*, 2018), and these insects are likely to disseminate PuWB phytoplasma-associated diseases, increasing the risk of severe epidemics and reductions of *C. moschata* production.

ACKNOWLEDGEMENT

This research was funded by the Research Start-up Funds for High-level Researchers in Inner Mongolia Agricultural University (Grant Numbers NDYB2018-3, NDYB2019-1), and the Natural Science Foundation of Inner Mongolia, China (Grant Numbers 2019MS03021).

COMPLIANCE WITH ETHICAL STANDARDS

Funding: This study was funded by the Research Start-up Funds for High-level Researchers in Inner Mongolia Agricultural University (Grant Numbers NDYB2018-3, NDYB2019-1), and the Natural Science Foundation of Inner Mongolia, China (Grant No. 2019MS03021).

Ethical approval: This article does not contain any studies with human participants or animals performed by any of the authors.

Informed consent: Informed consent was obtained from all individual participants included in the described research.

LITERATURE CITED

Bertaccini A., Lee I-M., 2018. Phytoplasmas: an update. In: Phytoplasmas: Plant Pathogenic Bacteria-I (G.P. Rao, A. Bertaccini, N. Fiore, L.W. Liefting, eds.), Springer, Singapore, 1–29.

Bertaccini A., 2019. The phytoplasma classification between '*Candidatus* species' provisional status and ribosomal grouping system. *Phytopathogenic Mollicutes* 9: 1-2.

Chen P., Liu Q-Z., Qiao X-F., Wang J-W., Zhang T., 2018. Identification and phylogenetic analysis of pear psyllids (Hemiptera: Psyllidae) in Chinese pear orchards. *Journal of Economic Entomology* 111: 2908–2913.

Cheng M., Dong J., Zhang L., Laski P., Zhang Z., McBeath J., 2012. Molecular characterization of stolbur group subgroup E (16SrXII-E) phytoplasma associated with potatoes in China. *Plant Disease* 96: 1372–1372.

Cheng C., Liang X., Xiang B., Zheng Y., 2013. Analysis of Cucumber mosaic virus satellite RNA and RNA3 sequence of processing tomato and pumpkin in Shihezi of Xinjiang. *Acta Agriculturae Boreali-Occidentalis Sinica* 5: 83–90.

Contaldo N., Bertaccini A., Paltonieri S., Windsor H.M., Windsor G.D., 2012. Axenic culture of plant pathogenic phytoplasmas. *Phytopathologia Mediterranea* 51: 607–617.

Contaldo N., Satta E., Zambon Y., Paltrinieri S., Bertaccini A., 2016. Development and evaluation of different complex media for phytoplasma isolation and growth. *Journal of Microbiological Methods* 127: 105–110.

Contaldo N., Bertaccini A., 2019. Phytoplasma Cultivation. In: *Phytoplasmas: Plant Pathogenic Bacteria-III* (A. Bertaccini, K. Oshima, M. Kube, G. Rao, eds.), Springer, Singapore, 89–104.

Deng S., Hiruki C., 1991. Genetic relatedness between two nonculturable mycoplasmalike organisms revealed by nucleic acid hybridization and polymerase chain reaction. *Phytopathology* 81: 1475–1479.

Devi N., Prasad R., Sagarika N., 2018. A review on health benefits and nutritional composition of pumpkin seeds. *International Journal of Chemical Studies* 6: 1154–1157.

Doi Y., Teranaka M., Yora K., Asuyama H., 1967. Mycoplasma- or PLT Group-like microorganisms found in the phloem elements of plants infected with mulberry dwarf, potato witches' broom, aster yellows, or paulownia witches' broom. *Japanese Journal of Phytopathology* 33: 259–266.

Galdeano E., Guzmán F.A., Fernández F., Conci L.R., 2013. Genetic diversity of 16SrIII group phytoplasmas in Argentina. Predominance of subgroups 16SrIII-J and B and two new subgroups 16SrIII-W and X. *European Journal of Plant Pathology* 137: 753–764.

Gao Y., Qiu P.P., Liu W.H., Su W.M., Gai S.P., Liang Y.C., Zhu X.P., 2013. Identification of '*Candidatus* Phytoplasma solani' associated with tree peony yellows disease in China. *Journal of Phytopathology* 161: 197–200.

Gundersen D.E., Lee I-M., 1996. Ultrasensitive detection of phytoplasmas by nested-PCR assays using two universal primer pairs. *Phytopathologia Mediterranea* 35: 144–151.

Hogenhout S.A., Segura M., 2010. Phytoplasma genomics, from sequencing to comparative and functional genomics-What have we learnt. In: *Phytoplasmas: Genomes, Plant Hosts Vectors* (P.G. Weintraub, P. Jones, eds.), CAB International, Wallingford, UK, 19–36.

IRPCM, 2004. '*Candidatus* Phytoplasma', a taxon for the wall-less, non-helical prokaryotes that colonize plant phloem and insects. *International Journal of Systematic Evolutionary Microbiology* 54: 1243–1255.

Kollar A., Seemüller E., Bonnet F., Saillard C., Bové J-M., 1990. Isolation of the DNA of various plant pathogenic mycoplasmalike organisms from infected plants. *Phytopathology* 80: 233–237.

Kumar V., Mishra D., Yadav G., Yadav S., Kumar S., 2018. Determining relationships between yield and biochemical traits in pumpkin. *The Pharma Innovation Journal* 7: 14–18.

Lee I-M., Gundersen-Rindal D.E., Davis R.E., Bartoszyk I.M., 1998. Revised classification scheme of phytoplasmas based on RFLP analyses of 16S rRNA and ribosomal protein gene sequences. *International Journal of Systematic Evolutionary Microbiology* 48: 1153–1169.

Montano H., Brioso P., Pimentel J., Figueiredo D., Cunha Junior J., 2006. *Cucurbita moschata*, new phytoplasma host in Brazil. *Journal of Plant Pathology* 88: 226.

Nejat N., Sijam K., Abdullah S.N.A., Vadamalai G., Dickinson M., 2010. Molecular characterization of an aster yellows phytoplasma associated with proliferation of periwinkle in Malaysia. *African Journal of Biotechnology* 9: 2305–2315.

Omar A.F., Foissac X., 2012. Occurrence and incidence of phytoplasmas of the 16SrII-D subgroup on solanaceous and cucurbit crops in Egypt. *European Journal of Plant Pathology* 133: 353–360.

Peng B., Kang B., Wu H., Liu L., Liu L., Fei Z., ... Gu Q., 2019. Detection and genome characterization of a novel member of the genus *Polerovirus* from zucchini (*Cucurbita pepo*) in China. *Archives of Virology* 164: 2187–2191.

Quanhong L., Caili F., 2005. Application of response surface methodology for extraction optimization of germinant pumpkin seeds protein. *Food Chemistry* 92: 701–706.

Rao G., Gopala G.S., Rao A., 2017. First report of a '*Candidatus* Phytoplasma asteris'-related strain (16SrI-B subgroup) associated with witches' broom disease in *Cucurbita pepo* in India. *New Disease Reports* 35: 33.

Salehi M., Siampour M., Esmailzadeh Hosseini S., Bertaccini A., 2015. Characterization and vector identification of phytoplasmas associated with cucumber and squash phyllody in Iran. *Bulletin of Insectology* 68: 311–319.

Schneider B., Seemüller E., Smart C., Kirkpatrick B., 1995. Phylogenetic classification of plant pathogenic mycoplasma-like organisms or phytoplasmas. In: *Molecular and diagnostic procedures in Mycoplasmology* (S. Razin, J. Tully, ed.), Academic Press, New York, USA, 369–380.

Schneider B., Gibb K.S., Seemüller E., 1997. Sequence and RFLP analysis of the elongation factor Tu gene used in differentiation and classification of phytoplasmas. *Microbiology* 143: 3381–3389.

Tanaka M., Osada S., Matsuda I., 2000. Transmission of rhus (*Rhus javanica* L.) yellows by Hishimonus sellatus and host range of the causal phytoplasma. *Journal of General Plant Pathology* 66: 323–326.

Wei W., Lee I-M, Davis R.E., Suo X., Zhao Y., 2008. Automated RFLP pattern comparison and similarity coefficient calculation for rapid delineation of new and distinct phytoplasma 16Sr subgroup lineages. *International Journal of Systematic Evolutionary Microbiology* 58: 2368–2377.

Weintraub P.G., Beanland L., 2006. Insect vectors of phytoplasmas. *Annual Review of Entomology* 51: 91–111.

Weisburg W., Tully J., Rose D., Petzel J., Oyaizu H., Yang D., ... van Etten J., 1989. A phylogenetic analysis of the mycoplasmas: basis for their classification. *Journal of Bacteriology* 171: 6455–6467.

Wu W., Cai H., Wei W., Davis R., Lee I-M., Chen H., Zhao Y., 2012. Identification of two new phylogenetically distant phytoplasmas from *Senna surattensis* plants exhibiting stem fasciation and shoot proliferation symptoms. *Annals of Applied Biology* 160: 25–34.

Yang R., Wang G., Wang S., Zhang D., Wei L., Chen H., ... Hu X., 2016. Molecular identification and diversity of '*Candidatus* Phytoplasma solani' associated with red-leaf disease of *Salvia miltiorrhiza* in China. *Journal of Phytopathology* 164: 882–889.

Yu X., Ai C., Wang J., Fu L., An M., Wang H., Sun Q., 2016. First report of a 16SrXII-A subgroup phytoplasma associated with *Artemisia scoparia* witches' broom disease in China. *Plant Disease* 100: 1494–1494.

Zhang Y., Lu L., Yong K.J., 2013. Review of the leafhopper genus *Macrosteles* Fieber (Hemiptera: Cicadellidae: Deltocephalinae) from China. *Zootaxa* 3700: 361–392.

Zhao Y., Wei W., Lee I-M., Shao J., Suo X., Davis R.E., 2009. Construction of an interactive online phytoplasma classification tool, *i*PhyClassifier, and its application in analysis of the peach X-disease phytoplasma group (16SrIII). *International Journal of Systematic Evolutionary Microbiology* 59: 2582–2593.

Zhao Y., Davis R.E., 2016. Criteria for phytoplasma 16Sr group/subgroup delineation and the need of a platform for proper registration of new groups and subgroups. *International Journal of Systematic Evolutionary Microbiology* 66: 2121–2123.

Phytopathologia Mediterranea
The international journal of the
Mediterranean Phytopathological Union

Firenze University Press
www.fupress.com/pm

Research Papers

Reduced fitness cost and increased aggressiveness in fenhexamid-resistant *Botrytis cinerea* field isolates from Chile

Marcela ESTERIO*, Claudio OSORIO-NAVARRO, Madelaine AZÓCAR, Charleen COPIER, Mauricio RUBILAR, Lorena PIZARRO+, Jaime AUGER

Departamento de Sanidad Vegetal, Facultad de Ciencias Agronómicas, Universidad de Chile, Santiago, Chile
+ *Current affiliation: Instituto de Ciencias Agroalimentarias, Animales y Ambientales (ICA3), Universidad de O'Higgins, Ruta 90 km 3, San Fernando, Chile*
*Corresponding author. E-mail: mesterio@uchile.cl

OPEN ACCESS

Citation: M. Esterio, C. Osorio-Navarro, M. Azócar, C. Copier, M. Rubilar, L. Pizarro, J. Auger (2021) Reduced fitness cost and increased aggressiveness in fenhexamid-resistant *Botrytis cinerea* field isolates from Chile. *Phytopathologia Mediterranea* 60(1): 69-77. doi: 10.36253/phyto-10723

Accepted: November 3, 2020

Published: May 15, 2021

Data Availability Statement: All relevant data are within the paper and its Supporting Information files.

Competing Interests: The Author(s) declare(s) no conflict of interest.

Editor: Tito Caffi, Università Cattolica del Sacro Cuore, Piacenza , Italy.

Summary. Disease management programmes in Chilean table grape vineyards use the hydroxyanilide fenhexamid as a pivotal fungicide for *Botrytis cinerea* control. However, fenhexamid-resistant populations of this pathogen have progressively increased in vineyards under fungicide use. *Botrytis cinerea* isolates were collected in 'Thompson Seedless' vineyards under fenhexamid control programmes (>two sprays per season) from three regions of Central Chile, during the 2013–2014, 2014–2015 and 2015–2016 growing seasons. Focusing on the 2015–2016 growing season when the greatest level of resistance was measured, only 8% of recovered isolates were sensitive to fenhexamid with 92% of isolates exceeding the sensitivity threshold for mycelium growth. All fenhexamid resistant isolates analyzed carried a mutation in the *Erg27* gene, which encodes for 3-keto reductase (3-KR) enzyme. The largest proportion of isolates presented a single-point mutation, leading to a substitution of phenylalanine by serine or isoleucine in the 412 residue of 3-KR (*erg27*^{F412S}, 27%; *erg27*^{F412I}, 48%). Substitution by valine in this position was observed in a lower proportion of isolates (*erg27*^{F412V}, 2%). In contrast to a previous report indicating high fitness cost in isolates carrying *erg27*^{F412S} or *erg27*^{F412I}, mycelium growth and sclerotia development under different restrictive temperatures were not affected compared to wildtype *Erg27* ^{F412} in Chilean mutant isolates. At 0°C, *erg27*^{F412S} and *erg27*^{F412I} generated larger lesions than *erg27*^{F412V} and *Erg27*^{F412} isolates in wounded and unwounded berry assays. Another five mutations were detected in low-resistance *Erg27* ^{F412} isolates; one was a previously unreported mutation: *erg27*^{R330P}. This study has demonstrated a significant loss of sensitivity to fenhexamid, limited fitness cost and high aggressiveness levels (*erg27*^{F412S} and *erg27* ^{F412I}) in field isolates carrying *Erg27* mutations, giving dirctions for the design of *Botrytis* control programmes based on fenhexamid.

Keywords: *Botrytis* fitness cost, *Erg27* mutations, resistance, increased virulence.

INTRODUCTION

Gray mold (caused by *Botrytis cinerea* Pers.: Fr.) is the most economically important disease in Chilean table grape production. *Botrytis cinerea* infection is favoured under wet conditions with temperatures below 22°C; it is a cool-season disease. Environmental conditions between late winter and spring in Chile usually provide the requirements for *B. cinerea* infection in the table grape growing area, causing blossom blight during the bloom period at the beginning of the season. *Botrytis cinerea* infections may also remain latent (Keller *et al*., 2003; Viret *et al*., 2004), leading to disease appearance after harvest either during storage or after purchase by consumers.

Control of *B. cinerea* on diverse crops is commonly achieved with combinations of pesticide and agronomic practices. Agronomic practices alone cannot prevent the disease in central Chile, so chemical treatments must be applied (Esterio *et al*., 2011). Because of the epidemiological traits of *B. cinerea*, disease forecasting models are not commonly used. Instead, treatments are applied at fixed phenological plant stages: bloom, bunch closure, veraison, and pre-harvest. However, more sprays may be scheduled under specific weather events that increase the risks of disease outbreaks. Among the wide range of fungicides registered for use against *B. cinerea*, fenhexamid, a hydroxyanilide derivate, has become a key component of gray mold management in Chilean table grape vineyards.

The sterol-3-ketoreductase enzyme (3-KR) encoded by the *Erg27* gene is the biological target of fenhexamid. This enzyme is required for C4 demethylation during ergosterol biosynthesis (Debieu *et al*., 2001). Inhibition of 3-KR leads to ergosterol depletion and accumulation of cytotoxic-ergosterol precursors, triggering defects in central cellular processes (Akins, 2005). Resistance to fenhexamid in *B. cinerea* has been reported in vineyards from Europe and the United States of America (Fillinger and Walker, 2016), and is linked to several mutations in the *Erg27* gene. High level of resistance occurs in isolates carrying single point mutations in codon 412 (Fillinger *et al*., 2008).

Since the introduction of fenhexamid in 1999, this fungicide has been widely used to *B. cinerea* control in table grape vineyards in Chile, being applied mainly during the grapevine bloom period. Fenhexamid resistance was reported in *B. cinerea* isolates from the Central Valley of Chile in the 2006–2007 growing season (Esterio *et al*., 2007; Esterio *et al*., 2011). Therefore, alternation of fungicides with different modes of action has been the strategy widely used for *B. cinerea* chemical control, in order to reduce the selection pressure.

Acquisition of high-level specific resistance to fenhexamid in *B. cinerea* has been described in isolates carrying mutation in codon 412 of *Erg27*, and has been associated with important decreases in pathogen fitness, including reduced conidium germination, myceliuml growth, and sclerotium development. Consequently, field problems associated with loss of efficacy of fenhexamid have not been reported to date (Ziogas *et al*., 2003; De Guido *et al*., 2007; Billard *et al*., 2012). In recent years, however, loss of sensitivity to fenhexamid has progressively and persistently increased in table grape fields in central Chile (Esterio *et al*., 2017). In order to maintain and promote fenhexamid effectiveness, the fitness cost of fenhexamid-resistance isolates from central Chile must be determined, and these should be included during construction of comprehensive and updated *B. cinerea* control programmes. For this purpose, *B. cinerea* isolates were recovered from six 'Thompson Seedless' vineyards managed with at least two fenhexamid applications per growing season to: (i) assess their sensitivity of the isolates to fenhexamid; (ii) determine their *Erg27* genotype; and (iii) evaluate fitness parameters.

MATERIALS AND METHODS

Botrytis cinerea *isolation and culture media*

Botrytis cinerea isolates were recovered during the 2013–2014, 2014–2015 and 2015–2016 growing seasons, from grapevine flowers collected at the full bloom and berries with 16.5° Brix stages, from six cv. Thompson Seedless vineyards located in the Chilean Central Valley, covering the three most important table grape production areas of Valparaíso Region (VR), Metropolitan Region (MR) and O'Higgins Region (OR). These vineyards had been undergoing field programmes with high fungicide pressure, being sprayed at least twice with fenhexamid per growing season. *Botrytis cinerea* single-conidium cultures isolated from these three regions were grown on malt yeast agar (20 g L^{-1} malt extract, 5 g L^{-1} Bacto yeast extract, 12.5 g L^{-1} agar) maintained at 20°C in constant darkness until conidiation. In total, 132 isolates from VR, 118 from MR, and 158 from OR were used in this study.

Fenhexamid sensitivity assay

Fenhexamid sensitivity was evaluated *in vitro* using colony growth tests. Colony growth tests were made on plates containing Sisler synthetic medium (2 g L^{-1}

KH_2PO_4, 1.5 g L^{-1} K_2HPO_4, 1 g L^{-1} $(NH_4)_2$ SO_4, 0.5 g L^{-1}, $MgSO_4 \cdot 7H_2O$, 10 g L^{-1} glucose, 2 g L^{-1} yeast extract and 12.5 g L^{-1} agar) (Leroux *et al*., 1999) supplemented with different concentrations of fenhexamid (0; 0.03; 0.1; 0.3; 1; 3 and 10 mg L^{-1}). Four-day-old mycelium plugs were seeded on the plates, and the cultures were then kept for 5 days at 20°C in darkness. Colony growth was determined by measuring the diameter of the resulting colonies. Three replicate plates were analyzed for each fenhexamid concentration in colony growth experiments. EC_{50} values (effective inhibitory dose that gave half-maximum inhibitory responses) were calculated for each isolate using the Minitab Version 12 statistical software program.

Erg27 genotyping: amplification and sequencing

Botrytis cinerea genomic DNA was isolated from 7-day-old mycelia using the DNeasy Plant mini kit (QIAGEN). A fragment of the *Erg27* gene was amplified using primers erg1800down and erg27End, which amplify a 1052 pb fragment, previously described by Fillinger *et al*. (2008). The PCR mix was composed of 50-100 ng genomic DNA, 1X GoTaq® Green Master Mix (Promega) and 0.2 µM each primer; 25µL volume was completed with nanopure water (Promega). The PCR product was purified and used for sequencing (Macrogen). Identification of *Erg27* genotypes was performed by alignment of the sequences using BioEdit software (Hall, 1999).

Pathogenicity test

To assess the pathogenicity on grape berries *B. cinerea* isolates were inoculated onto wounded and unwounded berries of 'Thompson Seedless', at harvest stage based on soluble solids content (16.5°Brix). The berries were washed in 1% sodium hypochlorite solution for 0.5 min, rinsed twice with sterile distilled water and allowed to dry under a laminar flow hood. Subsequently, a 10 µL droplet of *B. cinerea* isolate suspension (10^6 conidia mL^{-1}) was inoculated on the surface of each unwounded or wounded berries. Wounding was made by puncturing each berry with a sterile needle to a depth of 2 mm. Inoculated berries were incubated at 0 or 20°C in sealed humidity chambers (80% relative humidity) for 4 days and the diameter of the gray mold lesion on each berry was measured. Eighteen berries were used for each *Erg27* genotype separated into three replicates. The experiment was repeated twice independently, firstly using table grape berries from seasons 2016–2017 and and second from 2018–2019.

Evaluations of colony growth, conidium production and sclerotium development

Six isolates for each identified *Erg27* genotype were used in this study, including wild type (no mutations in the *Erg27* gene). The exception was for *erg27*^{F412V}, where only three isolates were found. In each case, 4-days-old non-sporulating mycelium plugs grown in Potato Dextrose Agar (PDA) were transferred onto a fresh PDA plate for phenotype evaluation. Three plates were used for each genotype in two independent experimental repetitions.

Mycelium radial growth was evaluated for 4 or 5 days in continuous darkness, under three temperature conditions: 15, 20 or 25°C. Conidium production was evaluated after 17 days of continuous colonial growth in darkness at 20°C. For each evaluation, total sporulating mycelium was recovered in a vial with 15 mL of sterile water, which was stirred, and conidia concentration was determined using a haematocytometer. For sclerotium development, plates were incubated for 40 days in darkness at 5 or 20°C. Number and mass of sclerotia in each plate were recorded, and the Sclerotium Index was defined as the ratio of total number of sclerotia to total sclerotium mass per plate.

Statistical analyses

Statistical analyses were carried out using ANOVA and the Bonferroni *post hoc* test in InfoStat software (Di Rienzo *et al*., 2015).

RESULTS

Sensitivity of Botrytis cinerea *isolates to fenhexamid*

Sensitivity to fenhexamid of each isolate was evaluated through the mycelium growth EC_{50}. The isolates were then classified as sensitive (Fen^S) or resistant (Fen^R) to fenhexamid, using the recommended cutoff value for field applications of fenhexamid (0.17 mg L^{-1}; Teldor-Bayer). Thirty-six isolates were obtained from VR vineyards in the 2013–2014 season and 11% of these were Fen^S, 72 isolates were obtained in 2014–2015 and 6% were Fen^S, and 24 isolates were obtained in 2015–2016 and 13% were Fen^S (Figure 1A, Table 1). In the 2013–2014, 2014–2015 and 2015–2016 seasons, 35, 36, and 47 isolates from the MR vineyards were analyzed, and 23%, 25%, and 0% of them were Fen^S (Figure 1B, Table 1). Of the isolates from OR vineyards 40, 72, and 46 isolates were obtained in the seasons 2013–2014, 2014–2015 and 2015–2016, respectively, among them 18%, 15% and 19% presented sensitivity to the fungicide (Figure 1C, Table

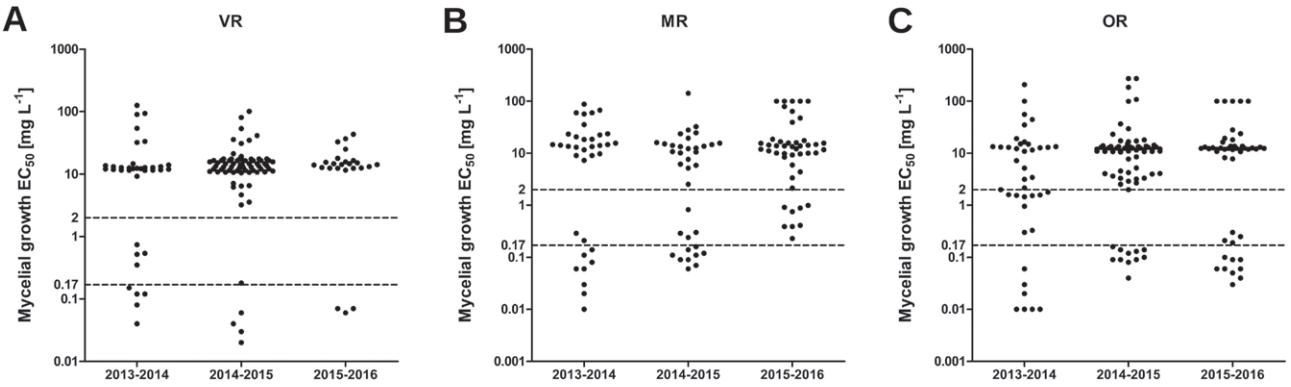

Figure 1. Sensitivity to fenhexamid of *Botrytis cinera* isolates obtained in the 2013-2014, 2014-2015 and 2015-2016 growing seasons from three regions of the Chilean Central Valley: Valparaíso Region (VR; N = 132), Metropolitan Region (MR; N = 118), and O'Higgins Region (OR; N = 158). Fenhexamid effective concentration (mg L^{-1}) was evaluated by EC_{50} value (effective concentration that reduces mycelial growth by 50%). Isolates were considered as low resistance when 0.17 mg L^{-1} > EC_{50} ≥ 2mg L^{-1} and high resistance when the EC_{50} ≥ 2 mg L^{-1}; bothof these sensitivity limits are shown by dashed lines.

1). Resistance to fenhexamid was classified as low when 0.17 mg L^{-1} > EC_{50} ≥ 2 mg L^{-1} and high when EC_{50}≥ 2 mg L^{-1}, considering the cutoff value described by Fillinger *et al*. (2008). The frequency of fenhexamid-resistant and highly resistant isolates in the *B. cinerea* population analysed in this study increased with time and this occurred in the three geographical regions under study.

Genetic characterization of Erg27 *in* Botrytis cinerea *isolates*

Mutations in wild type *Erg27* allele in *B. cinerea* isolates from the field and laboratory-generated strains have been associated with different ranges of loss of sensitivity to fenhexamid (Fillinger *et al*. 2008; Esterio *et al*. 2011; Grabke *et al*. 2013; Amiri and Peres, 2014). In particular, mutations in 412 codon of *Erg27* trigger high resistance to this fungicide (Fillinger *et al*., 2008; Debieu and Leroux, 2015; Fillinger and Walker, 2016).

The *Erg27* genotypes of isolates from the three regions (2015–2016 season) were evaluated in order to find a genetic factor associated with resistance to fenhexamid. Of a total of 24 isolates from the VR region, 29% carried a serine substitution (*erg27*^{F412S}) and 58% the isoleucine substitution (*erg27*^{F412I}) at position 412, and only 13% of total isolates maintained phenylalanine at the 412

Table 1. Sensitivity to fenhexamid of *Botrytis cinerea* isolates from Central Chile, from Valparaíso Region (VR), Metropolitan Region (MR) and O'Higgins Region (OR).

Region	Season	Total isolates	% S[a]	% LR[b]	% HR[c]	*Mean* EC_{50}[d]	*Min* EC_{50}[e]	*Max* EC_{50}[f]
	2013–14	36	11.11	11.11	77.78	19.16	0.04	125.50
VR	2014–15	72	5.56	1.39	93.05	16.19	0.02	100.70
	2015–16	24	12.50	0.00	87.50	15.73	0.06	43.26
	2013–14	35	22.86	5.71	71.43	18.67	0.01	87.08
MR	2014–15	36	25.00	11.11	63.89	12.75	0.06	142.30
	2015–16	47	0.00	17.39	82.61	23.43	0.23	100.00
	2013–14	40	17.50	22.50	60.00	16.41	0.01	208.10
OR	2014–15	72	15.28	1.39	83.33	21.80	0.04	273.60
	2015–16	46	19.15	8.51	72.34	19.05	0.03	100.00

[a] Frequency occurrence (%) of sensitive isolates (EC_{50} < 0.17 mg L^{-1}).
[b] Frequency occurrence (%) of low-resistant isolates (0.17 mg L^{-1} < EC_{50} ≤ 2.0 mg L^{-1}).
[c] Frequency occurrence (%) of high-resistant isolates (EC_{50} > 2.0 mg L^{-1}).
[d] Mean EC_{50} (mg L^{-1}).
[e] Minimum value of EC_{50} (mg L^{-1}).
[f] Maximum value of EC_{50} (mg L^{-1}).

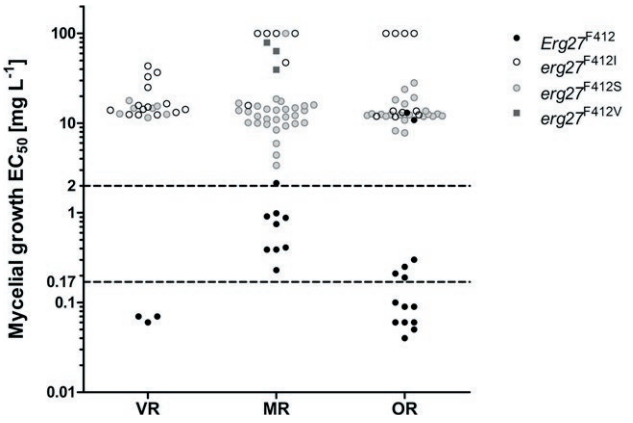

Figure 2. Fenhexamid sensitivity levels of *Botrytis cinerea* isolates carrying a mutation *Erg27*^{F412} from Valparaíso Region (VR; N =24), Metropolitan Region (MR; N = 47) and O'Higgins Region (OR; N = 46) in the 2015-2016 growing season, based on EC_{50} values (effective concentration that reduced mycelium growth by 50%). Sensitivity limits are shown by dashed lines: low resistance = 0.17 mg L^{-1} > EC_{50} ≥ 2 mg L^{-1} and high resistance = EC_{50}≥ 2 mg L^{-1}.

position (*Erg27*^{F412}) (Table 2, Figure 2). As expected, all isolates from this region carrying the mutations in the 412 position of *Erg27* were highly resistant to fenhexamid, and the isolates without mutation in this codon were fenhexamid sensitive. From the MR region, 47 isolates were tested. Substitutions *erg27*^{F412S} was at frequency of 62%, and *erg27*^{F412I} at 13%, while 19% of the isolates had no mutation in *Erg27*^{F412} (Table 1, Figure 2). Three isolates (6%) carried a non-common mutation of valine instead phenylalanine at 412 position (*erg27*^{F412V}, 6%) (Table 1, Figure 2). All the highly resistant isolates in this population had mutations in codon 412 of *Erg27*, as expected. However, nine isolates with no mutation in *Erg27*^{F412} showed some resistance to fenhexamid, suggesting that mutations in other positions of *Erg27* or on another gene could be responsible for the resistance.

In the 46 isolates from OR, 48% carried the *erg27*^{F412S} mutation and 22% the *erg27*^{F412I} mutation, exhibiting high resistance to fenhexamide (Table 1, Figure 2). In this case, 30% of the isolates had no mutation at *Erg27*^{F412}; two of these isolates showed high resistance to the fungicide and four had low resistance.

The low and high resistance in isolates from the MR and OR regions that lacked mutations in *Erg27*^{F412} raised the possibility of another codon of *Erg27* being mutated and conferring resistance to fenhexamid. To answer this, the sequence of the *Erg27* gene was scrutinized to identify other mutations. Five other mutations were found in the *Erg27* gene, including *erg27*^{L195F}, *erg27*^{P238S}, *erg27*$^{\Delta 298}$, *erg27*^{R330P} and *erg27*^{N369D}. These mutations were found in different combinations, in the 117 isolates analyzed from

Table 2. Numbers of *Botrytis cinerea* isolates of *Erg27* genotype at the 412 position, obtained from Central Chile, from Valparaíso Region (VR), Metropolitan Region (MR) and O'Higgins Region (OR).

Region	Total isolates	*Erg27*^{F412}		*erg27*^{F412I}		*erg27*^{F412S}		*erg27*^{F412V}	
		%[a]	Mean EC_{50}[b]	%[a]	Mean EC_{50}[b]	%[a]	Mean EC_{50}[b]	%[a]	Mean EC_{50}[b]
VR	24	13	0.07	58	19.85	29	14.99	-	-
MR	47	19	0.79	13	77.18	62	17.90	6	60.59
OR	46	30	1.81	22	47.65	48	13.90	-	-

[a] Frequency occurrence of genotype in percentage
[b] Mean EC_{50} (mg L^{-1}) for genotype of *Erg27* at the 412 position.

the three regions. *erg27*^{P238S}, *erg27*$^{L195F/\Delta 298}$ and *erg27*$^{\Delta 298/R330P}$ were present in isolates that lacked mutation in position 412 of *Erg27* and were resistant to fenhexamid (Figure 3A), suggesting that these mutations could lead to resistance to fenhexamide. However, *erg27*$^{\Delta 298}$ by itself possibly did not affect resistance to this fungicide. Similarly, *erg27*^{N369D} combined with *erg27*$^{P238F/N369D}$ did not give resistance to fenhexamid, although *erg27*^{P238S} by itself correlated with fenhexamid resistance. Mutations in other positions were also detected in the isolates carrying *erg27*^{F412S}or *erg27*^{F412I} (Figure 3B-D). However clear correlations between their presence and fenhexamid resistance were not detected, indicating that mutations in position 412 are more relevant for fenhexamid resistance.

Evaluation of growth parameters and virulence of the Botrytis cinerea *isolates carrying mutations in* Erg27

Growth parameters and virulence were analyzed to evaluate the performance of fenhxamid resistant isolates from VR, OR, and MR carrying mutations in the 412 position of the *Erg27* gene. Mycelium growth was evaluated under suboptimal (15°C) and optimal temperature conditions (20 or 25°C). No differences in mycelium radial growth were observed among field isolates with non-mutated *Erg27*^{F412} and *erg27*^{F412S}, *erg27*^{F412I} or *erg27*^{F412V} at the three growing temperature tested (Figure 4A, 4B and 4C).

Development of sclerotia as survival structures is essential for overwintering of *B. cinerea* inoculum in the field. Therefore, sclerotium development was evaluated in two contrasting temperature conditions: 5 or 20°C. Numbers of sclerotia, sclerotia masses and sclerotia indices (ratio of numbers to masses) were quantified. No statistically significant differences were observed between *Erg27*^{F412}, *erg27*^{F412S} or *erg27*^{F412I} at 5°C, but at this temperature, the restriction of sclerotium develop-

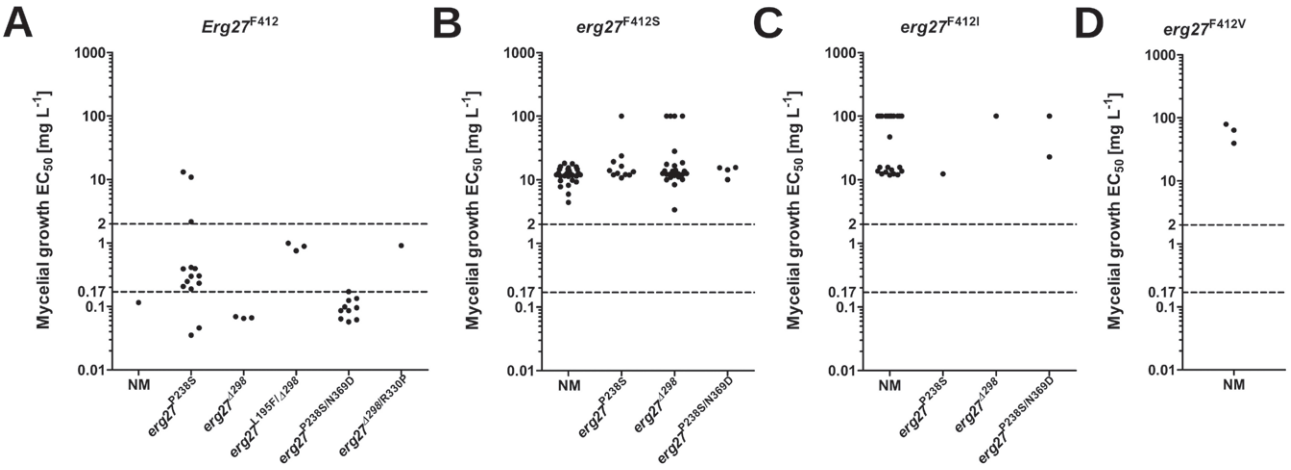

Figure 3. Sensitivity to fenhexamid in *Botrytis cinerea* isolates *Erg27*^{F412} (A), *erg27*^{F412S} (B), *erg27*^{F412I} (C) and *erg27*^{F412V} (D) carrying additional mutations is shown based on EC_{50} values (effective concentration that reduces mycelium growth by 50%). Five other mutations were detected: *erg27*^{L195F}, *erg27*^{P238S}, *erg27*$^{\Delta 298}$, *erg27*^{R330P} and *erg27*^{N369D}. Dashed lines indicate sensitivity limits: low resistance = 0.17 mg L^{-1} > EC_{50} ≥ 2 mg L^{-1} and high resistance = EC_{50}≥ 2 mg L^{-1}.

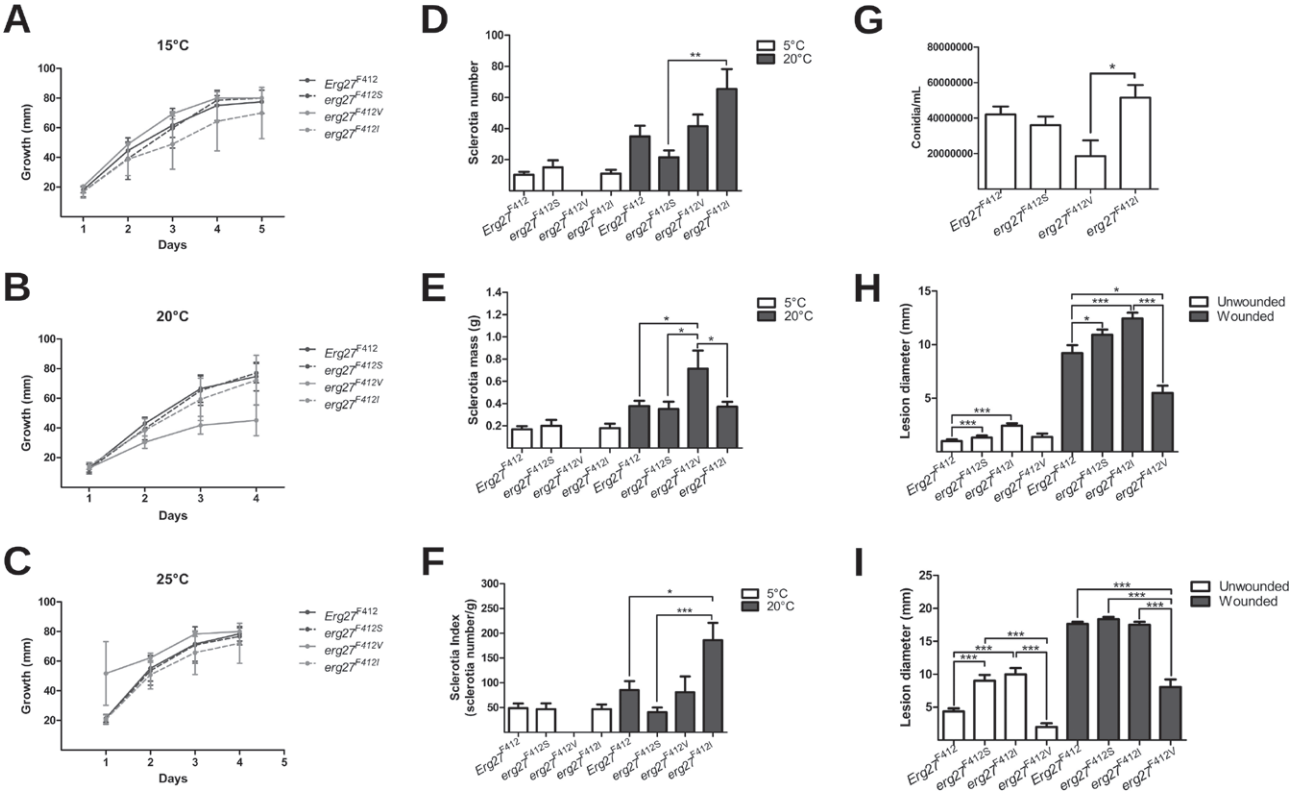

Figura 4. Comparation on fitness parameters between *Erg27*^{F412}, *erg27*^{F412S}, *erg27*^{F412I} and *erg27*^{F412V} isolates of *Botrytis cinerea*. Radial mycelium growth was evaluated at 15°C (A), 20°C (B) or 25°C (C). Sclerotium development was measured using numbers of sclerotia (D), sclerotium mass (E) and Sclerotia Index (F), evaluated at 5°C or 20°C. Conidium production was also evaluated (G). Wounded and Unwounded detached table grape berries were used to evaluate aggressiveness levels at 0 or 20°C in *Erg27* mutant isolates (H, I). Asterisks indicate significant differences (* $P < 0.05$; ** $P < 0.01$; *** $P < 0.001$)

ment did not occur with *erg27*^{F412V} isolates (Figur 4D, 4E and 4F). At 20°C, *erg27*^{F412S} produced fewer of sclerotia than *erg27*^{F412I}, but equivalent numbers to *Erg27*^{F412} and *erg27*^{F412V} (Figure 4D). The sclerotium mass was greater in *erg27*^{F412V} compared to other isolates carrying mutant alleles (Figure 4E). Evaluation of the sclerotium indices showed greater values in strains carrying *erg27*^{F412I} (Figure 4F).

Conidium production was investigated to establish the propagation capacity of isolates carrying different *Erg27* mutations at optimal temperature for *B. cinerea* development. No differences in conidium production were observed between *erg27*^{F412S}, *erg27*^{F412I} and isolates carrying the wild type *Erg27*. However, significantly fewer conidia were produced by *erg27*^{F412V} isolates (Figure 4G), indicating that this mutation impaired conidium development.

The infection capacity of the *Erg27* mutants was measured on detached 'Thompson Seedless' grape berries using six isolates of each genotype. On unwounded berries incubated at 0°C, *erg27*^{F412I} isolates developed larger rot lesions than berries inoculated with *Erg27*^{F412}, *erg27*^{F412S} or *erg27*^{F412V} isolates. In wounded berries, *erg27*^{F412S} and *erg27*^{F412I} generated larger lesions compared to the *Erg27* ^{F412} genotype, while *erg27*^{F412V} produced smaller lesions than the *Erg27* ^{F412} genotype isolates (Figure 4H). At 20°C, unwounded berries inoculated with *erg27*^{F412I} or *erg27*^{F412S} isolates developed enhanced infection damage compared with *Erg27*^{F412}. However, the necrotic damage observed in wounded berries infected by *erg27*^{F412S} or *erg27*^{F412I} did not differ from that caused by *Erg27*^{F412} isolates. In contrast, *erg27*^{F412V} isolates were less aggressive than *Erg27*^{F412} isolates in both unwounded and wounded berries (Figure 4I). Together, these results indicate that growth in the *erg27*^{F412S}, *erg27*^{F412I} and *erg27*^{F412V} isolates was not affected, although they carried a mutation in *Erg27*, and isolates carrying *erg27*^{F412S} and *erg27*^{F412I} were of increased aggressiveness on both unwounded and wounded berries.

DISCUSSION

Table grape vines are cultivated mostly in the Central Valley of Chile because this region has favorable agroecological conditions for grape production. Grape vineyards in Chile are threatened by *Botrytis* outbreaks due to the frequent cool springs and wet weather conditions. Therefore, fungicides are commonly applied to vineyards in this region. Development of resistance to fungicides has been observed in *B. cinerea* in this area, endangering the ability to control gray mold (Latorre *et al*., 2015; Esterio *et al*., 2017).

In the present study *B. cinerea* populations collected from 'Thompson Seedless' table grape vineyards from three regions of Central Chile were shown to have reduced sensitivity to fenhexamid. This reduced sensitivity increased progressively in the the three successive growing seasons tested. Nevertheless, fenhexamid is still one of the main fungicides regularly used in the local *B. cinerea* control programmes, with at least two applications of this chemical in each growing season.

Botrytis cinerea resistant isolates to fungicides with unisite modes of action have been widely reported in the last 10 years, after intensive application programmes, accompanied by reduced fungicide efficacy (van den Bosch *et al*. 2015; Fillinger and Walker, 2016). The *Erg27* mutation in position 412 is one of the most common changes linked to fenhexamid resistance (Fillinger *et al*., 2008; Billard *et al*., 2012; Debieu and Leroux, 2015). We reported isolates carrying *erg27*^{F412S}, *erg27*^{F412I} and *erg27*^{F412V} mutations; these have been previously reported in *B. cinerea* isolated from fields in France, Germany and the United States of America, and have been associated with high fenhexamid-resistance levels (Grabke *et al*., 2013; Amiri and Peres, 2014; Rupp *et al*., 2017). Isolates carrying mutant versions of *Erg27* were predominant, including *erg27*^{F412I} from VR and *erg27*^{F412S} from MR and OR. Strong correlations were observed between the presence of mutations at codon 412 of *Erg27* and high resistance to fenhexamid ($EC_{50} \geq 2$ mg L^{-1}). The *erg27*^{F412I} and *erg27*^{F412V} genotypes showed the greatest EC_{50} values in each population, while *erg27*^{F412S} presented the lowest EC_{50} among the mutants. This indicates that this mutation conferred less resistance to fenhexamid. In all the Chilean regions analyzed in this study, progressive increases of the resistant isolates were detected over the three growing seasons assessed, demonstrating the effects of constant fungicide pressure on *B. cinerea* population.

In addition to high fenhexamid resistance related to mutation in *Erg27*, particularly in the 412 position, we detected other mutations that produced moderate levels of resistance in other *Erg27* codons: *erg27*^{P238S}, *erg27*$^{L195F/\Delta 298}$ and *erg27*$^{\Delta 298/ R330P}$. Isolates carrying mutations *erg27*^{L195F} and *erg27*^{R330P} are the first reported in Chile. Particularly, *erg27*^{R330P} associated with moderate resistance to fenhexamid has not been previously reported (Debieu and Leroux, 2015). The presence of *erg27*^{P238S} and *erg27*^{N369D} together suppressed resistance to fenhexamid more than in isolates carrying *erg27*^{P238S} alone. However, the level of resistance to fenhexamid remained unchanged in strains *erg27*^{F412S} and *erg27*^{F412I} when

erg27^{N369D} was also present, suggesting that changes close to the 3-KR transmembrane domain were more relevant in the interaction between fenhexamid and 3-KR. Our data also suggest that the presence of *erg27*^{F412S} produced a second functional change within the *Erg27* sequence, in contrast to *erg27*^{F412I} and *erg27*^{F412V}.

Mutations in position 412 of *Erg27* have been previously reported to reduce isolate performance (Billard *et al*. 2012)**.** However, the isolates *erg27*^{F412I} and *erg27*^{F412S}, identified in the present study grew similarly to fenhexamid-sensitive strains at 15°C, 20°C and 25°C. Sclerotium development and conidium production were also not affected in *erg27*^{F412I} and *erg27*^{F412S} isolates, in contrast to previous reports that showed growth retardation in fenhexamid-resistant strains (Billard *et al*., 2012; Saito *et al*., 2014). *erg27*^{F412I} and *erg27*^{F412S} *B. cinerea* isolates were more pathogenic, particularly in unwounded grape berries at all the temperatures tested. It is possible that the low effects on fitness and the increase in infection capacity observed in *erg27*^{F412I} and *erg27*^{F412S} were due to accumulation of additional mutations that conferred adaptive advantages for survival under high fungicide selection pressure (Ishii, 2015), overcoming the negative effect reported in strains carrying *erg27*^{F412I} and *erg27*^{F412S} (Billard *et al*., 2012). Isolates carrying *erg27*^{F412V} exhibited fitness costs, producing few conidia and possessing only minor increases in infection capacity. This suggests that this mutation may be rare in the field *B. cinerea* populations, being found only three times in isolates obtained in the present study.

Amino-pyrazolinone fenpyrazamine was recently introduced as a Botryticide for gray mold control in Chile. Fenpyrazamine, like fenhexamid, targets 3-KR (Kimura *et al*., 2017), but *Erg27* changes associated with resistance to fenpyrazamine have not been studied. Fenpyrazamine could potentially control fenhexamid-resistant isolates by inhibiting 3-KR, targeting the enzyme independently of the amino-acid at position 412. Therefore, experiments determining fenpyrazamine efficacy on fenhexamid-resistant isolates are required, to provide a basis for restructuring chemical control strategies to reduce occurrence of highly resistant *B. cinerea* populations.

The present research has highlighted the prevalence of fenhexamid resistance linked to the *Erg27* genotype in *B. cinera* populations isolated from 'Thompson Seedless' vineyards treated with this fungicide in the Central Valley of Chile. These results show an overall reduction of fitness in fenehxamid-resistant *B. cinera* isolates, suggesting the appearance of adapted strains resistant to this fungicide. This poses serious risks for field control of gray mold in table grape production in Chile.

ACKNOWLEDGEMENTS

This research was financially supported by Grant FIA PYT-2016-0243. We thank Veronica Estrada for technical support.

LITERATURE CITED

Amiri A., Peres N.A., 2014. Diversity in the *erg27* Gene of *Botrytis cinerea* field isolates from strawberry defines different levels of resistance to the hydroxyanilide fenhexamid. *Plant Disease* 98(8): 1131–1137.

Akins R.A., 2005. An update on antifungal targets and mechanisms of resistance in *Candida albicans*. *Medical Mycology* 43(4): 285–318.

Billard A., Fillinger S., Leroux P., Lachaise H., Beffa R., Debieu D., 2012. Strong resistance to the fungicide fenhexamid entails a fitness cost in *Botrytis cinerea*, as shown by comparisons of isogenic strains. *Pest Management Science* 68(5): 684–691.

Debieu D., Bach J., Hugon M., Malosse C., Leroux P., 2001. The hydroxyanilide fenhexamid, a new sterol biosynthesis inhibitor fungicide efficient against the plant pathogenic fungus *Botryotinia fuckeliana* (*Botrytis cinerea*). *Pest Management Science* 57(11): 1060–1067.

Debieu D., Leroux P., 2015. Sterol Biosynthesis Inhibitors: C-4 Demethylation. In: *Fungicide Resistance in Plant Pathogens* (H. Ishii, D.W. Hollomon, ed.) Springer, Japan, 217–232.

De Guido M.A., De Miccolis Angelini R.M., Pollastro S., Santomauro A., Faretra F., 2007. Selection and genetic analysis of laboratory mutants of *Botryotinia fuckeliana* resistant to fenhexamid. *Journal of Plant Pathology* 89: 203–210.

Di Rienzo J.A., Casanoves F., Balzarini M.G., González L., Tablada M., Robledo C.W., 2015. InfoStat. InfoStat Group, FCA, Universidad Nacional de Córdoba,
Argentina. http://www.infostat.com.ar

Esterio M., Auger J., Ramos C., García H., 2007. First report of fenhexamid resistant isolates of *Botrytis cinerea* on grapevine in Chile. *Plant Disease* 91(6): 768.

Esterio M., Muñoz G., Ramos C., Cofré G., Estévez R., … Auger J., 2011. Characterization of *Botrytis cinerea* isolates present in Thompson Seedless table grapes in the Central Valley of Chile. *Plant Disease* 95(6): 683–690.

Esterio M., Copier C., Román A., Araneda M.J., Rubilar M., … Auger J., 2017. Frequency of fungicide-resistant *Botrytis cinerea* populations isolated from

'Thompson Seedless' table grapes in the Central Valley of Chile. *Ciencia e Investigación Agraria* 44(3): 295–306.

Fillinger S., Leroux P., Auclair C., Barreau C., Al Hajj C., Debieu D., 2008. Genetic analysis of fenhexamid-resistant field isolates of the phytopathogenic fungus *Botrytis cinerea*. *Antimicrobial Agents and Chemotherapy* 52 (11): 3933–3940.

Fillinger S., Walker A.S., 2016. Chemical Control and Resistance Management of Botrytis Diseases. In: *Botrytis – the Fungus, the Pathogen and its Management in Agricultural Systems* (S. Fillinger, Y. Elad, ed.) Springer, Switzerland, 189–216.

Grabke A., Fernández-Ortuño D., Schnabel G., 2013. Fenhexamid resistance in *Botrytis cinerea* from strawberry fields in the Carolinas is associated with four target gene mutations. *Plant Disease* 97(2): 271–276.

Hall T.A., 1999. BioEdit: a user-friendly biological sequence alignment editor and analysis program for Windows 95/98/NT. *Nucleic Acids Symposium Series* 41: 95–98.

Ishii H., 2015. Stability of Resistance. In: *Fungicide Resistance in Plant Pathogens* (H. Ishii, D.W. Hollomon, ed.) Springer, Japan, 35–48.

Keller M., Viret O., Cole M., 2003. *Botrytis cinerea* infection in grape flowers: defence reaction, latency and disease expression. *Phytopathology* 93: 316–322.

Kimura N., Hashizume M., Kusaba T., Tanaka S., 2017. Development of the novel fungicide fenpyrazamine. *Journal of Pesticide Science* 42(3): 137–143.

Latorre B.A., Elfar K., Ferrada E.E., 2015. Gray mold caused by *Botrytis cinerea* limits grape production in Chile. *Ciencia e Investigación Agraria* 42(3): 305–330.

Leroux P., Chapeland F., Desbrosses D., Gredt M., 1999. Patterns of cross-resistance to fungicides in *Botryotinia fuckeliana* (*Botrytis cinerea*) isolates from French vineyards. *Crop Protection* 18: 687–697.

Rupp S., Weber R.W., Rieger D., Detzel P., Hahn M., 2017. Spread of *Botrytis cinerea* strains with multiple fungicide resistance in German horticulture. *Frontiers in Microbiology* 7: 2075.

Saito S., Cadle-Davidson L., Wilcox W.F., 2014. Selection, fitness, and control of grape isolates of *Botrytis cinerea* variably sensitive to fenhexamid. *Plant Disease* 98(2): 233–240.

van den Bosch F., Paveley N., Fraaije B., van den Berg F., Oliver R., 2015. Evidence-Based Resistance Management: A Review of Existing Evidence. In: *Fungicide Resistance in Plant Pathogens* (H. Ishii, D.W. Hollomon, ed.) Springer, Japan, 63–76.

Viret O., Keller M., Jaudzems V.G., Cole F.M., 2004. *Botrytis cinerea* infection of grape flowers: light and electron microscopical studies of infection sites. *Phytopathology* 94(8): 850–857.

Ziogas B.N., Markoglou A.N., Malandrakis A.A., 2003. Studies on the inherent resistance risk to fenhexamid in *Botrytis cinerea*. *European Journal of Plant Pathology* 109: 311–317.

Phytopathologia Mediterranea
The international journal of the
Mediterranean Phytopathological Union

Firenze University Press
www.fupress.com/pm

Research Papers

Neocosmospora spp. associated with dry root rot of citrus in South Africa

Vladimiro GUARNACCIA[1,2,3,*], Jan VAN NIEKERK[3,4], Pedro W. CROUS[5], Marcelo SANDOVAL-DENIS[5]

[1] *Centre for Innovation in the Agro-Environmental Sector, AGROINNOVA, University of Torino, Largo Braccini 2, 10095 Grugliasco (TO), Italy*
[2] *Department of Agricultural, Forest and Food Sciences (DISAFA), University of Torino, Largo Braccini 2, 10095 Grugliasco (TO), Italy*
[3] *Department of Plant Pathology, University of Stellenbosch, Private Bag X1, Matieland 7602, South Africa*
[4] *Citrus Research International, P.O. Box 28, Nelspruit 1200, South Africa*
[5] *Westerdijk Fungal Biodiversity Institute Uppsalalaan 8, 3584 CT, Utrecht, The Netherlands*
*Corresponding author. E-mail: vladimiro.guarnaccia@unito.it

Summary. Citrus is one of the most important fruit crops cultivated in South Africa. Internationally, citrus dry root rot is a common disease in major citrus production areas. Several abiotic and biotic factors are involved in disease development, in which *Neocosmospora* species are important biotic agents. The diversity of *Neocosmospora* species associated with dry root rot symptoms of *Citrus* trees cultivated in South Africa was evaluated using morphological and molecular analyses. Multi-locus analysis was conducted, based on fragments of seven loci including: ATP citrate lyase (*acl1*), calmodulin (*cal*), internal transcribed spacer region of the rRNA (ITS), large subunit of the rRNA (LSU), RNA polymerase largest subunit (*rpb1*), RNA polymerase second largest subunit (*rpb2*), and translation elongation factor 1-alpha (*tef1*). A total of 62 strains representing 11 *Neocosmospora* species were isolated from crowns, trunks and roots of citrus trees affected by dry root rot, as well as from soils sampled in affected citrus orchards. The most commonly isolated taxa were *N. citricola*, *N. ferruginea* and *N. solani*, while rarely encountered taxa included *N. brevis*, *N. crassa*, *N. hypothenemi* and *N. noneumartii*. Furthermore, four *Neocosmospora* species are also newly described, namely *N. addoensis*, *N. citricola*, *N. gamtoosensis* and *N. lerouxii*.

Keywords. Citrus decline, morphology, multigene phylogeny, systematics.

OPEN ACCESS

Citation: V. Guarnaccia, J. van Niekerk, P. W. Crous, M. Sandoval-Denis (2021) *Neocosmospora* spp. associated with dry root rot of citrus in South Africa. *Phytopathologia Mediterranea* 60(1): 79-100. doi: 10.36253/phyto-12183

Accepted: January 24, 2021

Published: May 15, 2021

Data Availability Statement: All relevant data are within the paper and its Supporting Information files.

Competing Interests: The Author(s) declare(s) no conflict of interest.

Editor: Alan J.L. Phillips, University of Lisbon, Portugal.

INTRODUCTION

Citrus is one of the most important world fruit crops, and South Africa is among the largest producers and exporters of citrus fruit (FAOSTAT, 2019). Citrus dry root rot (DRR) is a common problem among citrus growers, reported in major production areas such as Australia (Broadbent, 2000), Florida, California and Texas in the United States of America (Graham *et*

al., 1985), Italy (Polizzi *et al*., 1992), Oman (Nemec *et al*., 1980; Bender, 1985), Pakistan (Kore and Mane, 1992; Conzulex *et al*., 1997; Verma *et al*., 1999; Rehman *et al*., 2012), Turkey (Kurt *et al*., 2020), Tunisia, Greece and Egypt (El-Mohamedy, 1998; Yaseen and D'Onghia, 2012).

While the aetiology of DRR is multifactorial and not completely understood, it is usually attributed to *Neocosmospora* (*Fusarium*) *solani* sensu lato. However, several species of *Neocosmospora*, but also *Fusarium*, are commonly found in orchard soils and citrus plants. These two closely related fusarioid genera encompass important plant pathogens, and are associated with major diseases of citrus (Menge, 1988; Derrick and Timmer, 2000; Sandoval-Denis *et al*., 2018), including DRR, root rot, feeder root rot, wilt, twig dieback and citrus decline (Menge, 1988; Spina *et al*., 2008). *Fusarium equiseti* was recovered from citrus roots in Florida (Smith *et al*., 1988), while *F. proliferatum*, *F. sambucinum* and *Neocosmospora solani* were found in Greece (Malikoutsaki-Mathioudi *et al*., 1987). *Fusarium oxysporum* f. sp. *citri* was reported as responsible for the wilt of citrus in Tunisia (Hannachi *et al*., 2014). *Fusarium oxysporum* and strains first assigned to "*F. ensiforme*" and later reidentified as *Neocosmospora brevis* were also reported from DRR in Italy (Sandoval-Denis *et al*., 2018; 2019), while a number of *Neocosmospora* species have been reported in association with DRR of citrus in Europe (Sandoval-Denis *et al*., 2018).

Neocosmospora (*Hypocreales*, *Nectriaceae*), comprises species with varied ecologies, including saprobes, endophytes, and plant and animal pathogens. Pathogenic species of *Neocosmospora* are known to affect more than 100 plant host families and diverse animal species, including humans (Sandoval-Denis *et al*., 2019). Although *Neocosmospora* (1899) is an old and well-established name, recent phylogenetic, morphological and ecological data (Lombard *et al*., 2015) provided additional support for this genus as one of several distinct fusarioid genera in the *Nectriaceae*. Follow-up revisions have corrected the taxonomy of most *Neocosmospora* species known to date, including the main pathogenic clades (Sandoval-Denis and Crous, 2018; Sandoval-Denis *et al*., 2019).

Previous studies have demonstrated how DRR, caused by the association between stressed plants and *Neocosmospora* species, can generate sudden decline of plants weakened by abiotic and biotic factors, such as root injuries, Phytophthora root rot, graft incompatibility, poor drainage, poor soil aeration, excess fertilizer, or soil pH (Menge, 1988; Polizzi *et al*., 1992). Chlorosis, poor vigour, wilt, leaf abscission and degeneration are visible in affected plants for several years before they suddenly die. Examination of scaffold roots, crowns and basal trunks usually shows wood staining (Timmer *et al*., 1979; Timmer 1982). Rot of the fibrous roots is also visible and associated with canopy size reductions, defoliation, dieback and sloughing of root cortices (Nemec and Baker, 1992). This disease has been managed by planting resistant rootstocks. However, during the last decade, trifoliate orange (*Poncirus trifoliata*) rootstocks, which are very susceptible to DRR, have been widely used, due to their resistance to virus and soilborne pathogens (i.e.: Citrus Tristeza Virus) (Fang *et al*., 1998).

Since 2013, sudden, devastating decline and death of citrus trees has been reported in the Gamtoos and Sundays River Valleys production areas in the Eastern Cape province of South Africa. This decline is typically observed on 4– to 10-year-old trees with the trifoliate rootstocks Carrizo citrange and Swingle citrumelo. As scions, these declining trees are of various citrus types, including lemons, oranges and mandarins. To date, little is known about DRR-like diseases in citrus orchards in South Africa. Given the importance of citrus production, and specifically in the two areas of South Africa, as well as the relevant economic impact of DRR in other countries, further research was needed to increase understanding of the aetiology of this disease.

Morphological, cultural and molecular characteristics of the fungal species associated with symptomatic trees were investigated in this study by employing large-scale sampling to isolate the pathogens involved, and to identify their strains according to modern taxonomic concepts *via* morphological characterization and multi-locus DNA sequence data. In 2018 several surveys were conducted in citrus orchards with the aims to: (1) conduct extensive surveys to sample symptomatic plant material; (2) cultivate as many of the associated fungi as possible; (3) conduct DNA multi-locus sequence analyses combined with morphological characterization of isolates obtained; and (4) compare the obtained results with known wood decay fungi previously associated with trees displaying characteristic DDR symptoms.

MATERIALS AND METHODS

Sampling, fungal collection and isolation

The Patensie (Gamtoos River Valley) and Kirkwood (Sundays River Valley) areas were surveyed during the second half of 2018. During these visits, the external and internal symptoms of diseased trees were examined. Scaffold roots, crown and trunk portions taken from between soil level and scion unions, were collected in

both the survey areas. Samples were each transversally cut into 3-cm-thick discs, which allowed observation of internal wood decay symptoms.

Wood fragments (3 × 3 mm) were cut from necrotic and healthy tissues and also from the margins between them. Each fragment was then surface sterilised by soaking in 70% ethanol for 5 s, 4% sodium hypochlorite for 90 s, sterile water for 60 s and then dried on sterile filter paper. Fragments were placed on potato dextrose agar (PDA) amended with 100 µg mL^{-1} streptomycin (PDA-S), and were then incubated at 25°C. Characteristic *Neocosmospora* colonies were collected from these plates by hyphal tipping onto clean PDA-S plates. The isolates used in this study are maintained in the culture collection of the Department of Plant Pathology, University of Stellenbosch, Stellenbosch, South Africa, and at the Westerdijk Fungal Biodiversity Institute (CBS), Utrecht, The Netherlands (Table 1).

Morphological studies of isolates

Morphological studies were carried out as indicated elsewhere (Leslie and Summerell, 2006; Sandoval-Denis and Crous, 2018; Sandoval-Denis *et al*., 2019). Macroscopic characteristics and fungal colony appearance of each isolate was determined after culturing on oatmeal agar (OA), potato dextrose agar (PDA) and synthetic nutrient-poor agar (SNA; Nirenberg, 1976), and incubation for 7–14 d at 24°C in darkness under a 12 h/12 h light/darkness cycle using cool fluorescent light. Colour nomenclature follows that of Rayner (1970). Fungal micromorphology was studied using 7–14-d-old cultures on carnation leaf agar (CLA; Fisher *et al*., 1982) and SNA, incubated at 24°C in a 12 h/12 h near UV light/dark cycle. Photomicrographs were captured using a Nikon Eclipse 80i microscope with Differential Interference Contrast (DIC) optics and a Nikon AZ100 dissection microscope, both equipped with a Nikon DS-Ri2 high definition colour digital camera. Measurements were recorded using Nikon NIS-elements D software v. 4.50, from at least 50 randomly selected elements for each structure.

Molecular studies of isolates

Total genomic DNA was extracted from isolates grown on malt extract agar (MEA; Crous *et al*., 2019), incubated for 7 d at room temperature (approx. 24°C). Mycelium was scraped from the colony surfaces with the aid of sterile scalpels, and DNA was isolated using the Wizard® Genomic DNA purification Kit (Promega Corporation) following the manufacturer's protocol.

Seven gene fragments were PCR amplified using the following primer combinations with protocols described elsewhere: acl1-230up and acl1-1220low for the larger subunit of the ATP citrate lyase (*acl1*; Gräfenhan *et al*. 2011), CAL-228F and CAL2Rd for calmodulin (*cal*; Carbone and Kohn, 1999; Quaedvlieg *et al*., 2014), ITS4 and ITS5 for the internal transcribed spacer region of the rRNA (ITS; White *et al*., 1990), LR0R and LR5 for a partial fragment of the large subunit of the rRNA (LSU; Vilgalys and Hester, 1990; Vilgalys and Sun, 1994), Fa and G2R for the RNA polymerase largest subunit (*rpb1*; O'Donnell *et al*., 2010), 5f2 and 7cr plus 7cf and 11ar for two non-contiguous fragments of the RNA polymerase second largest subunit (*rpb2*: Liu *et al*., 1999; Sung *et al*. 2007), and EF-1 and EF-2 for the translation elongation factor 1-alpha gene (*tef1*: O'Donnell *et al*., 2008). Sequencing was carried out in both directions on an ABI Prism 3730XL DNA Analyzer (Applied Biosystems) using the same primer pairs used for amplification, plus the internal sequencing primers F6, F8 and R8 for *rpb1* (O'Donnell *et al*., 2010). Consensus sequences were assembled using Seqman Pro v. 10.0.1 (DNASTAR).

Sequence alignments were constructed and analysed individually for each gene partition, including DNA sequences representing the phylogenetic diversity of *Neocosmospora* selected according to recently published phylogenies (Guarnaccia *et al*., 2019; Sandoval-Denis *et al*., 2019). Alignments were achieved using MAFFT (Katoh *et al*., 2019) as implemented on the European Bioinformatics Institute (EMBL-EBI) portal (www.ebi.ac.uk), and were visually inspected and then manually corrected if needed using MEGA v. 6 (Tamura *et al*., 2013).

Phylogenetic analyses were based on two independent algorithms: Maximum-Likelihood, using Random Accelerated (*sic*) Maximum Likelihood (RAxML) v. 8.2.10 (Stamatakis, 2014) and Bayesian inference (BI) under MrBayes v. 3.2.6 (Huelsenbeck and Ronquist, 2001; Ronquist and Huelsenbeck, 2003). The analyses were carried out using the CIPRES Science Gateway portal (www.phylo.org: Miller *et al*., 2012). Single-gene phylogenies were compared visually to check for topological conflict between significantly supported clades, and then as combined multilocus phylogenies (Mason-Gamer and Kellogg, 1996; Wiens 1998). A first analysis based on combined *rpb2* and *tef1* sequence data was directed to identify *Neocosmospora* spp. from isolates obtained from symptomatic citrus trees. A second analysis including the combined seven gene dataset was directed to clarify the phylogeny of South African citrus *Neocosmospora* isolates with uncertain phylogenetic position or deter-

Table 1. Collection data and GenBank accession numbers of isolates included in this study.

Species	Strain number[1]	Country	Host	GenBank sequence accession number[2]						
				acl	*cal*	ITS	LSU	*rpb1*	*rpb2*	*tef1*
Geejayessia atrofusca	NRRL 22316	USA	Staphylea trifolia	-	-	AF178423	AF178392	JX171496	EU329502	AF178361
Geejayessia cicatricum	CBS 125552	Slovenia	Dead twig	HQ728171	-	HQ728145	MH875038	-	HQ728153	HM626644
Neocosmospora addoensis	CBS 146508 = VG268 = CPC 37126	South Africa	*Citrus sinensis* - crown	MW218003	MW218050	MW173040	MW173031	MW218096	MW446573	MW248739
	CBS 146509 = VG279 = CPC 37127	South Africa	*Citrus sinensis* - crown	MW218004	MW218051	MW173041	MW173032	MW218097	MW446574	MW248740
	CBS 146510^{T} = VG281 = CPC 37128	South Africa	*Citrus sinensis* - crown	MW218005	MW218052	MW173042	MW173033	MW218098	MW446575	MW248741
Neocosmospora ampla	CBS 202.32^{T}	German East Africa	*Coffea* sp.	-	-	LR583701	LR583909	-	LR583815	LR583594
Neocosmospora bataticola	CBS 144397	USA	Ipomoea batatas	MW218006	MW218053	AF178407	AF178376	MW218099	EU329509	AF178343
	CBS 144398^{T}	USA	Ipomoea batatas	MW218007	MW218054	AF178408	AF178377	MW218100	FJ240381	AF178344
Neocosmospora borneensis	CBS 145462^{ET}	Indonesia	Bark or recently dead tree	-	-	AF178415	AF178384	-	EU329515	AF178352
Neocosmospora bostrycoides	CBS 144.25^{NT}	Honduras	Soil	MW218008	MW218055	LR583704	LR583912	MW218101	LR583818	LR583597
	CBS 392.66	Unknown	Bertholletia excelsa	MW218009	MW218056	LR583705	LR583913	MW218102	LR583819	LR583598
Neocosmospora brevicona	CBS 204.31^{ET}	Indonesia	*Gladiolus* sp.	MW218010	MW218057	LR583707	LR583915	MW218103	LR583821	LR583600
Neocosmospora brevis	CBS 130326	USA	Human eye	-	-	DQ094351	DQ236393	-	EF470136	DQ246869
	VG150	South Africa	*Citrus sinensis* - crown	-	-	MW173043	-	-	MW446576	MW248742
	VG152	South Africa	*Citrus sinensis* - crown	-	-	MW173044	-	-	MW446577	MW248743
	VG157	South Africa	*Citrus sinensis* - crown	-	-	MW173045	-	-	MW446578	MW248744
Neocosmospora catenata	CBS 143228	USA	*Stegostoma fasciatum*	MW218011	MW218058	KC808255	KC808255	MW218104	KC808354	KC808213
	CBS 143229^{T}	USA	*Stegostoma fasciatum*	MW218012	MW218059	KC808256	KC808256	MW218105	KC808355	KC808214
Neocosmospora citricola	CBS 146511 = VG302 = CPC 37129	South Africa	*Citrus sinensis* - crown	MW218013	MW218060	MW173046	MW173034	MW218106	MW446579	MW248745
	CBS 146512 = VG307 = CPC 37130	South Africa	*Citrus sinensis* - crown	MW218014	MW218061	MW173047	MW173035	MW218107	MW446580	MW248746
	CBS 146513^{T} = VG343 = CPC 37131	South Africa	*Citrus sinensis* - crown	MW218015	MW218062	MW173048	MW173036	MW218108	MW446581	MW248747
	VG17	South Africa	*Citrus sinensis* - crown	-	-	MW173049	-	-	MW446582	MW248748
	VG30	South Africa	*Citrus sinensis* - crown	-	-	MW173050	-	-	MW446583	MW248749
	VG139	South Africa	*Citrus sinensis* - crown	-	-	MW173051	-	-	MW446584	MW248750
	VG140	South Africa	*Citrus sinensis* - crown	-	-	MW173052	-	-	MW446585	MW248751
	VG183	South Africa	*Citrus sinensis* - crown	-	-	MW173053	-	-	MW446586	MW248752
	VG197	South Africa	*Citrus sinensis* - root scaffold	-	-	MW173054	-	-	MW446587	MW248753
	VG203	South Africa	*Citrus sinensis* - crown	-	-	MW173055	-	-	MW446588	MW248754

(Continued)

Table 1. (Continued).

Species	Strain number[1]	Country	Host	GenBank sequence accession number[2]						
				acl	*cal*	ITS	LSU	*rpb1*	*rpb2*	*tef1*
	VG287	South Africa	*Citrus sinensis* - crown	-	-	MW173056	-	-	MW446589	MW248755
	VG332	South Africa	*Citrus sinensis* - crown	-	-	MW173057	-	-	MW446590	MW248756
	VG358	South Africa	*Citrus sinensis* - crown	-	-	MW173058	-	-	MW446591	MW248757
	VG389	South Africa	*Citrus sinensis* - crown	-	-	MW173059	-	-	MW446592	MW248758
	VG399	South Africa	*Citrus sinensis* - crown	-	-	MW173060	-	-	MW446593	**MW248759**
Neocosmospora crassa	CBS 144386^{T}	France	Unknown	**MW218016**	**MW218063**	LR583709	LR583917	**MW218109**	LR583823	LR583604
	VG211 = CPC 37122	South Africa	*Citrus sinensis* - crown	-	-	**MW173061**	**MW173037**	-	**MW446594**	**MW248760**
Neocosmospora cucurbitae	CBS 410.62	Netherlands	*Cucurbita viciifolia*	-	-	LR583710	LR583918	-	LR583824	DQ247640
	CBS 616.66^{T}	Netherlands	*Cucurbita viciifolia*	-	-	LR583711	LR583919	-	LR583825	DQ247592
Neocosmospora cyanescens	CBS 518.82^{T}	Netherlands	Human foot	**MW218017**	**MW218064**	AB190389	LR583920	**MW218110**	LR583826	LR583605
	CBS 637.82	Netherlands	Human foot	**MW218018**	**MW218065**	LR583712	LR583921	**MW218111**	LR583827	LR583606
Neocosmospora diminuta	CBS 144390^{T}	Unknown	*Coelocaryon preusii*	-	-	LR583713	LR583922	-	LR583828	LR583607
Neocosmospora elegans	CBS 144395	Japan	*Xanthoxylum piperitum*	**MW218019**	**MW218066**	AF178394	AF178363	**MW218112**	EU329496	AF178328
	CBS 144396^{ET}	Japan	*Xanthoxylum piperitum*	**MW218020**	**MW218067**	AF178401	AF178370	**MW218113**	FJ240380	AF178336
Neocosmospora falciformis	CBS 475.67^{T}	Puerto Rico	Human mycetoma	**MW218021**	**MW218068**	MG189935	MG189915	**MW218114**	LT960558	LT906669
	CBS 121450	Syria	Declined grape vine	**MW218022**	**MW218069**	JX435211	JX435211	**MW218115**	JX435261	JX435161
	VG296	South Africa	soil - citrus orchard	-	-	**MW173062**	-	-	**MW446595**	**MW248761**
Neocosmospora ferruginea	CBS 109028^{T}	Switzerland	Human subcutaneous nodule	-	-	DQ094446	DQ236488	-	EU329581	DQ246979
	VG21	South Africa	*Citrus sinensis* - crown			MW440622			MW446596	MW446558
	VG22	South Africa	*Citrus sinensis* - crown			MW440623			MW446597	MW446559
	VG51	South Africa	*Citrus sinensis* - root scaffold			MW440624			MW446598	MW446560
	VG98	South Africa	*Citrus sinensis* - crown			MW440625			MW446599	MW446561
	VG109	South Africa	*Citrus sinensis* - crown			MW440626			MW446600	MW446562
	VG133	South Africa	*Citrus sinensis* - root scaffold			MW440627			MW446601	MW446563
	VG159	South Africa	*Citrus sinensis* - root scaffold			MW440628			MW446602	MW446564
	VG191	South Africa	*Citrus sinensis* - crown			MW440629			MW446603	MW446565
	VG195	South Africa	*Citrus sinensis* - root scaffold			MW440630			MW446604	MW446566
	VG205	South Africa	*Citrus sinensis* - root scaffold			MW440631			MW446605	MW446567

(Continued)

Table 1. (Continued).

Species	Strain number[1]	Country	Host	GenBank sequence accession number[2]						
				acl	*cal*	ITS	LSU	*rpb1*	*rpb2*	*tef1*
	VG289	South Africa	*Citrus sinensis* - root scaffold			MW440632			MW446606	MW446568
	VG370	South Africa	*Citrus sinensis* - crown			MW440633			MW446607	MW446569
	VG371	South Africa	*Citrus sinensis* - crown			MW440634			MW446608	MW446570
	VG394	South Africa	*Citrus sinensis* - root scaffold			MW440635			MW446609	MW446571
	VG403	South Africa	*Citrus sinensis* - crown			MW440636			**MW446610**	**MW446572**
Neocosmospora gamsii	CBS 143207^{T}	USA	Human bronchoalveolar lavage fluid	-	-	DQ094420	DQ236462	-	EU329576	DQ246951
	CBS 143211	USA	Humidifier coolant	-	-	DQ094563	DQ236605	-	EU329622	DQ247103
Neocosmospora gamtoosensis	CBS 146502^{T} = VG16 = CPC 37120	South Africa	*Citrus sinensis - crown*	**MW218023**	**MW218070**	**MW173063**	**MW173038**	**MW218116**	**MW446611**	**MW248762**
Neocosmospora haematococca	CBS 119600^{ET}	Sri Lanka	Dying tree	-	-	KM231797	KM231664	-	LT960561	DQ247510
Neocosmospora hypothenemi	CBS 145464^{T}	Benin	*Hypothenemus hampei*	**MW218024**	-	LR583715	LR583923	**MW218117**	JF741176	JF740850
	CBS 145466	Uganda	*Hypothenemus hampei*	**MW218025**	**MW218071**	-	-	**MW218118**	-	-
	VG11	South Africa	*Citrus sinensis* - crown	-	-	**MW173064**	-	-	**MW446612**	**MW248763**
	VG14	South Africa	*Citrus sinensis* - crown	-	-	**MW173065**	-	-	**MW446613**	**MW248764**
	VG49	South Africa	*Citrus sinensis* - root scaffold	-	-	**MW173066**	-	-	**MW446614**	**MW248765**
	VG189	South Africa	*Citrus sinensis* - crown	-	-	**MW173067**	-	-	**MW446615**	**MW248766**
	VG328	South Africa	*Citrus sinensis* - crown	-	-	**MW173068**	-	-	**MW446616**	**MW248767**
Neocosmospora ipomoeae	CBS 353.87	Netherlands	*Gerbera* sp.	**MW218026**	**MW218072**	LR583717	LR583925	**MW218119**	LR583831	DQ247639
	CBS 833.97	Netherlands	*Rosa* sp.	**MW218027**	**MW218073**	LR583719	LR583927	**MW218120**	LR583833	LR583611
Neocosmospora keratoplastica	CBS 490.63^{T}	Japan	Human	**MW218028**	**MW218074**	LR583721	LR583929	**MW218121**	LT960562	LT906670
	CBS 144389	Belgium	Greenhouse humic soil	**MW218029**	**MW218075**	LR583722	LR583930	**MW218122**	LR583836	LR583613
Neocosmospora lerouxii	CBS 146514^{T} = VG48 = CPC 37132	South Africa	*Citrus sinensis* - root scaffold	**MW218030**	**MW218076**	**MW173069**	**MW173039**	**MW218123**	**MW446617**	**MW248768**
Neocosmospora lichenicola	CBS 509.63	Brazil	Air	-	-	LR583728	LR583936	-	LR583843	LR583618
	CBS 623.92^{ET}	Germany	Human necrotic wound	-	-	LR583730	LR583938	-	LR583845	LR583620
Neocosmospora liriodendri	CBS 117481^{T}	USA	*Liriodendron tulipifera*	**MW218031**	**MW218077**	AF178404	AF178373	**MW218124**	EU329506	AF178340
Neocosmospora longissima	CBS 126407^{T}	New Zealand	Tree bark	-	-	LR583731	LR583939	-	LR583846	LR583621
Neocosmospora macrospora	CBS 142424^{T}	Italy	*Citrus sinensis*	**MW218032**	**MW218078**	LT746266	LT746281	**MW218125**	LT746331	LT746218
	CPC 28193	Italy	*Citrus sinensis*	**MW218033**	**MW218079**	LT746268	LT746283	**MW218126**	LT746333	LT746220

(Continued)

Table 1. (Continued).

Species	Strain number[1]	Country	Host	GenBank sequence accession number[2]						
				acl	*cal*	ITS	LSU	*rpb1*	*rpb2*	*tef1*
Neocosmospora martii	CBS 115659^{ET}	Germany	*Solanum tuberosum*	-	-	JX435206	JX435206	-	JX435256	JX435156
Neocosmospora metavorans	CBS 135789^{T}	Greece	Human pleural effusion	**MW218034**	**MW218080**	LR583738	LR583946	**MW218127**	LR583849	LR583627
	CBS 143219	Spain	Human foot	**MW218035**	**MW218081**	LR583744	LR583948	**MW218128**	LR583851	LR583629
Neocosmospora mori	CBS 145467^{T}	Japan	*Morus alba*	-	-	DQ094305	DQ236347	-	EU329499	AF178358
	CBS 145468	Japan	*Morus alba*	-	-	DQ094306	DQ236348	-	EU329493	AF178359
Neocosmospora noneumartii	CBS 115658^{T}	Israel	*Solanum tuberosum*	**MW218036**	**MW218082**	LR583745	LR583949	**MW218129**	**MW446618**	LR583630
	VG87 = CPC 37135	South Africa	*Citrus sinensis* - root scaffold	-	-	**MW173070**	**MW173345**	-	**MW446619**	**MW248769**
	VG88 = CPC 37136	South Africa	*Citrus sinensis* - root scaffold	-	-	**MW173071**	**MW173346**	-	**MW446620**	**MW248770**
Neocosmospora oblonga	CBS 130325^{T}	USA	Human eye	-	-	LR583746	LR583950	-	LR583853	LR583631
Neocosmospora paraeumartii	CBS 487.76^{T}	Argentina	*Solanum tuberosum*	-	-	LR583747	LR583951	-	LR583855	DQ247549
Neocosmospora parceramosa	CBS 115695^{T}	South Africa	Soil	**MW218037**	**MW218083**	JX435199	JX435199	-	JX435249	JX435149
Neocosmospora perseae	CBS 144142^{T}	Italy	*Persea americana*	**MW218038**	**MW218084**	LT991940	LT991947	**MW218130**	LT991909	LT991902
Neocosmospora petroliphila	CBS 203.32	South Africa	*Pelargonium* sp.	**MW218039**	**MW218085**	DQ094320	DQ236362	**MW218131**	LR583857	DQ246835
	CBS 224.34	Cuba	Human toenail	**MW218040**	**MW218086**	DQ094383	DQ236425	**MW218132**	LR583858	DQ246910
Neocosmospora piperis	CBS 145470^{T}	Brazil	*Piper nigrum*	-	-	AF178422	AF178391	-	EU329513	AF178360
Neocosmospora pisi	CBS 123669^{ET}	USA	Progeny of parentals from *Pisum sativum* and soil	-	-	LR583753	LR583957	-	LR583862	LR583636
	CBS 142372	Germany	*Trifolium subterraneum*	-	-	LR583755	LR583959	-	LR583864	KY556454
Neocosmospora protoensiformis	CBS 145471^{T}	Venezuela	Dicot tree	-	-	AF178399	AF178368	-	EU329498	AF178334
Neocosmospora pseudoradicicola	CBS 145472^{T}	Papua New Guinea	Diseased cocoa pods	**MW218041**	**MW218087**	JF740899	JF740899	**MW218133**	JF741084	JF740757
Neocosmospora quercicola	CBS 141.90^{T}	Italy	*Quercus cerris*	-	-	LR583760	LR583964	-	LR583869	DQ247634
Neocosmospora regularis	CBS 230.34^{T}	Netherlands	*Pisum sativum*	-	-	LR583763	LR583967	-	LR583873	LR583643
Neocosmospora silvicola	CBS 123846^{T}	USA	*Liriodendron tulipifera*	-	-	LR583766	LR583971	-	LR583876	LR583646
Neocosmospora solani	CBS 140079^{ET}	Slovenia	*Solanum tuberosum*	**MW218042**	**MW218088**	KT313633	KT313633	**MW218134**	KT313623	KT313611
	VG36	South Africa	*Citrus sinensis* - root scaffold	-	-	**MW173072**	-	-	**MW446621**	**MW248771**
	VG38	South Africa	*Citrus sinensis* - root scaffold	-	-	**MW173073**	-	-	**MW446622**	**MW248772**

(Continued)

Table 1. (Continued).

Species	Strain number[1]	Country	Host	GenBank sequence accession number[2]						
				acl	*cal*	ITS	LSU	*rpb1*	*rpb2*	*tef1*
	VG46	South Africa	*Citrus sinensis* - root scaffold	-	-	**MW173074**	-	-	**MW446623**	**MW248773**
	VG53	South Africa	*Citrus sinensis* - root scaffold	-	-	**MW173075**	-	-	**MW446624**	**MW248774**
	VG63	South Africa	*Citrus sinensis* - root scaffold	-	-	**MW173076**	-	-	**MW446625**	**MW248775**
	VG68	South Africa	*Citrus sinensis* - root scaffold	-	-	**MW173077**	-	-	**MW446626**	**MW248776**
	VG78	South Africa	*Citrus sinensis* - root scaffold	-	-	**MW173078**	-	-	**MW446627**	**MW248777**
	VG93	South Africa	*Citrus sinensis* - root scaffold	-	-	**MW173079**	-	-	MW446628	MW248778
	VG99	South Africa	Soil - citrus orchard	-	-	**MW173080**	-	-	**MW446629**	**MW248779**
	VG115	South Africa	*Citrus sinensis* - crown	-	-	**MW173081**	-	-	**MW446630**	**MW248780**
	VG147	South Africa	*Citrus sinensis* - crown	-	-	**MW173082**	-	-	**MW446631**	**MW248781**
	VG169	South Africa	*Citrus sinensis* - crown	-	-	**MW173083**	-	-	**MW446632**	**MW248782**
	VG175	South Africa	*Citrus sinensis* - root scaffold	-	-	**MW173084**	-	-	**MW446633**	**MW248783**
	VG193	South Africa	*Citrus sinensis* - root scaffold	-	-	**MW173085**	-	-	**MW446634**	**MW248784**
	VG415	South Africa	*Citrus sinensis* - crown	-	-	**MW173086**	-	-	**MW446635**	**MW248785**
Neocosmospora sp. (FSSC12)	CBS 143212	USA	Turtle egg	**MW218043**	**MW218089**	DQ094587	DQ236629	**MW218135**	EU329625	DQ247128
	CBS 143226	USA	Kemps Ridley turtle	**MW218044**	**MW218090**	KC808244	MG189922	**MW218136**	KC808342	KC808202
Neocosmospora spathulata	CBS 145474^{T}	USA	Human synovial fluid	**MW218045**	**MW218091**	EU329674	EU329674	**MW218137**	EU329542	DQ246882
Neocosmospora stercicola	CBS 142481^{T}	Germany	Compost yard debris	-	-	LR583779	LR583984	-	LR583887	LR583658
	CBS 144388	Belgium	Greenhouse humic soil	-	-	LR583780	LR583985	-	LR583888	LR583659
Neocosmospora suttoniana	CBS 143214^{T}	USA	Human wound	**MW218046**	**MW218092**	DQ094617	DQ236659	**MW218138**	EU329630	DQ247163
	CBS 143224	USA	Equine eye	**MW218047**	**MW218093**	MG189940	MG189925	**MW218139**	KC808336	KC808197
Neocosmospora tonkinensis	CBS 115.40^{T}	Vietnam	*Musa sapientum*	**MW218048**	**MW218094**	MG189941	MG189926	**MW218140**	LT960564	LT906672
	CBS 118931	UK	*Solanum lycopersicum*	**MW218049**	**MW218095**	LR583784	LR583989	**MW218141**	LR583891	LR583662
Neocosmospora vasinfecta	CBS 446.93	Japan	Soil	-	-	LR583791	LR583996	-	LR583898	LR583670
	CBS 533.65	India	Unknown	-	-	LR583792	LR583997	-	LR583899	LR583671

[1] CBS: Westerdijk Fungal Biodiverity Institute (WI), Utrecht, The Netherlands; CPC: Collection of P.W. Crous, held at WI; NRRL: Agricultural Research Service Culture Collection, National Center for Agricultural Utilization Research, USDA, Peoria, IL, USA; VG: Working collection of J. Van Niekerk held at Department of Plant Pathology, University of Stellenbosch, South Africa; ET: Ex-epitype, IT: Ex-isotype, NT: Ex-lectotype.

[2] *acl*: ATP citrate lyase largest subunit; *cal*: calmodulin; ITS: internal transcribed spacer region of the rDNA; LSU: large subunit of the rDNA; *rpb1*: RNA polymerase largest subunit; *rpb2*: RNA polymerase second largest subunit; *tef1*: translation elongation factor 1-alpha. Sequences generated in the present study are shown in **bold font**.

mined as putative novel species in the previous analyses. For RAxML analyses, the default parameters were selected and clade stability was determined by bootstrap (BS) analysis using 1000 repetitions. Bayesian analyses consisted of two parallel runs of 5 M generations, with the stop-rule on, set to 0.01. The sampling frequency was set to 1000 generations, and consensus trees and posterior probability values (PP) were calculated after discarding the first 25% of sampled trees as the burn-in fraction. The best evolutionary model for each gene partition was determined using MrModelTest v. 2.3 (Nylander, 2004).

RESULTS

Sampling, fungal collection and isolation

In the Patensie and Kirkwood areas, diseased trees initially showed yellowing, wilting leaves and dieback of branch tips. Symptoms subsequently progressed with defoliation and sudden decline before the plants died. Inspection of affected trees showed cracks or blisters on the trunks above the crowns with, rarely, gum exudates (Figure 1). If each trunk was transversely cut, brown to black discolouration and necrosis of the vascular tissue became visible with different extensions (Figure 2). Similar discolouration and stains were visible into the scaffold roots. Symptoms were observed in orchards older than 8 years. Incidence of symptomatic plants was in some cases up to 50% of affected trees in orchards.

A total of 62 monosporic isolates resembling those of *Neocosmospora* were collected from the sampled citrus trees. Among them, 33 isolates were obtained from the Kirkwood area and 29 from Patensie. Thirty-eight were isolated from trunk portions, 22 from scaffold roots, and two from soil surrounding infected roots. Among the isolates collected from trunks, 17 were from necrotic tissue, two from healthy tissue and 14 from the margins between necrotic and healthy tissues.

Phylogenetic studies and identification of the pathogens

A first analysis, based on combined *rpb2* and *tef1* loci, was conducted to identify the *Neocosmospora* isolates obtained from symptomatic citrus trees. The dataset contained 129 isolates, representing 62 South African isolates, as well as 67 ex-type or reference strains representing 46 taxa in *Neocosmospora,* and two outgroup taxa (*Geejayessia atrofusca* NRRL 22316 and *G. cicatricum* CBS 125552). The alignment included 2290 positions (1614 *rpb2*, 676 *tef1*) of which 748 were variable (480 *rpb2*, 268 *tef1*), and 562 positions were phylogenetically informative sites (379 *rpb2*, 183 *tef1*). For both gene partitions, a GTR + I + G model was selected and incorporated in the analyses. The BI lasted for 1,855,000 generations, and the consensus tree and PP were calculated from 1392 trees after discarding 494 trees as burn-in fraction. Phylogenetic trees inferred using ML and BI analyses resulted in very similar topologies, and therefore only the ML tree is presented in Figure 3a. The South African isolates were distributed among 11 distinct phylogenetic lineages, of which seven corresponded to known *Neocosmospora* species, which were, in order of frequency of isolation: *N. ferruginea* and *N. solani* (15 isolates each), *N. hypothenemi* (five isolates), *N. brevis* (three isolates), *N. noneumartii* (two isolates), and *N. crassa* and *N. falciformis* (one isolate each). The remaining 20 South African isolates grouped within four undescribed phylogenetic lineages, among which 15 isolates clustered in a well-supported clade ("*Neocosmospora* sp. 1", BS = 93/PP = 0.96), sister to *N. bataticola*; three isolates (VG268, 279 and 281) clustered in a fully-supported clade ("*Neocosmospora* sp. 2", BS = 100/PP = 100), sister to *N. metavorans*; while two isolates (singletons VG16 and VG48) were resolved as single lineages (respectively, "*Neocosmospora* sp. 3" and "*Neocosmospora* sp. 4"); however, with low statistical support values compared with those in the *rpb2* and *tef1* analyses.

To further assess the phylogenetic position of the putative novel phylogenetic clades, a second, more robust multi-locus phylogenetic analysis was performed using seven loci (*acl*, *cal*, ITS, LSU, *rpb1*, *rpb2* and *tef1*) and selected strains representing closely related species, as determined in the previous phylogenetic assessment of the genus *Neocosmospora*. The combined dataset included 5904 positions (616 *acl*, 573 *cal*, 467 ITS, 480 LSU, 1489 *rpb1*, 1613 *rpb2* and 666 *tef1*) from 47 strains, representing a subset of 28 phylogenetic clades of *Neocosmospora*, plus two outgroup taxa. From the total sites included, 1405 were variable (188 *acl*, 103 *cal*, 100 ITS, 34 LSU, 372 *rpb1*, 390 *rpb2* and 218 *tef1*), and 856 were phylogenetically informative (81 *acl*, 82 *cal*, 70 ITS, 22 LSU, 196 *rpb1*, 266 *rpb2* and 139 *tef1*). Optimal model selection for each gene partition was determined as follows: GTR + G for *tef1*, GTR + I + G for LSU and ITS; K80 + G for *acl*, K80 + I + G for *cal*, and SYM + I + G for *rpb1* and *rpb2*. The BI lasted for 1,520,000 generations, and PP were calculated from 1141 trees after discarding 380 trees as the burn-in fraction. The BI analysis (shown in Figure 3 b) confirmed the topology obtained by ML.

The analyses confirmed the results obtained in the two-gene phylogeny, and the four novel lineages were resolved with high BS and PP support. *Neocosmospora* sp. 2 and representative isolates of clade *Neocosmospora*

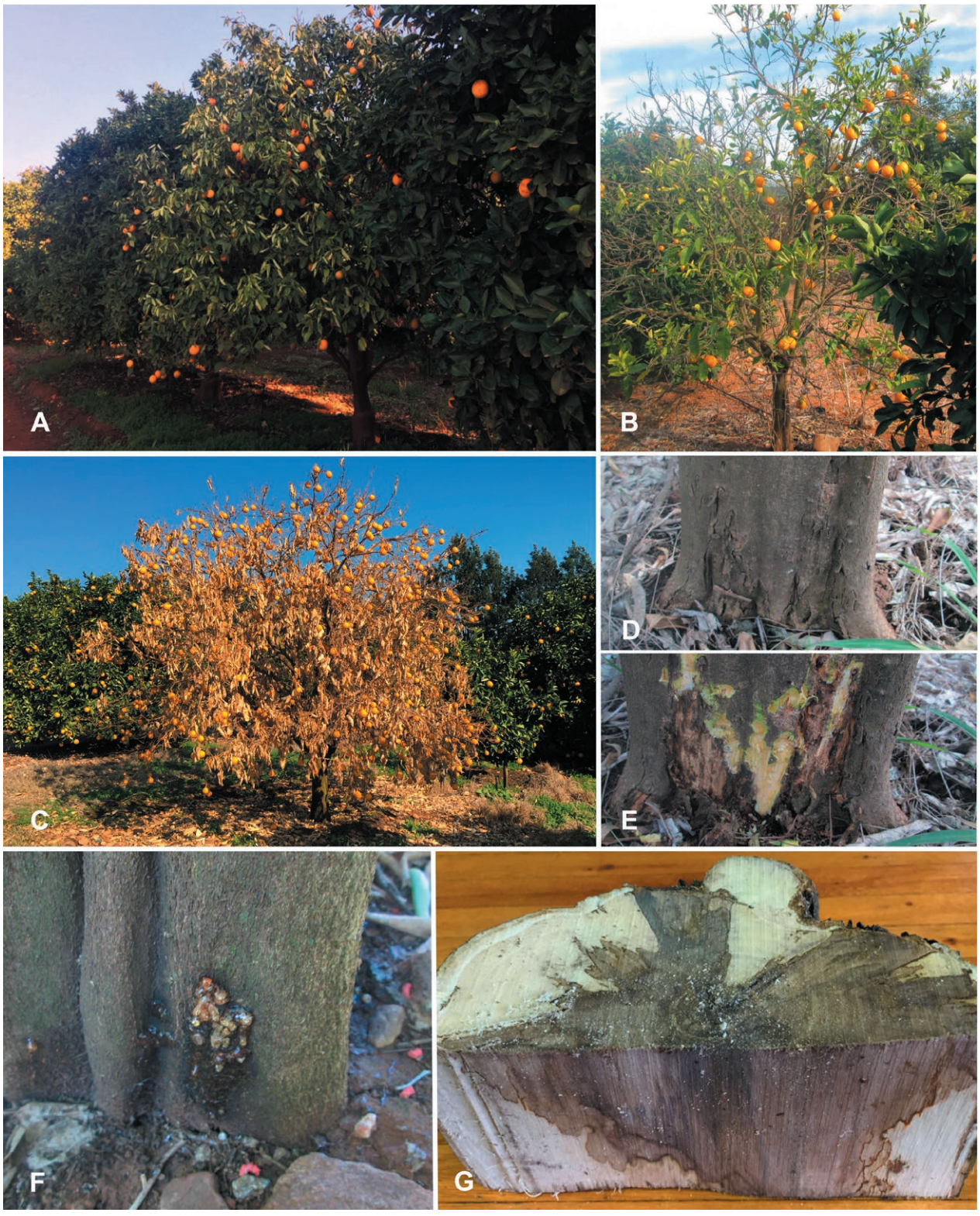

Figure 1. Dry root rot symptoms of citrus observed in South Africa. Tree decline progression: initial leaves wilting (A), yellowing, loss of leaves, and dieback of branch tips (B) and plant death (C). External cracks or blisters on the trunk portion above the crown (D) and internal dry rot (E) of the same plant. Gum exudate at the crown level (F). Brown to black discolouration and necrosis of the vascular tissue visible in longitudinal and transverse sections (G).

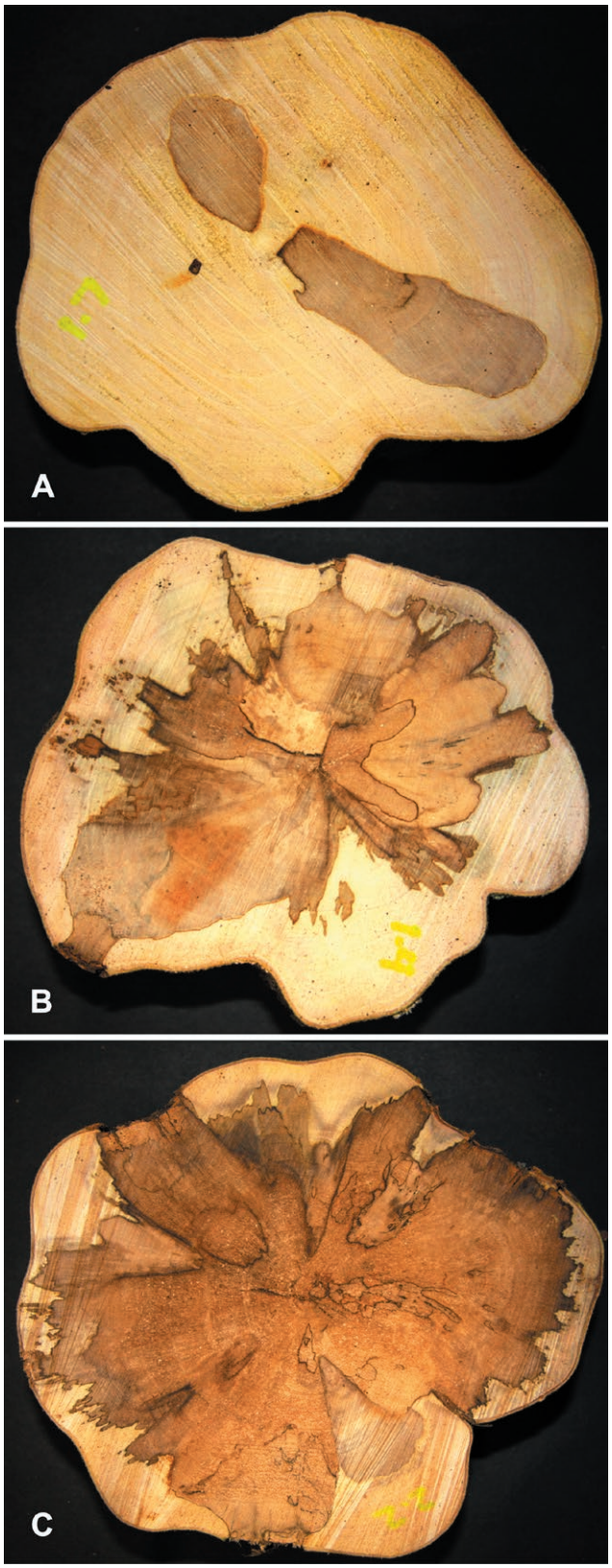

Figure 2. Small (A), medium (B) or large (C) extensions of internal discolouration in transverse sections through citrus tree trunks.

sp. 1 were both resolved as fully supported clades (BS = 100/PP = 100), while the lone lineages *Neocosmospora* sp. 3 and *Neocosmospora* sp. 4 were confidently resolved as well-supported branches (respectively, BS = 96/PP = 0.97 and BS = 86/PP = 0.96). These four phylogenetic lineages are therefore here proposed as the novel species *Neocosmospora addoensis*, *N. citricola*, *N. gamtoosensis* and *N. lerouxii*.

Taxonomy

Neocosmospora addoensis Sand.-Den. & Guarnaccia, *sp. nov.* – MycoBank MB837939; Figure 4.

Etymology. Named after the geographical area Addo, South Africa where first collected.

Typus. South Africa, Eastern Cape, Kirkwood, from *Citrus sinensis* crown, May 2018, *V. Guarnaccia* (holotype CBS H-24565 designated here, culture ex-type CBS 146510 = CPC 37128 = VG281).

Conidiophores borne on aerial mycelium, 53.5–425 µm long, unbranched or less commonly laterally branched, bearing terminal single phialides, proliferating percurrently; aerial phialides monophialidic, subulate to subcylindrical, smooth- and thin-walled, 34–64.5 × 2–4 µm, with short and flared apical collarettes and inconspicuous periclinal thickening; *aerial conidia* arranged in false heads on phialide tips, hyaline, broadly ellipsoidal to clavate and slightly asymmetrical, smooth- and thin-walled, aseptate, (5.5–)7–10(–14.5) × (2–)3–4 µm (av. 8.5 × 3 µm). *Sporodochia* pale luteous to pale peach coloured, formed abundantly on carnation leaves. *Sporodochial conidiophores* unbranched or laterally and irregularly branched bearing apical groups of 2–3 monophialides; *sporodochial phialides* subulate to subcylindrical, 12.5–25 × 2–4.5 µm, smooth and thin-walled, commonly proliferating sympodially, collarettes and periclinal thickening absent or inconspicuous. *Sporodochial conidia* falcate, slightly curved dorsoventrally to almost straight, broadest near the half portion or the upper third, tapering towards both ends, with blunt and slightly curved apical cells and blunt, sometimes inconspicuous foot-like basal cells, (1–)2–5-septate, predominantly 4-septate, hyaline, smooth- and thick-walled; one-septate conidia: (18.5–)19–24(–25) × 3–4.5 µm (av. 21.5 × 4 µm); two-septate conidia: (24–)26–30 × 3.5–5 µm (av. 27.5 × 4.5 µm); three-septate conidia: (27–)33–43(–45) × (3–)4–5.5(–6) µm (av. 38 × 5 µm); four-septate conidia: (39–)42–47.5(–51.5) × 4.5–6 µm (av. 49 × 5.5 µm); five-septate conidia: (37.5–)42.5–51 × 5–6 µm (av. 47 × 5.5 µm). *Chlamydospores* subspherical to spherical, hyaline to pale yellow, smooth-walled or slightly roughened, thick-walled, 4–10 µm, single or in chains, terminal or intercalary on hyphae and conidia.

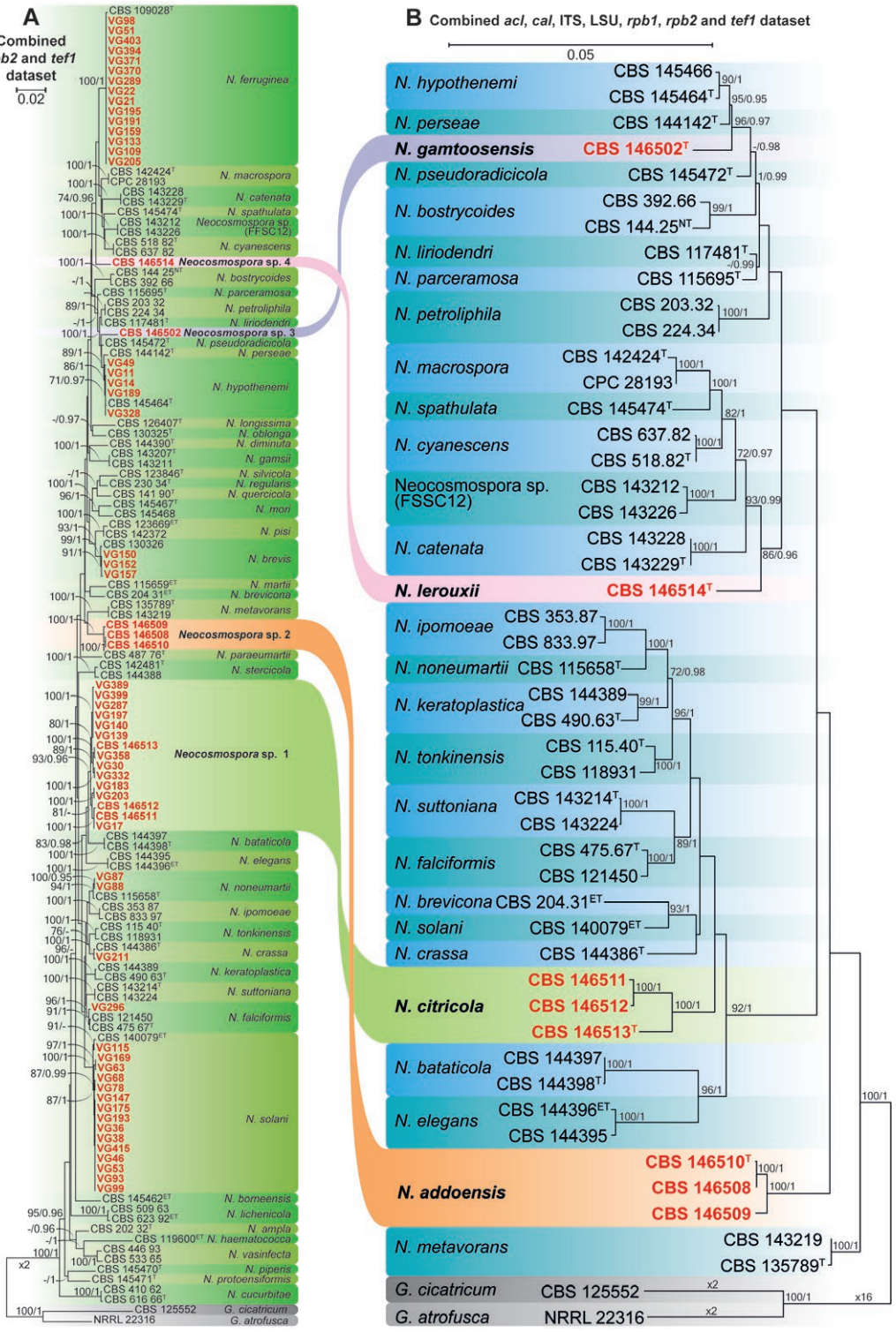

Figure 3. Maximum-likelihood (ML) phylograms obtained from combined *rpb2* and *tef1* (A) and *acl*, *cal* ITS, LSU, *rpb1*, *rpb2* and *tef1* (B) sequences, of 62 isolates of *Neocosmospora* spp. from South African *Citrus* (shown in red), and representative and ex-type isolates of *Neocosmospora*. Names of new species described here are shown in **bold font**. Numbers on the nodes are ML bootstrap values greater than 70% followed by Bayesian posterior probability values greater than 0.95. Branch lengths are proportional to distance. Ex-type, ex-epitype and ex-neotype strains are indicated, respectively, with ^{T}, ^{ET} and ^{NT}. The trees are rooted to *Geejayesia atrofusca* (NRRL 22316 and *G. cicatricum* (CBS 125552).

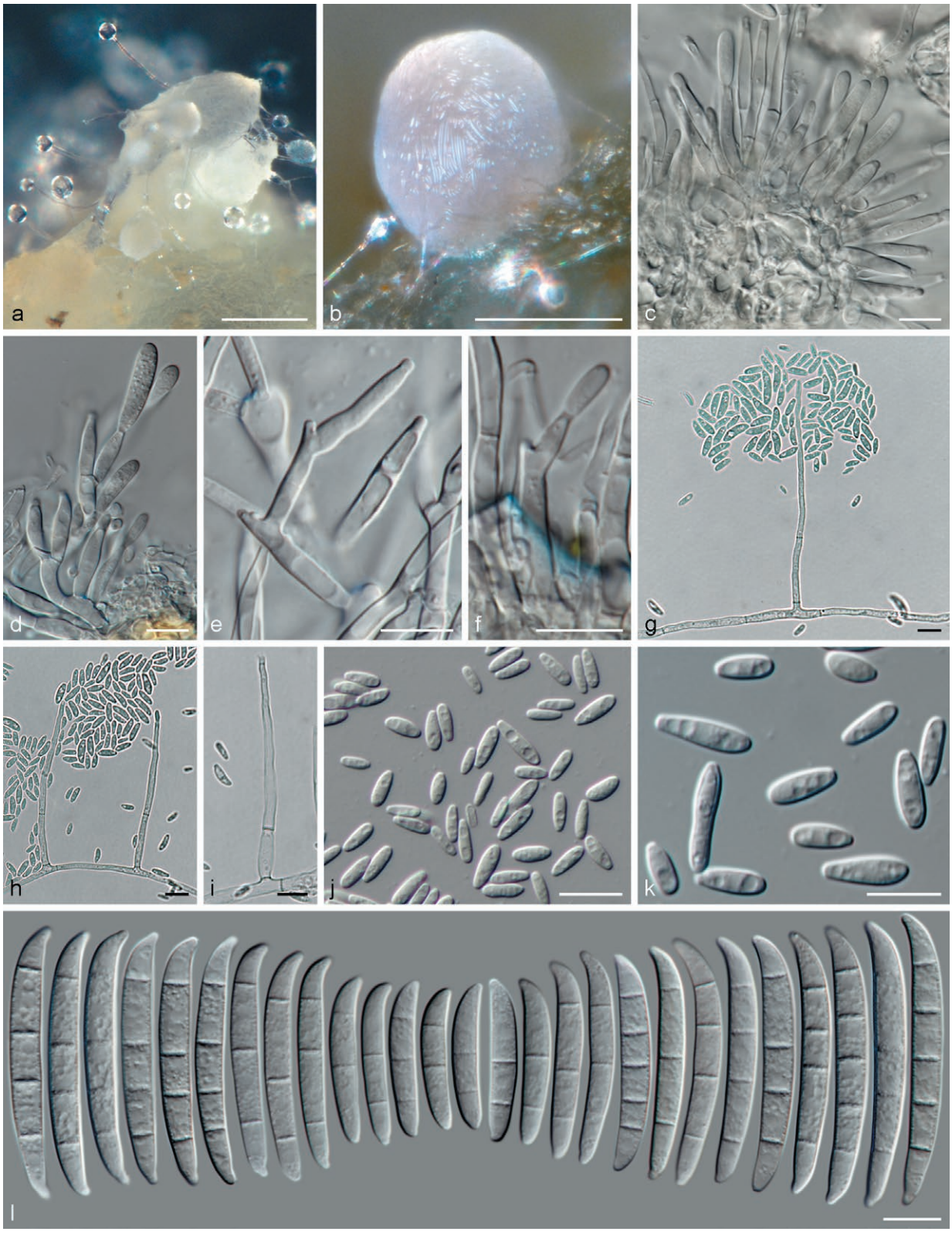

Figure 4. *Neocosmospora addoensis* (ex-type culture CBS 146510). (a and b) sporodochia formed on the surface of carnation leaves; (c to f) sporodochial conidiophores and phialides; (g to i) aerial conidiophores; (j and k. aerial conidia; (l) sporodochial conidia. Scale bars: a and b = 100 µm; c to l = 10 µm.

Culture characteristics. Colonies on PDA reaching 79 mm diam. at 24°C after 7 d (growth rate: 4.1–5.6 mm d^{-1}). Colony surface white to primrose, becoming scarlet to bay, flat with abundant dense aerial mycelium, cottony to woolly; colony reverse pale luteous to sulphur yellow, a vivid scarlet to rust pigment can be formed. On SNA, white to pale buff, membranous to woolly with scant aerial mycelium, becoming powdery; colony reverse white to pale buff. On OA, pale luteous to pale rosy buff, flat, membranous to cottony; colony reverse pale luteous to pale rosy buff.

Additional materials examined. South Africa, Eastern Cape, Patensie, from *Citrus sinensis* crown, May 2018, *V. Guarnaccia* (CBS 146508 = CPC 37126 = VG 268, CBS 146509 = CPC 37127 = VG279).

Notes. Both phylogenetic analyses resolved *Neocosmospora addoensis* as the closest genetic relative to *N. metavorans* (96 to 98% sequence similarity among individual gene datasets). *Neocosmospora metavorans* is a frequent opportunistic pathogen of animals, including humans (Sandoval-Denis *et al*., 2019). Nevertheless, in addition to its genetic exclusivity, these two species are morphologically quite distinct, particularly in the size and septation of the aerial conidia (aseptate, up to 14.5 µm in *N. addoensis* and multiseptate, up to 25 µm in *N. metavorans*), while sporodochial conidia of *N. addoensis* are more slender (up to 6 µm wide) than those of *N. metavorans* (up to 7.5 µm wide).

Neocosmospora addoensis is characterized by its small and slender macroconidia, which are much smaller than the average macroconidial type in *Neocosmospora*. Based on its macroconidial size, this species is close to *N. brevis* and *N. pseudoradicicola*; however, these two species are well-delimited phylogenetically, clustering in far separate lineages of the genus (96% sequence similarity with *N. brevis* and 97% with *N pseudoradicicola*). Morphologically, *N. addoensis* differs from *N. pseudoradicicola* by its macroconidial shape and curvature, with more rounded apical cells, rather inconspicuous foot cells and less pronounced dorsoventral curvature; and from *N. brevis* by the absence of aerial macroconidia and slightly more elongated and hooked macroconidial apical cells.

Neocosmospora citricola Guarnaccia & Sand.-Den., *sp. nov.* – MycoBank MB837940; Figure 5.

Etymology. In reference to occurrence of this fungus on *Citrus* plants.

Typus. South Africa, Eastern Cape, Patensie, from *Citrus sinensis* crown, May 2018, *V. Guarnaccia* (holotype CBS H-24566 designated here, culture ex-type CBS 146513 = CPC 37131 = VG343).

Conidiophores borne on aerial mycelium, 66.5–198.5 µm long, unbranched or irregularly laterally branched, bearing terminal single phialides; *aerial phialides* monophialidic, subulate to subcylindrical, smooth- and thin-walled, 39.5–73.5 × 2–4.5 µm, each showing a discrete flared collarette and inconspicuous to evident periclinal thickening; *aerial conidia* arranged in false heads on phialide tips, hyaline, broadly ellipsoidal to obovoidal, rarely clavate, smooth- and thin-walled, 0–1-septate, (6–)9–17(–24.5) × 3–5(–6.5) µm (av. 13 × 4.5 µm). *Sporodochia* pale luteous to pale orange, formed abundantly on carnation leaves and on the agar surface. *Sporodochial conidiophores* laterally and irregularly branched, bearing single terminal monophialides or terminal groups or up to three monophialides; *sporodochial phialides* subulate to subcylindrical, 11–27.5 × 3–5.5 µm, smooth and thin-walled, with inconspicuous or absent apical collarettes and periclinal thickening. *Sporodochial conidia* falcate, curved dorsoventrally to almost straight, each with broadening in the upper third, tapering towards both ends, with a blunt to papillate and slightly curved apical cell and a blunt, foot-like basal cell, (2–)3–5(–6)-septate, predominantly five-septate, hyaline, robust, smooth- and thick-walled; two-septate conidia, 44 × 5.7 µm; three-septate conidia: 33.5–49.5(–58) × 4.5–6 µm (av. 43 × 5.5 µm); four-septate conidia: (46.5–)47.5–56(–59.5) × 5–6.5 µm (av. 52 × 6 µm); five-septate conidia: (49.5–)53–60.5(–65) × (4.5–)5.5–6.5(–7) µm (av. 57 × 6 µm); six-septate conidia: 60 × 6 µm. *Chlamydospores* subspherical to spherical, hyaline to pale golden brown, smooth to slightly roughened and thick-walled, 5–10 µm, single or in chains, terminal or intercalary on hyphae and conidia.

Culture characteristics: Colonies on PDA reaching 69 mm diam. at 24°C after 7 d (growth rate: 3.2–4.9 mm d^{-1}). Colony surfaces straw, buff to pale luteous, with pale luteous to orange centres and abundant aerial mycelium, flat, felty, woolly to cottony with abundant concentric rings of aerial mycelium, colony reverse pale luteous to orange. On SNA, white and translucent, flat, woolly, becoming slightly pulverulent with sporulation, colony reverse white. On OA, saffron to peach, flat, membranous to cottony, colony reverse intense peach to flesh.

Additional materials examined. South Africa, Eastern Cape, Patensie, from *Citrus sinensis* crown, May 2018, *V. Guarnaccia* (CBS 146511 = CPC 37129 = VG302, CBS 146512 = CPC 37130 = VG307).

Notes. *Neocosmospora citricola* resolved as a highly supported monophyletic clade, basal to a fully supported lineage containing *N. bataticola* and *N. elegans*, which clearly differentiated genetically (96 to 98% sequence similarity to *N. citricola* in the single gene datasets).

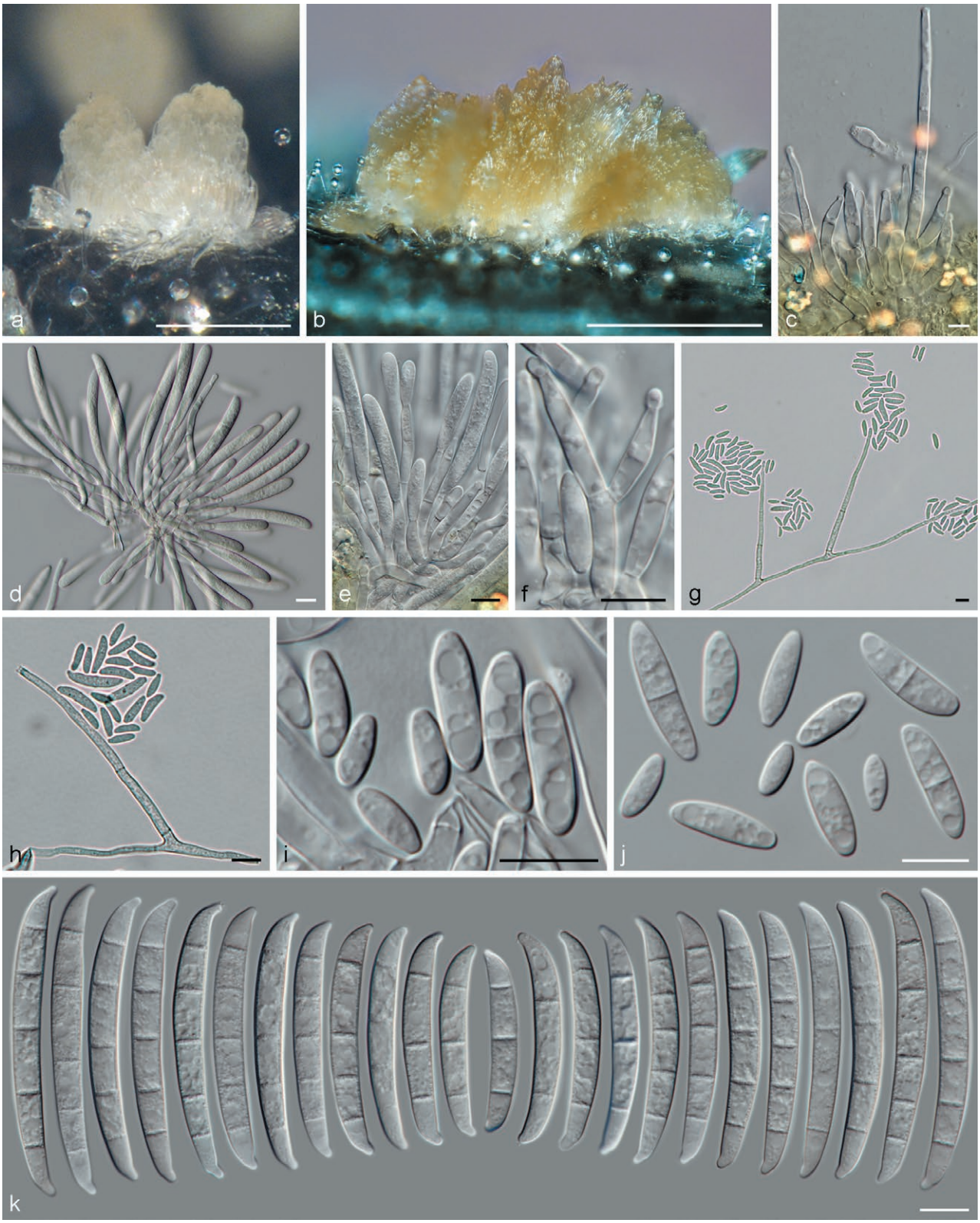

Figure 5. *Neocosmospora citricola* (ex-type culture CBS 146513). (a and b) sporodochia formed on the surface of carnation leaves; (c to f) sporodochial conidiophores and phialides; (g and h) aerial conidiophores;(I and j) aerial conidia; (k) sporodochial conidia. Scale bars: a and b = 100 µm; c to k = 10 µm.

Although genetically distant, *Neocosmospora citricola* is morphologically similar to *N. nirenbergiana*, *N. piperis* and *N. protoensiformis* (92% sequence similarity with *N. nirenbergiana* and 96% with *N. piperis* and *N. protoensiformis*; data not shown), the four species producing very similar macroconidia in shape and overall size. Nevertheless, *N. citricola* differs from *N. nirenbergiana* and *N. piperis* by the absence of aerial macroconidia. Conversely, *N. nirenbergiana* and *N. piperis* do not produce aerial microconidia, and the aerial conidiophores of *N. citricola* are much more robust than those of *N. nirenbergiana* and *N. piperis*. *Neocosmospora protoensiformis* also lacks aerial macroconidia; however, in addition to forming smaller microconidia (up to 15 µm long, average size 7.6 × 3.6 µm in *N. protoensiformis vs* up to 24 µm long, average size 13 × 4.5 µm in *N. citricola*), and shorter sporodochial phialides (up to 19.5 µm long in *N. protoensiformis vs* up to 27.5 µm long in *N. citricola*), macroconidia of *N. protoensiformis* differ from those of *N. citricola* by usually being more tapered at both ends.

Neocosmospora gamtoosensis Sand.-Den. & Guarnaccia, *sp. nov.* – Mycobank MB837941; Figure 6.

Etymology. Named after the valley where this fungus was collected, Gamtoos River Valley, South Africa.

Typus. South Africa, Eastern Cape, Patensie, from *Citrus sinensis* crown, May 2018, *V. Guarnaccia* (holotype CBS H-24564 designated here, culture ex-type CBS 146502 = CPC 37120 = VG16).

Conidiophores borne on aerial mycelium, 96.5–291 µm long, unbranched or irregularly laterally branched, bearing terminal single phialides; *aerial phialides* monophialidic, subulate to subcylindrical, smooth- and thin-walled, 17.5–61 × 2–3.5 µm, collarettes and periclinal thickening evident; *aerial conidia* arranged in false heads on phialide tips, hyaline, broadly ellipsoid, obovoid to short clavate, smooth- and thin-walled, aseptate, (4.5–)5.5–9(–11.5) × 2–3.5(–6) µm (av. 7 × 3 µm). *Sporodochia* citrine to honey, formed abundantly on carnation leaves. *Sporodochial conidiophores* commonly unbranched and densely packed, bearing terminal, single monophialides or groups of 2–3 phialides; *sporodochial phialides* lageniform to ampulliform, 7.5–17 × 3–5 µm, smooth and thin-walled, each with an often conspicuous periclinal thickening and a reduced, flared collarette. *Sporodochial conidia* falcate, slightly curved dorsoventrally to almost straight on their ventral faces, broadening in the upper third, tapering towards both ends, with blunt and hooked apical cells and blunt to slightly pointed and extended foot-like basal cells, (4–)5–6(–7)-septate, predominantly five-septate, hyaline, smooth- and thick-walled; four-septate conidia: (37–)40–55(–56.5) × 4.5–5.5 µm (av. 48.5 × 5 µm); five-septate conidia: (46.5–)51.5–60(–62) × 4.5–5.5 µm (av. 56 × 5 µm); six-septate conidia: 55.5–64(–65) × 4.5–5.5 µm (av. 60 × 5 µm); seven-septate conidia: 60.5 × 5 µm. *Chlamydospores* subspherical, hyaline to pale yellow, inconspicuously roughened, thick-walled, 5–12 µm diam., single or forming chains or clusters, terminal or intercalary on hyphae.

Culture characteristics: Colonies on PDA reaching 60 mm diam. at 24°C after 7 d (growth rate: 3.8–4.3 mm d^{-1}). Colony surfaces pale luteous, amber to pure yellow, flat with abundant dense aerial mycelium in radial patches, cottony to woolly, colony reverse pale luteous to vivid pure yellow. On SNA, colonies white to pale buff, translucent, flat, woolly with scant aerial mycelium, becoming slightly powdery; reverse white to pale buff. On OA, the colonies are pale luteous, pale buff to primrose, flat, membranous to cottony, and colony reverse pale luteous to pale rosy buff.

Notes. In the combined *rpb2* and *tef1* analysis, *Neocosmospora gamtoosensis* formed an unsupported lone lineage, basal to a larger lineage containing *N. hypothenemi*, *N. perseae* and *N. pseudoradicicola*. The combined seven-loci analysis resolved *N. gamtoosensis* within the larger lineage, with high statistical support for all the earlier listed species. Base pair similarities between the novel species and its closest relatives ranged from 98% in the combined dataset to between 96 and 99% in the individual gene datasets.

Neocosmospora gamtoosensis is morphologically reminiscent of *N. hypothenemi*, both species having predominantly five-septate macroconidia of very similar size and shape; however, *N. gamtoosensis* has conspicuously flared collarettes on its aerial phialides, also producing shorter (length up to 11.5 µm, average = 7 µm in *N. gamtoosensis vs* up to 13.5 µm, average = 8.2 µm in *N. hypothenemi*), aseptate aerial conidia, and honey coloured sporodochia (yellow-green in *N. hypothenemi*), and lacking reddish pigments on PDA. *Neocosmospora noneumartii*, another genetically distant (97% sequence similarity in the combined analysis), but morphologically similar species, differs from *N. gamtoosensis* by forming dimorphic conidia from aerial phialides and longer sporodochial conidia (five-septate sporodochial conidia of average length 56 µm *vs* 63 µm in *N. noneumartii*). *Neocosmospora gamtoosensis* is also morphologically very similar to *N. lerouxii*. However, *N. gamtoosensis* has shorter (five-septate sporodochial conidia average length 63 µm in *N. lerouxii*) and more curved sporodochial conidia.

Neocosmospora lerouxii Guarnaccia & Sand.-Den., *sp. nov.* – Mycobank MB837942; Figure 7.

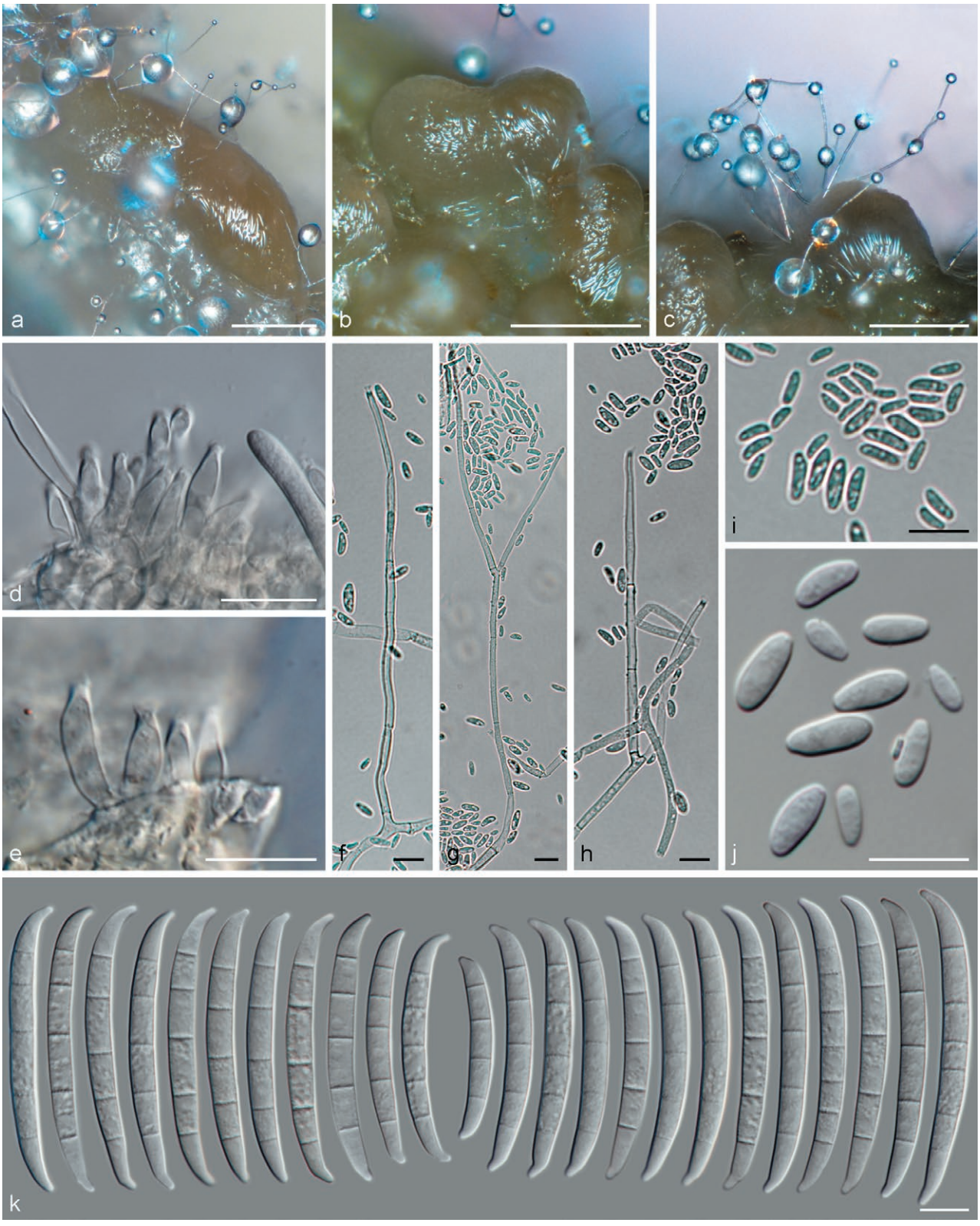

Figure 6. *Neocosmospora gamtoosensis* (ex-type culture CBS 146502). (a toc) sporodochia formed on the surface of carnation leaves; (d and e) sporodochial conidiophores and phialides; (f to h) aerial conidiophores; (I and j) aerial conidia; (k) sporodochial conidia. Scale bars: a and b = 100 µm; c to k = 10 µm.

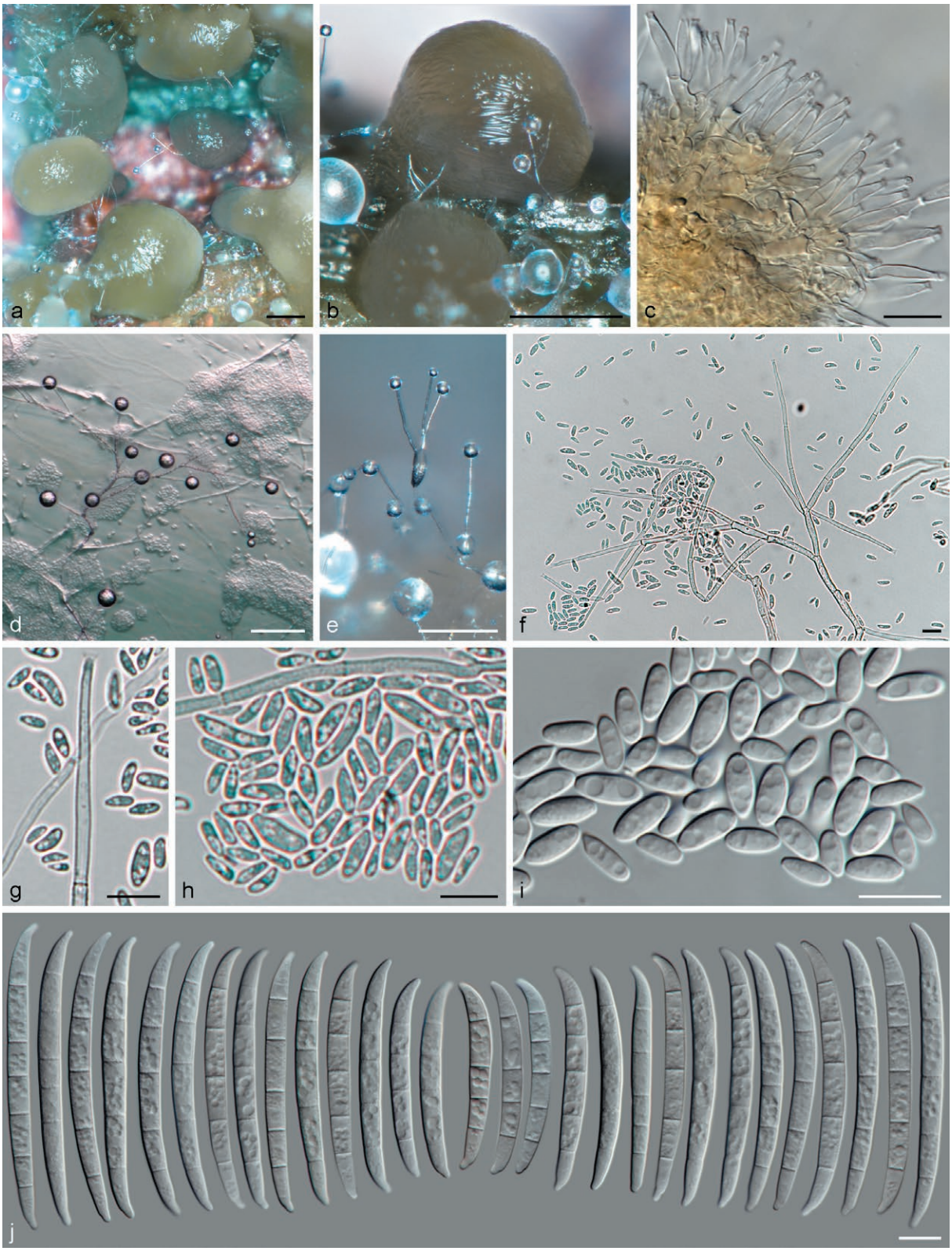

Figure 7. *Neocosmospora lerouxii* (ex-type culture CBS 146514). (a and b) sporodochia formed on the surface of carnation leaves; (c) sporodochial conidiophores and phialides; (d tog) aerial conidiophores and phialides; (h and i) aerial conidia; (j) sporodochial conidia. Scale bars: a and b = 100 µm; d and e = 50 µm; f to j = 10 µm.

Etymology. In memory of Dr Hennie Le Roux (10 Jul 1967 – 4 Oct. 2016), who made major contributions to the South African and international citrus industries.

Typus. South Africa, Eastern Cape, Patensie, from *Citrus sinensis* root scaffold, May 2018, *V. Guarnaccia* (holotype CBS H-24567 designated here, culture ex-type CBS 146514 = CPC 37132 = VG48).

Conidiophores borne on aerial mycelium, 139.5–295 µm long, simple or most commonly abundantly and irregularly branched, proliferating percurrently, bearing terminal single phialides; *aerial phialides* monophialidic, subulate to subcylindrical, smooth- and thin-walled, 37–61.5 × 2–4 µm, with periclinal thickening and collarettes abundant; *aerial conidia* arranged in false heads on phialide tips, hyaline, ovate, broadly ellipsoidal to short clavate, smooth- and thin-walled, 0(–1)-septate, (4.5–)6–10(–18.5) × 2–5 µm (av. 8 × 3.5 µm). *Sporodochia* pale luteous, ochreous to citrine, formed abundantly on carnation leaves and on agar surfaces. *Sporodochial conidiophores* verticillately and laterally branched and densely packed, smooth- and thin-walled, bearing apical whorls of up to four monophialides; *sporodochial phialides* subulate to subcylindrical, (12–)14.5–19.5(–22.5) × 2.5–4.5 µm, smooth- and thin-walled, with conspicuous periclinal thickening and short, flared collarettes. *Sporodochial conidia* falcate, almost straight or gently curved dorsiventrally, each broadening in the centre and upper third, tapering towards both ends, with a conical and slightly curved apical cell and a notched foot-like basal cell, (2–)4–6-septate, predominantly five-septate, hyaline, smooth- and thick-walled; two-septate conidia, 29 × 4 µm; three-septate conidia: 40 × 5 µm; four-septate conidia: (44–)45–49(–50.5) × (4–)4.5–5 µm (av. 47 × 5 µm); five-septate conidia: (46.5–)56.5–67(–73.5) × 4.5–5(–6.5) µm (av. 62 × 5 µm); six-septate conidia: 60–74 × 4.5–5.5 µm (av. 67 × 5 µm). *Chlamydospores* subspherical to spherical, hyaline to pale yellow-brown, smooth- and thick-walled, 4–8 µm diam., single or in chains, terminal or intercalary on hyphae.

Culture characteristics. Colonies on PDA reaching 61 mm diam. at 24°C after 7 d (growth rate: 3.5–4.3 mm d^{-1}). Surfaces buff, pale luteous to pale flesh, with abundant and dense whitish aerial mycelium, flat to slightly raised, felty to cottony. Colony reverse pale luteous, quickly becoming amber to sulphur yellow, with or without pale apricot patches. On SNA, colonies white and translucent, flat, felty, with white reverse sides. On OA, colonies white, saffron to buff, flat, membranous to cottony, with reverse sides buff to pale luteous with pale salmon patches.

Notes. The combined *rpb2* plus *tef1* analysis showed this taxon to form a well-supported (BS = 74, PP = 0.96) lone lineage, basal to a larger, unsupported linage containing *N. catenata*, *N. cyanescens*, *N. ferruginea*, *N. macrospora*, and *N. spathulata*, and the undescribed phylogenetic species FSSC 12. The analysis of the combined seven-gene dataset confirmed the previous results, with all the species described here resolved as highly- to fully-supported monophyletic clades. Genetic similarity between *N. lerouxii* and its closest phylogenetic relatives also support phylogenetic exclusivity of *N. lerouxii* (98% sequence similarity with all the above taxa in the combined alignment, and 97 to 99% similarity for the individual gene datasets).

Morphologically, *Neocosmospora lerouxii* most closely resembles the three distantly related species *N. gamtoosensis*, *N. hypothenemi* and *N. noneumartii* (respectively, 97, 98 and 97% sequence similarity, in the seven-loci combined dataset). While the three species were clustered in well-separated lineages in all analyses, morphologically they share very similar characteristics. Although *N. lerouxii* has similar macroconidial shape to *N. gamtoosensis* and *N. hypothenemi*, the macroconidia of *N. lerouxii* are longer and straighter than in the other two species (five-septate macroconidia average length 62 µm *vs* 56 µm in *N. gamtoosensis* and 59 µm in *N. hypothenemi*). Macroconidia of *N. lerouxii* also have thinner walls in comparison to those of *N. noneumartii*. In addition, has a slower growth rate in culture than *N. noneumartii*, (3.5–4.3 mm d^{-1} for *N. lerouxii vs* 4.7–8 mm d^{-1} in *N. noneumartii*).

DISCUSSION

Since 2013, severe sudden decline and death of citrus plants has been observed in citrus production areas of the Eastern Cape province of South Africa. Several species of *Colletotrichum*, *Diaporthaceae* and *Botryosphaeriaceae* have been reported as causing wood decay of citrus plants internationally (Guarnaccia and Crous, 2018; Mayorquin *et al*., 2019; Berraf-Tebbal *et al*., 2020; Esparham *et al*., 2020; Bezerra *et al*., 2021). Considering the very large economic losses to the South African citrus industry due to the observed sudden decline of trees, and because no surveys and isolations had been previously conducted for this disease and associated pathogens in the Eastern Cape citrus production area, a large-scale survey of affected citrus plants was required. The present study provides the first preliminary survey and sampling of citrus trees affected by dry root rot, and characterization of *Neocosmospora* diversity related to the observed disease in two important citrus production areas of South Africa.

Neocosmospora species are well-established in geographical areas with Mediterranean, sub-tropical or tropical climates, where these fungi are associated with diseases of important agricultural crops (Sandoval-Denis *et al*., 2018; Guarnaccia *et al*., 2018; 2019).

Fusarium oxysporum, *F. proliferatum* and *N. solani* s. str. were previously considered as pathogens associated with dry root rot of citrus plants. (Menge, 1988; Adesemoye *et al*., 2011). Specifically *F. oxysposrum* and *N. solani* were previously reported from South Africa. Diversity of *Fusarium* (three species) and *Neocosmospora* (five species) was revealed associated with dry root rot in restricted areas of three European countries by Sandoval-Denis *et al*. (2018). However, that study considered it likely that many other *Neocosmospora* spp. would also be isolated if a wider sampling area was surveyed.

In the present study, several citrus orchards in two major citrus production area of South Africa were investigated. A total of 62 *Neocosmospora* strains were collected from symptomatic tree trunks, roots and soil surrounding the roots. Phylogenetic analyses as well as morphological characters, revealed ten *Neocosmospora* species associated with infections on *Citrus* in South Africa, plus one species (*N. falciformis*) from soil from affected citrus orchards. The analyses included several of the closest related taxa to each of the *Neocosmospora* species recovered, based on BLAST searches of NCBI's GenBank nucleotide database. The final phylogenetic tree revealed four previously undescribed species (*N. addoensis*, *N. citricola*, *N. gamtoosensis*, *and N. lerouxii*) and six known species (*N. brevis*, *N. crassa*, *N. ferruginea*, *N. hypothenemi*, *N. noneumartii*, and *N. solani*) all of which were always associated with abovementioned symptomatic material.

Neocosmospora citricola, *N. ferruginea* and *N. solani* were the predominant species, largely found associated with the affected tissues of symptomatic plants cultivated in all the investigated orchards. Although follow-up studies will conduct pathogenicity trials to confirm these observations, it is assumed that these species represent the major biotic factors causing DRR of citrus in South Africa as they were consistently associated with the symptoms described from the diseased trees. These results also partially confirm what was recently demonstrated after surveys conducted in Mediterranean countries, where *N. ferruginea* (formerly FSSC28) and *N. solani* were isolated from typical DRR of citrus (Sandoval-Denis *et al*., 2018). *Neocosmospora citricola* was not found before the present study, and considering the broad distribution on affected plants, this fungus is likely to be important in DRR. *Neocosmospora addoensis* was isolated with low frequency, from one orchard and from necrotic trunk tissue. The other novel species described in this study, *N. gamtoosensis and N. lerouxii*, were found only sporadically, and are thus not considered as important pathogens. However, their description provides new insights into the taxonomy of *Neocosmospora*. *Neocosmospora brevis*, *N. crassa*, *N. hypothenemi* and *N. noneumartii* were also isolated sporadically, and future studies will investigate their roles in DRR. The complexity of pathogens associated with artificially reproducing DRR of citrus is well-known (Graham *et al*., 1985), but needs to be confirmed in further field trials. Furthermore, additional surveys in South Africa and other citrus-producing areas, and pathogenicity trials of *Neocosmospora* spp. in association with abiotic factors, should also be conducted.

The present study has provided the first overview of *Neocosmospora* diversity associated with DRR of citrus trees in South Africa, and has given useful information about taxonomic characterization within *Neocosmospora*. All the *Neocosmospora* species were isolated from crowns, trunks, roots and soil from the affected citrus orchards. Infected propagation material and soil can spread the pathogens nationally and internationally as the fungi can survive as chlamydospores in the soil and systemic infections in plant material. Further studies are required to resolve the host range and pathogenicity of all the species recovered. These fungi can survive as endophytes or as latent infections within citrus plants, so healthy propagation material should be used by growers. Favourable climatic conditions and, especially, plant stress factors could also play major roles in disease development. Further research on the epidemiology of DRR of citrus should be conducted to develop specific knowledge as the basis for effective disease prevention and management.

LITERATURE CITED

Adesemoye A.O., Eskalen A., Faber B., Bender G., O'connell N., ... Shea, T. 2011. Current knowledge on Fusarium dry root rot of citrus. *Citrograph* 2: 29–33.

Bender G.S. 1985. Dry Root Rot of Citrus—Factors Which Increase the Susceptibility of Trees to Infection by *Fusarium solani.* PhD dissertation, University of California, Riverside, CA, USA.

Berraf-Tebbal A., Mahamedi A.E., Aigoun-Mouhous W., Špetík M., Čechová J., … Eichmeier A. 2020. *Lasiodiplodia mitidjana* sp. nov. and other *Botryosphaeriaceae* species causing branch canker and dieback of *Citrus sinensis* in Algeria. *PloS one* 15: e0232448.

Bezerra J.D.P, Crous P.W., Aiello D., Gullino M.L., Polizzi G., Guarnaccia V. 2021. Genetic diversity and pathogenicity of *Botryosphaeriaceae* species aassociated with symptomatic citrus in Europe. *Plants* 10: 492.

Broadbent P. 2000. Dry root rot or sudden death. In: Timmer LW, Garnsey SM, Graham JH (eds) Compendium of Citrus Diseases, 2nd edn. APS Press, St. Paul, p. 71

Carbone I., Kohn L.M. 1999. A method for designing primer sets for speciation studies in filamentous ascomycetes. *Mycologia* 91: 553–556.

Conzulex W., Ramallo J., Ploper L.D. 1997. Identification of *Fusarium solani* (Mart.) associated with decline and root rot of grapefruit (*Citrus paradisi*). *Avana Agroindustrial* 18: 7–8.

Crous P.W., Verkley G.J.M., Groenewald J.Z., Houbraken, J. 2019. *Westerdijk Laboratory Manual Series* 1: Fungal Biodiversity. Westerdijk Fungal Biodiversity Institute, Utrecht, The Netherlands.

Derrick K.S., Timmer L.W. 2000. Citrus Blight and other diseases of recalcitrant etiology. *Annual Review of Phytopathology* 38: 181–205.

El-Mohamedy R.S.R. 1998. Studies on Wilt and Root Rot Disease of Some Citrus Plants in Egypt. PhD thesis, Fac Agric Ain Shams Univ, Cairo, Egypt, 227 pp.

Esparham N., Mohammadi H., Gramaje D. 2020. A survey of trunk disease pathogens within citrus trees in Iran. *Plants* 9: 754.

Fang D.Q., Federici C.T., Roose M.L. 1998. A high-resolution linkage map of the citrus tristeza virus resistance gene region in *Poncirus trifoliata* (L.) Raf. *Genetics* 150: 883–890.

FAOSTAT 2019. Food and Agriculture Organization of the United Nations. http://www.fao.org/faostat/en/#home. Accessed 26 February 2020.

Fisher N.L., Burguess L.W., Toussoun T.A., Nelson P.E. 1982. Carnation leaves as a substrate and for preserving cultures of *Fusarium* species. *Phytopathology* 72: 151–153.

Gräfenhan T., Schroers H.J., Nirenberg H.I., Seifert K.A. 2011. An overview of the taxonomy, phylogeny, and typification of nectriaceous fungi in *Cosmospora*, *Acremonium*, *Fusarium*, *Stilbella*, and *Volutella*. *Studies in Mycology* 68: 79–113.

Graham J.H., Brlansky R.H., Timmer L.W., Lee R.F., Marais, L.J. 1985. Comparison of citrus tree declines with necrosis of major roots and their association with *Fusarium solani*. *Plant Disease* 69: 1055–1058.

Guarnaccia V., Crous P.W. 2018. Species of *Diaporthe* on *Camellia* and *Citrus* in the Azores Islands. *Phytopathologia Mediterranea* 57: 307–319.

Guarnaccia V., Sandoval-Denis M., Aiello D., Polizzi G., Crous, P.W. 2018. *Neocosmospora perseae* sp. nov., causing trunk cankers on avocado in Italy. *Fungal Systematics and Evolution* 1: 131–140.

Guarnaccia V., Aiello D., Polizzi G., Crous, P.W., Sandoval-Denis M. 2019. Soilborne diseases caused by *Fusarium* and *Neocosmospora* spp. on ornamental plants in Italy. *Phytopathologia Mediterranea* 58: 127–137.

Hannachi I., Rezgui S., Cherif M. 2014. First report of mature citrus trees being affected by Fusarium wilt in Tunisia. *Plant Disease* 98: 566.

Huelsenbeck J.P., Ronquist F. 2001. MrBayes: Bayesian inference of phylogeny. *Bioinformatics* 17: 754–755.

Katoh K., Rozewicki J., Yamada K.D. 2019. MAFFT online service: multiple sequence alignment, interactive sequence choice and visualization. *Briefings in Bioinformatics* 20: 1160–1166.

Kore S.S., Mane A.V. 1992. A dry root rot disease of kagzilime (*Citrus aurantifolia*) seedling caused by *Fusarium solani*. *Journal of Maharashtra Agricultural Universities* 17: 276–278.

Kurt Ş., Uysal A., Soylu E., Kara M., Soylu S. 2020. Characterization and pathogenicity of *Fusarium solani* associated with dry root rot of citrus in the eastern Mediterranean region of Turkey. *Journal of General Plant Pathology* 86: 326–332.

Leslie J.F., Summerell B.A. 2006. *The Fusarium laboratory manual*. Blackwell Publishing, Ames.

Liu Y.J., Whelen S., Hall B.D. 1999. Phylogenetic relationships among ascomycetes: evidence from an RNA polymerase II subunit. *Molecular Biology and Evolution* 16: 1799–1808.

Lombard L., Van der Merwe N.A., Groenewald J.Z., Crous P.W. 2015. Generic concepts in Nectriaceae. *Studies in Mycology* 80: 189–245.

Malikoutsaki-Mathioudi M., Bourbos V.A., Skoudridakis M.T. 1987. La pourriture sèche des racines – une maladie très grave des agrumes en Grèce. *EPPO Bulletin* 17: 335–340.

Mason-Gamer R., Kellogg E. 1996. Testing for phylogenetic conflict among molecular data sets in the tribe *Triticeae* (*Gramineae*). Systematic Biology 45: 524–545.

Mayorquin J.S., Nouri M.T., Peacock B.B., Trouillas F.P., Douhan G.W., … Eskalen A. 2019. Identification, Pathogenicity, and Spore Trapping of *Colletotrichum karstii* associated with twig and shoot dieback in California. *Plant Disease* 103: 1464–1473.

Menge J.A. 1988. Dry root rot. In: Whiteside JO, Garnsey SM, Timmer LW (eds), *Compendium of Citrus diseases*, 14–15. APS Press, USA.

Miller M.A., Pfeiffer W., Schwartz T. 2012. The CIPRES science gateway: enabling high-impact science for phylogenetics researchers with limited resources. In: *Proceedings of the 1st Conference of the Extreme Science and Engineering Discovery Environment: Bridging from the extreme to the campus and beyond*, 1–8. Association for Computing Machinery, USA.

Nemec S., Baker R. 1992. Observations on *Fusarium solani* naphthazarin toxins, their action, and potential role in citrus plant disease. *Proceedings of the 7th meeting of the International Society of Citriculture*, Acireale, Italy, International Society of Citriculture, Riverside, pp. 832–837.

Nemec S., Baker R., Burnett H. 1980. Pathogenicity of *Fusarium solani* to citrus roots and its possible role in blight etiology. *Proceedings of the Florida State Horticultural Society* 93: 36–41.

Nirenberg H.I. 1976. Untersuchungen über die morphologische und biologische differenzierung in der Fusarium-Sektion Liseola. *Mitteilungen der Biologischen Bundesanstalt für Land- und Forstwirtschaft Berlin-Dahlem* 169: 1–117.

Nylander J.A.A. 2004. MrModeltest v2. Program distributed by the author. Evolutionary Biology Centre, Uppsala University.

O'Donnell K., Sutton D.A., Fothergill A., McCarthy D., Rinaldi M.G., … Geiser D.M. 2008. Molecular phylogenetic diversity, multilocus haplotype nomenclature, and in vitro antifungal resistance within the *Fusarium solani* species complex. *Journal of Clinical Microbiology* 46: 2477–2490.

O'Donnell K, Sutton DA, Rinaldi MG, Sarver, B. A., Balajee, S. A., … Aoki T. 2010. Internet-accessible DNA sequence database for identifying fusaria from human and animal infections. *Journal of Clinical Microbiology* 48: 3708–3718.

Polizzi G., Magnano di San Lio G., Catara A. 1992. Dry root rot of citranges in Italy. *Proceedings of the International Society of Citriculture*. VII International Citrus Congress, Acireale 1992: 890–893.

Quaedvlieg W., Binder M., Groenewald J.Z., Summerell, B.A., Carnegie, A.J., … Crous P.W. 2014. Introducing the consolidated species concept to resolve species in the Teratosphaeriaceae. *Persoonia* 33: 1–40.

Rayner R.W., 1970. *A Mycological Colour Chart*. Kew, UK: Commonwealth Mycological Institute.

Rehman A., Rehman A., Javed N., Mehboob S. 2012. Toxin production by *Fusarium solani* from declining citrus plants and its management. *African Journal of Biotechnology* 11: 2199–2203.

Ronquist F., Huelsenbeck J.P. 2003. MrBayes 3: Bayesian phylogenetic inference under mixed models. *Bioinformatics* 19: 1572–1574.

Sandoval-Denis M., Crous P.W. 2018. Removing chaos from confusion: assigning names to common human and animal pathogens in *Neocosmospora*. *Persoonia* 41: 109–129.

Sandoval-Denis M., Guarnaccia V., Polizzi G., Crous P.W. 2018. Symptomatic *Citrus* trees reveal a new pathogenic lineage in *Fusarium* and two new *Neocosmospora* species. *Persoonia* 40: 1–25.

Sandoval-Denis M., Lombard L., Crous P.W. 2019. Back to the roots: a reappraisal of *Neocosmospora*. *Persoonia* 43: 90–185.

Smith I.M., Dunez J., Phillips D.H., Lelliott R.A., Archer S.A. 1988. European handbook of plant diseases. Blackwell Scientific Publications, UK.

Spina S, Coco V, Gentile A, Catara A., Cirvilleri G. 2008. Association of *Fusarium solani* with rolabc and wild type Troyer Citrange. *Journal of Plant Pathology* 90: 479–486.

Stamatakis A. 2014. RAxML version 8: a tool for phylogenetic analysis and post-analysis of large phylogenies. *Bioinformatics* 30: 1312–1313.

Sung G.H., Sung J.M., Hywel-Jones N.L., Spatafora J. W. 2007. A multi-gene phylogeny of Clavicipitaceae (Ascomycota, Fungi): Identification of localized incongruence using a combinational bootstrap approach. *Molecular Phylogenetics and Evolution* 44: 1204–1223.

Tamura K., Stecher G., Peterson D., Filipski A., Kumar S. 2013. MEGA6: Molecular Evolutionary Genetics Analysis version 6.0. *Molecular Biology and Evolution* 30: 2725–2729.

Timmer L.W. 1982. Host range and host colonization, temperature effects, and dispersal of *Fusarium oxysporum* f. sp. *citri*. *Phytopathology* 72: 698–702.

Timmer L.W., Garnsey S.M., Grimm G.R., El-Gholl N.E., Schoulties C.L. 1979. Wilt and dieback of Mexican lime caused by *Fusarium oxysporum*. *Phytopathology* 69: 730–734.

Verma K.S., Nartey S., Singh N. 1999. Occurrence and control of dry root rot of citrus seedlings. *Plant Disease Research* 14: 31–34.

Vilgalys R., Hester M. 1990. Rapid genetic identification and mapping of enzymatically amplified ribosomal DNA from several *Cryptococcus* species. *Journal of Bacteriology* 172: 4238–4246.

Vilgalys R., Sun B.L. 1994. Ancient and recent patterns of geographic speciation in the oyster mushroom *Pleurotus* revealed by phylogenetic analysis of ribosomal DNA sequences. *Proceedings of the National Academy of Sciences of the United States of America* 91: 4599–4603.

White T.J., Bruns T., Lee S., Taylor J. 1990. Amplification and direct sequencing of fungal ribosomal RNA genes for phylogenetics. In: Innes MA, Gelfand DH, Sninsky *et al.* (eds), *PCR Protocols: a Guide to Methods and Applications*: 315–322. Academic Press, USA.

Wiens J.J. 1998. Testing phylogenetic methods with tree congruence: phylogenetic analysis of polymorphic morphological characters in phrynosomatid lizards. *Systematic Biology* 47: 427–444.

Yaseen T., D'Onghia A.M. 2012. *Fusarium* spp. associated to citrus dry root rot: An emerging issue for Mediterranean citriculture. *Acta Horticulturae* 940: 647–655.

Phytopathologia Mediterranea
The international journal of the
Mediterranean Phytopathological Union

Firenze University Press
www.fupress.com/pm

New or Unusual Disease Reports

Molecular and serological detection of Parietaria mottle virus in *Phytolacca americana*, a new host of the virus

Giuseppe PARRELLA[1,*], Elisa TROIANO[1], Adriano STINCA[2], Maria Isabella POZZI[1]

[1] *Institute for Sustainable plant Protection of National Research Council (IPSP-CNR), Piazzale Enrico Fermi 1, 80055 Portici (NA), Italy*
[2] *Department of Environmental, Biological and Pharmaceutical Sciences and Technologies, University of Campania Luigi Vanvitelli, Via Vivaldi 43, 81100 Caserta, Italy*
*Corresponding author: giuseppe.parrella@ipsp.cnr.it

Summary. Parietaria mottle virus (PMoV) is an emerging virus in Mediterranean countries, responsible for severe disease in tomato and pepper crops in the field and protected cultivation. The principal wild reservoir of PMoV is *Parietaria officinalis*, and only few additional wild plants have been described as natural reservoirs of the virus. During field survey in southern Italy, several plants of *Phytolacca americana* showing virus-like symptoms were collected. Serological and molecular assays showed that these plants were infected by PMoV. Sequence comparison of the movement protein gene of the PMoV isolate from *P. americana* showed the greatest similarity to the corresponding sequence from tomato plants growing nearby. These results indicate that *P. ameriacana* is a new natural host of PMoV, and further investigation is warranted to establish the potential of this host as reservoir of the virus in the field.

Keywords. PMoV, alien species, American pokeweed, natural host, emerging viruses.

OPEN ACCESS

Citation: G. Parrella, E. Troiano, A. Stinca, M. I. Pozzi (2021) Molecular and serological detection of Parietaria mottle virus in *Phytolacca americana*, a new host of the virus. *Phytopathologia Mediterranea* 60(1): 101-104. doi: 10.36253/phyto-12207

Accepted: January 27, 2021

Published: May 15, 2021

Data Availability Statement: All relevant data are within the paper and its Supporting Information files.

Competing Interests: The Author(s) declare(s) no conflict of interest.

Editor: Arnaud G Blouin, New Zealand Institute for Plant and Food Research, Auckland, New Zealand.

INTRODUCTION

Phytolacca americana L. (*Phytolaccaceae*), commonly known as "American pokeweed", "pokeweed" or "dragonberries", is a poisonous perennial geophyte herb native to North America. It was introduced in Europe where it is invasive in many countries, including Italy (Galasso *et al*., 2018). This neophyte plant mainly spreads in anthropic and disturbed environments (Stinca and Motti, 2017; Bonanomi *et al*., 2018). In July 2020, during a survey of tomato virus diseases in southern Italy (Campania region), several individuals of *P. americana* were noticed showing virus-like symptoms, comprising mosaic, chlorotic spots and lines and leaf distortions (Figure 1). The detected plants were growing close to a family garden, located in the Sorrento peninsula, were Parietaria mottle virus (PMoV) was detected in a local variety of tomato with high incidence. Distances from pokeweed plants to the tomato plants ranged between 5 to 20 m. The presence of thrips individuals on

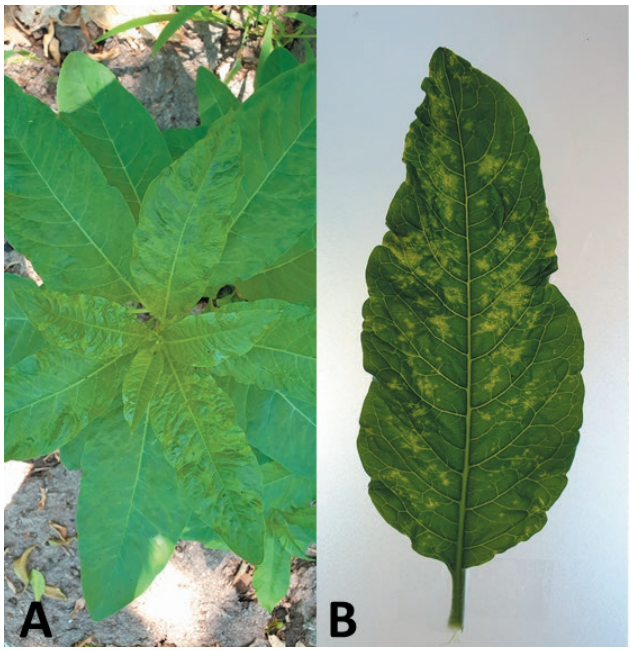

Figure 1. Symptoms associated to Parietaria mottle virus infection in *Phytolacca americana* L.: (A) mosaic on the apical leaves, and (B) details of symptoms on a leaf.

tomato and pokeweed plants was also observed. Overall, field observations suggested possible implication of PMoV as the cause of the symptoms observed in pokeweed plants.

MATERIALS AND METHODS

Leaf-sap from three symptomatic and two asymptomatic *P. americana* plants, and two symptomatic tomato plants, was mechanically inoculated to *Chenopodium quinoa* Willd., *C. amaranticolor* (H.J.Coste & A.Reyn.) H.J.Coste & A.Reyn., *Vigna unguiculata* (L.) Walp. 'Black eye' and *Nicotiana tabacum* L. 'Xanthi nc.'.

The same samples were tested by antigen-coated-plate enzyme-linked immunosorbent assay (ACP-ELISA) with a specific PMoV polyclonal antibody (Lisa *et al.*, 1998), following the procedure of Parrella (2020). In addition, samples were tested by cucumber mosaic virus (CMV) and tomato spotted wilt virus (TSWV)-specific lateral flow (LF) kits (Pocket Diagnostic), since in tomato symptoms induced by PMoV resembling those induced by CMV and TSWV in single or mixed infections have also been reported (Ramasso *et al.*, 1997; Roggero *et al.*, 2000).

Total RNAs were extracted with the E.Z.N.A.® Plant RNA Kit (Omega Bio-tek), and RT-PCR using the PMoV specific primers PMoVMP1a and PMoVMP2b, encompassing the entire PMoV movement protein (Parrella *et al.*, 2016). Amplicons of the expected size (916 bp) obtained from symptomatic samples were cloned into pGEM-T vector (Promega), and were sequenced at Microsynth Seqlab (Göttingen, Germany). Blast analysis was performed online (http://blast.ncbi.nlm.nih.gov/Blast.cgi), and fifteen sequences of other PMoV isolates (Table 1) were downloaded and were used to determine

Table 1. Parietaria mottle virus isolates used in the present study.

Isolate	Host	Geographic origin	Year of collection	Accession No.
Pha1	*Phytolacca americana*	Campania, Italy	2020	MW248388
390	*Solanum lycopersicum*	Campania, Italy	2020	MW456562
391A	*Solanum lycopersicum*	Campania, Italy	2020	MW456563
Sar-1	*Solanum lycopersicum*	Sardinia, Italy	2019	MN782302
Ruc1	*Diplotaxis tenuifolia*	Campania, Italy	2016	KX866978
Ruc2	*Diplotaxis tenuifolia*	Campania, Italy	2016	KX866979
Fri-1	*Capsicum annuum*	Campania, Italy	2015	LT160068
Fri-2	*Capsicum annuum*	Campania, Italy	2015	LT160070
Pap-1	*Capsicum annuum*	Campania, Italy	2015	LT160069
M31A	*Solanum lycopersicum*	Catalonia, Spain	2006	AM182749
G34H	*Solanum lycopersicum*	Catalonia, Spain	2006	AM182744
AC1	*Solanum lycopersicum*	Catalonia, Spain	2006	AM182743
SD2	*Solanum lycopersicum*	Catalonia, Spain	2006	AM182745
RAMS1	*Solanum lycopersicum*	Catalonia, Spain	2006	AM182748
So7J	*Solanum lycopersicum*	Catalonia, Spain	2006	AM182746
JBT1	*Solanum lycopersicum*	Catalonia, Spain	2006	AM182747
CR8	*Solanum lycopersicum*	Catalonia, Spain	2001	FJ858204
T32	*Solanum lycopersicum*	Piedmont, Italy	1979	KT005245

the phylogenetic relationships among them and the pokeweed isolate (named Pha1). Multiple sequence alignment was performed using the ClustalW algorithm of MEGA 6.0 (Tamura *et al*., 2013), with gap opening penalty of 15 and gap extension penalty of 6.66. A phylogenetic tree was constructed using the neighbor-joining (NJ) method with 1000 bootstrap replicates, and genetic distance was calculated by the Tamura three-parameter model which was determined as the best-fitting model of substitution using MEGA 7.0.

RESULTS AND DISCUSSION

Inoculated host plants showed the following symptoms after 1 to 3 weeks, consistent with symptoms caused by PMoV (Ramasso *et al.,* 1997; Marchoux *et al*., 1999): large chlorotic local lesions followed by dieback and wilting in *C. quinoa*; large chlorotic local lesions followed by mosaic in *C. amaranticolor*; necrotic local lesions in *V. unguiculata*; and pinpoint necrotic local lesions followed by mosaic, leaf distortions, vein necrosis and necrotic patches on the apical non-inoculated leaves of *N. tabacum*. PMoV infection in symptomatic hosts was confirmed by RT-PCR. Host plants inoculated with leaf sap of the asymptomatic pokeweed plants showed no symptoms.

PMoV was detected by ACP-ELISA in all symptomatic plants, with an average optical density (O.D.) at 450 nm of 0.96 ± 0.60 (n = 3), and 0.12 ± 0.03 for asymptomatic plants (n = 2), after 1 h of substrate incubation. Tests for the potential additional presence of TSWV and CMV by LF were negative.

The ACP-ELISA results were confirmed with reverse transcription (RT)-PCR. The expected 916 bp fragment was obtained from symptomatic pokeweed (Figure 2) and tomato plants tested, while no amplicon was obtained from asymptomatic plants. Sequences obtained from symptomatic *P. americana* shared 100% nucleotide similarity, and the corresponding sequence of the isolate Pha1 was deposited in GenBank (Accession n. MW248388). The Pha1 sequence shared greatest nucleotide similarity with sequences of the two PMoV tomato isolates from hosts growing nearby: 99.67% with the tomato isolate 390 (Accession n. MW456562) and 99.78% similarity with isolate 391A (Accession n. MW456563). This indicated virus movement between the American pokeweed and tomato hosts. These three isolates also clearly grouped in the phylogenetic tree, forming a distinct clade together with the isolates Ruc1, identified previously from *Diplotaxis tenuifolia* (L.) DC., and Fri-2, from *Capsicum annuum* L., in the same Italian region (Parrella *et al*., 2017; Parrella *et al*., 2016). Nevertheless, overall phylogenetic grouping showed no clear correlation with host or geographic origin, although the existence of four distinct phylogenetic groups of PMoV isolates was indicated based on the MP gene (Figure 3). These results confirm those previously obtained and based on the coat protein (CP) phylogenetic relationships of PMoV isolates (Galipienso *et al*., 2015).

PMoV is an emerging virus, due to its increasing incidence in tomato and other cultivated plants, such as *Cap-*

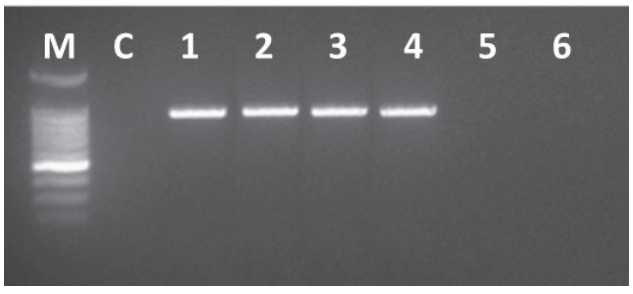

Figure 2. RT-PCR detection of Parietaria mottle virus in symptomatic *Phytolacca americana* L. leaves. Lanes M, 100 bp DNA ladder; C, control without total RNAs; 1, Positive control (PMoV infected tomato plants); 2 to 4, symptomatic *P. americana* leaves from three different plants; 5 and 6, asymptomatic *P. americana* leaves from two different plants.

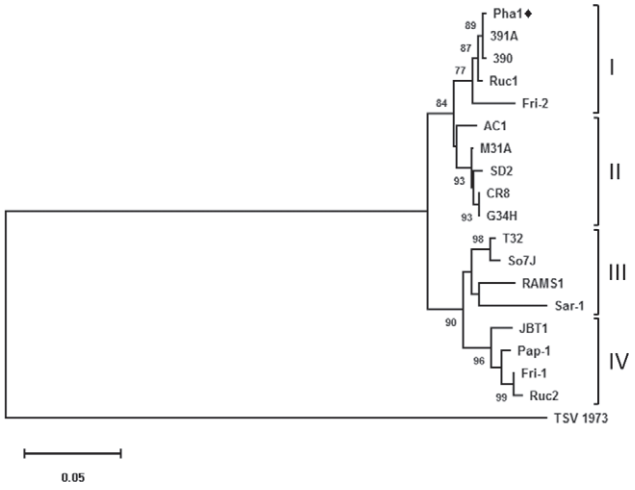

Figure 3. Phylogenetic analysis based on the movement protein (MP) gene of the Parietaria mottle virus (PMoV) isolates examined in this study (Pha1, 390 and 391A), and 15 other PMoV isolates available in GenBank. The accession numbers, isolate names, hosts, geographic origins and years of sampling for each isolate are listed in Table 1. The isolate from *Phytolacca americana* (Pha1) is indicated in the tree with the symbol ♦. The phylogenetic tree was constructed using the neighbor joining (NJ) method, with 1000 bootstrap replicates, and genetic distances were calculated by the Tamura three-parameter model using MEGA 7.0. The isolate of tobacco streak virus TSV 1973 (Accession n. JX463336) was used as an outgroup.

sicum annuum, *Diplotaxis tenuifolia*, and the ornamental plant *Mirabilis jalapa* L. (Parrella, 2002; Janssen *et al*., 2005; Parrella *et al*., 2016; Parrella *et al*., 2017; Caruso *et al*., 2018; Parrella *et al*., 2020). The discovery of a new natural host of PMoV, i.e. *Phytolacca americana*, confirms the tendency of the virus to occupy new ecological niches. Within Caryophyllales, *Phytolaccaceae* are closely related to *Nyctaginaceae*, the plant family to which *Mirabilis jalapa* belongs, and this host is another unusual natural host of PMoV (Rettig *et al*., 1992; Cuénoud *et al*., 2002; Lee *et al*., 2013). After the present discovery, further investigations would be useful to increase knowledge of the possible role of American pokeweed as a reservoir of PMoV, and the impacts of epidemics of this pathogen on susceptible crops such as tomato and pepper.

ACKNOWLEDGEMENT

This research was supported by the Campania Region (Italy), Plan of Phytosanitary Action for 2020, URCOFI project: Unit for coordination and development of surveillance, research, monitoring and training activities for phytosanitary purposes.

LITERATURE CITED

Bonanomi G., Incerti G., Abd El-Gawad A. M., Sarker T.C., Stinca A., … Saracino A., 2018. Windstorm disturbance triggers multiple species invasion in a Mediterranean forest. *iForest* 11: 64–71.

Caruso G., Parrella G., Giorgini M., Nicoletti R., 2018. Crop systems, quality and protection of *Diplotaxis tenuifolia*. *Agriculture* 8: 55.

Cuénoud P., Savolainen V., Chatrou L.W., Powell M., Grayer R.J., Chase M.W., 2002. Molecular phylogenetics of Caryophyllales based on nuclear 18S rDNA and plastid rbcL, atpB, and matK DNA sequences. *American Journal of Botany* 89: 132–144.

Galasso G., Conti F., Peruzzi L., Ardenghi N.M.G., Banfi E., … Bartolucci F., 2018. An updated checklist of the vascular flora alien to Italy. *Plant Biosystems* 152: 556–592.

Galipienso L., Martinez C., Willemsen A., Alfaro-Férnandez A., Font-San Ambrosio I., … Rubio L., 2015. Genetic variability and evolutionary analysis of Parietaria mottle virus: role of selection and genetic exchange. *Archives of Virology* 160: 2611–2616.

Janssen D., Saez E., Segundo E., Martin G., Gil F., Cuadrado I.M., 2005. *Capsicum annuum* – a new host of *Parietaria mottle virus*. *Plant Pathology* 54: 567.

Lee J., Kim S.Y., Park S.H., Ali M.A., 2013. Molecular phylogenetic relationships among members of the family Phytolaccaceae sensu lato inferred from internal transcribed spacer sequences of nuclear ribosomal DNA. *Genetics and Molecular Research* 12: 4515–4525.

Lisa V., Ramasso E., Ciuffo M., Roggero P., 1998. Tomato apical necrosis caused by a strain of Parietaria mottle virus. In: *Proceedings of the Ninth Conference of the ISHS Vegetable Virus Working Group, Recent Advances in Vegetable Virus research,* Torino, 22–27 August. [Unpublished abstracts book], pp. 1–5.

Marchoux G., Parrella G., Gebre-Selassie K., Gognalons P., 1999. Identification de deux ilarvirus sur tomate dans le sud de la France. *Phytoma*, 522: 53–55.

Parrella G., 2002. First report of *Parietaria mottle virus* in *Mirabilis jalapa*. *Plant Patho*logy 51: 401.

Parrella G., Greco B., Troiano E., 2016. Severe symptoms of mosaic and necrosis in bell pepper associated with Parietaria mottle virus in Italy. *Plant Disease* 100: 1514.

Parrella G., Greco B., Troiano E., 2017. First report of Parietaria mottle virus associated with yellowing disease in *Diplotaxis tenuifolia* in Italy. *Plant Dis*ease 101: 850–851.

Parrella G., Troiano E., Cherchi C., Giordano P., 2020. Severe outbreaks of Parietaria mottle virus in tomato in Sardinia, southern Italy. *Journal of Plant Pathology*, 102: 915.

Parrella G., 2020. Sources of resistance in wild *Solanum* germplasm (section *Lycopersicon*) to Parietaria mottle virus, an emerging virus in the Mediterranean basin. *Plant Pathology* 69: 1018–1025.

Ramasso E., Roggero P., Dellavalle G., Lisa V., 1997. Necrosi apicale del pomodoro causata da un Ilarvirus. *Informatore Fitopatologico* 1: 71–77.

Rettig J.H., Wilson H.D., Manhart J.R., 1992. Phylogeny of the Caryophyllales - gene sequence data. *Taxon* 41: 201–209.

Roggero P., Ciuffo M., Katis N., Alioto D., Crescenzi A., … Gallitelli D., 2000. Necrotic disease in tomatoes in Greece and southern Italy caused by a tomato strain of *Parietaria mottle virus*. *Journal of Plant Pathology* 82: 159.

Stinca A., Motti R., 2017. Alien plant invasions in Astroni crater, a decades-long unmanaged forest in southern Italy. *Atti della Società Toscana di Scienze Naturali, Memorie Serie B* 124: 101–108.

Tamura K., Stecher G., Peterson D., Filipski A., Kumar S., 2013. MEGA6: Molecular evolutionary genetics analysis version 6.0. *Molecular Biology & Evolution* 30: 2725–2729.

Phytopathologia Mediterranea
The international journal of the
Mediterranean Phytopathological Union

Firenze University Press
www.fupress.com/pm

New or Unusual Disease Reports

First report of blast of durum wheat in Bangladesh, caused by *Magnaporthe oryzae* pathotype *Triticum*

Krishna Kanta ROY[1,*], Md MUZAHID-E-RAHMAN[1], KISHOWAR-E-MUSTARIN[1], Md Mostofa Ali REZA[1], Paritosh Kumar MALAKER[1], Naresh Chandra DEB BARMA[1], Xinyao HE[2], Pawan Kumar SINGH[2,*]

[1] *Bangladesh Wheat and Maize Research Institute (BWMRI), Nashipur, Dinajpur-5200, Bangladesh*
[2] *International Maize and Wheat Improvement Centre (CIMMYT), El Batan, Texcoco, Mexico*
*Corresponding authors. E-mail: rkrishnaroy666@gmail.com; pk.singh@cgiar.org

Summary. Durum wheat (*Triticum turgidum* var. *durum* Desf.) is an important cereal crop in many regions of the world. In March of 2018 and 2019, symptoms typical of blast were frequently observed on durum wheat plants under field conditions in Jashore, Bangladesh. The putative causal pathogen was isolated from infected wheat spike specimens onto potato dextrose agar and oatmeal agar, and was identified from mono-conidium cultures as *Magnaporthe oryzae*, based on morphological features. The pathotype of the fungus was identified as *Triticum*, based on comparative molecular analyses of ITS sequences and MoT3 specific markers. BLAST analysis revealed >99.8% similarity with *M. oryzae/P. oryzae,* retrieved from the NCBI Genebank. This was confirmed through amplification of the predicted products with MoT3 primers in PCR analysis. Pathogenicity was confirmed by inoculating healthy durum wheat seedling leaves and spikes with a conidium suspensions of *M. oryzae* isolate DuBWMRI1901.2A. The fungus produced similar symptoms on inoculated leaves and spikes as those observed in the field, and was subsequently re-isolated, fulfilling Koch's postulates. This is the first report of blast of durum wheat caused by *Magnaporthe oryzae* pathotype *Triticum* in Bangladesh.

Keywords. Isolation, morphological detection, molecular analysis, pathogenicity.

OPEN ACCESS

Citation: K. Kanta Roy, Md Muzahid-E-Rahman, Kishowar-E-Mustarin, Md M. A. Reza, P. K. Malaker, N. C. Deb Barma, X. He, P. K. Singh (2021) First report of blast of durum wheat in Bangladesh, caused by *Magnaporthe oryzae* pathotype *Triticum*. *Phytopathologia Mediterranea* 60(1): 105-111. doi: 10.36253/phyto-11821

Accepted: November 3, 2020

Published: May 15, 2021

Data Availability Statement: All relevant data are within the paper and its Supporting Information files.

Competing Interests: The Author(s) declare(s) no conflict of interest.

Editor: Andy Tekauz, Cereal Research Centre, Winnipeg, MB, Canada.

INTRODUCTION

Durum wheat (*Triticum turgidum* var. *durum*) is the second most cultivated species of wheat after bread wheat, accounting for 5 to 8% of global wheat production, and is the 10th most important cereal crop overall (Kabbaj *et al*., 2017). Durum wheat is cultivated under diverse climatic conditions in West Asia and North Africa (WANA) and is the most sustainable wheat type in the Mediterranean basin due to its tolerance to hot and dry environmental conditions. It remains a significant staple food crop for mar-

ginalized farmers due to its potential for large-scale production and high monetary returns (Yahyaoui *et al*., 2000; Sall *et al*., 2019). The largest durum wheat producer is the European Union, with projected production in 2020 of 309 million bushels, followed by Canada (162), Turkey (132), Algeria (118), U.S.A. (59) and Morocco (48) (NDWC, 2020). The high protein grain content and hard structure make durum wheat ideal for producing pasta products, and it is therefore often referred as 'pasta wheat'. In addition, it can also be used to make bulgur, couscous, freekeh, puffed cereals, desserts, filler for pastries, and unleavened breads. In Bangladesh, wheat crops are only grown during winter. Although durum wheat is a non-traditional minor cereal in Bangladesh, it still has significant commercial importance (BARI, 2015). The Bangladesh Wheat and Maize Research Institute (BWMRI) produces durum grain on a limited field scale (<0.2 ha) to explore its production and marketing potential in Bangladesh. Despite its current limited production, durum wheat may have good prospects in future as a niche market crop in the country.

Durum wheat can be severely affected by several pests and diseases. The most important diseases include stripe rust, Septoria tritici blotch, Fusarium head blight, stem rust, leaf rust, tan spot, root rot, crown rot, and common bunt (Yahyaoui *et al*., 2000; Haile *et al*., 2019). Under favourable environmental conditions yield losses in the WANA region due to diseases can reach 40% (Yahyaoui *et al*., 2000). In March of 2018 and 2019, a disease with symptoms similar to those of wheat blast, previously identified on bread wheat in Bangladesh (Malaker *et al*., 2016), was observed on durum wheat for the first time in experimental field plots in Jashore, Bangladesh. Blast is caused by the hemi-biotrophic ascomycete fungus *Magnaporthe oryzae* (Catt.) B. C. Couch 2002 (anamorph *Pyricularia oryzae* Cavara 1892) (Couch and Kohn 2002; Couch *et al*., 2005; Zhang *et al*., 2016). There was no record of blast on durum wheat under field conditions in Bangladesh prior to this report. *Magnaporthe oryzae* is versatile in nature, having a group of sub-species, and can attack 50+ species in the 'Poaceae', including wheat, rice, triticale, barley, millet, oat, and others (Sundaram *et al*., 1972; Ou, 1985; Igarashi *et al*., 1986; Urashima *et al.,* 1993; Kato *et al*., 2000; Urashima *et al*., 2004; Roy *et al*., 2020). The pathogen is host-specific: the *Triticum* pathotype is responsible for infecting wheat, the *Oryza* pathotype, rice, the *Setaria* pathotype, millet, the *Lolium* pathotype, annual and perennial ryegrass, among others. The first epidemic of the *Triticum* pathotype occurred in Parana, Brazil in 1985 (Igarashi *et al*., 1986). The initial outbreak outside of South America was observed in wheat in Bangladesh in February 2016 (Malaker *et al*., 2016), devastating the season's harvest. This pathotype can also attack other barley and triticale, as observed in Bangladesh in 2019 and confirmed by morphological and molecular analyses (Roy *et al*., 2020; Roy, unpublished). Positive cross-infection of MoT isolates on wheat, triticale, durum, and barley was observed under laboratory conditions at BWMRI (Roy, unpublished).

In the present investigation, symptoms of blast were observed in durum wheat under field conditions. Hence, the aim of the present study was to identify the causative pathogen by confirming morphological features, conducting molecular analyses using ITS sequences and pathotype-specific markers, and conducting pathogenicity tests.

MATERIALS AND METHODS

Isolation, purification, and detection of the pathogen

To isolate the disease-causing pathogen, four to five diseased spikes were randomly collected from blast-affected plots in Jashore, Bangladesh in 2018, and brought to the BWMRI pathology laboratory. The infected spikes were partially or fully bleached with shriveled grains, indicating pathogen infections at an early stage of grain development. Special care was taken to ensure samples were fresh and therefore less likely to be contaminated with other fungi. Small portions (<1 cm^2) of symptomatic spike tissues were surface disinfected in 1% Clorox (NaOCl) solution for 20–30 sec, and were then rinsed twice with sterile distilled water. The samples were incubated in darkness at 25–28°C on three-layer moistened Whatman blotter paper to promote fungal sporulation. After 24 h, conidiophores and conidia developed on the tissue samples. Single conidia were transferred onto Petri dishes containing potato dextrose agar (PDA) (200 g sliced potato, 15 g agar powder, and 12 g dextrose in 1000 mL distilled water). These were incubated for 5–7 d in a laminar air flow chamber with continuous fluorescent light at 28 ± 2°C and 40–42% relative humidity to produce single-conidium isolate cultures. The morphology of two isolates was recorded, including colony characteristics and conidium colour, shape, and size.

Molecular analyses with ITS sequences and MoT3 primers

The pathotype of the two isolates was confirmed through molecular analyses using ITS sequencing (White *et al*., 1990) and PCR amplification with MoT3

primer sets (Pieck *et al*., 2017). To confirm the pathotype of two of the isolates through ITS sequencing, total genomic DNA was extracted from mycelia of the isolates separately using a Wizard Genomic DNA Purification Kit (Promega) following the manufacturer's protocol. Molecular confirmation was first performed using the internal transcribed spacer (ITS) region of the ribosomal DNA by amplifying the isolates with ITS5 (GGAAGTAAAAGTCGTAACAAGG) and ITS4 (TCCTCCGCTTATTGATATGC) primers. The primers were synthesized by First BASE Laboratories (Malaysia), and the resulting products were sequenced and aligned using BioEdit 7.2. The sequences were submitted to GenBank under the following accession numbers: LC554422 (isolate DuBWMRI1901.2A) and LC554423 (isolate DuBWMRI1902.76C), and were analyzed using BLAST (https: //blast.ncbi.nlm.nih.gov/Blast). A phylogenetic tree was constructed with the neighbour-joining likelihood method with 1000 bootstrap replications using the MEGA-X model (Kumar *et al*., 2018). To confirm the pathotype with MoT3 primer sets (MoT3 primers are responsible for the identification of wheat blast fungi), the protocol described above was used to extract genomic DNA from the isolates. PCR amplification was performed on the samples in 100 µL PCR tubes using the GoTaq G2 Green Master Mix (Promega) and the MoT3 specific primers- MoT3F (GTCGTCATCAACGTGACCAG) and MoT3R (ACTTGACCCAAGCCTCGAAT). PCR was performed as described by Pieck *et al.* (2017) using a Thermal Cycler (Veriti, Applied Biosystems). The PCR cycling conditions were as follows: initial denaturation occurred at 94°C for 3 min, followed by 30 cycles of denaturation at 94°C for 1 min, annealing at 62°C for 2 min, extension at 72°C for 1 min 30 sec, and final elongation at 72°C for 10 min. Five microliters of each amplification mixture were verified by agarose (1% w/v) gel electrophoresis in 0.5× Tris-borate-EDTA (TBE) buffer. The presence or absence of the 361 bp MoT-specific PCR band was observed after electrophoresis. To test the specificity of MoT3 primers, several other blast-causing isolates from wheat (positive), rice, triticale, barley, and foxtail millet were included, and water was used as a negative control.

Pathogenicity tests on spikes and seedling leaves

Pathogenicity tests were carried out using seedling leaves and spikes of durum wheat genotype BDW 08. The seedlings were grown in 4 × 3 × 2.5 cm plastic pots, and adult plants in 15 × 13 × 7 cm pots, under laboratory conditions. There were four pots each for seedlings and for adult plants, with ten seedlings or adult plants in each pot. Seedlings at the two-leaf stage (12–14 d after sowing) and spikes (2–3 d after initiation of heading) were inoculated with isolate DuBWMRI1901.2A. To prepare conidia for MoT inoculation, inocula were multiplied on oatmeal agar (OMA) (50 g oatmeal and 15 g agar powder in 1000 mL distilled water). Sections of PDA-cultured MoT fungus growth were transferred onto OMA, and were then incubated at 27–29°C and 40–45% relative humidity for 7–10 d to promote conidium production. and then harvested. A conidium suspension was then prepared by scraping the conidia from OMA plates into a 100 mL capacity beaker using a camel hair brush. The suspension was filtered through two layers of cheesecloth, and two drops of 0.01% Tween 20 solution were added to 100 mL of aqueous conidium suspension. The suspension was stirred gently for 10 min to thoroughly disperse the conidia. The test seedlings and adult (headed) plants were inoculated using the suspension of 30,000 conidia mL^{-1} using a hand sprayer. The suspension was applied onto plant leaves and spikes to run-off. Two series of inoculations using seedling leaves and adult-plant spikes were performed using the same procedure. Some leaves and spikes were sprayed with water only to serve as negative controls. The inoculated leaves were incubated in continuous darkness for 36 h and spikes for 48 h, at 27 ± 2°C and 80 to 85% relative humidity (RH) in a 'polyhood' chamber (a metallic framework covered with a transparent polyethylene sheet). Following incubation, all pots were removed from the chamber and placed onto a laboratory bench for symptom expression.

RESULTS AND DISCUSSION

Putative blast symptoms were observed in three durum wheat plots, one of 6 m^2 in 2018, and two of 1 m^2 in 2019. In these plots, 30–50% of the total spikes were infected. Symptoms were found primarily on spikes, but also on leaves and stems. Spike symptoms were partially bleached spikes typical of blast (Figure 1, A_1 and A_2). These had visible dark gray or brown infection points on each rachis, and sometimes exhibited gray to white fungus sporulation (Figure 1 D). Infection of heads at the initial stage of anthesis led to aborted or shriveled and distorted grains with low test weights. Leaves with blasted symptoms had typical eye-shaped or elongated lesions with white centres and brown margins (Figure 1 B). Foliar symptoms were mostly observed on old leaves and rarely on young or flag leaves. Elongated lesions were also observed on stems; these had white centres and brown or black margins (Figure 1 B). They were

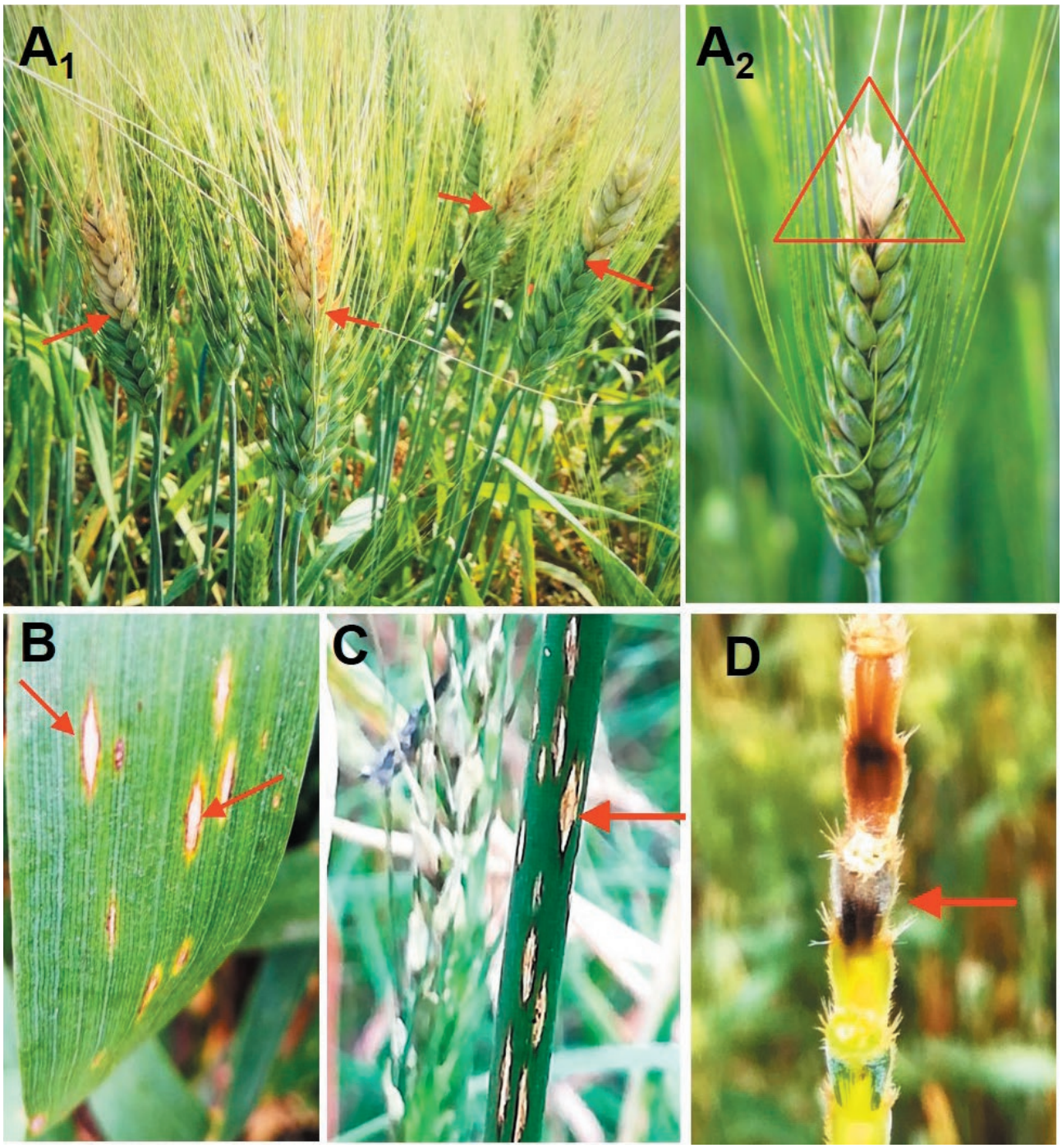

Figure 1. Field symptoms of durum wheat blast on different plant parts: (A_1 and A_2) typical partially-bleached spikes; (B) elongated or eye-shaped lesions on durum leaf with white centers surrounded by brown margins; (C) elongated lesion on stem with white center and dark brown or black margins; and (D) dark gray or brown infection points and gray to white sporulation in rachis.

observed rarely, and may have only developed when conditions particularly favoured disease development.

Microscope examination of affected samples showed vegetative and reproductive growth of the pathogen. Fungus growth was observed on rachis surfaces and on foliar lesions under a light microscope after 24–36 h of incubation (Figure 2, A and B). Young conidia of both isolates were pyriform, two-septate (three-celled), and

translucent; over time these became grayish or slightly darkened (Figure 2 G), and sometimes appeared to be single-celled. Conidia were of uniform shape, although their sizes varied from 16–25 × 7-10 µm. The middle cell of each conidium was wider and darker than the terminal cells, and each conidium tapered towards its apex. When conidia were water-mounted on glass slides, germtubes were evident within 2–3 h. Conidiophores were observed as coloured, erect, and cylindrical, with darkened basal portions and apical conidia. Conidiophores each bore seven to nine conidia acrogenously.

Colonies of the two isolates on PDA were gray to dark gray after 7 to 10 d incubation (Figure 2, C and E). Colonies of isolate DuBWMRI1901.2A were darker than those of DuBWMRI1902.76C. Puffy mycelial growth and a single concentric ring were observed in both isolates. On OMA, profuse grayish to white conidium masses were found after 8–12 d incubation (Figure 2, D and F). In the laminar flowhood, optimum conditions for conidium production were 28–29°C and 40–45%, and continuous florescent light. Conidium production on rachis tissues was more profuse than on leaf tissues.

The morphological features of the conidia were identical to *Magnaporthe oryzae* as described by Subramanian (1968). Both isolates were placed in long-term storage on dried filter paper at -81°C at the BWMRI pathology laboratory for future use. These can be accessed universally.

The pathotype of the isolated *M. oryzae* was confirmed by molecular analyses of the two representative isolates, DuBWMRI1901.2A and DuBWMRI1902.76C, using the internal transcribed spacer (ITS) region primer

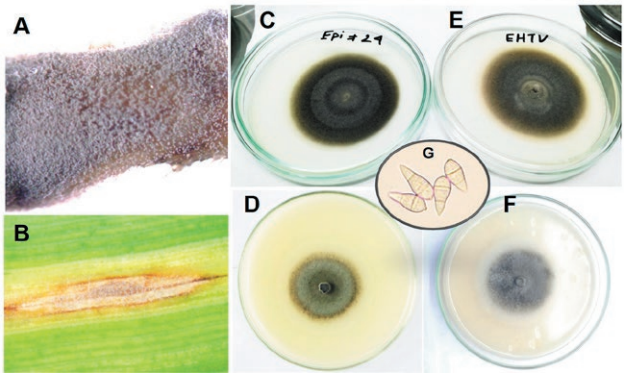

Figure 2. Growth of durum blast pathogen isolates on infected rachis and leaf tissues, and in PDA and OMA cultures after incubation under laboratory conditions. (A) gray to dark gray conidia of the fungus on an incubated rachis; (B) grayish conidia spores on an incubated leaf lesion; mono-conidium colonies of isolate DuBWMRI1901.2A on PDA (C), and OMA (D), and of DuBWMRI1902.76C PDA (E) and OMA (F); and (G) compound light microscope image of two-septate pyriform conidia.

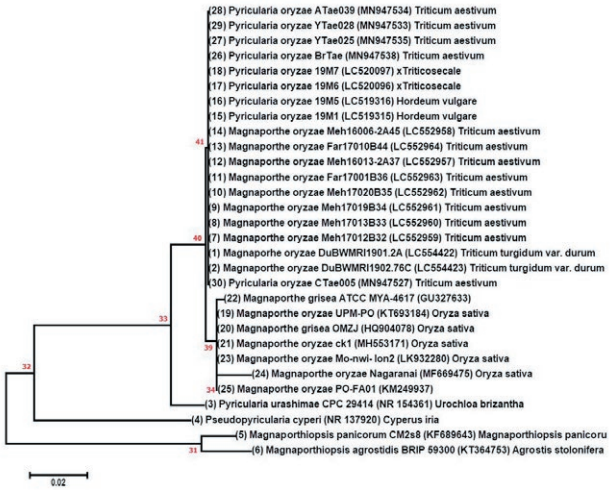

Figure 3. Neighbour-joining phylogenetic tree of *Magnaporthe oryzae* isolates DuBWMRI1901.2A and DuBWMRI1902.76C with 28 related rDNA-ITS sequences from GenBank. Numbers at the nodes indicate bootstrap values generated from 1000 replicates, and the scale bar indicates the number of nucleotide substitutions.

sets and the pathotype-specific MoT3 primers. The ITS sequences of the isolates were >99.8% similar to several *M. oryzae/P. oryzae* sequences available in GenBank. The phylogenetic tree (Figure 3) grouped the Bangladeshi durum blast isolates together with other *M. oryzae/P. oryzae* isolates from *Triticum aestivum*, × *Triticosecale* and *Hordeum vulgare* from Paraguay and Bangladesh. Based on the aligned sequences of ITS, the constructed neighbour-joining likelihood phylogenetic tree confirmed that the two blast isolates were identical to *Magnaporthe oryzae* (Subramanian 1968). Similarly, MoT3 primer results demonstrated that the two blast isolates were amplified with the band (361 bp) identical to those of wheat, triticale and barley blast isolates during PCR assay, while there was no PCR amplification found with rice and foxtail millet blast isolates (Figure 4).

The pathogenicity tests of the *M. oryzae* isolates gave at 48–72 h post-inoculation, eye-shaped water-soaked lesions developed on the seedling leaf blades (Figure 5 A), while there were no symptoms observed on water-treated plants (controls). The lesions had gray centres and dark green margins. The lesions became elongated and developed grayish centres with brown margins (Figure 5 B); ultimately whole leaves became blighted. In contrast, the inoculated spikes were only partially bleached 13–15 d after inoculation (Figure 5 C). The water-inoculated spikes remained symptomless. *Magnaporthe oryzae* was re-isolated on PDA plates (Figure 5 E) from the symptomatic leaves of inoculated plants, which produced profuse conidia within 24 h of incubation

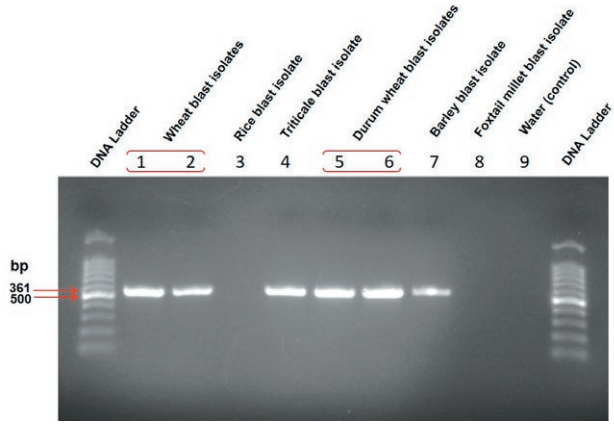

Figure 4. PCR amplification of durum wheat blast isolates DuBWMRI1901.2A (lane 5) and DuBWMRI1902.76C (lane 6), and blast isolates from wheat (lanes 1 and 2), rice (lane 3), triticale (lane 4), barley (lanes 7), and foxtail millet (lane 8), using MoT3 primer sets for confirming the *Triticum* pathotype of the *Magnaporthe oryzae* pathogen, during molecular detection assay.

(Figure 5 D). Conidia of the re-isolated pathogen were identical to those used for inoculations, and thus fulfilling Koch's postulates for the inoculated fungi (Cohen 1994).

Based on the morphological features of the selected isolates (conidium shape, size and colour), molecular analyses (ITS sequences and MoT3 markers) and pathogenicity tests, the causal organism of durum wheat blast observed in field plots was confirmed to be *Magnaporthe oryzae* pathotype *Triticum*. This is the first report of blast of durum wheat in Bangladesh, by *Magnaporthe oryzae* pathotype *Triticum*.

ACKNOWLEDGEMENTS

This study was financially supported by grants from the Australian Centre for International Agricultural Research (ACIAR), and CRP WHEAT and Krishi Gobeshona Foundation (KGF), Bangladesh.

LITERATURE CITED

BARI, 2015. Bangladesh Agricultural Research Institute, Joydebpur, Dhaka. *Annual Report* (2014–2015), 7 p.

Cohen J., 1994. Fulfilling Koch's postulates. *Science* 266: 1647.

Couch B.C., Kohn L.M., 2002. A multilocus gene genealogy concordant with host preference indicates segre-

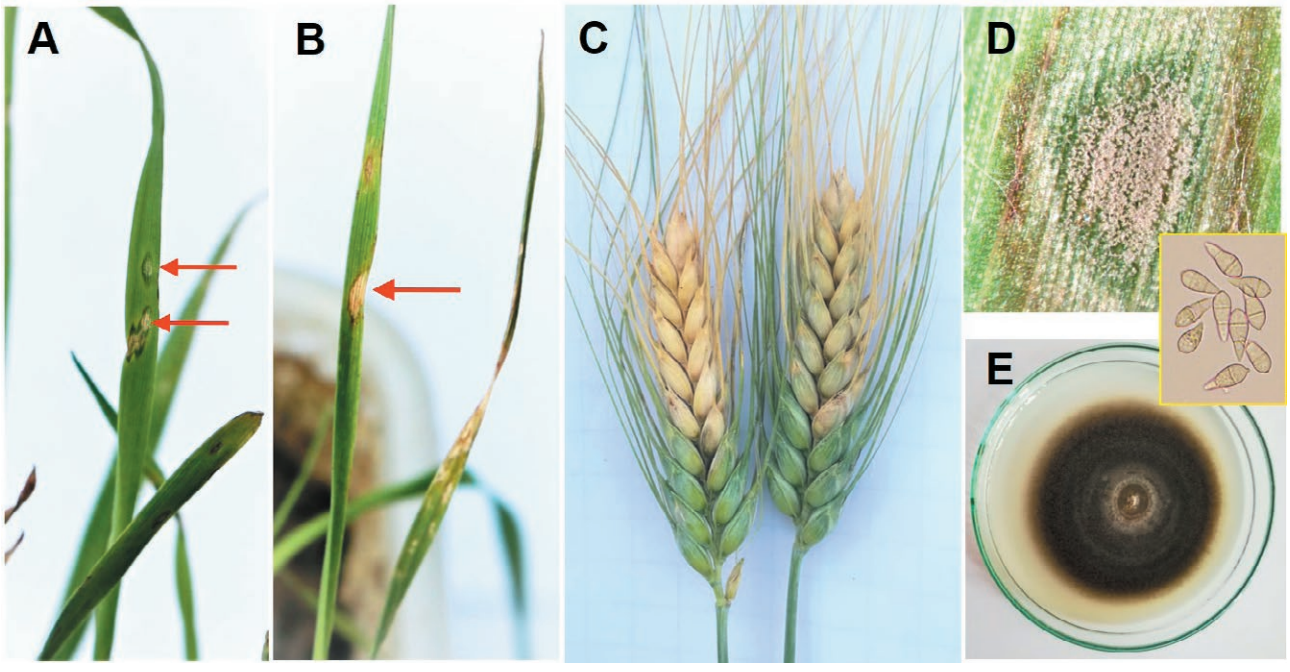

Figure 5. Results from pathogenicity tests of the *Magnaporthe oryzae* putative pathogen used to fulfill Koch's postulates. (A) typical eye-shaped water-soaked lesions on seedling leaves 48–72 h after inoculation with isolate DuBWMRI1901.2A; (B) elongated lesion with a grayish centre and brown margins 5–7 d post-inoculation; (C) partially bleached spikes 12–14 d post-inoculation; (D) gray conidium growth on a detached leaf lesion after 24 h incubation on moist blotter paper; and (E) re-isolated inoculated isolate, and conidia (inset).

gation of a new species, *Magnaporthe oryzae*, from *M. grisea*. *Mycologia* 94: 683–693.

Couch B., Fudal I., Lebrun M., Tharreau D., Valent B., ... Kohn L., 2005. Origins of host-specific populations of the blast pathogen *Magnaporthe oryzae* in crop domestication with subsequent expansion of pandemic clones on rice and weeds of rice. *Genetics* 170: 613–630.

Haile J.K., N'Diaye A., Walkowiak S., Nilsen K.T., Clarke J.M., … Pozniak C.J., 2019. Fusarium Head Blight in Durum Wheat: Recent Status, Breeding Directions, and Future Research Prospects. *Phytopathology* 109 (10): 1664–1675.

Igarashi S., Utiamada C.M., Igarashi L.C., Kazuma A.H., Lopes R.S., 1986. Occurrence of *Pyricularia* sp. in wheat (*Triticum aestivum* L.) in the State of Parana, Brazil. *Fitopatologia Brasileira* 11: 351–52.

Kabbaj H., Sall A.T., Al-Abdallat A., Geleta M., Amri A., ... Bassi F.M., 2017. Genetic diversity within a global panel of durum wheat *(Triticum durum)* landraces and modern germplasm reveals the history of alleles exchange. *Frontiers in Plant Science* 8: 1277.

Kato H., Yamamoto M., Yamaguchi-Ozaki T., Kadouchi H., Iwamoto Y., ... Naoki M.O.R.I., 2000. Pathogenicity, mating ability and DNA restriction fragment length polymorphisms of *Pyricularia* populations isolated from Gramineae, Bambusideae and Zingiberaceae plants. *Journal of General Plant Pathology* 66: 30–47.

Kumar S., Stecher G., Li M., Knyaz C., Tamura K., 2018. MEGA X: Molecular evolutionary genetics analysis across computing platforms. *Molecular Biology and Evolution* 35(6): 1547–1549.

Malaker P.K., Barma N.C.D., Tiwari T.P., Collis W.J., Duveiller. E., ... Valent B., 2016. First report of wheat blast caused by *Magnaporthe oryzae* pathotype *triticum* in Bangladesh. *Plant Disease* 100(11): 2330.

NDWC, 2020. World Durum Production. (Source: International Grains Commission Xldata/world/all wheat/wheat/prod). Available at: https: //www.ndwheat.com/uploads/6/world-web-charts

Ou S.H., 1985. Blast. *In*: Ou, S. H. (ed.). Rice Diseases, 2nd edition. CABI, Wallingford, UK, 109–201 pp.

Pieck M.L., Ruck A., Farman M.L., Peterson G.L., Stack J.P., ... Pedley K.F., 2017. Genomics based marker discovery and diagnostic assay development for wheat blast. *Plant Disease* 101: 103–109.

Roy K. K., Rahman M.M.E., Reza M.M.A., Mustarin K.E., Malaker P.K., … Singh P.K., 2020. First report of triticale blast caused by the fungus *Magnaporthe oryzae* pathotype *Triticum* in Bangladesh. *Canadian Journal of Plant Pathology* (DOI: 10.1080/07060661.2020.1793223).

Sall A.T., Chiari T., Legesse W., Seid-Ahmed K., Ortiz R., ... Bassi F.M., 2019. Durum wheat (*Triticum durum* Desf.): origin, cultivation, and potential expansion in Sub-Saharan Africa. *Agronomy* 9: 263.

Subramanian C.V., 1968. *Pyricularia oryzae*. CMI Descriptions of Pathogenic Fungi and Bacteria.

Sundaram N.V., Palmer L.T., Nagarajan K., Prescott J.M., 1972. Disease survey of sorghum and millet in India. *Plant Disease* 56: 740–743.

Urashima A.S., Igarashi S., Kato H., 1993. Host range, mating type and fertility of *Pyricularia grisea* from wheat in Brazil. *Plant Disease* 77: 1211–1216.

Urashima A.S., Lavorent N.A., Goulart A.C.P., Mehta Y.R., 2004. Resistance spectra of wheat cultivars and virulence diversity of *Magnaporthe grisea* isolates in Brazil. *Fitopatologia Brasileira* 29: 511.

White T.J., Bruns T., Lee S., Taylor J., 1990. Amplification and direct sequencing of fungal ribosomal RNA genes for phylogenetics. A Guide to Methods and Applications. Academic Press, San Diego, 315–322 pp.

Yahyaoui A., Hakim S., Al-Naimi M., Nachit M.M., 2000. Multiple disease resistance in durum wheat (*Triticum turgidum* L. var. *durum*). *In*: Royo C., Nachit M., DiFonzo N., and Araus J. L. (eds.). Durum wheat improvement in the Mediterranean region: New challenges. CIHEAM, Zaragoza, Spain, 387–392 pp.

Zhang N., Luo J., Rossman A.Y., Aoki T., Chuma I., … Xu J.R., 2016. Generic names in Magnaporthales. *IMA Fungus* 7: 155–159.

Phytopathologia Mediterranea
The international journal of the
Mediterranean Phytopathological Union

Firenze University Press
www.fupress.com/pm

Short Notes

Temperature and incubation period affect *Septoria pistaciarum* conidium germination: disease forecasting and validation

Thomas THOMIDIS[1,*], Konstantinos MICHOS[2], Fotis CHATZIPADOPOULOS[2], Amalia TAMPAKI[2]

[1] *International Hellenic University, Department of Human Nutrition and Diabetics, Campus of Sindos, 57400, Greece*
[2] *Neuropublic S.A., Information Technologies & Smart Farming Services, Piraeus, 18545, Attica, Greece*
*Corresponding author. E-mail: thomi-1@otenet.gr, thomidis@cp.teithe.gr

Summary. Septoria leaf spot is an important disease of pistachio trees in Greece. This study aimed to determine effects of temperature and the incubation period on germination of conidia of *Septoria pistaciarum*, and to evaluate a generic model to forecast pistachio leaf spot under the field conditions of Aegina Island, Greece. The optimum temperature for conidium germination was 23°C, and germination was inhibited at 35 and 4°C. At constant temperature of 23°C, conidia commenced germination after 9 h. The predictive model indexed disease risk close to 100 at 10 May at two locations (Rachi Moschona and Vigla) in 2017, and first leaf spot symptoms were observed on 17 May. Moderate to high disease severity (>25% leaves infected) were observed in unsprayed trees at the end of May. In 2018, the model indexed risk close to 100 on 9 May at Rachi Moschona, and first symptoms were observed on 18 May. Moderate to high disease severity (>25% leaves infected) were observed in unsprayed trees on 25th of May. This study has shown that the forecasting model can be used in Aegina Island, Greece, to predict the severity of Septoria leaf spot of pistachio.

Keywords. Generic model, temperature.

OPEN ACCESS

Citation: T. Thomidis, K. Michos, Fotis Chatzipa-Padopoulos, A. Tampaki (2021) Temperature and incubation period affect *Septoria pistaciarum* conidium germination: disease forecasting and validation. *Phytopathologia Mediterranea* 60(1): 113-117. doi: 10.36253/phyto-11216

Accepted: October 17, 2020

Published: May 15, 2021

Data Availability Statement: All relevant data are within the paper and its Supporting Information files.

Competing Interests: The Author(s) declare(s) no conflict of interest.

Editor: Tito Caffi, Università Cattolica del Sacro Cuore, Piacenza, Italy.

INTRODUCTION

Septoria leaf spot is an important disease of pistachio trees in Greece. Three species of *Septoria* have been reported on pistachio worldwide; *Septoria pistaciarum, S. pistaciae* and *S. pistacina* (Teviotdale *et al*., 2001). In Greece, the fungus was identified as *Mycosphaerella pistaciarum* by Chitzanidis (1956), and the pycnidial stage of *S. pistaciarum*. Eskalen *et al.* (2001) reported *S. pistaciarum* as the causal agent of leaf spot of pistachio in the Eastern Mediterranean and Southeast Anatolian regions. The main symptoms of this disease are development of round to irregular lesions (each of 1–2 mm diam. and containing one to many (~20) pycnidia per lesion (Young and Michailides, 1989; Aghajani *et al*., 2009). The lesions form between small

veins on both sides of affected leaves. These spots may increase slightly in size with time, but generally remain small and isolated from one another. Hundreds of spots may develop on each infected leaf. Over time, large sections of the leaf turn tan in colour. In severe cases, trees defoliate prematurely which reduces the amount of carbohydrates produced and stored, ultimately decreasing tree vigour.

Meteorological factors play key roles in infection caused by Septoria leaf spot fungi. The onset and severity of the disease was affected by wet weather and temperatures from 15–25°C in Arizona, United States of America (Young and Michailides, 1989; Matheron and Call, 1998). In South Greece, these climate conditions occur mainly in the period from May to June each year.

Many models have been developed for forecasting the probability of infections for particular plant pathogens (Newlands, 2018). Modelling approaches have strengths and weakness, and model selection depends upon several factors. Magarey *et al.* (2005) developed a generic infection model based on temperature and wetness duration. This model is generic in the sense that it was developed to describe any pathosystem when appropriate parameters are supplied. The successful development of a plant disease forecasting system also requires the proper validation of a developed model to reduce the risk of two false predictions a) false positive predictions, in which a forecast was made for a disease when in fact no disease was found in a location, and b) false negative predictions, in which a forecast was made for a disease not to occur when in fact the disease was found (Esker *et al*., 2008).

The main aims of this study were a) to investigate the minimum, maximum and optimum temperatures for the conidia germination of *S. pistaciarum*, b) to examine the minimum duration of incubation period (in hours) for the conidia germination of *S. pistaciarum* and c) the evaluation of the generic model developed by Magarey *et al.* (2005) to forecast the pistachio leaf spot disease under the field conditions of Aegina Island, Greece.

METHODS

Assessment of effects of temperature and time on conidium germination

Leaves with typical symptoms of Septoria leaf spot were collected from a commercial pistachio orchard on Aegina Island, Greece in 2016. Identification of the pathogen as *S. pistaciarum* was based on the description of Crous *et al.* (2013). To enhance sporulation, infected leaves were placed in damp chambers for 2 d. Conidium suspensions were made by flooding the surface of leaf spots with sterile distilled water and filtering the resulting suspension through four layers of cheesecloth. Conidium concentration was adjusted to 10^5 conidia mL^{-}with a haemocytometer. One mL of suspension was spread into each Petri dish containing 2% malt extract agar (MEA), and the dishes were placed in a growth chamber (Emmanuel E. Chryssagis, Growth Plant Chambers - GRW 500/CMP2) (98 ± 3% relative humidity) under continuous wetness for 24 h at 4, 8, 10, 15, 20, 23, 25, 30, 32 or 35°C. The proportions of germinated conidia in the Petri dishes incubated at 23°C were recorded at 3, 6, 9, 12, 24, 36 and 48 h after placing in the growth chamber. Conidium germination was determined for 100 conidia, using a microscope at 400× magnification. A conidium was considered germinated when the germ tube length was at least equal to the greatest diameter of the swollen conidium. There were four Petri dishes for each treatment (Dhingra and Sinclair, 1985; Dantigny *et al*., 2006). This experiment was conducted twice.

General linear regression analysis was performed (SPSS Grad Pack 23, SPSS Inc.) to determine relationships between temperature, incubation period and conidium germination.

Disease prediction model

The following parameters were used to run a Septoria leaf spot predictive model based on the results produced in the above experiments: Minimum Temperature (Tmin) = 8°C, Maximum Temperature (Tmax) = 32°C, Optimum Temperature (Topt) = 23°C, Minimum Leaf Wetness (Wmin) = 9 h, Maximum Leaf Wetness (Wmax) = 24 h (based on the above results). This model was evaluated under the field conditions of Aegina Island. Leaf wetness was estimated from the hourly data: if the leaf wetness sensor indexed the hour as wet, it was designated as 1, or when the sensor indexed the hour dry, it is designated 0 (so the dry hours were not counted and were not considered). Continuous wet hours were summed to determine leaf wetness. However, if there was an interruption of fewer than or equal to 24 dry hours (based on the preliminary results produced in the laboratory) the summation of hours was continued. If the interruption of dry hours was longer than 24 dry hours, a new summation of hours was immediately started. Temperature was the average temperature during each wet period.

Cultivar susceptibility or inoculum level were not considered because insufficient information was available about their effects on the occurrence of infection.

Model accuracy in predicting the day of infection was evaluated by comparing actual and predicted times of symptom appearance. In the Aegina Island, which is one of the most important pistachio production areas in Greece, a telemetric meteorological station (Neuropublic S.A., Information Technologies & Smart Farming Services, Piraeus, 18545, Attica, Greece) was established to record weather data, and these data were used to run the model. The model was operated hourly, starting from 00.01 h on 1 May [aiming to include the periods favourable for development of the disease (May to June), and unfavourable for the development of the disease (July-August)], and ending at 31 August, using hourly leaf wetness and temperatures as driving variables for calculations The date of the first observation of leaf spot symptoms (in young leaves) was used to verify the indexing of the models, and the final intensity of the symptoms was recorded 15 d later by calculating the percentage of infected leaves in a sample of 100 leaves randomly selected from each of ten trees. The period of possible appearance of the disease was calculated on each day when Risk (LW, T) > 30, considering an incubation period indicated from our preliminary studies (incubation period estimated at 5 to 15 d in leaves). The model predictions were from 0 (when Disease Risk = 0) to 100 (Disease Risk = the greatest possible value). All the other values were distributed between 0 and 100. Previous preliminary study showed that no or very light symptoms were observed when the model predictions were from 0 to 29.

Two commercial pistachio fields (trees of cv. Aegina, 10–12 years old) were chosen to record the appearance of Septoria leaf spot symptoms in the locations Rachi Moschona and Vigla in 2017, and the experiment was repeated in the same field at Rachi Moschona in 2018. No results could be collected in 2018 from the Vilga location because of technical problems with the meteorological station). Selected trees did not show any symptoms of the disease before starting the trials. The trees (kept unsprayed) were inspected twice each week to determine the time of symptoms onset. When symptoms were unclear, the trees were carefully inspected for the appearance of the first symptoms. Leaves with leaf spot symptoms were marked and observed during the following surveys. Inspections ceased after the appearance of the first disease symptoms.

The predicted period of disease onset was then compared with the actual onset of disease. The model was judged to have provided accurate prediction of disease when the observed symptom onset coincided with the time interval predicted by the model (Giosuè *et al.*, 2000).

RESULTS AND DISCUSSION

Effects of temperature and time on conidium germination

There were no significant differences between the two years for effects of temperatures ($P = 0.175$) or incubation period ($P = 0.207$), so the data from the two experiments were combined. Temperature influenced ($P < 0.001$, SE = 0.259) conidium germination. The optimum temperature for germination was 23°C, germination was strongly reduced at 32 and 8°C, and was inhibited at 35 and 4°C. The estimates of the parameters from the quadratic function are presented in Figure 1. Incubation period also influenced ($P < 0.001$, SE = 0.107) conidium germination. Under constant temperature at 23°C, germination was first observed after 9 h incubation. The greatest percentage of conidium germination was observed after 24 h incubation. No significant differences were detected in the proportions of germinated conidia after 24, 36 or 48 h incubation. Estimates of the parameters from the quadratic function are presented in Figure 2. According to Matheron and Call (1998), the onset and severity of Septoria leaf spot of pistachio in Arizona was affected by summer rainfall temperatures ranging from 15 to 25°C.

Control of the Septoria leaf spot has been based on disease prognosis. This method is adequate, but has disadvantages of inopportune and unnecessary spray applications. These increase the costs pistachio production and also possible environmental pollution with pes-

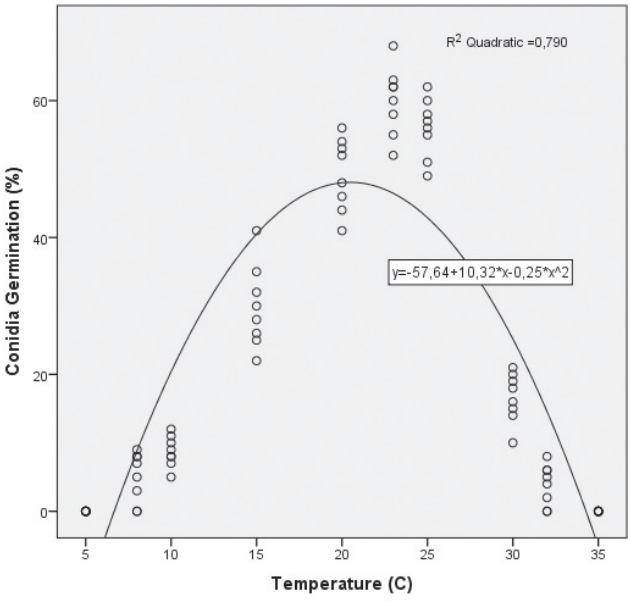

Figure 1. Proportions (%) of germinated *Septoria pistaciarum* conidia in Petri dishes held at different temperatures.

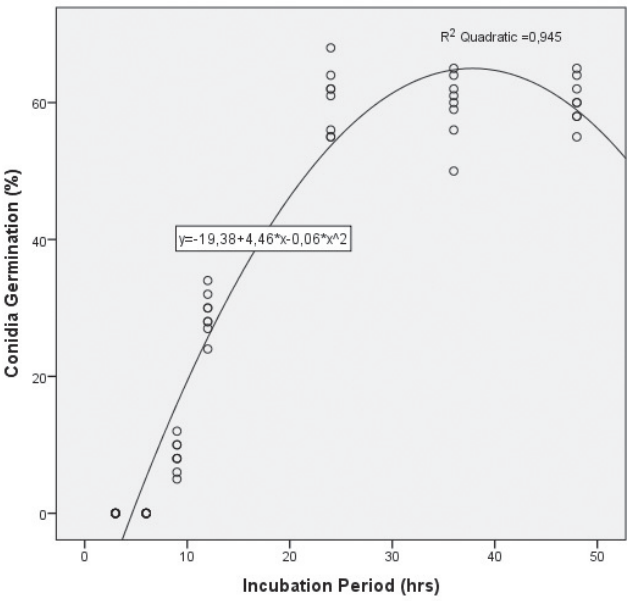

Figure 2. Proportions (%) of germinated *Septoria pistaciarum* conidia in Petri dishes held at 23°C for different incubation periods.

ticides. Disease forecasting has become an established component of quantitative epidemiology. Although it is difficult to exactly predict disease incidence, estimating possible ranges of disease intensity (risk) can be relatively easy. This improvement will provide disease management decision makers with valuable information. The introduction of predictive models to forecast disease appearance could reduce the number of spray applications required for disease control, and improve the effectiveness of spray applications conducted.

Predictive models for forecasting plant diseases are typically developed in specific climates and regions. Before using a model not field tested or validated for a specific location, the model must be tested for one or more seasons under local conditions to verify that it has good precision in that location. Predictive models may contain assumptions about site-specific conditions that may not apply for all areas. Input variables may need to be adjusted due to pathogen biology, and host phenology and variety in a specific area.

Magarey *et al.* (2005) developed a generic model appropriate for predicting the appearance of several plant diseases. This model requires climate parameters such as minimum, maximum and optimum temperatures, and minimum and maximum number of hours of leaf wetness. In the present study this approach was evaluated under field conditions for predict the appearance of pistachio leaf spot. The model indexed risk close to 100 on May 10 at two locations (Rachi Moschona and Vigla) in 2017 (Figure 3), and first symptoms of the disease were observed on May 17. Moderate to high intensity of the symptoms of the disease (>25% of leaves

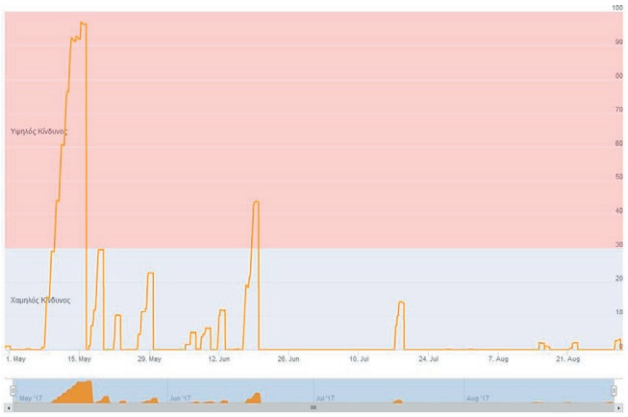

Location Rachi Moschona, 2017

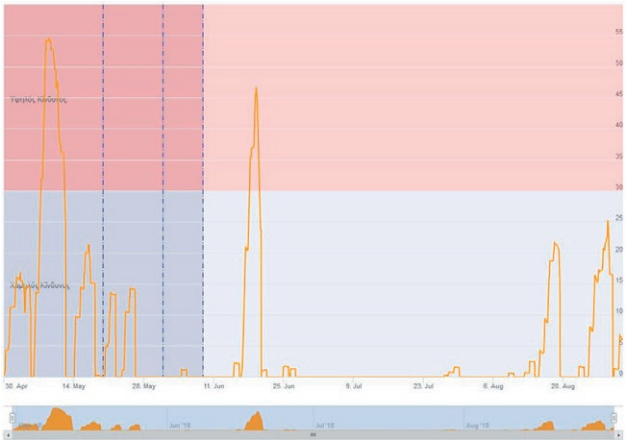

Location Rachi Moschona, 2018

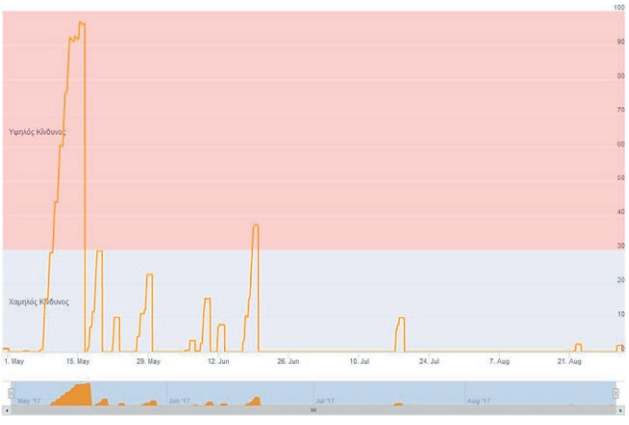

Location Vigla, 2017

Figure 3. Indexing of the generic predictive model (orange line) to forecast infections by *Septoria pistaciarum* on pistachio trees at two locations in 2017 and one location in 2018.

infected) were observed in the unsprayed trees at the end of May. In 2018, the model indexed risk close to 100 on May 9 at Rachi Moschona. The first symptoms of the disease were observed on May 18. Moderate to high intensity of the symptoms (>25% of leaves infected) were observed in the unsprayed trees on May 25. These results showed that the model correctly indexed infection periods.

Based on the results of this study, the Septoria leaf spot prediction model can be used on the Aegina Island, Greece. Greek pistachio producers now have the option to spray their trees only when the model predicts risks of infections. More investigations should be conducted to determine possible correlations between disease risk levels and the proportions of disease, and to determine the number of spray applications which are economically acceptable for pistachio production.

ACKNOWLEDGEMENTS

The authors acknowledge financial assistance provided by the NEUROPUBLIC AE.

LITERATURE CITED

Aghajani M.A., Aghapour B., Michailides T.J., 2009. First report of Septoria leaf spot of pistachio in Iran. *Australasian Plant Pathology Notes* 4: 29–31

Chitzanidis A., 1956. Species of Septoria on the leaves of Pistaciavera L., and their perfect stages. *Annals Institute Phytopathological Benaki* 10: 29–44.

Crous W.P., Quaedvlieg W., Sarpkaya K., Can C., Erkılıç A., 2013. Septoria-like pathogens causing leaf and fruit spot of pistachio. *IMA Fungus* 4: 187–199, doi: 10.5598/imafungus.2013.04.02.04

Dantigny P., Bensoussan M., Vasseur V., Lebrihi A., Buchet C., ... Roussos S., 2006. Standardisation of methods for assessing mould germination: A workshop report. *International Journal of Food Microbiology* 108: 286–291.

Dhingra O.D., Sinclair J.B. 1985. *Basic Plant Pathology Methods*. CRC Press, Florida, USA.

Eskalen A., Küse M., Danisti L., Karadag, S., 2001. *Fungal diseases in pistachio trees in East-Mediterranean and Southeast Anatolian regions*. In: Ak B.E. (ed.). XI GREMPA Seminar on Pistachios and Almonds. Zaragoza: *CIHEAM*, pp. 261–264 (*Cahiers Options Méditerranéennes*; n. 56)

Esker P.D., Sparks A.H., Campbell L., Guo Z., Rouse M., ... Garrett, K.A., 2008. Ecology and epidemiology in R: Disease forecasting and validation. *The Plant Health Instructor* DOI:10.1094/PHI-A-2008-0129-01.

Giosuè S., Spada G., Rossi V., Carli G., Ponti, I., 2000. Forecasting infections of the leaf curl disease on peaches caused by *Taphrina deformans*. *European Journal of Plant Pathology* 106**:** 563–571.

Magarey R.D., Sutton T.B., Thayer C.L., 2005. A simple generic infection model for foliar fungal plant pathogens. *Phytopathology* 95: 92–100.

Matheron M.E., Call R.E., 1998. Factors affecting the development and management of Septoria leaf spot of pistachio in Arizona. *Acta Horticulturae* 470: 592–595.

Newlands N.K., 2018. Model-based forecasting of agricultural crop disease risk at the regional scale, integrating airborne inoculum, environmental, and satellite-based monitoring data. *Frontiers in Environmental Science* (Open Access) https://doi.org/10.3389/fenvs.2018.00063

Teviotdale B.L., Michailides T.J., MacDonald J., 2001. Diseases of pistachio (*Pistacia vera* L.). *Common Names of Plant Diseases*. APS St Paul, MN, USA.

Young D.J., Michailides T.J., 1989. First report of Septoria leaf spot of pistachio in Arizona. *Plant Disease* 73: 775.

Phytopathologia Mediterranea
The international journal of the
Mediterranean Phytopathological Union

Firenze University Press
www.fupress.com/pm

Research Papers

Virulence and diversity of *Puccinia striiformis* in South Russia

Galina V. VOLKOVA, Olga A. KUDINOVA*, Irina P. MATVEEVA

FSBI Federal State Budgetary Scienti!c Institution, All-Russian Scienti!c Center of Biological Plant Protection, 350039 Krasnodar, Russia
*Corresponding author. E-mail: alosa@list.ru

Summary. *Puccinia striiformis* causes wheat yield losses in all countries where wheat is cultivated. Virulence and diversity of the *P. striiformis* were assessed in 2013–2018 in South Russia, and this showed that the North Caucasian population of the pathogen was diverse. One hundred and eighty two virulence phenotypes were identified in 186 *P. striiformis* isolates. Among isolates collected in 2014, 2015, and 2018, all phenotypes were unique. In the 2013 and 2017 populations, phenotypes with few (one to eight) virulence alleles prevailed. In the 2014, 2015, and 2018 populations, most of the phenotypes contained greater numbers (nine to 19) of virulence alleles. Over the 5 years of research, the pathogen population lacked isolates virulent to the host *Yr* resistance genes *3, 5, 26,* and *Sp*. Single (from 1 to 5%) occurrences of isolates virulent to host lines with *Yr* genes *3a, 17, 24, 3b + 4a + H46,* and *3c + Min* were identified. Differences in frequencies of virulence alleles between years in the *P. striiformis* populations (Ney indices, N) were generally non-significant (N = 0.11 to 0.23), with the exception of the populations in 2013 and 2017 (N = 0.37). The minimum N values was found for the populations of 2015 and 2018 (N = 0.10). Over the five years of this study, the dynamics of the virulence of the population and jumps in the frequency of isolates with respect to many *Yr* genes were identified. This feature of the *P. striiformis* populations in South Russia, combined with high phenotypic diversity, indicates the ability for rapid race formation and morphogenesis in response to changes in biotic and abiotic factors.

Keywords. Yellow rust, virulence, effective resistance genes, pathogen population.

OPEN ACCESS

Citation: G. V. Volkova, O. A. Kudinova, I. P. Matveeva (2021) Virulence and diversity of *Puccinia striiformis* in South Russia. *Phytopathologia Mediterranea* 60(1): 119-127. doi: 10.36253/phyto-12396

Accepted: February 11, 2021

Published: May 15, 2021

Data Availability Statement: All relevant data are within the paper and its Supporting Information files.

Competing Interests: The Author(s) declare(s) no conflict of interest.

Editor: Diego Rubiales, Institute for Sustainable Agriculture, (CSIC), Cordoba, Spain.

INTRODUCTION

The yellow rust pathogen (*Puccinia striiformis* West. f. sp. *tritici* Erikss. et Henn.) causes wheat yield losses in all countries where this crop is grown (Singh *et al*., 2004; Bux *et al*., 2011; Hovmøller *et al*., 2017). This pathogen can also infect barley, rye and more than 50 species of herbs (Waqar *et al*., 2018). *Puccinia striiformis* has rapid coupled evolution with the formation of new virulent races that can infect previously resistant wheat varieties (Wellings and McIntosh, 1990; Hovmøller and Justesen, 2007). Recent spread of the pathogen has been limited to regions with temperate climates. Since 2010, new races of *P. striiformis* have caused serious yellow rust epidemics in India, Iran, Pakistan (Afshari, 2008; MacKenzie, 2011), the United States of

America and Canada (Wan and Chen, 2014), Australia (Wellings and Kandel, 2004), Ethiopia (Gebreslasie *et al*., 2020), Egypt (Ashmawy *et al*., 2019; Shahin *et al*., 2020) and other countries.

In Russia, until the end of the 1960s, yellow rust had no economic significance, although the disease was periodically recorded (Morozova, 1974). Since 1990, in the south of Russia, there has been a steady expansion of the area affected by this disease (Chuprina *et al*., 1999; Shumilov and Volkova, 2013). The main regions of South Russia are Krasnodar, Stavropol and Rostov. These regions are leading in the production of winter cereal crops (49% of the total Russian production), and are characterized by favourable weather conditions for the development of phytopathogens, including *P. striiformis*. Foci of infection appear in epiphytotic years due to migration of the pathogen from the Transcaucasus, where a maternal *P. striiformis* population with high variability is formed, to foothills in Dagestan, Ossetia, Ingushetia, Kabardino-Balkaria, adjacent steppe regions of the Stavropol and Krasnodar Regions (Chuprina *et al*., 1999). The infected area in 1995 to 1997 in some regions of southern Russia was 56 to 63% (Berdysh, 2002). In 1997, in Krasnodar region, the infected area varied between 30 and 90% (Dobryanskaya *et al*., 1999). In 2001, an epiphytotic of yellow rust occurred (Berdysh, 2002). In 2004 and 2008, the development of yellow rust, especially in the southern foothill zone of the region, reached 20 to 40% with wheat yield losses of 10 to 15% (Sanin and Nazarova, 2010). The proportion of *P. striiformis* in the pathocomplex during 2001 to 2008 averaged 8% and varied from 5 to 22%. In 2004, moderate yellow rust development was noted, while in 2001 to 2003 and 2005 to 2007, low level of this disease occurred. In 2009-2011, the development of yellow rust ranged from 0.3 to 6.1%. In 2012, the pathogen was not detected in the region, which is most likely due to the low temperatures that occurred in winter. In 2013 to 2017, development and spread of yellow rust remained at the level of previous years and fluctuated from 0.2 to 3.5%. In 2018, the development of the disease was less than 2% (Volkova *et al*., 2018; Matveeva, Volkova, 2019).

Traditionally, in large areas of cultivation, yellow rust is controlled by the use of effective fungicides. However, with the trend towards "greening" of agricultural production, biosafety methods for protecting wheat from yellow rust are becoming increasingly important, with method being the use of disease-resistant wheat varieties (Aktar-Uz-Zaman *et al*., 2017). To effectively use their potential, a substantiated strategy for host variety distribution in agrolandscape niches is necessary, but this cannot be achieved without knowledge of virulence of phytopathogen population (Wellings, 2011). Thus, monitoring the virulence dynamics of the *P. striiformis* population is an important tool for disease management (Chen, 2005; Ali *et al*., 2017).

The aim of the present study was to assess diversity and virulence dynamics of *P. striiformis* populations in southern Russia during 2013 to 2018.

MATERIALS AND METHODS

Route surveys and sample collection

The collection of yellow rust material was carried out in late May to early June of each year, from wheat crops and plant breeding sites in the main grain-producing regions of southern Russia, including Krasnodar, Stavropol and Rostov. Leaves with urediniopustules were wrapped in filter paper and labelled with dates and localities of collection, and were stored during the survey periods in a portable refrigerator. When storing samples in the laboratory, collected leaves were dried and then placed in a refrigerator at 2–4°C.

Weather conditions of growing seasons

In 2013, spring was prolonged with frequent rains, which favourably affected development of yellow rust. In 2014, positive deviations of air temperature prevailed in the early spring period. Heavy rains fell in the second half of March, which contributed to the development of yellow rust on crops. The spring of 2015 was early, unstable, and protracted, with intense frosts in late March to early April, and there were intense frosts (-1 to -5°C). The cold weather in April reduced growth and development of diseases, but these conditions did not affect yellow rust development. In spring of 2017, frequent rains and low temperatures favoured yellow rust development. 2018 was an unfavourable year for development of yellow rust. The combination of high temperatures and low soil moisture in spring limited development of the pathogen.

Multiplication of Puccinia striiformis *isolates*

Multiplication of infectious material for isolation of *P. striiformis* monopustule isolates was carried out on the highly susceptible wheat variety Kaw (United States of America). This was carried out in a greenhouse, using optimal temperature (15 to 18°C), humidity (60 to 80%) and lighting (12,000 to 15,000 lux) for development of

the pathogen (Anpilogova and Volkova, 2000). Wheat plants were grown in 0.5 L capacity pots, five to eight plants in each pot, until their second leaves appeared (germination phase). The wax bloom was then removed from the plants by lightly rubbing the leaves with slightly moistened fingers, and suspensions of urediniospores of the respective populations were applied at low concentration. Water was then applied to the plants with a pump sprayer and the plants were placed in a humid chamber for 18 to 20 h at 13 to 16°C, after which they were transferred to isolated boxes in a greenhouse. After 13 to 14 d, when first signs of disease appeared, only one plant with a single chlorotic spot was left in each pot. This plant was covered with an insulator 10 cm in diameter, with a double layer of gauze fixed on top.

Multiplication of *P. striiformis* isolates was carried out on the same variety using the methods described above. Urediniospores were collected into test tubes, which were identified isolate identifications and agroclimatic zones.

Virulence analysis of Puccinia striiformis *isolates*

To study the virulence of the pathogen population, standard sets of host differentials and lines, carrying 41 resistance genes (Table 1), were used. Perforated pots each containing 25 mL of sand were placed on trays, and were irrigated with Knop's nutrient solution (stock solution: 100 g calcium nitrate, 25 g potassium phosphate, 25 g of magnesium sulphate, 12.5 g potassium chloride, 0.1 g of ferric chloride, in 1 L water). For irrigation, 100 mL of the stock solution was diluted in 10 L of water and the trays were filled with the nutrient mixture (Smirnova and Alekseeva, 1988).

Sprouted seeds of differentials and near isogenic lines were sown into pots, at five seed per pot. In the 1-2 true leaf phase, When resulting plants were at the one to two leaf stage, they were inoculated with each of *P. striiformis* isolates. A tray with each set of varieties and lines was designated by the isolate number with which the plants were infected. At 14 to 18 d after inoculation, when the type of reaction was well pronounced, the reaction was assessed. The type of reaction was determined using the Gassner and Streib scale (Roelfs *et al*., 1992). Varieties and lines with reaction type i, 0, 1 and 2 were considered resistant to the isolate, and type 3.4 as susceptible. a virulence formula was then determined, where the effective resistance genes of each host plant were indicated in the numerator, and the ineffective genes were indicated in the denominator (Green, 1965).

Table 1. Sets of host plant differentials, near isogenic lines of variety Avocet and additional varieties with known resistance genes for characterizing *Puccinia striiformis* virulence.

Varieties and lines	*Yr* Gene(s)	Varieties and lines	*Yr* Gene(s)
International set		Fielder	6+20
Chinese 166*	1	Tyee	Tye
Lee*	7+22+23	Tres	Tr1+Tr2
Heines Kolben	2+6	Hyak	17
Vilmorin 23	3a+4a+V23	Express	Exp1+Exp2
Moro*	10+Mor	*Australian set on the base of*	
Strubes Dickkopf	SD+25	*variety Avocet*	
Suwon 92× Omar	SU	Yr1 / 6 Avocet S	1
Clement*	2+9+Cle	Yr5 / 6 Avocet S*	5
T. spelta album	5	Yr6 / 6 Avocet S	6
European set		Yr7 / 6 Avocet S	7
Hybrid 46	3b+4b+H46	Yr8 / 6 Avocet S*	8
Reichersberg 42	7+25	Yr9 / 6 Avocet S*	9
Heines Peko	2+6+25	Yr10 / 6 Avocet S	10
Nord Desprez	3a+4a+ND	Yr15 / 6 Avocet S	15
Compair*	8+19	Yr17 / 6 Avocet S	17
Carstens V	25+32	Yr24 / 6 Avocet S	24
Spaldings prolific	Sp+25	Yr26 / 6 Avocet S	26
Heines VII*	2+HVII	Yr27 / 6 Avocet S	27
American set		Yr32 / 6 Avocet S	32
Lemhi	21	YrSp / 6 Avocet S	Sp
Paha	Pa1+Pa2+Pa3	Avocet Resistans	A
Druchamp	3a+Dru+Dru2	Jupateco 73 R	18
Produra	Pr1+Pr2	additional varieties	
Yamhill	2+3a+Yam	Minister	3c+Min
Stephens	3a+Ste+Ste2	Vuka	4b

* Host varieties and lines also included in the American set of differentiator varieties.

Statistical analyses of results

The level of diversity of *P. striiformis* phenotypes was assessed using the Shannon index (Hw) according to the formula (Kolmer *et al*., 2003):

$$H_w = -\sum pi \ln(pi)/\ln(n)$$

where *pi* is the frequency of *i*-th phenotype in the population, and *n* is = the total number of isolates of the population.

The diversity of the *P. striiformis* population The frequencies of virulence genes was described using the Ney diversity index (H_s) (Kosman and Leonard, 2007):

$$H_s\,(P) = \Sigma[1 - q_i^2 - (1 - q_i)^2]/k,\ 1 \le i \le k,$$

where q_i is the frequency of i-th gene in this population, and k= number of genes.

The differences of frequencies of virulence genes between the *P. striiformis* populations were assessed using Ney's genetic distance (Kosman, 1996):

$$N = \Sigma \Sigma x_{ij} y_{ij} / \sqrt{\Sigma\Sigma x^2_{ij} \Sigma\Sigma y^2_{ij}},$$

where x_{ij} and y_{ij} indicate frequencies of i-th allele, in the j-th year in compared populations.

RESULTS

Virulence of the wheat yellow rust pathogen population

For the period from 2013 to 2018, virulence of 186 isolates of *P. striiformis* was described (Table 2). Of 41 host lines with resistance genes, 38 showed different responses to *P.* striiformis infection.

Over the 5 years of study, the pathogen population lacked isolates virulent to the *Yr* resistance genes *3, 5, 26,* or *Sp*. Single (from 1 to 5%) occurrences were observed of isolates virulent to lines with the *Yr* genes *3a, 17, 24, 3b + 4a + H46,* or *3c + Min*. In 2009, 1010 and 2011, isolates affecting varieties with *Yr17* occurred with a frequency of 30%, while isolates virulent to the *Yr3c + Min* gene were absent in the population (Shumilov *et al*., 2015). The frequency of *P. striiformis* isolates virulent to the lines with the *Yr* genes *4 + 12, 6, 7 + 25, 2 + HVII, 32, 2 + 9,* or *SD* remained at an average level and varying from 6 to 20%.

The frequency of isolates on host lines with the *Yr* genes *1, 2, 4b, 21, SU, 2 + 6, 7 + 22 + 23,* or *8 + 19* remained stably high (30-80%). On differentiator varieties with the *Yr* genes *39 + Alp* and *Da1 + Da2* the frequency of isolates was high in all years of study, except 2017. On varieties and lines with *Yr* genes *7, 9, 10, 15, 18, 25, 10 + Mor , 3a + 4a + V23,* or *25 + 32*, high polymorphism of the pathogen reaction types was observed. There was also a decrease in the frequency of isolates for the line with the *Yr8* gene, and an increase for the line with the *Yr3a + 4a + ND* genes.

Table 2. Frequency (%) of isolates with virulence alleles in the North Caucasian population of *Puccinia striiformis f. tritici* during 2013 to 2018.

Yr genes of virulence	*Yr* gene frequency (%) and Years of assessment				
	2013	2014	2015	2017	2018
1	30.6	87.8	78.3	40	52.7
2	50.0	69.4	65.7	30	45.1
3a	0.0	2.0	0.0	5	1.6
4+12	8.3	6.1	7.0	20	5.8
4b	25.0	81.6	71.6	55	42,4
6	0.0	6.1	8.2	0	2.8
7	11.1	8.2	10.4	40	0.0
8	19.4	10.2	11.8	5	0.0
9	0.0	67.3	12.5	45	22.2
10	16.7	79.6	18.1	10	5.1
15	11.1	81.6	37.4	30	13.9
17	0.0	4.1	1.2	0	4.8
18	8.3	51.0	10.6	40	62.7
21	58.3	79.6	44.8	30	64.3
24	0.0	4.1	0.0	0	2.8
25	19.4	85.7	20.2	30	18.6
27	11.1	2.0	2.1	0	0.0
29	30.6	69.4	56.7	15	49.1
32	0.0	12.2	10.1	5	17.2
2+9	0.0	12.2	10.8	20	10.8
SU	22.2	57.1	48.3	15	44.4
SD	5.6	8.2	5.2	5	7.2
10+Mor	5.6	46.9	10.1	20	5.6
3a+4a+V23	16.7	51.0	34.1	35	28.4
2+6	48.9	73.5	51.0	40	46.1
7+22+23	41.7	75.5	59.7	45	52.5
2+HVII	11.1	6.1	10.9	20	19.4
25+32	0.0	65.3	1.2	15	14.8
8+19	55.6	65.3	31.8	40	41.4
3a+4a+ND	19.4	10.2	16.1	20	35.6
2+6+25	8.3	30.0	24.6	35	16.7
7+25	19.4	8.2	6.1	20	10.4
3b+4a+H46	0.0	2.0	0.0	5	3.6
A	19.4	63.3	54.4	35	72.2
Da1+Da2	13.9	32.7	27.5	0.0	18.4
39+Alp	41.7	57.1	49.8	0.0	51.3
3, 5, 26, Sp	0.0	0.0	0.0	0.0	0.0
3c+Min	2.8	0.0	0.0	0.0	1.6
Number of isolates	36	49	45	20	36

Diversity of Puccinia striiformis *populations by virulence phenotypes*

The study of the phenotype composition of the North Caucasian population of the wheat yellow rust pathogen revealed significant diversity; 182 virulence phenotypes were identified from 186 *P. striiformis* isolates. Among the isolates from the populations of 2014, 2015, and 2018, all the phenotypes were unique. In the 2013 pathogen population, four phenotypes occurred twice. Diversity of the populations (frequencies of virulence alleles) remained at a moderate average level (Table 3).

Table 3. Ney and Shannon indices for *Puccinia striiformis* populations in South Russia, during 2013 to 2018.

Year	Number of *P. striiformis* isolates	Number of phenotypes	Ney index (Hs)	Shannon index (Sh)
2013	36	32	0.21	0.96
2014	49	49	0.27	1.0
2015	45	45	0.26	1.0
2017	20	20	0.27	1.0
2018	36	36	0.27	1.0

Table 4. Ney indices for *Puccinia striiformis* populations in South Russia during 2013 to 2018, as indicated by the frequencies of virulence alleles.

Compared pairs	Year of assessments of *Puccinia striiformis* populations			
	2013	2014	2017	2018
2013		0.23	0.37	0.17
2014			0.15	0.14
2015	0.18	0.11	0.21	0.10
2017				0.20

Differences between Puccinia striiformis *populations in 2013 to 2018 by frequencies of virulence alleles*

The populations of *P. striiformis* in 2013 to 2018 was compared for the number of virulent alleles (Figure 1). The population of the pathogen in 2013 was characterized by reduced virulence, and phenotypes with small numbers (1-8) of virulence alleles. In contrast, the 2014 population was characterized by a predominance of highly virulent isolates with medium and high levels of virulence alleles.

The 2015 *P. striiformis* population was also dominated by isolates with medium numbers of virulence alleles. In the 2017 population of the pathogen, isolates with short virulence formulae prevailed, although isolates with a medium and high content of virulent alleles totalled 50%. The 2018 population was characterized by an approximately equal ratio of isolates containing medium and large numbers of virulence alleles. Thus, from year to year, the virulence of the populations varies greatly, which indicated the pathogen ability for rapid race formation in response to changes in biotic and abiotic factors.

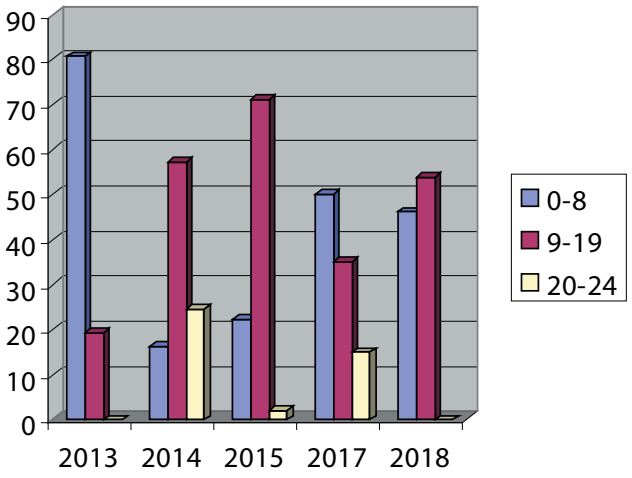

Figure 1. Frequency of *Puccinia striiformis* phenotypes with different numbers of virulence alleles in South Russia during 2013 to 2018.

The differences in frequencies of virulence alleles in the *P. striiformis* populations between years, as shown by Ney indices were generally insignificant (Table 4), with the exception of populations in 2013 and 2017 (N = 0.37).

The minimum Ney index value was found between *Puccinia striiformis* populations in 2015 and 2018 (N = 0.10).

DISCUSSION

The established diversity of the *P. striiformis* population in southern Russia in terms of virulence phenotypes, noted earlier in previous studies (Shumilov *et al.*, 2015; Volkova, 2020), has been primarily associated with the large number of cultivated winter wheat varieties. In the Krasnodar region, about 98 varieties are grown, in the Rostov region, 125 varieties, and in the Stavropol region, 140 winter wheat varieties are used.

The effective *Yr* genes *3, 5, 26,* and *Sp* partially retained their efficiency shown in previous years. For host lines with resistance genes *Yr5* and *YrSp*, this tendency has continued since 2009 (Shumilov, 2013), although the moderate frequency of isolates virulent to *Yr26* in 2009 to 2011 was about 6%. In populations of the *P. striiformis* in other continents, the effectiveness of a number of resistance genes has been similar. For example, in western Canada for many years (1984 to 2013) the host lines with *Yr* genes *1, 5, 15,* and *SP* were not affected by the pathogen, and starting in 2010, isolates virulent to *Yr* genes 24 and *26* started to occur (Brar *et al.*, 2016; 2018). In the United States of America, *Yr* genes *5,* and *15* have been effective since 1960 (Liu *et al.*, 2017). In contrast, in Kazakhstan, *Yr5, Yr9, Yr26,* and *Yr27* are considered to be effective genes (Rsaliev, 2008), while in South Russia *Yr9* has lost its effectiveness and the frequency of *P. striiformis* isolates infecting

Yr27 was from 2 to 11% (Table 2). Isolates from Pakistan and the United States of America were avirulent to lines with genes *Yr5*, *Yr15*, and *YrSP* (Bux *et al*., 2012). The *Yr26* gene, which was effective in South Russia, is gradually losing effectiveness in regions of China, which are especially prone to yellow rust. This is probably due to active use of this gene in wheat breeding in these regions (Han *et al*., 2015). In 2015, *P. striiformis* isolates virulent to *Yr26* were also found in Mexico (Huerta-Espino and Singh, 2017). In Europe, western and central Asia and Africa, this gene has retained effectiveness (Howmoller *et al*., 2020). The appearance and spread of new races in Europe and North Africa, which are annually recorded in new territories, causes concern. For example, the race "Warrior" (*PstS7*), discovered in 2011 in the United Kingdom (virulence profile *Yr1, 2, 3, 4, 6, 7, 9, 17, 25, 32, Sp, AvS,* and *Amb),* and introduced into the European population of the pathogen, caused increased yield losses in many varieties (Rahmatov, 2016). In 2016, a virulent race was found in Ukraine and Azerbaijan (Hovmøller *et al*., 2018). In Russia, *Yr3* and *YrSp* still retain their effectiveness, but the appearance of virulent races in neighbouring regions dictates the need for careful monitoring of the virulence of *P. striiformis* populations.

Thus, the *Yr5, Yr15*, and *Yr26* genes have remained effective in different regions of the world for many years. This is probably due to their origins. The *Yr5* gene was obtained from the wild species *Triticum spelta album*, the *Yr 15* gene from *Triticum dicoccoides*, (Gerechter-Amitai *et al*. 1989), and the *Yr26* gene was transferred from durum wheat to soft wheat via amphiploid with *Aegilops tauschii* (McIntosh and Lagudah, 2000). These three genes belong to the group of so-called *ASR* genes, which are distinguished by their efficacy at all stages of plant growth (Wang and Chen, 2017). For the *P. striiformis* population in southern Russia, the frequency of isolates virulent to lines with *Yr15* genes varied from 11 to 82%.

Dynamics of the frequency of *P. striiformis* isolates to some differential varieties and lines with *Yr* genes can be traced, starting from 2009 (Figure 2 and Figure 3) (*Shumilov*, 2013).In 2014, there was a sharp increase in the frequency of pathogen isolates virulent to varieties and lines with genes *Yr25 + 32* and *Yr10 + Mor.* In subsequent years, the frequencies decrease. A similar surge was observed for most of the other *Yr* genes, including *1, 2, 4b, 9, 10, 15, 21, 25, 29, SU, 3a + 4a + V23, 2 + 6,* and *7 + 22 + 23.* In general, however, there were no significant differences between the 2014 population and other populations. This indicates that the pathogen populations were clonal, and the variability was probably due to weather conditions or rotation of varieties, and not from pathogen introductions from outside the region.

Comparing the frequencies of virulence alleles with similar results in previous years indicates that the resistance of some effective genes has gradually been lost (see Figures 2, and 3). For example, the frequency of isolates virulent to testers with the genes *Yr3a + 4a + ND* and *Yr2 + 9* in 2009 to 2011 did not exceed 5%, while from 2013 to 2015 this was greater ranging from 6 to 19%.

A specific feature of the North Caucasian *P. striiformis* populations has been the low or moderate frequency of occurrence of isolates virulent to a number of differential lines based on the wheat variety Avocet, as compared to pathogen populations in Canada and the United States of America. For example, in the pathogen population in Canada in 2012, there was high frequency of pathogen isolates (70 to 100%) with virulence to *YrA, Yr2, Yr6, Yr7, Yr8, Yr9, Yr17, Yr26, Yr27, Yr31* and *Yr32* (Kumar *et al*., 2012). In the South Russian population, the frequency of isolates virulent to most of these lines ranged from 6 to 17%. Therefore, for a complete

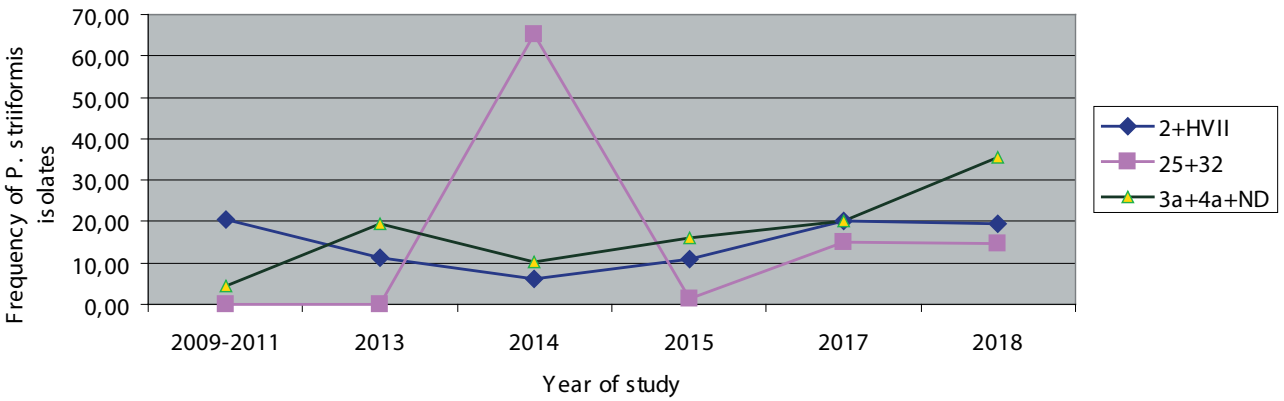

Figure 2. Frequencies of *Puccinia striiformis* isolates in South Russia from 2009 to 2018 with virulence to the European set of differential wheat varieties.

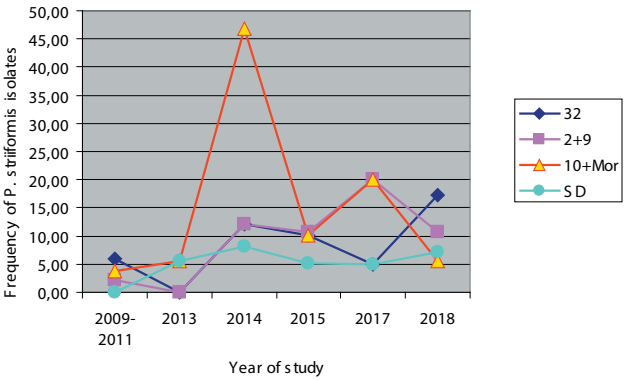

Figure 3. Frequencies of *Puccinia striiformis* isolates in South Russia during 2009 to 2018, with virulence to the host varieties and lines of the International and Australian differential sets.

and objective analysis of the virulence of the *P. striiformis* population, differentiation in the southern region of Russia was carried out using the international, American, European and Australian host differential sets.

CONCLUSIONS

These studies of the *P. striiformis* populations in South Russia have shown that even in conditions unfavourable for the pathogen, yellow rust of wheat occurred in the region every year, and in some areas there were foci of the disease with of up to 50% severity. Effective host genes for resistance to *P. striiformis* were the *Yr* genes *3, 5, 26,* and *Sp*. At the same time, host lines with genes *Yr5* and *Yr Sp* have continued to be resistant since 2009. Single (from 1 to 5%) occurrences of isolates virulent to host lines with several *Yr* genes were observed, including gene *3a, 17, 24, 3b + 4a + H46,* and *3c + Min*. According to the Shannon diversity indices, phenotypic composition of the *P. striiformis* population in South Russia has been established. This confirms is a characteristic feature of the population, as described in previous studies (Shumilov *et al*., 2015; Volkova *et al*., 2020). The differences in *P. striiformis* populations in the frequency of virulence genes between years are insignificant. During the five years of the present study, there were intensive virulence dynamics and changes in the frequency of virulence to host *Yr* genes in the pathogen population. This feature in South Russia, combined with high phenotypic diversity, indicates the ability of *P. striiformis* for rapid race formation and morphogenesis in response to changes in biotic and abiotic environmental factors. This dictates the need for continued monitoring of an important pathogen in this region. The obtained long-term data on the dynamics of virulence of *P. striiformis* are important for understanding the interaction mechanisms of this host-pathogen system, and provide a necessary link in breeding for resistance to yellow rust in South Russia.

ACKNOWLEDGEMENTS

Researchers of the Laboratory of Immunity of Cereal Crops to Fungal Diseases of the Federal Scientific Center for Biological Plant Protection assisted in this research. Mrs. A. V. Danilova and Mrs. O. Miroshnichenko helped with collection of yellow rust affected plant material, and Mrs. O. Vaganova, Mrs. Gladkova E. V. gave technical assistance. The research was carried out in accordance with State Assignment No. 075-00376-19-00 of the Ministry of Science and Higher Education of the Russian Federation, within the framework of Topic No. 0686-2019-0008.

LITERATURE CITED

Afshari F., 2008. Prevalent pathotypes of *Puccinia striiformis* f. sp. *tritici* in Iran. *Journal of Agricultural Science and Technology* 10: 67–78.

Aktar-Uz-Zaman M., Tuhina-Khatun M., Hanafi M.M., Sahebi M., 2017. Genetic analysis of rust resistance genes in global wheat cultivars: an overview. *Biotechnology & Biotechnological Equipment* 31(3): 431–445.

Ali S., Rodriguez-Algaba J., Thach T., Sorensen C.K., Hansen … Hovmoller M.S., 2017. Yellow rust epidemics worldwide were caused by pathogen races from divergent genetic lineages. *Frontiers in Plant Science* 8: 1057.

Anpilogova L.K., Volkova G.V., 2000. *Development Methods of Artificial Infectious Backgrounds and Wheat Varieties Assessment for Resistance to Harmful Diseases (spike fusarium, rust, powdery mildew).* Recommendations. Krasnodar: RAAS, ARRIBPP, 28 pp. (in Russian)

Ashmawy M.A., Shahin A.A., Samar M.E., Hend A.N., 2019. Virulence dynamics and diversity of *Puccinia striiformis* populations in Egypt during 2017/18 and 2018/19 growing seasons. *Journal of Plant Protection and Pathology* 10 (12): 655–666.

Berdysh Yu. I., 2002. *Phytosanitary Monitoring and Scientific Substantiation of Winter Wheat Protection Against Pests on Black Earth Soil of Western Ciscaucasia*. PhD Thesis, Krasnodar, Russia, 173 pp. (in Russian)

Brar G.S., McCallum B.D., Gaudet D.A., Puchalski B.J., Fernandez M.R., Kutcher H.R., 2016. Stripe rust disease dynamics in southern Alberta, Saskatchewan, and Manitoba, 2009-2014. *Canadian Journal of Plant Pathology* 38: 114–115.

Brar G.S., Dhariwal R., Randhawa H.S., 2018. Resistance evaluation of differentials and commercial wheat cultivars to stripe rust (*Puccinia striiformis*) infection in hot spot regions of Canada. *European Journal of Plant Pathology* 152: 269.

Bux H., Ashraf M., Chen X., Mumtaz A.S., 2011. Effective genes for resistance to stripe rust and virulence of *Puccinia striiformis* f. sp. *tritici* in Pakistan. *African Journal of Biotechnology* 10(28): 5489–5495.

Bux H., Rasheed A., Mangrio S.M., Abro S.A., Shah S.J.A., … Chen X., 2012. Comparative virulence and molecular diversity of stripe rust (*Puccinia striiformis* f. sp. *tritici*) collections from Pakistan and United States. *International Journal of Agricultural Biology* 14: 851–860.

Chen X. M., 2005. Epidemiology and control of stripe rust (*Puccinia striiformis* f. sp. *tritici*) on wheat. *Canadian Journal of Plant Pathology* 27: 314–337.

Chuprina V.P., Sokolov M.S., Anpilogova L.K., Kobileva E.A., Levashova G.I., Pikushova V.V., 1999. Protection of wheat crops against stripe rust, taking into account the epiphytotic and biotrophic characteristics of its pathogen *Puccinia striiformis* West. *Agrochemistry* 7: 81–94. (in Russian)

Dobryanskaya M.V., Anpilogova L.K., Vysotskaya N.I., 1999. Model of sporulation of the stripe rust pathogen. *Protection and Quarantine of Plants* 8: 25–26. (in Russian)

Gerechter-Amitai Z.K., Sifhou C.H., Grama A., Kleitman F., 1989. Yr15: a new gene for resistance to *Puccinia striiformis* in *Triticum dicoccoides* sel. G-25. *Euphytica* 43: 187–190.

Gebreslasie Z.S., Huang S., Zhan G., Badebo A., Zeng Q.,... Kang Z., 2020. Stripe rust resistance genes in a set of Ethiopian bread wheat cultivars and breeding lines. *Euphytica* 216(2): 17.

Green G.J., 1965. Stem rust of wheat, rye and barley in Canada in 1964. *Plant Disease Survey* 45(1): 23–39.

Han D.J., Wang Q.L., Chen X.M., Zeng Q.D., Wu J.H., ... Kang, Z. S., 2015. Emerging Yr26-virulent races of *Puccinia striiformis f. tritici* are threatening wheat production in the Sichuan Basin, China. *Plant Disease* 99(6): 754–760.

Hovmøller M.S., Justesen A.F., 2007. Rates of evolution of avirulence phenotypes and DNA markers in a northwest European population of *Puccinia striiformis* f. sp. *tritici. Molecular Ecology* 16: 4637–4647.

Hovmøller M.S., Rodriguez-Algaba J., Thach, T., Sørensen, C.K., 2017. Race typing of *Puccinia striiformis* on wheat. In: *Wheat rust diseases*. Humana Press, New York, NY, USA 29–40.

Hovmøller M.S., Rodriguez-Algaba J., Thach T., Justesen, A.F., Hansen J.G., 2018. Report for *Puccinia striiformis* race analyses and molecular genotyping 2017. Global Rust Reference Center (GRRC), Aarhus University, Flakkebjerg, DK-4200 Slagelse, Denmark. Available at: https://agro.au.dk/fileadmin/Summary_of_Puccinia_striiformis_race_analysis_2017.pdf

Hovmøller M.S., Rodriguez-Algaba J., Thach T., Justesen A.F., Hansen J.G., 2020. GRRC annual report 2019: Stem and yellow rust genotyping and race analyses. Aarhus University, Department of Agroecology, DK-4200 Slagese, Denmark. Available at: https://agro.au.dk/fileadmin/www.grcc.au.dk/International_Services/Pathotype_YR_results/GRRC_annual_report_2019.pdf

Huerta-Espino J., Singh R.P., 2017. First detection of virulence in *Puccinia striiformis* f. sp. tritici to wheat resistance genes Yr10 and Yr24 (= Yr26) in Mexico. *Plant Disease* 101(9): 1676–1676.

Kolmer J.A., Long D.L., Kosman, E., Hughes, M.E., 2003. Physiologic specialization of *Puccinia triticina* on wheat in the United States in 2001. *Plant Disease* 87: 859–866.

Kosman E., 1996. Difference and diversity of plant pathogen populations: a new approach for measuring. *Phytopathology* 86: 1152–1155.

Kosman E., Leonard K.J., 2007. Conceptual analysis of methods applied to assessment of diversity within and distance between populations with asexual or mixed mode of reproduction. *New Phytologist* 174: 683–696.

Kumar K., Holtz M.D., Xi K., Turkington T.K., 2012. Virulence of *Puccinia striiformis* on wheat and barley in central Alberta. *Canadian Journal of Plant Pathology* 34(4): 551–561.

Line R.F., 2002. Stripe rust of wheat and barley in North America: A retrospective historical review. *Annual Review of Phytopathology* 40: 75–118.

Liu T., Wan A., Liu D., Chen X., 2017. Changes of races and virulence genes in *Puccinia striiformis* f. sp. *tritici,* the wheat stripe rust pathogen, in the United States from 1968 to 2009. *Plant Disease* 101(8): 1522–1532.

MacKenzie D., 2011. Crop disease to add to east Africa's woes [Electronic resource]. 1 p. Available at: http://www.newscientist.com/article/mg21128214.100-crop-disease-to-add-to-east-africas-woes.html

Matveeva I.P., Volkova G.V. 2019. Wheat yellow rust: Distribution, harmfulness, control measures (review).

Bulletin of the Ulyanovsk State Agricultural Academy 2 (46):102-116. (in Russian)

McIntosh R.A. Lagudah E.S., 2000. Cytogenetical studies in wheat. XVIII. Gene Yr24 for resistance to stripe rust. *Plant Breeding* 119: 81–83.

Morozova A.A., 1974. Species composition of winter wheat rust and their distribution in the Krasnodar Territory. *Proceedings of the Kuban Agricultural Institute* 79 (107): 49–55. (in Russian)

Rahmatov M., 2016. *Genetic Characterisation of Novel Resistance Alleles to Stem Rust and Stripe Rust in Wheat-Alien Introgression Lines*. PhD Thesis, Alnarp, Swedish University of Agricultural Sciences, Sweden, 76 pp.

Roelfs A.P., Singh R.P., Saari E.E., 1992. *Rust Diseases of Wheat: Concepts and Methods Management*. CIMMIT, Mexico, 81 pp.

Rsaliev Sh.S., 2008. A new method for differentiating wheat yellow rust. *Science News of Kazakhstan* 2: 143-146. (in Russian)

Sanin S.S., Nazarova L.N., 2010. Phytosanitary situation on wheat crops in the Russian Federation (1991-2008). *Protection and Quarantine of Plants* 2: 20 p. (in Russian)

Shahin A., Ashmawy M., El-Orabey W., Esmail S., 2020. Yield Losses in Wheat Caused by Stripe Rust (*Puccinia striiformis*) in Egypt. *American Journal of Life Sciences* 8 (5): 127–134.

Shumilov Yu.V., 2013. *Agrobiological Substantiation of Methods of Reducing the Infectious Potential of the Wheat Stripe Rust Pathogen in the North Caucasus*. PhD Thesis, N.I. Vavilov Saratov State Agricultural University, Russia, 24 pp. (in Russian)

Shumilov Yu.V., Volkova G.V., 2013. Wheat stripe rust requires special attention. *Protection and Quarantine of Plants* 8: 13–14. (in Russian)

Shumilov Yu.V., Volkova G.V., Nadykta V.D., 2015. Structure of the wheat stripe rust pathogen population by virulence in the North Caucasus. *Mycology and Phytopathology* 49(3): 194–200. (in Russian)

Singh R.P., William H.M., Huerta-Espino J., Rosewarne G., 2004. Wheat Rust in Asia: Meeting the challenges with old and new technologies. In: *New directions for a diverse planet*. Proceed. 4th International Crop Science Congress, September 26 to October1, Brisbane, Australia. Available at: http://www.cropscience.org.au./icsc2004/symposia/3/7/141_singhrp.html

Smirnova L.A., Alekseeva T.P., 1988. An improved method of cultivation of seedlings of grain crops for immunological studies. *Selection and Seed Production* 4: 25–27. (in Russian)

Volkova G.V., Shulyakovskaya L.N., Kudinova O.A., Matveeva I.P., 2018. Wheat yellow rust in the Kuban. *Plant Protection and Quarantine* 4: 29. (in Russian)

Volkova G.V., Matveeva I.P., Kudinova O.A. 2020. Virulence of the wheat yellow rust pathogen population in the North Caucasus region of Russia. *Mycology and Phytopathology* 54(1): 33–41. (in Russian)

Waqar A., Khattak S.H., Begum S., Rehman T., Rabia A. … Ali. G.M., 2018. Stripe rust: A review of the disease, Yr genes and its molecular markers. *Sarhad Journal of Agriculture* 34(1): 188–201.

Wan A.M., Chen X.M., 2014. Virulence characterization of *Puccinia striiformis* f. sp. *tritici* using a new set of *Yr* single-gene line differentials in the United States in 2010. *Plant Disease* 98: 1534–1542.

Wang M., Chen X., 2017. Stripe rust resistance. In: *Stripe Rust* (Chen X., Kang Z. ed.), Springer, Dordrecht, 353–558.

Wellings C.R., McIntosh R.A., 1990. *Puccinia striiformis* f. sp. *tritici* in Australasia: pathogenic changes during the first 10 years. *Plant Pathology* 39 (2): 316–325.

Wellings C.R., Kandel K.R., 2004. Pathogen dynamics associated with historic stripe (yellow) rust epidemics in Australia in 2002 and 2003. In: *Proceedings of the 11th International Cereal Rusts and Powdery Mildews Conference*. Abstr. A2.74.1 p. Available at: http://www.crpmb.org/icrpmc11/abstracts.html

Wellings C.R., 2011. Global status of stripe rust: a review of historical and current threats. *Euphytica* 179: 129–141.

Phytopathologia Mediterranea
The international journal of the
Mediterranean Phytopathological Union

Firenze University Press
www.fupress.com/pm

Research Papers

Bioactive secondary metabolites produced by the emerging pathogen *Diplodia olivarum*

Roberta DI LECCE[1], Marco MASI[1,*], Benedetto Teodoro LINALDEDDU[2], Gennaro PESCITELLI[3], Lucia MADDAU[4], Antonio EVIDENTE[1]

[1] *Dipartimento di Scienze Chimiche, Università di Napoli Federico II, Complesso Universitario Monte Sant'Angelo, Via Cintia 4, 80126, Napoli, Italy*
[2] *Dipartimento Territorio e Sistemi Agro-Forestali, Università di Padova, Viale dell'Università 16, Legnaro 35020, Italy*
[3] *Dipartimento di Chimica e Chimica Industriale, Università di Pisa, Via Moruzzi 13, 56124 Pisa, Italy*
[4] *Dipartimento di Agraria, Sezione di Patologia Vegetale ed Entomologia, Università degli Studi di Sassari, Viale Italia 39, 07100, Sassari, Italy*
*Corresponding author. E-mail: marco.masi@unina.it

Summary. A new cleistanthane *nor*-diterpenoid, named olicleistanone (**1**), was isolated as a racemate from the culture filtrates of *Diplodia olivarum*, an emerging pathogen involved in the aetiology of branch canker and dieback of several plant species typical of the Mediterranean maquis in Sardinia, Italy. When the fungus was grown *in vitro* on Czapek medium, olicleistanone was isolated together with some already known phytotoxic diterpenoids identified as sphaeropsidins A, C, and G, and diplopimarane (**2**-**5**). Olicleistanone was characterized as 4-ethoxy-6a-methoxy-3,8,8-trimethyl-4,5,8,9,10,11-hexahydrodibenzo[*de,g*]chromen-7(6a*H*)-one. When *D. olivarum* was grown on mineral salt medium it produced (-)-mellein (**6**), sphaeropsidin A and small amounts of sphaeropsidin G and diplopimarane. Olicleistanone (**1**) exhibited strong activity against the insect *Artemia salina* L. (100% larval mortality) at 100 μg mL^{-1} but did not exhibit phytotoxic, antifungal or antioomycete activity. Among the metabolites isolated (**1**-**6**), sphaeropsidin A (**2**) was active in all bioassays performed exhibiting strong phytotoxicity on leaves of *Phaseolus vulgaris* L., *Juglans regia* L. and *Quercus suber* L. at 1 mg mL^{-1}. Sphaeropsidin A (**2**) also completely inhibited mycelium growth of *Athelia rolfsii, Diplodia corticola*, *Phytophthora cambivora* and *P. lacustris* at 200 μg per plug, and was active in the *Artemia salina* assay. Also in this assay, diplopimarane (**5**) and sphaeropsidin G (**4**) were active (100% larval mortality). Diplopimarane also showed antifungal and antioomycete activities. *Athelia rolfsii* was the most sensitive species to diplopimarane. Sphaeropsidin C (**3**) and (-)-mellein (**6**) were inactive in all bioassays. These results expand knowledge on the metabolic profile of *Botryosphaeriaceae*, and embody the first characterization of the main secondary metabolites secreted by *D. olivarum*.

Keywords. *Botryosphaeriaceae*, forest ecosystems, olicleistanone, toxins.

Citation: R. Di Lecce, M. Masi, B. T. Linaldeddu, G. Pescitelli, L. Maddau, A. Evidente (2021) Bioactive secondary metabolites produced by the emerging pathogen *Diplodia olivarum*. *Phytopathologia Mediterranea* 60(1): 129-138. doi: 10.36253/phyto-12170

Accepted: January 20, 2021

Published: May 15, 2021

Data Availability Statement: All relevant data are within the paper and its Supporting Information files.

Competing Interests: The Author(s) declare(s) no conflict of interest.

Editor: Luisa Ghelardini, University of Florence, Italy.

INTRODUCTION

Diplodia Fr. is a large genus in the *Botryosphaeriaceae*, typified by *Diplodia mutila* (Fr.: Fr.) Fr. (Alves *et al.*, 2014). Species of *Diplodia* are cosmopoli-

tan in temperate and subtropical regions, and occur on a wide range of angiosperm and gymnosperm hosts (Masi *et al.*, 2018). They exhibit diverse lifestyles, from endophytes inhabiting asymptomatic plant tissues to aggressive pathogens that cause severe diseases in various plant hosts (Pérez *et al.*, 2010; Adamson *et al.*, 2015; Martin *et al.*, 2017; Masi *et al.*, 2018). The increasing number of reports of new diseases caused by these pathogens has stimulated research into the virulence factors involved in their pathogenesis processes. Several bioactive secondary metabolites were isolated and characterized from the emerging *Diplodia* pathogenic species *D. africana, D. corticola, D. cupressi, D. fraxini, D. quercivora* and *D. sapinea*. These metabolites belong to different classes of organic compounds including pimarane diterpenoids, α-pyrones, furanones, diplobifuranylones, naphthoquinones, biphenols, cyclohexene oxides, furopyrans, isochromanones and melleins (Evidente *et al.*, 2012; Andolfi *et al.*, 2014; Cimmino *et al.*, 2016; Cimmino *et al.*, 2017a; Masi *et al.*, 2018). Some phytotoxins produced by *Diplodia* species (e.g. the tetracyclic pimarane diterpenoid, sphaeropsidin A) have broad-spectra of biological properties, including anticancer activity (Masi *et al.*, 2018).

Recently, *Diplodia olivarum* has emerged as an aggressive pathogen on different plant hosts in Italy. This fungus was first found on rotting olive drupes in southern Italy, and was described as a new species in 2008 (Lazzizera *et al.*, 2008). It was later reported as a cause of canker on carob tree (Granata *et al.*, 2011), lentisk (Linaldeddu *et al.*, 2016) and wild olive (Manca *et al.*, 2020). Symptoms caused by the pathogen in infected hosts include sunken cankers with characteristic wedge-shaped wood necroses on branches and stems. Foliar symptoms have also been observed especially on lentisk shoots (Figure 1).

Given the expansion of severe dieback caused by *D. olivarum* in several natural ecosystems in Italy, and the limited information available about bioactive secondary metabolites produced by this emerging pathogen, the study described here was conducted to isolate, identify and evaluate phytotoxic, antifungal, antioomycetes and zootoxic activities of the main compounds produced by *D. olivarum*

Figure 1. Foliar symptoms on lentisk shoots infected by *Diplodia olivarum*.

MATERIALS AND METHODS

Chemical characterization procedures

Optical rotations were measured in MeOH on a P-1010 digital polarimeter (Jasco, Tokyo, Japan), unless otherwise noted. IR spectra were recorded as a glass film deposits using a 5700 FT-IR spectrometer (Jasco), and UV spectra were measured in MeCN on a V-530 spectrophotometer (Easton). ^{1}H and ^{13}C NMR spectra were recorded, respectively, at 400 and 100 MHz in $CDCl_3$, on a Bruker spectrometer (Billerica), using the same solvent as internal standard. The multiplicities were determined by DEPT spectrum (Berger and Braun, 2004). COSY, HSQC, HMBC and NOESY spectra were recorded using Bruker microprograms. HR ESIMS spectra were recorded on a 6120 Quadrupole LC/MS instrument (Agilent Technologies). Analytical (0.25 mm thickness) and preparative TLC (0.50 mm thickness) were performed on silica gel (Kieselgel 60, F_{254},) and on reversed phase (Kieselgel 60 RP-18, F_{254}, 0.20 mm tickness) plates (Merck). Resulting spots were visualized by exposure to UV radiation (253 nm), or by spraying first with 10% H_2SO_4 in MeOH and then with 5% phosphomolybdic acid in EtOH, followed by heating at 110°C for 10 min. Column chromatography was performed using silica gel (Merck, Kieselgel 60, 0.063-0.200 mm).

Fungus strain

The *D. olivarum* strain used in this study was originally isolated from a cankered branch of lentisk collected in a natural area on Caprera Island (Italy). Representative genetic sequences from this strain were deposited in GenBank, with the accession numbers: ITS; KX833078), *tef1-α*; KX833079) and MAT1-2-1; MG015783 (Lopes *et al*., 2018). Pure cultures were maintained on potato dextrose agar (PDA) (Fluka, Sigma-Aldrich Chemic GmbH) and were stored at 4°C in the collection of the Dipartimento di Agraria, University of Sassari, Italy, as BL96.

Production, extraction and purification of secondary metabolites

Diplodia olivarum was grown on Czapek broth amended with 2% yeast extract or mineral salt medium (Pinkerton and Strobel, 1976), both at pH 5.7 in 1 L capacity Erlenmeyer flasks each containing 250 mL of medium. Each flask was seeded with 5 mL of a mycelium suspension and then incubated for 30 d at 25°C. Culture filtrates were obtained by filtering the cultures through filter paper in a vacuum system.

The filtrate (14.5 L), obtained growing the fungus on Czapek medium, was acidified to pH 4 with 2 N HCl and extracted exhaustively with EtOAc. The combined organic extracts were dried with Na_2SO_4 and evaporated under reduced pressure. The brown-red oil residue recovered (4.5 g) was fractioned by column chromatography on silica gel (90 × 4 cm) eluted with *n*-hexane-EtOAc (7:3). Eleven fractions were collected and pooled on the basis of similar TLC profiles. Fraction 2 (195.2 mg) was purified by column chromatography on silica gel, eluted with petroleum ether-EtOAc (9.5:0.5), and yielded 13 homogeneous fractions. The residue of the fourth fraction from this latter column (11.0 mg) was further purified by TLC, eluted with *n*-hexane-acetone (8.5:1.5), and yielded sphaeropsidin G, **4** [6.7 mg, 0.46 mg L^{-1}, R_f 0.82, eluent *n*-hexane-acetone (8.5:1.5)] as an amorphous solid. The residue of the third fraction (103.2 mg) was purified by column chromatography on silica gel (75 × 3 cm), eluted with $CHCl_3$-isoPrOH (93:7), and yielded eight homogeneous fractions. The residue of the third fraction from this latter column (23.0 mg) was crystallized with EtOAc-*n*-hexane (1:5) to give diplopimarane, **5** [14.2 mg, 0.97 mg L^{-1}, R_f 0.7, eluent *n*-hexane-EtOAc (7:3)] as white crystals. The residue of the eighth fraction (56.4 mg) was purified by preparative TLC, eluted with *n*-hexane-$CHCl_3$-isoPrOH (8:1.5:0.5), and yielded olicleistanone (**1**) as an amorphous solid [5.8 mg, 0.4 mg L^{-1}, R_f 0.45, eluent *n*-hexane-$CHCl_3$-isoPrOH (8:1.5:0.5)]. The residues from the fifth (290.3 mg) and sixth (278.9 mg) fractions from the first column were combined and crystallized with EtOAc-*n*-hexane (1:5) to give sphaeropsidin A, **2** [312.6 mg, R_f 0.5, eluent *n*-hexane-acetone (7:3), R_f 0.7, eluent *n*-hexane-EtOAc (6:4)] as white crystals. The residue of the seventh fraction (135.1 mg) from the first column was purified by CC on silica gel, eluent *n*-hexane-EtOAc-acetone (6:2.5:1.5), giving sphaeropsidin C, **3** [53.3 mg, 3.67 mg L^{-1}, R_f 0.52, eluent *n*-hexane-EtOAc-acetone (6:2.5:1.5), R_f 0.63, eluent *n*-hexane-EtOAc (6:4)] as a white solid, and a further amount of sphaeropsidin A, **2** (33.2 mg, total yield 23.7 mg L^{-1}).

The culture filtrate (10.0 L) obtained growing the fungus on modified mineral medium was extracted following the procedure described above to obtain 3.2 g of organic extract. This was fractioned by column chromatography on silica gel (80 × 4 cm) eluted with *n*-hexane-EtOAc (7:3), and yielded ten groups of homogeneous fractions. The residue of the third fraction (302.3 mg) was purified by column chromatography on silica gel (75 × 3 cm), eluted with *n*-hexane-$CHCl_3$-isoPrOH (7.5:2:0.5), and yielded diplopimarane (**5**; 1.4 mg, 0.01 mg L^{-1}) and (-)-mellein [**6**; 105.8 mg, 7.30 mg L^{-1}, R_f 0.65, eluent *n*-hexane-$CHCl_3$-isoPrOH (7.5:2:0.5)]. The residue of the fourth fraction of the first column (8.2 mg) was further purified by TLC, eluted with *n*-hexane-acetone (8.5:1.5), and yielded sphaeropsidin G (**4**; 1.5 mg, 0.10 mg L^{-1}). The residue of the fifth (815.9 mg) fraction of the first column was crystallized with EtOAc-*n*-hexane (1:5) to give sphaeropsidin A (**2**; 677 mg, 46.69 mg /L^{-1}).

Spectroscopic data of secondary metabolites

Olicleistanone (**1**): UV λ_{max} (log ε) 333 (2.98), 241 (3.55) nm; IR ν_{max} 1725, 1610, 1592, 1560, 1458 cm^{-1}; ^1H and ^{13}C NMR: Table 1; HRESI -MS (+) spectrum *m/z*: 735 $[2M+Na]^+$, 395 $[M + K]^+$, 379.1876 [$C_{22}H_{28}$ Na O_4, calcd. 379.1885, $M+Na]^+$, 311 $[M+H\text{-}CH_3CH_2OH]^+$.

Sphaeropsidin A (**2**): $[\alpha]_D^{25}$ +104 (*c* 0.4, MeOH); [lit. (Evidente *et al*., 1996): $[\alpha]_D^{25}$ +109.6 (*c* 0.2, MeOH); ^1H NMR is very similar to that previously reported (Evidente *et al*., 1996); HRESI-MS (+) spectrum *m/z*: 715 $[2M+Na]^+$, 369 $[M+Na]^+$, 347.1820 [$C_{20}H_{27}O_5$, calcd. 347.1780, $M+H]^+$.

Sphaeropsidin C (**3**): $[\alpha]_D^{25}$ +18.3 (*c* 0.7, MeOH); [lit. (Evidente *et al.,* 1997): $[\alpha]_D^{25}$ + 16.8 (*c* 1.0, MeOH)]; ^1H NMR is very similar to that previously reported (Evidente *et al.,* 1997); HRESI-MS (+) spectrum *m/z*:

703 [2M+K]$^+$, 687 [2M+Na]$^+$, 665 [2M+H]$^+$, 333.2037 [$C_{20}H_{29}O_4$, calcd. 333.2066, M+H]$^+$.

Sphaeropsidin G (**4**): $[\alpha]_D^{25}$ +48.6 (*c* 0.8, $CHCl_3$) [lit. (Cimmino *et al.*, 2016): $[\alpha]_D^{25}$ +51.4 (*c* 0.56, $CHCl_3$)]; ^{1}H NMR is very similar to that previously reported (Cimmino *et al.*, 2016); ESI-MS (+) spectrum *m/z*: 309 [M + K]$^+$, 293 [M + Na]$^+$, 271 [M + H]$^+$.

Diplopimarane (**5**): $[\alpha]_D^{25}$ +23.0 (*c* 0.1, $CHCl_3$) [lit. (Andolfi *et al.*, 2014): $[\alpha]_D^{25}$+25.8 (*c* 0.6, $CHCl_3$)]; ^{1}H NMR is very similar to that previously reported (Andolfi *et al.*, 2014); ESIMS (+) spectrum *m/z*: 623 [2M - 4H + Na]$^+$, 339 [M - 2H + K]$^+$, 325 [M + Na]$^+$, 323 [M - 2H + Na]$^+$.

(-)-Mellein (**6**): $[\alpha]^{25}$D -93.0 (*c* 0.3 MeOH) [lit. (Masi *et al.*, 2020): $[\alpha]^{25}_D$ -90 (*c* 0.2, CH_3OH)]; ^{1}H NMR is similar to that previously reported (Masi *et al.*, 2020); ESI MS (+) spectrum *m/z*: 179 [M + H]$^+$.

Computational methods

Molecular mechanics, Hartree-Fock (HF) and density functional theory (DFT) calculations were run with Spartan'18 (Wavefunction, Inc. 2018), with standard parameters and convergence criteria.

First, the conformers of (7*S*,15*S*)-**1** and (7*S*,15*R*)-**1** were investigated with the Monte Carlo algorithm using Merck molecular force field (MMFF). They were then screened by geometry optimizations at HF/3-21G level, single-point calculations at B3LYP/6-31G(d) level, and final geometry optimizations at the same level. Energies and populations were then estimated at the B97M-V/6-311+G(2df,2p) level. The procedure gave six energy minima for (7*S*,15*S*)-**1** and ten minima for (7*S*,15*R*)-**1** within the final energy threshold (10 kJ mol^{-1} at the B97M-V/6-31G(d) level). ^{13}C-NMR chemical shifts were then calculated with the GIAO method at the B3LYP/6-31G(d) level. An empirical correction was applied to each molecule depending on the number of bonds to the carbon and on the bond lengths (Hehre *et al.*, 2019). ^3J coupling constants were determined as Boltzmann averages of all the DFT structures described above, either with Karplus equations or at B3LYP/pcJ-0 levels (Fermi contact term only).

Leaf puncture assays

Leaves of *Phaseolus vulgaris* L, *Juglans regia* L. and *Quercus suber* L. were used for this assay, and each compound was tested at 1.0 mg mL^{-1}. The assays were performed as previously reported (Andolfi *et al.*, 2014), and each treatment was repeated three times. Leaves were observed daily and scored for symptoms after 5 d. The effects of the toxins on the leaves were observed up to 10 d . Lesions were estimated using APS Assess 2.0 software following the tutorials in the user's manual. Lesion size was expressed in mm^2.

Antifungal assays

All compounds (**1**-**6**) were preliminarily tested on four different plant pathogens including the two fungi (*Athelia rolfsii* and *D. corticola*) and the two oomycetes (*Phytophthora cambivora* and *P. lacustris*). The sensitivity of all four species to these compounds was evaluated, depending on the species, on carrot agar (CA) or potato dextrose agar (PDA), as inhibition of the mycelium radial growth. The assays were performed as previously reported (Masi *et al.*, 2016). Each metabolite was tested at 200 µg per plug. Methanol was used as negative controls. Metalaxyl-M (mefenoxam; p.a. 43.88%; Syngenta), a synthetic fungicide to which the oomycetes are sensitive, and PCNB (pentachloronitrobenzene) for ascomycetes and basidiomycetes, were used as positive controls. Each treatment consisted of three replicates, and the experiment was repeated two times

Artemia salina *bioassays*

All compounds were assayed on brine shrimp larvae (*Artemia salina* L.). The assay was performed in cell culture plates with 24 cells (Corning) as previously described (Andolfi *et al.*, 2014). The metabolites were tested at 100 mg mL^{-1}. Tests were performed in quadruplicate. The proportions (%) of larval mortality was determined after 36 h incubation at 27°C in the dark.

RESULTS AND DISCUSSION

The organic extract obtained from filtrates of *D. olivarum* culture grown on Czapek medium was purified to yield a new *nor*-diterpenoid cleistanthane (**1**; Figure 2), named here as olicleistanone, together with two known pimarane diterpenoids identified as sphaeropsidins A and C (respectively **2** and **3**; Figure 2), and two known *nor*-pimarane diterpenoids identified as sphaeropsidin G and diplopimarane (respectively, **4** and **5**; Figure 2). When the fungus was grown on mineral salt medium it produced (-)-mellein (**6**; Figure 2), sphaeropsidin A (**2**) and low amounts of sphaeropsidin G (**4**) and diplopimarane (**5**).

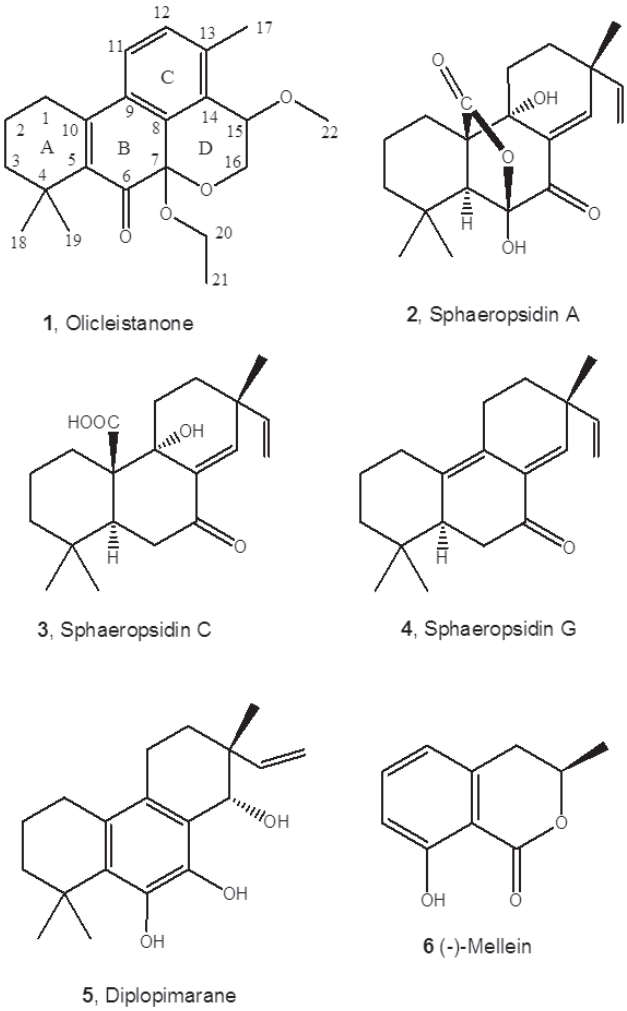

Figure 2. Structures of olicleistanone (**1**), sphaeropsidins A, C and G (**2**, **3** and **4**), diplopimarane (**5**) and (-)-mellein (**6**).

The known compounds (**2** to **6**) were identified comparing their physical (specific optical rotation) and spectroscopic data (^{1}H NMR and ESIMS) with those previously reported (Evidente *et al.*, 1996; Evidente *et al.*, 1997; Evidente *et al.*, 2010; Andolfi *et al.*, 2014; Abou-Mansour *et al.*, 2015; Cimmino *et al.*, 2016; Cimmino *et al.* 2017b; Masi *et al.*, 2018; Masi *et al.*, 2020).

Olicleistanone (**1**) has a molecular formula of $C_{22}H_{28}O_4$, as deduced from its HR ESIMS spectrum and consistent with nine hydrogen deficiencies. Preliminary investigation of its ^{1}H and ^{13}C NMR spectra (Table 1) showed that the compound is closely related to a tricyclic *nor*-diterpenoid, with aromatized and cyclohexadiene rings (C and B) joined to a dihydropyran ring (D) generated probably from a cleistanthane carbon skeleton (Devappa *et al.*, 2011). The signal at δ 195.5 in the ^{13}C NMR spectrum also showed the presence of a conjugated ketone group (Breitmaier and Voelter, 1987). These results are in full agreement with the bands typical for carbonyl and aromatic groups observed in the IR spectrum (Najkanishi and Solomns 1977) and the absorption maxima observed in the UV spectrum (Pretsch *et al.*, 2000).

The ^{1}H and COSY spectra (Berger and Braun, 2004) of olicleistanone (**1**) showed the presence of the typical signals of two *ortho*-coupled protons (H-11 and H-12) of a 1,2,3,4-tetrasubstituted C benzene ring, and the singlets of a methoxy group (CH_3-22), a vinyl methyl (CH_3-17) and two methyls (CH_3-19 and CH_3-18) bonded to a quaternary carbon. The two methyls represent the head of the geranylgeranyl biosynthetic precursor which generated the diterpenoid cleistanthane carbon skeleton. The same spectra showed the signal of an ethoxy group. A signal pattern due to pyran moiety (ring D) of the benzohydropyran system (C and D rings) appeared as an ABC system. The spectra also showed a signal typical of the three adjacent methylene groups (CH_2-1, CH_2-2 and CH_2-3) of the A ring (Pretsch *et al.*, 2000).

The correlations observed in the HSQC spectrum (Berger and Braun, 2004) allowed the chemical shifts to be assigned to the protonated carbons, as reported in Table 1 (Breitmaier and Voelter, 1987).

The long range couplings observed in the HMBC spectrum (Berger and Braun, 2004) (Table 1) allowed the quaternary carbons to be assigned. The signals at δ 34.0 correlated with H_2-2, H_2-3, H_3-18 and H_3-19 and were assigned to C-4, at 136.4 with H_2-1, H_2-3, H_3-18 and H_3-19 and assigned to C-5, at 195.5 with H_2-1 and assigned to C-6, at 92.3 with H-15, H_2-16 and H-20A and assigned to C-7, at 130.6 with H-12 and H_3-17 and assigned to C-8, at 146.1 with H_2-1, H_2-2, H-11 and assigned to C-10, at 138.7 with H-11 and H_3-17 and assigned to C-13, and at 130.2 with H-12, H-15 and H_2-16 and assigned to C-14. The remaining signal at δ 132.9 was assigned to C-9 (Breitmaier and Voelter, 1987). The correlation between C-7 and H-20A allowed the ethoxy group to be located at C-7 and consequently the methoxy group at C-15. Ethoxy groups are relatively rare in natural products, but not unprecedented, including several ethoxy-containing ketals like **1** (Wang *et al.*, 2006; Lim *et al.*, 2013; Xiong *et al.*, 2015; Shen *et al.*, 2015; Zhang *et al.*, 2016). We avoided the use of ethanol during the extraction or purification process, which could lead to **1** as an artifact (Maltese *et al.*, 2009; Capon, 2020).

Thus, the chemical shifts were assigned to all the carbons and the corresponding protons, which are reported in Table 1, and olicleistanone (**1**) was formulated as 4-ethoxy-6a-methoxy-3,8,8-trimethyl-4,5,8,9,10,11-hexahydrodibenzo[*de*,*g*]chromen-7(6a*H*)-one.

Table 1. ^{1}H and ^{13}C NMR and HMBC data for olicleistanone (**1**)[a,b].

Position	δ_C[c]	δ_H (*J* in Hz)	HMBC
1	27.4 t	2.77 (1H) dt (18.8, 6.1) 2.47 (1H) ddd (18.8, 12.2, 6.6)	H_2-2, H_2-3
2	18.6 t	1.80 m (2H)	H_2-1
3	40.5 t	1.62 (1H) m 1.49 (1H) m	H_2-1, H_2-2, H_3-18, H_3-19
4	34.0 s		H_2-2, H_2-3, H_3-18, H_3-19
5	136.4 s		H_2-1, H_2-3, H_3-18, H_3-19
6	195.5 s		H_2-1
7	92.3 s		H-15, H_2-16, H-20A
8	130.6 s		H-12, H_3-17
9	132.9 s		
10	146.1 s		H_2-1, H_2-2, H-11
11	125.0 d	7.31 (1H) d (7.9)	
12	131.3 d	7.18 (1H) d (7.9)	
13	138.7 s		H-11, H_3-17
14	130.2 s		H-12, H-15, H_2-16
15	69.5 d	4.20 (1H) d (3.3)[e]	H_2-16, H_3-22
16	60.5 t	4.22 (1H) dd (12.7, 3.3)[e] 4.41 (1H) d (12.7)	H-15
17	18.4 q	2.34 (3H) s	H-12
18[d]	27.7 q	1.23 (3H) s	H_3-19
19[d]	29.7 q	1.36 (3H) s	H_3-18
20	59.0 t	3.33 (1H) dq (14.2, 7.0) 3.64 (1H) dq (14.2, 7.0)	H_3-21
21	15.4 q	1.14 (3H) t (7.0)	
22	55.7 q	3.38 (3H) s	H-15

[a] 2D ^{1}H, ^{1}H (COSY) and ^{13}C, ^{1}H (HSQC) NMR experiments confirmed the correlations of all the protons and the corresponding carbons.
[b] Coupling constants (*J*) are given in parenthesis.
[c] Multiplicities were assigned with DEPT.
[d] These signals could be exchanged.
[e] These two signals are in part overlapped.

The structure assigned to **1** was supported by the other HMBC couplings reported in Table 1 and from the data of its HR ESIMS spectrum which showed the sodium dimer $[2M+Na]^+$, the potassium $[M+K]^+$ and the sodium $[M+Na]^+$ adducts at *m/z*: 735, 395, 379.1876. The significant ion $[M+H\text{-}CH_3CH_2OH]^+$ observed at *m/z* 311 was probably generated from a pseudo-molecular ion by loss of ethanol.

Attempts to assign the relative configuration of **1** were made recording a NOESY spectrum. The measured NOESY correlations are reported in Table 2, but since there is no clear correlation between the protons of the methoxy and ethoxy groups, these data alone were not sufficient to assign the relative configuration of the two chiral centres (C-7 and C-15). To better interpret

Table 2. NOESY data for olicleistanone (**1**).

Irradiated	Observed	Irradiated	Observed
H-11	H_2-1	OMe	H_3-17
H_2-20	H_3-21	H_3-18	H_2-20
H-15	H_3-17, OMe		

Table 3. Experimental and calculated $^{3}J_{HH}$ values (Hz) for olicleistanone (**1**)[a].

Experimental		Calculated (Karplus)	Calculated (DFT)	Calculated (Karplus)	Calculated (DFT)
		(7*S*,15*S*)-**1**		(7*S*,15*R*)-**1**	
H-15/H-16a	3.3	3.14	4.05	7.24	9.26
H-15/H-16b	n.d.	0.89	0.70	7.81	8.63

[a] *J* values calculated either by a Karplus curve or by DFT at B3LYP/pcJ-0 level in vacuo, as Boltzmann average of all structures obtained by DFT geometry optimization (see text).
n.d.: Not detected.

NMR data, a molecular modelling study was undertaken. First, two diastereomeric structures (7*S*,15*S*)-**1** and (7*S*,15*R*)-**1** were generated and their possible conformations were explored by means of a conformational search with molecular mechanics (Merck molecular force field, MMFF). Geometry optimizations were then run with the density functional method (DFT) at the B97M-V/6-311+G(2df,2p)//B3LYP/6-31G(d) level, using the computational protocol for the prediction of ^{13}C chemical shifts of flexible compounds, developed by Hehre *et al.* (2019). For the two diastereomers, six or ten conformers were found with detectable populations at room temperature. The various conformers differed in the conformation of the methoxy and ethoxy groups, but also in the puckering of ring A. A clear difference between the two diastereomers was the orientation of H-15, which was predominantly pseudo-equatorial in (7*S*,15*S*)-**1** and pseudo-axial (7*S*,15*R*)-**1**. Thus, we presumed that the coupling constants between H-15 and H-16a/H-16b could be used to discriminate between the two isomers. Experimentally, H-15 appears as a doublet with splitting of 3.3 Hz, meaning that one $J_{15/16}$ was small (3.3 Hz) and the other was negligible. This agreed with a pseudo-equatorial orientation. $^{3}J_{15/16}$ were then estimated with Karplus curve and spin-spin coupling calculations at B3LYP/pcJ-0 level. These results are shown in Table 3, and strongly support the assignment of **1** as (7*S**,15*S**)-**1**. ^{13}C-NMR calculations were then run at the B3LYP/6-31G(d) level. The estimated root-mean-square (rms) error between experimental and calculated ^{13}C chemical shifts was acceptable (2.4–2.5)

but similar for both isomers, confirming the (7*S**,15*S**)-**1** assignment but without further supporting it. Nevertheless, we consider that the argument based on *J*-couplings is accurate enough to assign the relative configuration.

For the absolute configuration, the ECD spectrum of a solution of **1** in acetonitrile (1 mM, 0.01 cm cell) was measured. The ECD spectrum was not distinguishable from the baseline over the whole range (185-400 nm, data not shown), despite the optimal absorption (0.3 to 0.8 for the absorption peaks). It therefore must be concluded that the isolated sample of **1** was a racemate. Racemic natural products are rare, and are thought to result from nonenzymatic reactions (Zask and Ellestad, 2018). The chirality centre at C-7 of **1** is a tertiary benzylic carbon in α position to carbonyl group and it is therefore easily subject to racemization. However, racemization of this centre does not occur in a post-synthetic step, otherwise two diastereomers would be obtained. On the other hand, the isolated (7*S*,15*S*)-**1** isomer was more stable than its (7*S*,15*R*) diastereomer by about 2 kcal mol^{-1} at the present level of calculation, suggesting that if the chiral centre at C-15 was biosynthesized in a later step than C-7, its configuration would be dictated by that at C-7.

All metabolites (**1** to **6**) isolated in this study were screened for phytotoxic, antifungal, antioomycete and zootoxic activities.

Except for compound **2**, phytotoxicity was not detected for any of the metabolites (at 1 mg mL^{-1}) when applied to leaves of *Phaseolus vulgaris*, *Quercus suber*, or *Juglans regia*. Sphaeropsidin A (**2**) caused necrotic lesions on leaves of all the plant species tested, with mean lesion sizes of 75.6 mm^2 on *P. vulgaris*, 163.3 mm^2 on *J. regia* and 15.1 mm^2 on *Q. suber*.

In the assays of antifungal activity, sphaeropsidin A (**2**) inhibited mycelium growth of all the plant pathogens tested (100% inhibition rate). Diplopimarane (**4**) completely inhibited growth of *Athelia rolfsii* and partially inhibited growth of *D. corticola*, *P. cambivora* and *P. lacustris*, inhibition from 56% to 75%. No colony growth inhibition was observed for the other four metabolites at the concentration used.

In the brine shrimp larvae bioassay, which is widely used for toxicology and ecotoxicology studies, compounds **1**, **4** and **6** (at 100 μg mL^{-1}) caused 100% larval mortality. Compound **2** caused 51% larval mortality, and compounds **3** and **5** were inactive.

Cleistanthane-type diterpenoids are produced by different fungi and plants, but few examples of cleistanthane *nor*-diterpenoids are reported. Among them there are aspergiloids A, B, F and G isolated from the fermentation broth extract of *Aspergillus* sp. YXf3, an endophytic fungus from *Ginkgo biloba*. However, no biological activities have been reported for these compounds (Guo *et al*., 2012; Yan *et al*., 2013).

Sphaeropsidin A, C and G, as well as B, D, E and F, previously isolated from *D. cupressi, D. mutila* (Sparapano *et al*., 2004), and *D. corticola* (Masi *et al*., 2018), belong to the group of tricyclic and tetracyclic unarranged pimarane diterpenoids, which are well-known fungus and plant metabolites (Reveglia *et al*., 2018). Smardesines and chenopodolins also belong to this group of compounds. These cytotoxic and phytotoxic metabolites were isolated from *Smardaea* sp. AZ0432 living in the moss *Ceratodon purpureus* (Wang *et al*., 2011), and from *Phoma chenopodiicola*, a fungus proposed for biocontrol of the weed plant *Chenopodoium album* (Cimmino *et al*., 2013; Evidente *et al*., 2015). Sphaeropsidin A and its 6-*O*-acetyl derivative also showed antimicrobial (Evidente *et al*., 2011) and anticancer activity (Lallemand *et al*., 2012; Ingels *et al*., 2017; Masi *et al*., 2018).

Melleins are 3,4-dihydroisocoumarins, which are produced by many fungi of various genera as well as plants, insects and bacteria. These compounds have several phytotoxic, zootoxic and antifungal effects (Reveglia *et al*., 2020). (-)-Mellein was toxic on grapevine leaves and grapevine calli (Djoukeng *et al*., 2009; Ramirez-Suero *et al*., 2014, Masi *et al*., 2018), and was detected in symptomatic and asymptomatic grapevine wood samples and green shoots (Djoukeng *et al*., 2009) from plants with Botryosphaeria dieback and leaf stripe. The role of this compound in pathogenesis was investigated by examining the extent to which it caused expression of defense-related genes in grapevine calli (Ramirez-Suero *et al*., 2014). Recently, (-)-mellein was also identified as a metabolite of *Lasiodiplodia euphorbiaceicola* during screening of phytotoxic metabolites isolated from *Lasiodiplodia* spp. infecting grapevine in Brazil (Cimmino *et al*., 2017b), and from *Sardiniella urbana*, a pathogen from declining European hackberry trees in Italy (Cimmino *et al.,* 2019).

It is well known that fungal phytotoxins are closely related to host plant interactions. These compounds play key roles inducing virulence and pathogenicity of fungi. The host/pathogen interaction is the first process of the complex mechanism of infection. Fungal pathogens produce enzymes to degrade host wood cell walls, and the fungal toxins penetrate vessels and metabolize dead host tissues. The toxins then translocate to branches and leaves distant from the infection points, inducing chlorosis and necrosis (Durbin *et al*., 1989; Ballio, 1991; Möbius and Hertweck 2009; Keller, 2019). Thus, the phytotoxicity of *D. olivarum* was probably due to production of sphaeropsidin A (**2**), as outlined in the present study.

Phytotoxins have also been shown to possess herbicidal, antimicrobial and insecticidal activities (Spara-

pano *et al*. 2004; Evidente *et al*. 2011; Cimmino *et al*. 2015; Barilli *et al*., 2017; Aznar *et al*. 2019). Drug-based phytotoxins can also be used in medicine against some important human diseases, such as cancer, malaria, dengue and yellow fevers, and against fungal and bacterial infections (Bajsa *et al*., 2007; Evidente *et al*., 2014, Masi *et al*. 2017; Masi *et al*., 2018; Roscetto *et al*., 2020). Some of these toxins could also be produced in industrial large scale, and be formulated for applications in agriculture and medicine. Among the toxins previously isolated, and also from *D. olivarum*, sphaeropsidin A (**2**) is a phytotoxin with strong potential for drug development (Ingles *et al*., 2017; Masi *et al*., 2018; Roscetto *et al*., 2020).

In conclusion, this study was the first to investigate secondary metabolites produced by *D. olivarum*, an emerging pathogen of forest trees in the Mediterranean region. The results confirm that *Botryosphaeriaceae* are sources of bioactive secondary metabolites, some of which have potential for applications in biotechnology sectors.

Among the metabolites produced *in vitro* by *D. olivarum*, sphaeropsidin A and diplopimarane inhibited vegetative growth of four plant pathogens belonging to different phyla. Additionally, the strong activity of the newly identified metabolite, olicleistanone (**1**), against *A. salina* deserves detailed investigation, because several applications of *A. salina* in toxicology and ecotoxicology continue to be widely used.

ACKNOWLEDGEMENTS

This study was partially supported by the "Fondo di Ateneo per la ricerca 2019", internal funding provided by the University of Sassari. Antonio Evidente is associated with the Istituto di Chimica Biomolecolare del CNR, Pozzuoli, Italy.

SUPPORTING INFORMATION

1D and 2D NMR data for **1** and HRESI-MS spectra of **1**-**3**.

LITERATURE CITED

Abou-Mansour E., Débieux J.L., Ramírez-Suero M., Bénard-Gellon M., Magnin-Robert M., … Serrano M., 2015. Phytotoxic metabolites from *Neofusicoccum parvum*, a pathogen of Botryosphaeria dieback of grapevine. *Phytochemistry* 115: 207–215.

Adamson K., Klavina D., Drenkhan R., Gaitnieks T., Hanso M., 2015. *Diplodia sapinea* is colonizing the native Scots pine (*Pinus sylvestris*) in the northern Baltics. *The European Journal of Plant Pathology* 143: 343–350.

Alves A., Linaldeddu B.T., Deidda A., Franceschini A., 2014. The complex of *Diplodia* specie associated with *Fraxinus* and some other woody hosts in Italy and Portugal. *Fungal Diversity* 67: 143–156.

Andolfi A., Maddau L., Basso S., Linaldeddu B.T., Cimmino A., … Evidente A., 2014. Diplopimarane, a 20-*nor*-*ent*-pimarane produced by the oak pathogen *Diplodia quercivora*. *Journal of Natural Products* 77: 2352–236.

Aznar-Fernández T., Cimmino A., Masi M., Rubiales D., Evidente A. 2019. Antifeedant activity of long-chain alcohols, and fungal and plant metabolites against pea aphid (*Acyrthosiphon pisum*) as potential biocontrol strategy. *Natural Product Research*, 33: 2471–2479.

Bajsa J., Singh K., Nanayakkara D., Duke S.O., Rimando A.M., Evidente A., Tekwani B.L. 2007. A survey of synthetic and natural phytotoxic compounds and phytoalexins as potential antimalarial compounds. *Biological and Pharmaceutical Bulletin*, 30: 1740–1744.

Ballio, A. 1991. Non-host-selective fungal phytotoxins: biochemical aspects of their mode of action. *Experientia* 47: 783–790.

Barilli E., Cimmino A., Masi M., Evidente M., Rubiales D., Evidente A. 2017. Inhibition of early development stages of rust fungi by the two fungal metabolites cyclopaldic acid and *epi*-epoformin. *Pest Management Science* 73: 1161–1168.

Berger S., Braun S., 2004. *200 and More Basic NMR Experiments: A Practical Course*. 1st ed. Wiley-VCH, Weinheim, Germany, 418 pp.

Breitmaier E., Voelter W., 1987. *Carbon-13 NMR Spectroscopy*. VCH, Weinheim, Germany, 183–280.

Capon, R., 2020. Extracting value: mechanistic insights into the formation of natural product artifacts–case studies in marine natural products. *Natural Product Reports* 37: 55–79

Cimmino A., Andolfi A., Zonno M.C., Avolio F., Santini A., … Evidente A., 2013. Chenopodolin: a phytotoxic unrearranged *ent*-pimaradiene diterpene produced by *Phoma chenopodicola*, a fungal pathogen for *Chenopodium album* biocontrol. *Journal of Natural Products* 76, 1291–1297.

Cimmino A., Masi M., Evidente M., Superchi S., Evidente, A. 2015. Fungal phytotoxins with potential herbicidal activity: chemical and biological characterization. *Natural Product Reports* 32: 1629–1653.

Cimmino A., Maddau L., Masi M., Evidente M., Linaldeddu B.T., Evidente A., 2016. Further secondary metabolites produced by *Diplodia corticola*, a fungal pathogen involved in cork oak decline. *Tetrahedron* 72: 6788–6793.

Cimmino A., Maddau L., Masi M., Linaldeddu B.T., Pescitelli G., Evidente A., 2017a. Fraxitoxin, a new isochromanone isolated from *Diplodia fraxini*. *Chemistry &. Biodiversity* 14: e1700325.

Cimmino A., Cinelli T., Masi M., Reveglia P., da Silva M.A., … Evidente A., 2017b. Phytotoxic lipophilic metabolites produced by grapevine strains of *Lasiodiplodia* species in Brazil. *Journal of Agricultural and Food Chemistry* 65: 1102–1107.

Cimmino A., Maddau L., Masi M., Linaldeddu B.T., Evidente A., 2019. Secondary metabolites produced by *Sardiniella urbana*, a new emerging pathogen on European hackberry. *Natural Product Research* 33: 1862–1869.

Devappa R.K., Makkar H.P., Becker K., 2011. Jatropha diterpenes: a review. *Journal of the American Oil Chemists' Society* 88: 301–322.

Djoukeng J.D., Polli S., Larignon P., Abou-Mansour E., 2009. Identification of phytotoxins from *Botryosphaeria obtusa*, a pathogen of 525 black dead arm disease of grapevine. *European Journal of Plant Pathology* 124: 303–308.

Durbin R.D., Ballio A., Graniti A., 1989. *Phytotoxins and Plant Pathogenesis*. Nato ASI Subseries H, Vol. 27, Springer-Verlag, Heidelberg, Germany, 508 pp.

Evidente A., Sparapano L., Motta A., Giordano F., Fierro O., Frisullo S., 1996. A phytotoxic pimarane diterpene of *Sphaeropsis sapinea* f. sp. *cupressi*, the pathogen of a canker disease of cypress. *Phytochemistry* 42: 1541–1546.

Evidente A., Sparapano L., Fierro O., Bruno G., Giordano F., Motta A., 1997. Sphaeropsidins B and C, phytotoxic pimarane diterpenes from *Sphaeropsis sapinea* f. sp. *cupressi* and *Diplodia mutila*. *Phytochemistry* 45: 705–713.

Evidente A., Punzo B., Andolfi A., Cimmino A., Melck D., Luque J., 2010. Lipophilic phytotoxins produced by *Neofusicoccum parvum*, a grapevine canker agent. *Phytopathologia Mediterranea* 49: 74–79.

Evidente A., Venturi V., Masi M., Degrassi G., Cimmino A., … Andolfi A., 2011. *In vitro* antibacterial activity of sphaeropsidins and chemical derivatives toward *Xanthomonas oryzae* pv. *oryzae*, the causal agent of rice bacterial blight. *Journal of Natural Products* 74: 2520–2525.

Evidente A., Masi M., Linaldeddu B.T., Franceschini A., Scanu B., … Maddau, L. 2012. Afritoxinones A and B, dihydrofuropyran-2-ones produced by *Diplodia africana* the causal agent of branch dieback on *Juniperus phoenicea*. *Phytochemistry* 77: 245–250.

Evidente A., Kornienko A., Cimmino A., Andolfi A., Lefranc F., … Kiss R. 2014. Fungal metabolites with anticancer activity. *Natural Product Reports* 31: 617–627.

Evidente M., Cimmino A., Zonno M.C., Masi M., Berestetskyi A., … Evidente A., 2015. Phytotoxins produced by *Phoma chenopodiicola*, a fungal pathogen of *Chenopodium album*. *Phytochemistry* 117: 482–488.

Granata G., Faedda R., Sidoti A., 2011. First report of canker caused by *Diplodia olivarum* on carob tree in Italy. *Plant Disease* 100: 2483–2491.

Guo Z.K., Yan T., Guo Y., Song Y.C., Jiao R.H., … Ge H.M., 2012. *p*-Terphenyl and diterpenoid metabolites from endophytic *Aspergillus* sp. YXf3. *Journal of Natural Products* 75: 15–21.

Hehre W., Klunzinger P., Deppmeier B., Driessen A., Uchida N., … Takata Y., 2019. Efficient protocol for accurately calculating ^{13}C chemical shifts of conformationally flexible natural products: scope, assessment, and limitations. *Journal of Natural Products* 82: 2299–2306.

Ingels A., Dinhof C., Garg A.D., Maddau L., Masi M., … Mathieu V., 2017. Computed determination of the *in vitro* optimal chemocombinations of sphaeropsidin A with chemotherapeutic agents to combat melanomas. *Cancer Chemotherapy and Pharmacology* 79: 971–983.

Lallemand B., Masi M., Maddau L., De Lorenzi M., Dam R., … Evidente A., 2012. Evaluation of *in vitro* anticancer activity of sphaeropsidins A–C, fungal rearranged pimarane diterpenes, and semisynthetic derivatives. *Phytochemistry Letters* 5: 770–775.

Lazzizera C., Frisullo S., Alves A., Lopes J., Phillips A.J.L., 2008. Phylogeny and morphology of *Diplodia* species on olives in southern Italy and description of *Diplodia olivarum* sp. nov. *Fungal Diversity* 31: 63–71.

Lim S.H., Low Y.Y., Subramaniam G., Abdullah Z.; Thomas N.F., Kam T.S., 2013. Lumusidines A–D and villalstonidine F, macroline–macroline and macroline–pleiocarpamine bisindole alkaloids from *Alstonia macrophylla*. *Phytochemistry* 87: 148–156.

Linaldeddu B.T., Maddau L., Franceschini A., Alves A., Phillips A.J.L., 2016. *Botryosphaeriaceae* species associated with lentisk dieback in Italy and description of *Diplodia insularis* sp. nov. *Mycosphere* 7: 962–977.

Lopes A., Linaldeddu B.T., Phillips A.J.L., Alves A., 2018. Mating type gene analyses in the genus *Diplodia*: from cryptic sex to cryptic species. *Fungal Biology* 122: 629–638.

Keller N.P. 2019. Fungal secondary metabolism: Regulation, function and drug discovery. *Nature Review Microbiology* 17: 167–180.

Maltese F., van der Kooy F., Verpoorte R. 2009. Solvent derived artifacts in natural products chemistry. *Natural Product Communication* 4: 447–454.

Manca D., Bregant C., Maddau L., Pinna C., Montecchio L., Linaldeddu B.T., 2020. First report of canker and dieback caused by *Neofusicoccum parvum* and *Diplodia olivarum* on oleaster in Italy. *Italian Journal of Mycology* 49: 85–91.

Martin D.K.H., Turcotte R.M., Miller T.M., Munck I.A., Aćimović S.G., … Kasson M.T., 2017. First report of *Diplodia corticola* causing stem cankers and associated vascular occlusion of northern red oak (*Quercus rubra*) in West Virginia. *Plant Disease* 101: 380.

Masi M., Maddau L., Linaldeddu B.T.; Cimmino A., D'Amico W., … Evidente A., 2016. Bioactive secondary metabolites produced by the oak pathogen *Diplodia corticola*. *Journal of Agricultural and Food Chemistry* 64: 217–225.

Masi M., Cimmino A., Tabanca N., Becnel J.J., Bloomquist J.R., Evidente A. 2017. A survey of bacterial, fungal and plant metabolites against *Aedes aegypti* (Diptera: Culicidae), the vector of yellow and dengue fevers and Zika virus. *Open Chemistry* 15: 156–166.

Masi M., Maddau L., Linaldeddu B.T., Scanu B., Evidente A., Cimmino A., 2018. Bioactive metabolites from pathogenic and endophytic fungi of forest trees. *Current Medicinal Chemistry* 25: 208–252.

Masi M., Aloi F., Nocera P., Cacciola S.O., Surico G., Evidente A., 2020. Phytotoxic metabolites isolated from *Neufusicoccum batangarum*, the causal agent of the scabby canker of cactus pear (*Opuntia ficus-indica* L.). *Toxins* 12: 126.

Mőbius N., Hertweck C. 2009. Fungal phytotoxins as mediators of virulence. *Current Opinion in Plant Biology* 12: 390–398.

Nakanishi K., Solomon P.H., 1977. *Infrared Absorption Spectroscopy*. 2nd ed. Holden Day, Oakland, California, USA, 17–44.

Pérez C., Wingfield M., Slippers B., Altier N., Blanchette R., 2010. Endophytic and canker-associated *Botryosphaeriaceae* occurring on non-native *Eucalyptus* and native *Myrtaceae* trees in Uruguay. *Fungal Diversity* 41: 53–69.

Pinkerton F., Strobel G., 1976. Serinol as an activator of toxin production in attenuated cultures of *Helminthosporium sacchari*. *PNAS* 73: 4007–4011.

Pretsch E., Bühlmann P., Affolter C., 2000. *Structure Determination of Organic Compounds – Tables of Spectral Data*. 3rd ed. Springer-Verlag: Berlin, Germany, 161–243.

Ramírez-Suero M., Bénard-Gellon M., Chong J., Lalou, H., Stempien E., … Bertsch, C., 2014. Extracellular compounds produced by fungi associated with Botryosphaeria dieback induce differential defence gene expression patterns and necrosis in *Vitis vinifera* cv. Chardonnay cells. *Protoplasma* 251: 1417–1426.

Reveglia P., Cimmino A., Masi M., Nocera P., Berova N., … Evidente, A., 2018. Pimarane diterpenes: Natural source, stereochemical configuration, and biological activity. *Chirality* 30: 1115–1134.

Reveglia P., Masi M., Evidente A., 2020. Melleins, intriguing natural compounds. *Biomolecules* 10: 772.

Roscetto E., Masi M., Esposito M., Di Lecce R., Delicato A., Maddau L., ... Catania M.R. 2020. Anti-biofilm activity of the fungal phytotoxin sphaeropsidin A against clinical isolates of antibiotic-resistant bacteria. *Toxins*, 12: 444.

Shen C.P., Luo J.G., Yang M.H., Kong L.Y. 2015. A pair of novel 2,3-seco cafestol-type diterpenoid epimers from the twigs of *Tricalysia fruticosa*. *Tetrahedron Letters* 56: 1328–1331.

Sparapano L., Bruno G., Fierro O., Evidente A., 2004. Studies on structure–activity relationship of sphaeropsidins A-F, phytotoxins produced by *Sphaeropsis sapinea* f. sp. *cupressi*. *Phytochemistry* 65: 189–198.

Wang H.; Wu F.H.; Xiong F.; Wu J. J.; Zhang L.Y.; … Zhao, S.X., 2006. Iridoids from *Neopicrorhiza scrophulariiflora* and their hepatoprotective activities in vitro. *Chemical and Pharmaceutical Bulletin* 54: 1144–1149.

Wang X.N., Bashyal B.P., Wijeratne E.K., U'Ren J.M., Liu M.X., … Gunatilaka, A.L., 2011. Smardaesidins A–G, isopimarane and 20-*nor*-isopimarane diterpenoids from *Smardaea* sp., a fungal endophyte of the moss *Ceratodon purpureus*. *Journal of Natural Products* 74: 2052–2061.

Xiong L., Zhou Q.M., Zou Y., Chen M.H., Guo L., … Peng C., 2015. Leonuketal, a spiroketal diterpenoid from *Leonurus japonicus*. *Organic Letters* 17: 6238–6241.

Yan, T., Guo, Z.K., Jiang, R., Wei, W., Wang, T., … Ge, H.M., 2013. New flavonol and diterpenoids from the endophytic fungus *Aspergillus* sp. YXf3. *Planta Medica* 79: 348–352.

Zask A., Ellestad G., 2018. Biomimetic syntheses of racemic natural products. *Chirality* 30: 157–164.

Zhang P., Tang C., Yao S., Ke C., Lin G., … Ye, Y., 2016. Cassane diterpenoids from the pericarps of *Caesalpinia bonduc*. *Journal of Natural Products* 79: 24–29.

Phytopathologia Mediterranea
The international journal of the
Mediterranean Phytopathological Union

Firenze University Press
www.fupress.com/pm

Research Papers

Antifungal activity of hydroxytyrosol enriched extracts from olive mill waste against *Verticillium dahliae*, the cause of Verticillium wilt of olive

Mounira Inas DRAIS[1,*], Elisa PANNUCCI[1], Rocco CARACCIOLO[1], Roberta BERNINI[1], Annalisa ROMANI[2], Luca SANTI[1], Leonardo VARVARO[1,*]

[1] *Department of Agriculture and Forest Sciences, University of Tuscia, Via S. Camillo de Lellis snc, Viterbo, Italy*
[2] *Department of Statistics, Computing, Applications "Giuseppe Parenti" DiSIA, PHYTO-LAB (Pharmaceutical, Cosmetic, Food supplement Technology and Analysis), University of Florence, Florence, Italy*
*Corresponding authors. E-mail: drais@unitus.it, varvaro@unitus.it

OPEN ACCESS

Citation: M. I. Drais, E. Pannucci, R. Caracciolo, R. Bernini, A. Romani, L. Santi, L. Varvaro (2021) Antifungal activity of hydroxytyrosol enriched extracts from olive mill waste against *Verticillium dahliae*, the cause of Verticillium wilt of olive. *Phytopathologia Mediterranea* 60(1): 139-147. doi: 10.36253/phyto-12019

Accepted: January 5, 2021

Published: May 15, 2021

Data Availability Statement: All relevant data are within the paper and its Supporting Information files.

Competing Interests: The Author(s) declare(s) no conflict of interest.

Editor: Epaminondas Paplomatas, Agricultural University of Athens, Greece.

Summary. Verticillium wilt (caused by *Verticillium dahliae* Kleb.) is an important disease affecting olive (*Olea europaea* L.) production. Effective control of this disease relies on integrated management strategies. *In vitro* antifungal activity of two hydroxytyrosol (HTyr) enriched extracts (HTE1 and HTE2) obtained from olive mill waste products (OMWP) was assessed against *V. dahliae*. Inhibitory effects of pure HTyr as a standard, and HTE1 and HTE2 at different concentrations, were evaluated on mycelium growth and conidium germination of *V. dahliae*. Chemical characterization of HTE1 and HTE2 allowed identification and quantification of HTyr as the main constituent in both extracts along with other low molecular weight phenols. HTE1 showed a higher inhibitory activity in both growth and conidium germination of *V. dahliae*. At the tested concentrations, low antifungal effects of HTyr were observed. After 3 d, 1 mg mL^{-1} of HTE1 gave greater inhibition of mycelium growth than HTE2 or HTyr. After 24 h, HTE1 gave 55% inhibition of conidium germination, and HTyr and HTE2 both gave 37% inhibition. This study has demonstrated that phenolic compounds derived from OMWP have antifungal activity against *V. dahliae*, indicating the potential of these compounds for eco-friendly control of Verticillium wilt.

Keywords. *Olea europaea*, enriched extracts, phenolic compounds, fungus inhibition.

INTRODUCTION

Verticillium wilt, caused by *Verticillium dahliae*, severely affects olive trees (*Olea europaea* L.), causing economic losses due to plant death (Jiménez-Díaz *et al.*, 1998; López-Escudero and Mercado-Blanco, 2011). The soil-borne fungus is considered one of the most serious threats to olive fruit and

oil production, and the disease is widely distributed in all Mediterranean olive-growing regions (Jiménez-Díaz *et al*., 2012). Olive trees are highly sectored with direct vascular connections of specific roots and shoots (Lavee *et al*., 1996). *Verticillium dahliae* infects host plants through their roots, and colonizes vascular systems, blocking water flow and eventually inducing wilt symptoms (Van Alfen, 1989). This damage results in significant reductions of leaf transpiration, which lead to leaf chlorosis and defoliation. Severe attacks cause trees to eventually die.

Since no control measures have proved to be successful when individually employed, an integrated strategy is recommended for management of Verticillium wilt of olive (VWO) (López-Escudero and Mercado-Blanco, 2011). Several studies have reported the use of antagonistic microorganisms as biological control agents (BCAs) against *V. dahliae* in olive (Mercado-Blanco *et al*., 2004; Triki *et al*., 2012; Markakis *et al*., 2016; Varo *et al*., 2016; Mulero-Aparicio *et al*., 2019). In addition, natural compounds could be complementary for integrated eco-friendly management of this important disease.

Beside the well-known antifungal activity of plant derived essential oils, which has been demonstrated for *V. dahliae* (López-Escudero *et al*., 2007; Varo *et al*., 2017), other classes of natural products also hold promise for disease management. Phenolic compounds have demonstrated, in parallel with strong antioxidant activity, antimicrobial activity in general and antifungal activity in particular (Yangui *et al*., 2009; Pannucci *et al*., 2019). These compounds can be obtained from the waste products of olive oil production; the two most prominent of these compounds are oleuropein obtained from leaves, and hydroxytyrosol (HTyr) from drupes (Thielmann *et al*., 2017). For HTyr, recent studies have demonstrated bactericidal and fungicidal activities of olive mill waste products (OMWP) obtained by a proprietary, environmentally friendly membrane technology (Pannucci *et al*., 2019). Several studies have examined the phenolic components of OMWP for use as biopesticides for crop protection (Mekki *et al*., 2006a, 2006b, 2008; Yangui *et al*., 2008, 2010; Larif *et al*., 2013; Lykas *et al*., 2014). These components would also fulfil the criteria for a sustainable economic development (Romani *et al*., 2016; Bernini *et al*., 2017).

The present study evaluated the effectiveness of two HTyr-enriched extracts from OMWP against *V. dahlia* using pure HTyr as standard. *In vitro* inhibitory effects on mycelium growth and conidium germination of a *V. dahliae* isolate were assessed. The aim was to determine the potential for using these extracts as part of integrated management of VWO.

MATERIALS AND METHODS

Plant extracts

Two HTyr enriched extracts (HTE1 and HTE2) were used. HTE1 was obtained from olive oil waste water (from olive cultivars 'Coratina' and 'Leccino'), collected from Molfetta (Puglia, Italy; 41°31′42.8″N, 12°47′31.3″E) in January 2017, using a previously described procedure (Pizzichini *et al*., 2011; Romani *et al*., 2016; Bernini *et al*., 2017; Pannucci *et al*., 2019). HTE2 was prepared from olive pomace (from cultivar 'Leccino') from Catania (Sicily, Italy; 37°29′32″N, 15°4′13″E) in January 2017, using the following procedure (Romani *et al*., 2016; Bernini *et al*., 2017). After olive oil production, the olives were de-oiled and pitted to obtain a pulp. This material was acidified to pH = 2.5–4.0, and then extracted at room temperature with an aqueous solvent using an electrical pneumatic extractor. The resulting solution was filtered by microfiltration, ultrafiltration, and nanofiltration. After a reverse osmosis step, the resulting fraction was concentrated under vacuum by using a scraper evaporator series (C & G Depurazione Industriale Company) combined with a heat pump (Romani *et al*., 2016; Bernini *et al*., 2017).

Chemicals

All solvents and chemical used for extractions were of the highest analytical grade (Sigma-Aldrich). Pure HTyr used as standard in experiments was synthetized to purity >98%, using a proprietary procedure (Bernini *et al*., 2008; 2010).

Characterization of HTE1 and HTE2

HTE1 and HTE2 were characterized using High Performance Liquid Chromatography/Diode Array Detector (HPLC/DAD) and Nuclear Magnetic Resonance (^{1}H NMR), and the analytical profiles were compared with HTyr. The HPLC/DAD analyses were carried out using an HP 1200 liquid chromatograph (Agilent Technologies), equipped with an analytical column (Lichrosorb RP18 250 × 4.60 mm i.d, 5 μm; Merck). The eluents were H_2O adjusted to pH = 3.2 with HCOOH (solvent A) and CH_3CN (solvent B). A four-step linear solvent gradient was used, starting from 100% of solvent A up to 100% of solvent B, for 88 min at a flow rate of 0.8 mL min^{-1} (Romani *et al*., 2016; Bernini *et al*., 2017). Phenolic compounds found in the extracts were identified by comparing retention times and UV/Vis spectra with those of the

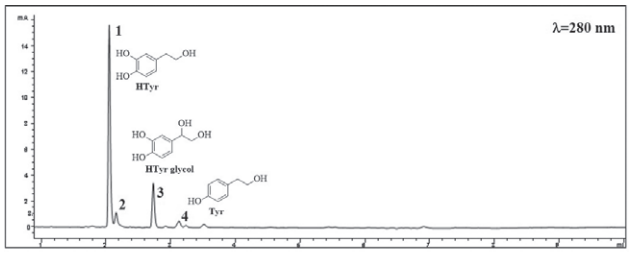

Compound	*mg/g*
(**1**) HTyr	115.24
(**3**) HTyr glycol	28.30
(**2**) and (**4**) Tyrosol and derivative	6.20
Total polyphenols	**149.74**

The results are the average of three replicates and the standard error is less than 2.5%

Figure 1. HPLC/DAD chromatographic profile of HTE2 at 280 nm.

authentic standards. Each compound was characterized using a five-point regression curve built with the available standards. Analytical data are reported in Figure 1.

^{1}H NMR spectra were recorded using a 400 MHz Nuclear Magnetic Resonance Spectrometer Avance III (Bruker). Chemical shifts were expressed in parts per million (δ scale) and referred to the residual protons of the solvent. Samples were prepared solubilizing 20-30 mg of each sample in methanol-d4. NMR spectra are shown in Figure 2.

Table 1. Fungi and strains used for the preliminary screening.

Fungi	Strain	Collection
Verticillium dahliae	VD22	Laboratory of plant pathology of DAFNE department, Tuscia University.
Botrytis cinerea	BC10	
Fusarium graminearum	3827	Laboratory of Plant pathology of the Department of Land, Environment, Agriculture and Forestry of Padova University.
Fusarium culmorum	5761	
Septoria tritici	MUCL 31967	
Bipolaris sorokiniana	DSMZ 62608	

Preliminary activity screening using HTyr against selected fungus isolates

Six fungus isolates were used (Table 1). Synthesized HTyr was used as standard for preliminary testing effects on the fungi, and to identify an active concentration of the compound to be used as reference for comparisons with HTE1 and HTE2. *Verticillium dahliae* and *B. sorokiniana* were inhibited by HTyr. The *V. dahliae* pathogen from olive was selected and additional tests were carried out to confirm the antifungal activity of HTyr and the two extracts. The other fungus isolates showed high variability and low susceptibility to the compounds and were not investigated further.

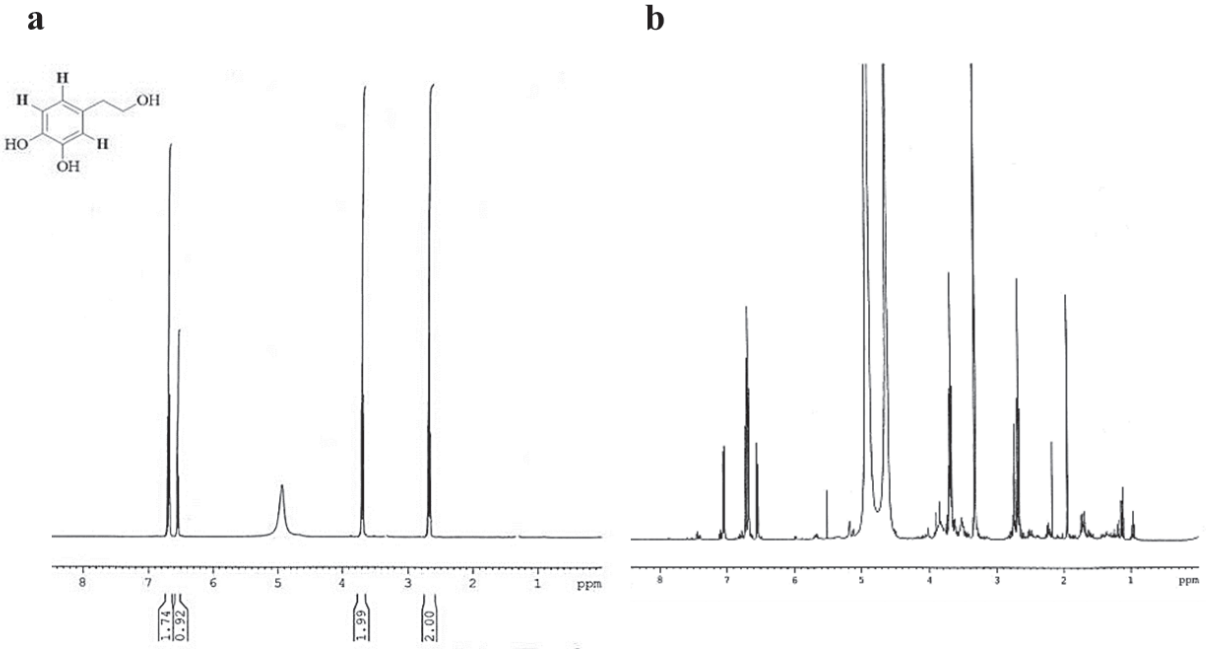

Figure 2. ^{1}H-NMR spectra of HTyr (a) and HTE2 (b).

Antifungal activity of HTyr, HTE1 or HTE2 on mycelium growth of Verticillium dahliae

The *V. dahliae* isolate VD 22 was grown on Potato dextrose Agar (PDA) for 7 d at 25°C before conducting the following experiments:

Disc diffusion assays. These were used to evaluate the antifungal activity of the HTyr standard against the *V. dahliae* isolate. The antifungal test was carried out by placing a mycelium plug in the centre of each PDA Petri dish, and at 3 cm from a paper disk (Oxoid) to which 1 mg of HTyr had been applied. After 72 h incubation at 25°C, the distance (mm) between the edge of the resulting fungus mycelium and the edge of the disk was measured (Balouiri *et al.*, 2016). Data are expressed as means of three independent replicas per treatment.

Modified top agar assays. These were used to evaluate the antifungal activity of HTyr, HTE1 and HTE2 obtained from OMWP against *V. dahliae*. HTyr was tested at concentrations of 0.25, 0.5 or 1 mg mL^{-1}. HTE1 was tested at 7.6, 15.2 or 30.4 mg mL^{-1}, and HTE2 was tested at 2.15, 4.3 or 8.6 mg mL^{-1}. These concentrations correspond to 0.25, 0.5 or 1 mg mL^{-1} of the corresponding HTyr content for each extract. The Top Agar was obtained by incorporating HTyr or the extracts at different concentrations into a final volume of 5 mL of PDA. The substrate obtained was poured into Petri dishes on top of 20 mL of previous solidified PDA. Solidified Top Agar was inoculated in the centre of each Petri dish with a mycelium plug of the *V. dahliae* isolate. Negative experimental controls were prepared by replacing the volume of samples with the same volume of sterile distilled water.

At 3, 5 and 7 days post-inoculation the diameter of mycelium growth in each Petri dish was measured (Figure 3), and these data were subsequently analyzed to calculate the percentage of mycelium growth inhibition (MGI%), using the following formula:

$$MGI\ \% = [(C-T)/C]\cdot 100,$$

where C = diameter of mycelium growth in the experimental control, and T= diameter of mycelium growth treated with HTyr or the extracts.

Antifungal activity of HTyr, HTE1 or HTE2 on Verticillium dahliae *conidium germination*

Effects of HTyr on conidium germination were evaluated by placing 5 μL of *V. dahliae* conidium suspension (10^5 conidia mL^{-1}) on a thin layer of water agar on a glass microscope slide. The water agar amended with 1 mg mL^{-1} of HTyr, HTE1 or HTE2. The Microscope slides were placed in Petri dishes lined with moist filter papers (100% RH.), and were incubated for 24 h at 25°C. Germinated conidia were counted after 6 h and 24 h, using a minimum of 100 conidia per replicate, with four replicates accessed (Khalil *et al.,* 1985). The results were expressed as percentages of inhibition of germination in relation to experimental controls, as follows:

$$\text{Percent inhibition} = [(C-T)/C]\ 100,$$

where C = conidium germination in the control, and T = conidium germination in treatment with HTyr or the extracts.

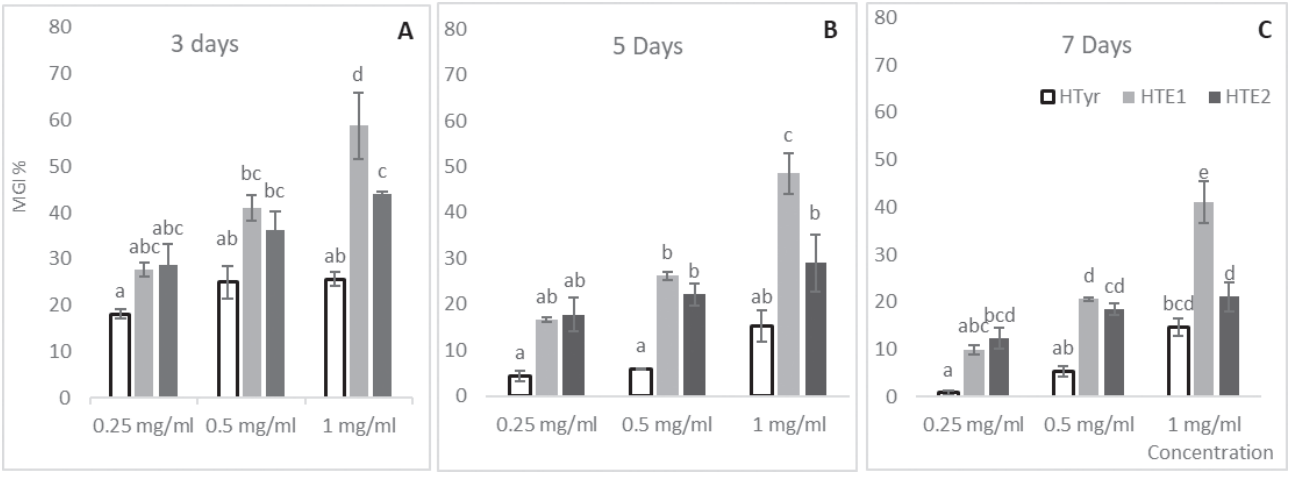

Figure 3. *V*erticillium *dahliae* mycelium growth inhibition percent (MGI %) in top agar assays. The data for different concentrations of HTyr, HTE1 and HTE2 are presented for 3 (A), 5 (B) and 7 (C) d of incubation. Bars indicate standard errors of triplicates and different letters indicate differences ($P < 0.05$), according Tukey's (HSD) multiple range test.

Data analyses

Differences (at $P < 0.05$) between means of the parameters measured were determined by analysis of variance (ANOVA) and Tukey's (HSD) multiple range test. IBM SPSS Statistics for Windows, Version 22.0, was used for these statistical analyses.

RESULTS

Phenolic profiles of HTE1 and HTE2

The qualitative and quantitative HPLC profiles of HTE1 have been previously described by Pannucci *et al.* (2019). In this extract, the main compound found was HTyr at 32.83 mg g^{-1}, representing the 64.7% w/w of the total phenols (50.7 mg g^{-1}). Minor components in this extract were verbascoside (12.9 mg g^{-1}, 25.4% w/w), tyrosol, gallic acid and verbascoside derivatives, which in total constituted the 9.6% w/w of total phenols.

This is the first description of HTE2. The chromatographic profile indicated that HTE2 contained 149.7 mg g^{-1} of polyphenols. The main compound in the extract was HTyr (115.2 mg g^{-1}, 77% w/w), and the secondary components were HTyr glycol and tyrosol (34.5 mg g^{-1}, 23% w/w).

The ^{1}H NMR spectrum of HTE2 confirmed the presence of HTyr as the main compound. The signals of the three aromatic protons (δ, ppm: dd, 6.53-6.56, J = 8.0 and 4.0 Hz, 1 H; d, 6.67, J = 4.0 Hz, 1 H; d, 6.70, J = 8.0 Hz, 1 H) were superimposable with those of HTyr.

Effects of HTyr, HTE1 and HTE2 on the mycelium growth of Verticillium dahliae

After 3 d incubation, the ANOVA of *V. dahliae* mycelium growth data showed significant differences among the treatments (HTyr, HTE1 or HTE2), and the related extract concentrations (0.25, 0.5 or 1 mg mL^{-1}) ($F(8, 18) = 11.98$, $P < 0.001$). Tuckey HSD analysis showed that at the lowest concentration (0.25 mg mL^{-1}) there was no statistically significant difference on the inhibition of the mycelium growth of *V. dahliae* between HTyr (mean = 18.1, SD = 1.77), HTE1 (mean = 27.7, SD = 2.66) and HTE2 (mean = 28.7, SD = 7.84). Similarly, at 0.5 mg mL^{-1}, no significant difference in the inhibition of the pathogen was observed between HTyr (mean = 25.0, SD = 6.05), HTE1 (mean = 40.9, SD = 4.69) and HTE2 (mean = 36.1, SD = 7.23). At 1 mg mL^{-1}, HTE1 (mean = 58.8, SD = 12.56) gave greater inhibition of *V. dahliae* than HTE2 (mean = 44.0, SD = 0.78) or HTyr (mean = 25.6, SD = 2.67).

After 5 d incubation, significant differences in mycelium growth were detected among the treatments and their concentrations ($F(8, 18) = 17.3$, $P < 0.001$). At 0.25 mg mL^{-1} there was no significant difference between HTyr (mean = 4.3, SD = 2.08), HTE1 (mean = 16.6, SD = 0.78) and HTE2 (mean = 17.7, SD = 6.50). Whereas at 0.5 mg mL^{-1} (Figure 3), HTE1 (mean = 26.1, SD = 1.55) and HTE2 (mean = 22.1, SD = 4.04) gave greater inhibition of mycelium growth than HTyr (mean = 5.9, SD = 0.07). At 1 mg mL^{-1} of HTyr, HTE1 (mean = 48.5, SD = 7.72) gave greater inhibition of *V. dahliae* than HTyr (mean = 15.2, SD = 5.88) and HTE2 (mean = 29.0, SD = 10.75).

After 7 d incubation, significant difference in mycelium growth were detected among treatments and their concentrations ($F(8, 18) = 28.60$, $P < 0.001$). At 0.25 mg mL^{-1}, no significant differences were detected between the HTyr (mean = 0.8, SD = 0.72) and HTE1 (mean = 9.9, SD = 1.66), or between HTE1 (mean = 9.9, SD = 1.66) and HTE2 (mean = 12.3, SD = 3.71), but a significant difference was found between HTyr (mean = 0.8, SD = 0.72) and HTE2 (mean = 12.3, SD = 3.71). At 0.5 mg mL^{-1} differences in mycelium growth were detected between HTyr (mean = 5.3, SD = 2.08) and HTE1 (mean = 20.5, SD = 0.73), and between HTyr and HTE2 (mean = 18.4, SD = 2.05), but not between HTE1 (mean = 20.5, SD = 0.73) and HTE2 (mean = 18.4, SD = 2.05). At 1 mg mL^{-1}, greater inhibition of *V. dahliae* was observed from HTE1 (mean = 41.0, SD = 7.74) compared to HTE2 (mean = 21.0, SD = 5.50) and HTyr (mean = 14.69, SD = 3.26), but no difference was measured between the effects of HTyr and HTE2.

For effects of different concentrations of each extract on growth of *V. dahliae*, from HTE1, after 3 d, there was no difference between the 0.25 mg mL^{-1} (mean = 27.7, SD = 2.66) and 0.5 mg mL^{-1} (mean = 40.9, SD = 4.69) treatments, but a significant difference was detected between the 1 mg mL^{-1} (mean = 58.7, SD = 12.56) and the 0.5 and 0.25 mg mL^{-1} treatments. Similarly, after 5 and 7 d of incubation, there was a difference in inhibition of *V. dahliae* from the greatest concentration of HTE1. For HTE2, there were no statistically significant differences in inhibition from the three different concentrations, after 3, 5 or and 7 d incubation.

Effects of HTyr, HTE1 or HTE2 on conidium germination of Verticillium dahliae

After 6 h incubation, HTyr gave 88% inhibition of conidium germination, while the two extracts caused greater inhibition, 99% from HTE1 and 95% from HTE2. After 24 h incubation, HTE1 gave the greatest inhibition (55%), while HTyr and HTE2 both gave 37% inhibition of conidium germination (Figure 4).

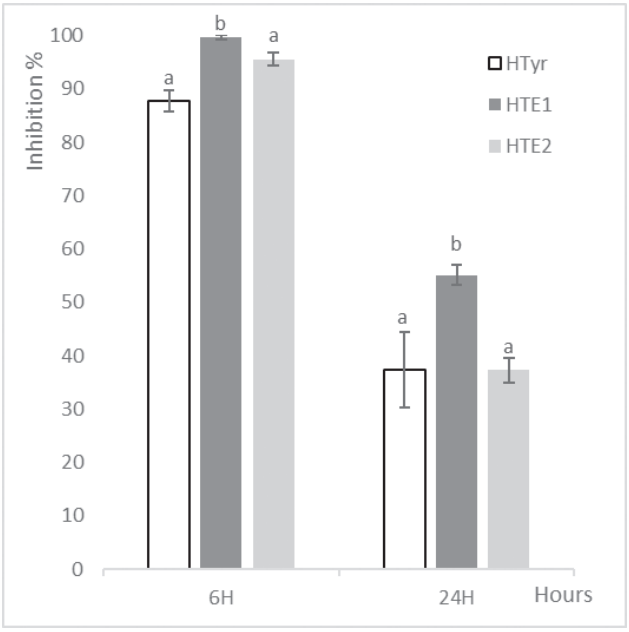

Figure 4. HTyr and HTE extracts mean inhibition (%) on *Verticillium dahliae* conidium germination. HTyr standard was tested at 1 mg mL^{-1} and HTE1 and HTE2 were tested at 1 mg mL^{-1} referred to the HTyr content in each extract. Germinated conidia were counted after 6 and 24 h incubation at 25°C in the dark, and means are for 100 conidia per replicate. Bars indicate standard errors, and different letters indicate significant differences ($P < 0.05$), Tukey's (HSD) multiple range test.

Statistically significant differences in inhibition of conidium germination were detected between the treatments with HTyr, HTE1 and HTE2 ($F(5,18) = 3.37$, $P < 0.05$). Application of 1 mg mL^{-1} of HTyr or the two extracts gave differences in percent germination after 6 h incubation between HTE1 (mean = 99.6, SD = 0.71) and HTE2 (mean = 95.5, SD = 2.31) Similar differences were observed between the effects of HTyr (mean = 87.7, SD = 3.82) and HTE1 (mean = 99.6, SD = 0.71). After 24 h incubation, no differences were detected between HTE2 (mean = 37.3, SD = 4.54) and HTyr (mean = 37.3, SD = 14.28). However, the difference between HTE1 (mean = 55.1, SD = 3.95) and HTE2 (mean = 37.3, SD = 4.54) was indeed statistically significant.

DISCUSSION

The increasing interest of the use of natural products in agricultural includes research on plant derived compounds for pest and disease management. This aims to meet the regulatory demands for reduction in the use of synthetic pesticides, to provide environmentally friendly approaches. Several reports have described effects of plant extracts on fungal plant pathogens. Phenolic compounds derived from OMWP have been shown to hold promise as natural fungicides against crop pathogens, including *Alternaria solani*, *Botrytis cinerea* and *Fusarium culmorum* (Winkelhausen *et al.*, 2005). In particular, HTyr is well-known and of interest to the pharmaceutical industry, because of the antioxidant, anti-inflammatory (Bernini *et al.*, 2015) and antimicrobial properties (Robles-Almazan *et al.*, 2018; Pannucci *et al.*, 2019) of this compound. OMWP enriched in HTyr, is a resource for agricultural applications. We have evaluated HTE1 and HTE2, obtained by OMWP, through a sustainable pilot process (Romani *et al.*, 2016; Bernini *et al.*, 2017) based on membrane technologies which mainly enrich HTyr, together with other low molecular weight phenols, as has been shown using HPLC and NMR analyses.

In the present study, the capacities have been demonstrated for HTyr, HTE1 and HTE2 to affect mycelium growth and conidium germination of *V. dahliae*, the cause agent of Verticillium wilt of olive trees. *In vitro* inhibitory effects of different concentrations were assessed. Inhibition of conidium germination is important because conidia are important for propagation of the disease.

HTE1 was the most effective treatment against mycelium growth and conidium germination of *V. dahliae*. The diameters of *V. dahliae* colonies decreased with increasing concentrations of this extract. At the tested concentrations, low antifungal effects of HTyr were detected, but greater inhibition was detected from HTE1 and HTE2 at the same relative concentrations of HTyr. HTE1 at 1 mg mL^{-1} gave greater inhibition of fungal growth than HTE2 or HTyr. However, even greater inhibition was achieved for *V. dahliae* conidium germination. Applying 1 mg mL^{-1} of HTyr, differences between HTE1 and HTE2 were detected. Similarly, significant differences between HTyr and HTE1 were observed for inhibition of conidium germination., However, no differences were noted between HTE2 and HTyr. The effects of 1 mg mL^{-1} of HTyr on conidium germination gave better results than detected for inhibition of growth of fungal colonies.

The results are similar to those of previous studies on HTyr enriched extracts from olive mill wastewater (OMWW) that were tested against the olive bacterium pathogens *Pseudomonas savastanoi* pv. *savastanoi* (Pss) and *Agrobacterium tumefaciens* (At) (Caracciolo *et al.*, 2019; Pannucci *et al.*, 2019). In those studies, HTE1 was also the most active extract, which completely inhibited the growth of Pss and at 0.5 mg mL^{-1} and at 1.0 mg mL^{-1}, compared to untreated controls. In contrast, HTyr

at 1.0 mg mL^{-1} only reduced bacterium growth. We have verified that HTyr and HTE1 as antifungal agents produced similar results. This provides results that can be explored in the future, which may provide mechanism of action relating to interactions of these compounds with specific bacterium or fungus cell membranes. Yangui *et al.* (2010) observed a severe reduction numbers of viable conidia of *V. dahliae* by at least 15 g L^{-1} of HTyr-rich OMWW or HTyr-rich extract with contact times greater than or equal to 30 min, or at 12.5 g L^{-1} with contact time of 60 min. Differently in the present study, we evaluated the inhibitory effects on *V. dahliae* mycelium growth and conidium germination, and the present results were obtained for HTE1 and HTE2 extracts from Italian olive cultivars from different geographical origins (Apulia and Sicily). Furthermore, a different extraction procedure based on membrane technology was used, which gave rise to a different phenolic content profile in the extracts.

For HTyr, HTE1 and HTE2, the greatest inhibition of *V. dahliae* mycelium growth was observed after the first 72 h of incubation. With longer periods of incubation, growth inhibition was less than that observed after 72 h. Decreasing growth inhibition with increasing incubation time possibly indicates that the active compounds were being metabolized by the fungus. Loss in inhibitory activity, and possibly stimulation of mycelium growth, is consistent with results for other fungi, such as *Aspergillus sp.* when growing on media containing rutin or quercetin, where the fugus produced an extracellular enzyme that degrades these glycosides (Westlake *et al.*, 1959). In the present study, the extracts may not have inhibited mycelium growth during long incubation periods because of breakdown by *V. dahliae* enzymes.

Concerning the stronger activity of HTE1 and HTE2 observed compared to HTyr, this could be due to a central role of the minor phenolic components in the extracts. Some of these have been shown to have antimicrobial activity when tested singularly. Gallic acid possesses a high antifungal activity against *Fusarium solani*; the hyphae became collapsed and shrunken after 24 h incubation (Nguyen *et al.*, 2013). Enriched, purified, but still complex mixtures of phenols could possibly provide multiple modes of action giving rise to synergistic antifungal effects.

Several mechanisms of action have been proposed for the antimicrobial activities of phenolic compounds. Their potency may result from the ability to compromise cell functions and membrane integrity, behaving as surface-active compounds (Yangui *et al.,* 2008). Therefore, alteration of microbe membrane permeability, with the consequent loss of cytoplasmic constituents, could explain phenolic activity against pathogenic fungi (Yangui *et al.,* 2009). The mechanisms by which polyphenols act are not entirely understood. However, results from the present study give evidence that the observed antifungal effects was directly related to the chemical composition of HTE1 and HTE2, and mainly to HTyr content of these extracts.

The present study showed that HTE1 and HTE2 have antifungal activity against *V. dahliae*. However, we consider that they are preliminary, since further research is required, including assessments on more pathogen isolates. In addition, studies of olive trees under field conditions are required to extend knowledge of management of this pathogen with these identified extract compounds. Some researchers have suggested that incorporation of OMWW into soil could be an eco-friendly alternative to soil fumigants for crop protection against *V. dahliae* (El-Abbassi *et al.*, 2017). Nevertheless, safe use of OMWP for efficient plant disease control, without negative effects on cultivated crops and soils, remains a challenge. It is also necessary to demonstrate that the phenolic contents of OMWP retains biocidal activity after large-scale applications, allowing sustainable agro-economic development.

ACKNOWLEDGEMENTS

This research was supported by "Agroalimentare e Ricerca" (AGER), Project AGER2-Rif.2016-0169: Valorization of Italian olive products through innovative analytical tools (VIOLIN), and by the Italian Ministry for Education, University and Research (MIUR), Project SAFE-Med, Law 232/216, Departments of Excellence.

LITERATURE CITED

Balouiri M., Sadiki M., Ibnsouda S.K., 2016. Methods for in vitro evaluating antimicrobial activity: A review. *Journal of Pharmaceutical Analysis* 6: 71–79.

Bernini R., Mincione E., Barontini M., Crisante F., 2008. Convenient synthesis of hydroxytyrosol and its lipophilic derivatives from tyrosol or homovanillyl alcohol. *Journal of Agricultural and Food Chemistry* 56: 8897-8904.

Bernini R., Mincione E., Barontini M., Crisante F., 2010. Procedimento per la preparazione di derivati dell'idrossitirosolo e di idrossitirosolo. Brevetto N. 0001381959

Bernini R.; Gilardini Montani M. S.; Merendino N.; Romani A. Velotti F. 2015. Hydroxytyrosol-derived

compounds: a basis for the creation of new pharmacological agents for cancer prevention and therapy. *Journal of Medicinal Chemistry* 58: 9089-9107.

Bernini R., Carastro I., Palmini G., Tanini A., Zonefrati R.,… Romani A., 2017. Lipophilization of hydroxytyrosol-enriched fractions from *Olea europaea* L. byproducts and evaluation of the in vitro effects on a model of colorectal cancer cells. *Journal of Agricultural and Food Chemistry* 65: 6506–6512

Caracciolo R., Pannucci E., Bernini R., Varvaro L., Santi L., 2019. Antibacterial activity of hydroxytyrosol-enriched extracts obtained from olive mill waste waters by membrane technologies against olive tree pathogens. 4th International Symposium on Biological Control of Bacterial Plant Diseases. Viterbo. *Journal of Plant Pathology* vol. 101: 8.

El-Abbassi A., Saadaoui N., Kiai H., Raiti J., Hafidi A., 2017. Potential applications of olive mill wastewater as biopesticide for crops protection. *Science of the Total Environment* 576: 10–21.

Jiménez-Díaz R.M., Tjamos E.C., Cirulli M., 1998. Verticillium wilt of major tree hosts: olive. *A compendium of Verticillium wilts in tree species. Ponsen and Looijen, Wageningen* (1998) 13–16.

Jiménez-Díaz R.M., Cirulli M., Bubici G., del Mar Jiménez-Gasco M., Antoniou P.P., Tjamos E.C., 2012. Verticillium wilt, a major threat to olive production: current status and future prospects for its management. *Plant Disease* 96: 304–329.

Khalil S. K., Shah M. A., Naeem M. (1985). Laboratory studies on the compatibility of the entomopathogenic fungus *Verticillium lecanii* with certain pesticides. *Agriculture, Ecosystems & Environment* 13: 329-334.

Larif M., Zarrouk A., Soulaymani A., Elmidaoui A., 2013. New innovation in order to recover the polyphenols of olive mill wastewater extracts for use as a biopesticide against the *Euphyllura olivina* and *Aphis citricola*. *Research on Chemical Intermediates* 39: 4303–4313.

Lavee S., Rallo L., Rapoport H.F., Troncoso de Arce A., 1996. The floral biology of the olive: effect of flower number, type and distribution on fruitset. *Scientia Horticulturae* 66(3-4): 149–158.

López-Escudero F.J., Mercado-Blanco J., 2011. Verticillium wilt of olive: a case study to implement an integrated strategy to control a soil-borne pathogen. *Plant Soil* 344: 1–50.

López-Escudero F.J., Mwanza C., Blanco-López M.A., 2007. Reduction of *Verticillium dahliae* microsclerotia viability in soil by dried plant residues. *Crop Protection* 26: 127–133.

Lykas C., Vagelas I., Gougoulias N., 2014. Effect of olive mill wastewater on growth and bulb production of tulip plants infected by bulb diseases. *Spanish journal of Agricultural Research*: 233–243.

Markakis E.A., Tjamos S.E., Antoniou P.P., Paplomatas E.J., Tjamos E.C., 2016. Biological control of Verticillium wilt of olive by *Paenibacillus alvei*, strain K165. *BioControl* 61: 293–303.

Mekki A., Dhouib A., Aloui F., Sayadi S., 2006a. Olive wastewater as an ecological fertiliser.

Mekki A., Dhouib A., Sayadi S., 2006b. Changes in microbial and soil properties following amendment with treated and untreated olive mill wastewater. *Microbiological Research* 161: 93–101.

Mekki A., Dhouib A., Feki F., Sayadi S., 2008. Assessment of toxicity of the untreated and treated olive mill wastewaters and soil irrigated by using microbiotests. *Ecotoxicology and Environmental Safety* 69: 488–495.

Mercado-Blanco J., Rodrıguez-Jurado D., Hervás A., Jiménez-Dıaz R.M., 2004. Suppression of Verticillium wilt in olive planting stocks by root-associated fluorescent Pseudomonas spp. *Biological Control* 30: 474–486.

Mulero-Aparicio A., Agustí-Brisach C., Varo Á., López-Escudero F.J., Trapero A., 2019. A non-pathogenic strain of *Fusarium oxysporum* as a potential biocontrol agent against Verticillium wilt of olive. *Biological Control* 139: 104045.

Nguyen D.M.C., Seo D.J., Lee H.B., Kim I.S., Kim K.Y.,… Jung W.J., 2013. Antifungal activity of gallic acid purified from *Terminalia nigrovenulosa* bark against *Fusarium solani*. *Microbial Pathogenesis* 56: 8–15.

Pannucci E., Caracciolo R., Romani A., Cacciola F., Dugo P.,… Santi L., 2019. An hydroxytyrosol enriched extract from olive mill wastewaters exerts antioxidant activity and antimicrobial activity on *Pseudomonas savastanoi* pv. *savastanoi* and *Agrobacterium tumefaciens*. *Natural Product Research*:1-8.

Pizzichini D., Russo C., Vitagliano M., Pizzichini M., Romani A.,… Vignolini P., 2011. Process for producing concentrated and refined actives from tissues and byproducts of *Olea europaea* with membrane technologies. Pat. No EP2338500A1 29.

Robles-Almazan M., Pulido-Moran M., Moreno-Fernandez J., Ramirez-Tortosa C., Rodriguez-Garcia C., Quiles J.L., Ramirez-Tortosa Mc., 2018. Hydroxytyrosol: bioavailability, toxicity, and clinical applications. *Food Research International* 105: 654–667.

Romani A., Pinelli P., Ieri F., Bernini R., 2016. Sustainability, innovation, and green chemistry in the production and valorization of phenolic extracts from *Olea europaea* L. *Sustainability* 8: 1002.

Thielmann J., Kohnen S., Hauser C., 2017. Antimicrobial activity of *Olea europaea* Linné extracts and their

applicability as natural food preservative agents. *International Journal of Food Microbiology* 251: 48-66.

Triki M.A., Hadj-Taieb S.K., Mellouli I.H., Rhouma A., Gdoura R., Hassairi A., 2012. Identification and screening of bacterial isolates from Saharan weeds for *Verticillium dahliae* control. *Journal of Plant Pathology*: 305–311.

Van Alfen N.K., 1989. Reassessment of plant wilt toxins. *Annual Review of Phytopathology* 27: 533-550.

Varo A., Raya-Ortega M.C., Trapero A., 2016. Selection and evaluation of micro-organisms for biocontrol of *Verticillium dahliae* in olive. *Journal of Applied Microbiology* 121: 767–777.

Varo A., Mulero-Aparicio A., Adem M., Roca L.F., Raya-Ortega M.C., López-Escudero F.J., Trapero A., 2017. Screening water extracts and essential oils from Mediterranean plants against *Verticillium dahliae* in olive. *Crop Prot*ection 92:168–175.

Westlake D.W.S., Talbot G., Blakley E.R., Simpson F.J., 1959. Microbial decomposition of rutin. *Canadian Journal of Microbiology* 5: 621–629.

Winkelhausen E., Pospiech R., Laufenberg G., 2005. Antifungal activity of phenolic compounds extracted from dried olive pomace. *Bulletin of the Chemists and Technologists of Macedonia* 24: 41–46.

Yangui T., Rhouma A., Gargouri K., Triki M.A., Bouzid J., 2008. Efficacy of olive mill waste water and its derivatives in the suppression of crown gall disease of bitter almond. *European Journal of Plant Pathology* 122: 495–504

Yangui T., Dhouib A., Rhouma A., Sayadi S., 2009. Potential of hydroxytyrosol-rich composition from olive mill wastewater as a natural disinfectant and its effect on seeds vigour response. *Food Chemistry* 117: 1–8.

Yangui T., Sayadi S., Gargoubi A., Dhouib A., 2010. Fungicidal effect of hydroxytyrosol-rich preparations from olive mill wastewater against *Verticillium dahliae*. *Crop Protection* 29: 1208–1213.

Phytopathologia Mediterranea
The international journal of the
Mediterranean Phytopathological Union

Firenze University Press
www.fupress.com/pm

Research Papers

Biocontrol agents and resistance inducers reduce Phytophthora crown rot (*Phytophthora capsici*) of sweet pepper in closed soilless culture

Giovanna GILARDI*, Athina VASILEIADOU, Angelo GARIBALDI, Maria Lodovica GULLINO

Centre for Innovation in the Agro-Environmental Sector, AGROINNOVA, University of Torino, Largo P. Braccini 2, 10095 Grugliasco (TO), Italy
*Corresponding author. E-mail: giovanna.gilardi@unito.it

OPEN ACCESS

Citation: G. Gilardi, A. Vasileiadou, A. Garibaldi, M. L. Gullino (2021) Biocontrol agents and resistance inducers reduce Phytophthora crown rot (*Phytophthora capsici*) of sweet pepper in closed soilless culture. *Phytopathologia Mediterranea* 60(1): 149-163. doi: 10.36253/phyto-11978

Accepted: January 5, 2021

Published: May 15, 2021

Data Availability Statement: All relevant data are within the paper and its Supporting Information files.

Competing Interests: The Author(s) declare(s) no conflict of interest.

Editor: Epaminondas Paplomatas, Agricultural University of Athens, Greece.

Summary. Twelve trials, in closed soilless culture under controlled conditions, were carried out to evaluate the efficacy of resistance inducers (based on K-phosphite and K-silicate used alone or in combination), and of experimental biocontrol agents (*Trichoderma* sp. TW2, a mixture of *Pseudomonas* FC 7B, FC 8B, and FC 9B, *Fusarium solani* FUS25, *Pseudomonas* sp. PB26), and a commercial formulation of *Trichoderma gamsii* + *T. asperellum*, against diseases caused by *Phytophthora capsici* of sweet pepper. The products were applied using three different protocols, and effects on incidence of Phytophthora crown, stem and root rots (% dead plants), disease development (area under the disease progress curve; AUDPC), and plant fresh weights were evaluated. Potassium phosphite, applied directly at standard P_2O_5:K_2O, 1.30 + 1.05 g L^{-1}) and at half standard rates, onto growing media, or via nutrient solution, and before infestation of peat plant growing medium with *P. capsici*, provided the best disease management in a dose-dependent manner, with an 80% reduction of Phytophthora crown, stem and root rots for the standard dosage and for both types of application. These treatments also reduced proportions of dead plants by 47% from the standard rate and by 62% at the half standard rate, when applied via the nutrient solution or directly to the substrate. K-silicate alone partially reduced the percentage of dead plants, with efficacy of 20–23%. No improvement in disease control was observed when K-silicate was applied in combination with phosphite, while K-silicate alone or combined with K-phosphite reduced disease development, compared to untreated controls. Biocontrol agents (BCAs), applied preventively, reduced Phytophthora crown, stem and root rots, with similar or better results than those from the commercial mixture of *Trichoderma asperellum* + *T. gamsii*. Among the tested BCAs, *Fusarium solani* FUS25 provided the most consistent disease reduction (60–65%) and gave increased plant fresh weights. All the tested BCAs reduced disease development, with a similar trend for different disease pressures. The least AUDPC values, compared to the non-treated controls, were from *Fusarium solani* FUS25, followed by the tested *Pseudomonas* strains and *Trichoderma* sp. TW2. These results indicate the potential for potassium phosphite and biocontrol agents in management of Phytophthora crown, stem and root rots of pepper grown in soilless systems.

Keywords. Hydroponics, *Phytophthora* control, *Capsicum annuum*, salts, microorganisms.

INTRODUCTION

Sweet pepper (*Capsicum annuum*) is a popular vegetable crop, which is greatly appreciated for its quality and taste for fresh consumption and for processing, and is increasingly grown in greenhouse environments. The commercial greenhouse production of this vegetable is extensive in European countries, including Spain (12,420 ha), Italy (2,370 ha), Poland (1,830 ha) and The Netherlands (1,320 ha) (2017 data; FAOSTAT 2019).

However, sweet pepper is frequently affected by pathogens, with soil-borne pathogens being important and causing severe crop losses (Owen-Going *et al*., 2003; Pernezny *et al*., 2003; Messelink *et al*., 2020). Among these *Phytophthora capsici*, which causes various diseases such as root, stem, and crown rots, resulted in economically important losses in most production areas (Matta and Garibaldi, 1981; Ristaino and Johnston, 1999; Hausbeck and Lamour, 2004; Granke *et al*., 2012). This pathogen is highly variable (Ristaino and Johnston, 1999; Matta and Garibaldi, 1981; Lee *et al*., 2001; Tamietti and Valentino, 2001; Foster and Hausbeck, 2010), and causes severe losses when grown either in soil or in soilless systems (Nielsen *et al*., 2006b), because it is difficult to manage (Messelink *et al*., 2020).

These diseases have been known in Italy since 1949 (Sibilia, 1952), and are still widespread, as a result of a lack of effective fumigants, no commercially acceptable resistant cultivars, and limited availability of resistant rootstocks which often only have partial resistance to the pathogen (Gilardi *et al*., 2014). Although several sweet pepper cultivars show full or partial resistance to *P. capsici*, stem blight, root rot and foliar blight of these cultivars are probably reduced by separate genetic systems, so that cultivars resistant to crown rot may not be resistant to foliar blight (Foster and Hausbeck, 2010). This complicates the use of genetic disease resistance in sweet pepper, increasing the need to improve marketable yield potential and good fruit quality (Barchenger *et al*., 2018; Acquadro *et al*., 2020). Development of pathogen resistance to fungicides, including the commonly used mefenoxam and metalaxyl (Bower and Coffey, 1985; Lamour and Hausbeck 2001; Parra and Ristaino, 2001; Tamietti and Valentino, 2001), and alternatives to phenylamides, such as cyazofamid, dimethomorph, flumorph and oxathiapoprolin (Bower and Coffey 1985; Kousik *et al*., 2008; Bi *et al*., 2014; Miao *et al*., 2016), has complicated management of these diseases.

Soilless cultivation is increasingly being adopted for many vegetable crops (Lee and Lee, 2015. Sambo *et al*., 2019), as this is a good option when crop rotation is not feasible and resistant cultivars are not available, and because of increasing limitations in the use of fumigants and fungicides (Garibaldi *et al*., 2014). Host species, plant growth substrate type and the target pathogen all play important roles in management of diseases in soilless cultivation (Zheng *et al*., 2000; van der Gaag and Wever, 2005; Khalil *et al*., 2009; Lee and Lee, 2015), and specific evaluations are required for new crops. The effects of soilless cultivation on sweet pepper have not been fully exploited, particularly in terms of effects on the reduction of soil-borne diseases, such as Phytophthora crown rot.

Apart from their intrinsic capability of reducing problems caused by soil-borne pathogens, soilless cultivation systems offer good opportunities for exploiting new disease management strategies, including the use of resistance inducers and biocontrol agents, where increasing limitations apply to use of traditional fungicides.

Several biocontrol agents (Rankin and Paulitz, 1994; Paulitz, 1997; Chatterton *et al*., 2004; Mercier and Manker, 2005; Calvo-Bado *et al*., 2006; Liu *et al*., 2007; Segarra *et al*., 2010; Köhl *et al*., 2011; Vallance *et al*., 2011; Gilardi *et al*., 2020), and other biocide products such as salts of phosphites and silicates, and nonionic surfactants (Stanghellini and Tomlinson, 1987; Cherif *et al*., 1994; Stanghellini and Rasmussen, 1994; Stanghellini *et al*., 1996; Stanghellini and Miller, 1997; Förster *et al*., 1998; Nielsen *et al*., 2006a; French-Monar *et al*., 2010; Song *et al*., 2016; Gilardi *et al*., 2020) have been tested against a number of soil-borne pathogens, including *P. capsici,* in soilless systems. However, most of the applications of these disease management tools require fine-tuning for type and application timing, particularly in soilless systems, before they can be practically implemented (Vallance *et al*., 2011).

The present study was carried out in an experimental closed soilless system, under controlled conditions, to evaluate the efficacy of host resistance inducers, based on K-phosphite and K-silicate, used alone or combined, and of experimental biocontrol agents, against *P. capsici* on sweet pepper. These treatments were compared with a commercial formulation of *Trichoderma gamsii* + *T. asperellum*. Different treatments and types and timing of application were tested, aiming to develop appropriate strategies for their application in practical soilless production systems.

MATERIALS AND METHODS

Soilless growing system and experimental layout

Twelve trials were carried out in a glasshouse at the AGROINNOVA Centre of Competence of the University

of Torino, in Grugliasco, Torino, Italy, at temperatures ranging from 22 to 30°C, using fully automated closed soilless system. This is a small-scale hydroponic system, with recirculating nutrient solution. Each hydroponic unit consisted of one channel (6 m long and 25 cm wide) connected to a storage tank (300 L capacity) filled with nutrient solution, which was automatically delivered to the plants using an electronic control unit (Idromat2, Calpeda S.p.a.). Nutrient solution (at 1.5–1.6 mS cm^{-1}) was pumped by emitters (one per pot) at a flow rate of 6 L h^{-1} from the storage tank, and fed to plants through drip emitters, and was left to drain back into the storage tank by gravity. The plants were fertigated with 5:3:8 N:P:K fertilizer (nutrient solution containing 120 mg L^{-1} total N, 30 mg L^{-1} P and 150 mg L^{-1}; conductivity 1.5–1.6 mS cm^{-1}). Nutrient solutions contained: 11.24 mM NO_3, 4.8 mM NH_4, 0.75 mM KH_2PO_4, 0.75 mM K_2SO_4, 0.012 mM Iron chelate EDTA, 2 mM MgO, 2 mM SO_3, 0.2 mM B, 0.001 mM Mo, 0.15 mM Zn, 3.1 mM CaO, 0.05 mM Cu^{++}, 0.25 mM Mn, and 12.2 mM K. The pH and conductivity of the nutrient solutions were checked regularly by using a pH meter and a SevenGo DUO TM SG23 conductivity meter (Tettler). The irrigation programme (three to six times per day) was revised according to the environmental conditions, particularly temperature. Each experimental unit consisted of six pots replicated five times (n = 30 pots). Two plants were planted in each pot, and six pots were each sub-replicate of 12 plants each. Five replicates were used per treatment (60 plants per treatment).

Plant material, and tested products and protocols

Fifteen-day-old plants of sweet pepper 'Corno di Toro' (Furia Sementi), which is susceptible to Phytophthora crown rot, were transplanted into 3 L capacity plastic pots filled with a growing medium containing: black peat soil (Brill Type 5: 15% of blond peat, 85% of black peat; pH 5.5–6.0, 1,100 g m^{-3} of N:P:K and traces of molybdenum, Georgsdorf) in all the trials.

Each set of trials included one untreated and inoculated experimental control, and different treatments with salt products or biocontrol agents tested alone or in combinations, which were applied according to three different protocols (Table 1). These were:

Protocols I and II. The fertilizer-based phosphite (Alexine 95PS: 52% P_2O_5 + 42% K_2O, Massò), which is labelled as a phosphorus supplement for soilless application, and potassium silicate (K_2SiO_3, 33.7 to 34.7%, Andrea Gallo S.r.l.) were tested (Trials 1 to 6) in 2018 and 2019, to select the optimal rates and types of application for potassium phosphite and potassium silicate, used alone or in combinations. K_2SiO_3 at 200 mg L^{-1} and K-phosphite were added directly to the nutrient solutions (NS) at the standard rate of 1.30 g L^{-1} P_2O_5 + 1.05 g L^{-1} K_2O, or at half this rate (0.65 P_2O_5 + 0.52 g L^{-1} K_2O + 0.525 g L^{-1}) in experimental Protocol I. The same products, alone or in combinations, were applied to each pot around the crown of the seedlings using 100 mL per pot of the suspension prepared according to Protocol II. The treatments were carried out three times every 7 d (Table 1).

Protocol III. The following BCAs, isolated from suppressive composts, were tested: *Pseudomonas* sp. PB26 (Pugliese *et al*., 2008), *Fusarium solani* FUS25 (Gullino and Pugliese, 2011), *Trichoderma* sp. TW2 (Cucu *et al*., 2020), and a 1:1:1 mixture of three *Pseudomonas* spp. strains: *Pseudomonas* sp. FC 7B (EU836174), *Pseudomonas putida* FC 8B (EU836171), and *Pseudomonas* sp. FC 9B (EU836172). These strains were previously isolated from a suppressive rockwool substrate in a soilless system (Clematis *et al*., 2009; Srinivasan *et al*., 2009) (Table 1). The bacterium strains were maintained at 4°C in Luria Bertani (LB) slants throughout the study. The fresh bacterium suspensions were each prepared by inoculating a loop-full of cells into 30 mL of LB medium in 100 ml capacity Erlenmeyer flasks, and then incubating the suspension on a rotary shaker at 600 rpm. The cell suspension was centrifuged and resulting pellets were re-suspended in sterile deionized water. The optical densities (OD_{600}) of cultures incubated for 48 h at 23°C were checked immediately before application, and was adjusted with sterile deionized water to 1×10^8 cells mL^{-1} before application. *Trichoderma* sp. TW2 was grown in a 1000 mL capacity flask containing 200 mL of potato dextrose broth (Sigma-Aldrich) and maintained under static conditions at 23°C. After 13 to 15 d, the produced conidia and mycelium were transferred to 200 mL of sterile distilled water and homogenized using a hand-held rotary mixer. The conidium suspension obtained for the *Trichoderma* sp. TW2 isolate was standardized to 1×10^7 cfu mL^{-1}.

The antagonist *Fusarium solani* FUS25 was propagated in 1000 mL capacity-flasks each containing 250 mL of potato dextrose broth maintained on a rotary shaker for 8 to 10 d at 160 rpm. The cultures were centrifuged at 8,000 g for 20 min at 4°C. Conidia and mycelium pellets were each transferred into 200 mL of sterile distilled water and homogenized using a rotary mixer. The inoculum suspensions were adjusted with sterile deionized water to 1×10^7 conidia mL^{-1} before application.

Each BCA suspension was applied at a final concentration of 1×10^7 cfu mL^{-1} to each pot and around the base of 15-d-old seedlings immediately after planting.

The BCAs were applied to the growing medium five times at 7 d intervals using 100 mL per pot of the suspension, following experimental Protocol III (Table 1). The experimental BCAs were compared with a commercial formulation of *Trichoderma asperellum* + *T. gamsii* (10% a.i.; 'Remedier', Isagro), applied at the label rate of 0.25 g per liter of peat substrate (Table 1).

Phytophthora capsici *strain and inoculation*

A highly virulent strain of *Phytophthora capsici* (coded PHC 6/16; AGROINNOVA culture collection), originally isolated from sweet pepper, was cultured on selective oomycete medium (Masago *et al*., 1977) at 20°C for 1 week. Zoospores were produced according to a modified protocol of that described by Kim *et al*., (1997). One mycelium/agar plug (5 mm in diam.), taken from an actively growing colony, was transferred to a 1000 mL capacity flask containing a wheat-hempseed medium (200 g wheat kernels, 100 g hempseeds, 320 mL water, sterilized at 121°C for 30 min), and then incubated at 22°C in a growth chamber under continuous light for 7 d, followed by 3 d at 15°C in darkness. Zoospore suspension was prepared by mixing 80 g of the oomycete biomass in 1 L of distilled water, mixing the suspension for 10 min, then removing the aqueous extract from solid sediment by filtering through two layers of cheesecloth and vigorously mixing it. Zoospores were released by chilling the liquid cultures at 4°C for 1 h, followed by 1 h at room temperature (25°C). The zoospore concentration was adjusted to 1×10^5 zoospores mL^{-1} using a haemocytometer. A 10 mL aliquot of the zoospore suspension was then pipetted onto the peat media around the base of each plant.

In trials 1 to 6, the first treatment with salts was carried out 48 h before infestation of the peat substrate, while in trials 7 to 12, the first treatment with BCAs was carried out 48–72 h before infestation of the peat substrate (Table 1).

Disease assessments, and statistical analyses

The sweet pepper plants were assessed starting from the first appearance of wilt caused by *P. capsici* root and crown infections. Disease incidence (DI) was evaluated at intervals of 3 to 7, d by counting and removing the dead plants with symptoms of Phytophthora root, crown and stem rot. At the final assessment, the remaining plants were removed by each pot and the total number of dead plants including those wilted, due to severe root

Table 1. Protocols adopted for different trials.

Experimental Protocol (Trial number, year)	Artificial inoculation	Tested treatment and concentration	Standard reference (dosage)	Application of the treatments	Number and interval between treatments
I (1, 2 and 3; 2018)	48 h after the first treatment, with 1×10^5 zoospores mL^{-1}	Potassium phosphite (P_2O_5: K_2O 0.65+ 0.525 g L^{-1}) and K-silicate (200 mg L^{-1}), alone or combined	Potassium phosphite (P_2O_5: K_2O 1.30 + 1.05 g L^{-1})	In nutrient solution (NS)	Three applications, at 7 d intervals
II (4, 5 and 6; 2019)	48 h after the first treatment, with 1×10^5 zoospores mL^{-1}	Potassium phosphite (P_2O_5 K_2O 0.65+ 0.525 g L^{-1}) and K-silicate (200 mg mL^{-1}), alone or combined	Potassium phosphite (P_2O_5 K_2O 1.30 + 1.05 g L^{-1})	To soil substrate	Three applications, at 7 d intervals
III (7, 8, 9, 10, 11 and 12; 2019-2020)	48-72 h after the first treatment, with 1×10^5 zoospores mL^{-1}	*Fusarium solani* FUS25 (1×10^7 cfu mL^{-1}) *Pseudomonas* (FC 7B, FC 8B, FC 9B) (1×10^7 cfu mL^{-1}) *Pseudomonas* sp. PB26 (1×10^7 cfu mL^{-1}) *Trichoderma* TW2 (1×10^7 cfu mL^{-1})	*Trichoderma gamsii* + *T. asperellum* (0.25 g L^{-1})	To soil substrate	Five applications, at 7 d intervals

infection by the pathogen, were counted. Final disease incidence (DI) was then calculated, expressed as percent, of dead and wilted plants over the total plants examined. Areas under the disease-progress curves (AUDPCs) were calculated using the formula of Shaner and Finney (1977), for a total number of observations per trial of three to five disease incidence assessments. The biomass of healthy plants (fresh weight from 1–2 cm above soil surface) in each experimental unit (six pots), was measured at the end of trials 7 to 12 in Protocol III.

The experimental units each consisted of a 3 L capacity pot with two plants (six pots), and sub-replicates contained 12 plants/treatment. Trials carried out using each of the three protocols were repeated at least three times (Tables 1 and 1S), and they were combined when the 'trial' factor was not statistically significant ($P > 0.05$).

Analysis of variance (ANOVA) with SPSS software (Version 26) was used to determine the effects of trial, treatments and their interactions, on disease incidence (DI) calculated at the end of each trial, AUDPC and fresh weight data. Prior to ANOVA, homogeneity of variances was evaluated and arcosin transformation of the percentage data was applied when necessary to normalize variances. When a statistically significant F test was obtained for treatments ($P \leq 0.05$), the data were subjected to mean separation using Tukey's test at $P \leq 0.05$.

RESULTS

Efficacy of resistance inducers (dosage, type of application) against Phytophthora crown rot

First symptoms of Phytophthora root and crown rot and sometimes black lesion on stems started to be visible between 4 to 7 d after inoculation during the trials carried out using Protocols I and II. These symptoms then developed quickly (average air temperature ranging from 24 to 28°C), with the final assessments carried out 27 to 33 d after planting (Protocol I), or 17 to 28 d after planting (Protocol II).

Both K-phosphite (df = 2, F = 261.324; $P \leq 0.0001$) and K-silicate, (df = 1, F = 5,220; $P \leq 0.024$), and K-phophite + K-silicate (df = 2, F = 13.685; $P \leq 0.0001$) affected the percentage of dead plants (DI) and the development of Phytophthora crown rot (AUDPC) (K-phospite: df = 2, F =161,784; $P \leq 0.0001$. K-silicate: df = 1; F = 5,747; $P \leq 0.018$. K-phosphote + K-silicate: df = 2; F = 13.823; $P \leq 0.0001$) (Table 2). Neither the type of application of K-phosphite (df = 2, F = 0.431; $P = 0.263$) or K-silicate (df = 1; F = 0.501; $P = 0.480$), nor the interaction of the K-phosphite + K-silicate treatment with the type of application (df = 2; F = 1.089; $P = 0.339$), affected disease incidence. Similarly, these treatments did on affect crown rot development (K-phosphite: df = 2, F = 0.679; $P = 0.359$. K-silicate: df = 1, F = 0.021; $P = 0.885$. K-phosphite + K-silicate: df = 2, F = 0.288; $P = 0.750$) (Table 2).

Table 2. Analyses of variance for disease incidence (DI) as percentage of dead and wilted plants and areas under disease progress curve (AUDPCs) for pepper 'Corno di toro' plants inoculated with *P. capsici* and treated with salts treatments (K-phospite, K-silicate or K-phospite + K-silicate), the type of application (in nutrient solution or to the soil substrate), and their interactions, calculated at the end of trails 1 to 6, according to F tests.

Considered factors and their interaction	df[a]	F values[b]	
		DI	AUDPC
K-phosphite treatment	2	261.324***	161.784***
K-silicate treatment	1	5.220*	5.747**
K-phosphite + K-silicate combined treatment	1	461.312***	90.003***
K-phosphite × K-silicate interaction	2	13.685***	13.823***
K-phosphite × type of application	1	0.431	0.679
K-silicate × type of application	1	0.501	0.021
K-phosphite × K-silicate × type of application	2	1.089	0.288

[a] Degrees of freedom between groups.
[b] Symbols *, **, *** indicate significance at, respectively, $P \leq 0.05$, $P \leq 0.001$ or $P \leq 0.0001$, according to F tests.

The DI and AUDPC data from each set of trials carried out according to Protocol I (Trials 1 to 3) or Protocol II (trials 4 to 6) were analyzed together for each experimental run (Tables 3 and 4), because statistically significant differences were not observed among trials ($P > 0.05$). The average incidence of Phytophthora root and crown rots was 46% in the untreated controls in trials 1, 2 and 3, and was greater (DI = 93%) in trials 4, 5 and 6 (Table 3).

The most efficacious control of the pathogen was observed from K-phosphite at the standard dosage (80% efficacy) in all the experiments for both types of application (Table 3), while efficacy the half rate treatments also reduced percentage of dead plants (compared to the untreated controls) by 47%, when applied via the nutrient solution, or by 62% when applied directly to the soil substrate.

K-silicate alone reduced the percentage of dead plants with 20–23% efficacy. No improvement in disease control was observed when K-silicate was applied in combination with K-phosphite for either of the tested doses. Slightly less disease control was observed for K-phosphite, at the standard dosage, combined with K-silicate, when applied via nutrient solution (68% efficacy) or to

Table 3. Mean disease incidences from K-silicate or K-phosphite salt treatments, alone or in combinations, when applied against Phytophthora crown rot caused by *Phytophthora capsici* on soilless grown sweet pepper 'Corno di Toro' plants. Data are average percentages of wilted and dead plants (disease incidence, DI) at the end of trials 1, 2 and 3, where Protocol I was used (see text), and trials 4, 5 and 6, where Protocol II was used.

Treatment (dosages: a.i.)[a]	Mean Disease Incidence (DI)					
	Treatments applied to the NS (Protocol I)			Treatments applied to the substrate (Protocol II)		
Untreated control	45.7 ± 3.2	d[c]	E %[d]	93.3 ± 2.0	d	E %
K-silicate (200 mg L^{-1})	35.0 ± 3.4	cd	23.4	73.3 ± 5.0	c	20.4
K-phosphite (P_2O_5:K_2O 0.65, + 0.525 g L^{-1})	24.4 ± 3.4	bc	46.5	35.6 ± 3.2	b	61.1
K-phosphite (P_2O_5:K_2O, 0.65 + 0.525 g L^{-1}) +K-silicate (200 mg L^{-1})	21.7 ± 2.5	b	52.6	34.4 ± 1.8	b	63.1
K-phosphite (P_2O_5:K_2O, 1.30 + 1.05 g L^{-1})	8.9 ± 2.1	a	80.5	18.3 ± 2.3	a	80.4
K-phosphite (P_2O_5:K_2O, 1.30 + 1.05 g L^{-1}) + K-silicate (200 mg L^{-1})	14.4 ± 1.3	ab	68.4	24.4 ± 2.6	ab	73.8
Trial[b]	df = 2; F = 2.888; P = 0.057			df = 2; F = 0.9555; P = 0.389		
K-phosphite	df = 1; F = 50.910; P < 0.0001			df = 1; F = 186.005; P < 0.0001		
K-silicate	df = 1; F = 7.704; P = 0.007			df = 1; F = 9.469; P = 0.003		
K-phosphite + K-silicate combined treatment	df = 1; F = 6,429; P = 0.017			df = 1; F = 9,870; P = 0.004		
K-phosphite × K-silicate interaction	df = 1; F = 8.432; P = 0.005			df = 1; F = 2.918; P = 0.05		
Treatments	df = 5; F = 24.040; P < 0.0001			df = 5; F = 97.006; P < 0.0001		

[a] K_2SiO_3 at 200 mg L^{-1} and K-phosphite (standard dosage of P_2O_5:K_2O, 1.30 + 1.05 g L^{-1} or half dosage of P_2O_5:K_2O, 0.65 + 0.525 g L^{-1}) or their combinations, were added directly to the nutrient solution NS (Protocol I), or to the soil substrate (Protocol II) in each pot using 100 mL/pot of suspension. The treatments were carried out three times, at 7 d intervals.

[b] Values from trials 1, 2 and 3 or trials 4, 5 or 6, each with five replicates per treatment, were combined when statistically significant differences were not observed (Trial P > 0.05). Significant according to the F tests and degrees of freedom (df) used in its calculation. Each mean is associated with its standard error (± SE).

[c] Means in the same column, followed by the same letter, do not differ according to Tukey's Test ($P \leq 0.05$). Each mean is associated with its standard error (± SE).

[d] E%: percentage reduction of disease incidence of wilted and dead plants, compared to the untreated controls, at the end of trials 1, 2 or 3, corresponding to, respectively, 30, 25 or 24 d after inoculation (Protocol I), and at the end of trials 4, 5 or 6, corresponding to, respectively, 35, 21 or 17 d after inoculation (Protocol II).

the substrate (74% efficacy) (Table 3). Similar effects were observed for K-phosphite, at a reduced dosage, combined with K-silicate, when applied via nutrient solution (53% efficacy) or to the substrate (63% efficacy) (Table 3).

For AUDPC values, K-silicate reduced disease development, compared to the untreated control, for both types of application. K-phosphite, at both tested dosages, applied alone or combined with K-silicate, affected AUDPC compared to the untreated control, and differences among these treatments (Table 4).

K-phosphite and K-silicate either alone or combined, applied via nutrient solution or when distributed to the growing medium, did not reduce the development of sweet pepper plants (data not shown).

Effects of biocontrol agents

First symptoms of Phytophthora root and crown rots started to be visible at 5 to 13 d after inoculations with *P. capsici* carried out 48–72 h after planting during the trials carried out using Protocol III. These symptoms rapidly under the experimental conditions used (average air temperature 24 to 28°C), with the final assessment carried out between 34 to 37 d after planting trials 7-9, and 23 to 26 d in trials 10-12 carried out with Protocol III.

The data from trials 7, 8 and 9 (DI, df = 2, F = 0.369, P = 0.545; AUDPC, df = 2, F = 0.073, P = 0.930), and from trials 10, 11 and 12 (DI, df = 2, F = 2.252, P = 0.111; AUDPC, df = 2, F = 0.781, P = 0.461), were combined when there was heterogeneity between the trial runs (Tables 5 and 6). Inoculation with the pathogen led to high disease incidence in the untreated controls (78% in trials 7, 8 and 9 and 63% in trials 10, 11 and 12), permitting evaluation of the different BCAs under study (Table 5). All the BCAs reduced DI in the trials 7, 8 and 9 (df = 5, F = 18.021, P < 0.0001) and in trials 10, 11 and 12 (df = 5, F = 15.538, P < 0.0001), compared to the untreated controls. The experimental biocontrol agents generally gave more disease control than the commercial formulation of *Trichoderma asperellum* + *T. gamsii*

Table 4. Mean areas under disease progress (AUDPCs) after treatments with K-silicate and K-phosphite salts, alone or in combinations, applied against Phytophthora crown rot caused by *Phytophthora capsici* to soilless grown plants of sweet pepper 'Corno di Toro'. These data were obtained at the end of trials 1, 2 and 3, using Protocol I, and trials 4, 5 and 6 using Protocol II (see text).

Treatment (Dosage a.i.)[a]	AUDPC[b]			
	Treatment applied to the NS (Protocol I)		Treatment applied to the substrate (Protocol II)	
Untreated control	846.4 ± 76.01	c[d]	1,376.9 ± 60.8	c
K-silicate (200 mg L^{-1})	533.6 ± 47.7	b	1,045.0 ± 105.9	b
K-phosphite (P_2O_5: K_2O 0.65 + 0.525 g L^{-1})	413.3 ± 59.7	ab	396.9 ± 46.2	a
K-phosphite (P_2O_5: K_2O 0.65 + 0.525 g L^{-1}) + K-silicate (200 mg L^{-1})	452.8 ± 54.3	ab	404.4 ± 33.4	a
K-phosphite (P_2O_5: K_2O 1.30 + 1.05 g L^{-1})	236.9 ± 45.2	a	219.2 ± 35.7	a
K-phosphite (P_2O_5: K_2O 1.30 + 1.05 g L^{-1}) + K-silicate (200 mg L^{-1})	259.4 ± 31.9	a	321.4 ± 43.2	a
Trial[d]	df = 2; F = 2.442; $P = 0.093$		df = 2; F = 0.388 $P = 0.244$	
K-phosphite	df = 1; F = 28.861; $P < 0.0001$		df = 1; F = 26.036; $P < 0.0001$	
K-silicate	df = 1; F = 9.202; $P = 0.003$		df = 1; F = 4.951; $P = 0.029$	
K-phosphite + K-silicate combined treatment	df = 1; F = 9,423; $P = 0.005$		df = 1; F = 5,311; $P = 0.014$	
K-phosphite × K-silicate interaction	df = 1; F = 9.485; $P = 0.003$		df = 1; F = 12.976; $P = 0.001$	
Treatment	df = 5; F = 16.800; $P < 0.0001$		df = 5; F = 61.923; $P < 0.0001$	

[a] K_2SiO_3 at 200 mg L^{-1} and K-phosphite (standard dosage of P_2O_5: K_2O 1.30 + 1.05 g L^{-1} or half dosage of P_2O_5: K_2O 0.65 + 0.525 g L^{-1}) or their combinations, added directly to the nutrient solution NS (Protocol I), or to the substrate in each pot using 100 mL per pot of the suspension prepared (Protocol II). The treatments were carried out three times every 7 days.

[b] AUDPC values were calculated for three to four assessments at 6-7 d intervals during trials 1, 2 and 3 (Protocol I), and four or five assessments at 3-6 d intervals during trials 4, 5 and 6 (Protocol II).

[c] Values from trials 1, 2 and 3 or trials 4, 5 and 6, each with five replicates per treatment, are combined when statistically significant differences (trial $P > 0.05$; F tests) were not observed.

[d] Means in each column followed by the same letter are not different ($P \leq 0.05$; Tukey's Test). Each mean is associated with its standard error (± SE).

Table 5. Mean Phytophthora crown rot incidences after applications of experimental BCA treatments, applied according to Protocol III, on for soilless grown sweet pepper 'Corno di Toro'. The data are average disease incidence (DI) at the end of trials 7, 8 and 9 and 10, 11 and 12.

Treatment[a]	Disease incidence (DI)					
	Trials 7, 8, and 9			Trials 10, 11 and 12		
Untreated control	77.8 ± 3.2	d[c]	% E[d]	62.5 ± 4.2	c	% E
Fusarium solani FUS 25	30.6 ± 4.0	a	60.7	22.2 ± 3.3	a	64.4
Pseudomonas sp. FC 7, FC 8, FC 9	42.8 ± 4.1	ab	45.0	30.4 ± 3.0	ab	51.4
Pseudomonas sp. PB 26	40.6 ± 3.5	ab	47.9	34.4 ± 3.2	ab	44.9
Trichoderma sp. TW 2	46.7 ± 4.7	b	40.0	36.9 ± 3.0	b	40.9
Trichoderma asperellum + T. gamsii	61.1 ± 4.2	c	21.4	36.4 ± 3.8	b	41.8
Trial[b]	df = 2; F = 0.369; $P = 0.545$			df = 2; F = 0.781; $P = 0.461$		
Treatment	df = 5; F = 18.021; $P < 0.0001$			df = 5; F = 15.538; $P < 0.0001$		

[a] The BCA suspensions were applied (at 1×10^7 cfu mL^{-1}) to each pot and around the base of 15 d-old seedlings after planting, six times at 5 d intervals using 100 mL per pot of the suspension. The experimental BCAs were compared with a commercial formulation of *Trichoderma asperellum + T. gamsii* (10% a.i., 'Remedier', Isagro), applied at the label rate of 0.25 g L^{-1} of peat substrate.

[b] Values from trials 7, 8 and 9 or trials 10, 11 and 12, each with five replicates per treatment, are combined when statistically significant differences ($P > 0.05$; F tests) were not observed.

[c] Means in each column followed by the same letter are not different ($P \leq 0.05$; Tukey's Test). Each mean is associated with its standard error (± SE).

[d] E%: percent disease incidence reduction, calculated as dead and wilted plants, compared to the untreated controls, at the end of the trials corresponding to 31, 31 or 34 d after inoculation for, respectively, trials 7, 8 and 9, and 23, 21 or 22 days after inoculation for, respectively, trials 10, 11 and 12.

Table 6. Mean areas under disease progress curves after applications of different experimental BCA treatments, applied according to Protocol III, for Phytophthora crown rot caused by *P. capsici* on soilless grown sweet peppers 'Corno di Toro'. The data are expressed as average area under disease progress (AUDPC) at the end of trials 7–9 and 10–12.

Treatment[a]	AUDPC[b]			
	Trials 7, 8 and 9		Trials 10, 11 and 12	
Untreated control	1,814.4 ± 75.7	d[d]	1,457.2 ± 62.9	c
Fusarium solani FUS 25	584.7 ± 72.2	a	442.6 ± 57.8	a
Pseudomonas sp. FC 7, FC 8, FC 9	852.8 ± 103.7	a-c	574.6 ± 55.5	ab
Pseudomonas sp. PB 26	806.1 ± 76.3	ab	673.3 ± 72.1	ab
Trichoderma sp. TW 2	947.2 ± 80.7	bc	727.5 ± 57.5	b
Trichoderma asperellum + *T. gamsii*	1,170.0 ± 77.2	c	660.3 ± 61.1	ab
Trial[c]	df = 2; F = 0.073; P = 0.930		df = 2; F = 2.252; P = 0.111	
Treatment	df = 5; F = 27.655; P < 0.0001		df = 5; F = 33.733; P < 0.0001	

[a] The BCA suspensions (1 ×10^7 cfu mL^{-1}) were applied five times after planting at 7 d intervals to individual pots around the base of 15 d-old seedlings, using 100 ml of suspension per pot. The experimental BCAs were compared with a commercial formulation of *Trichoderma asperellum* + *T. gamsii* (10% a.i.; 'Remedier', Isagro), applied at the label rate of 0.25 g L^{-1} of peat substrate.
[b] AUDPC values were calculated considering four to five assessments at 4 to 9 d intervals during trials 7, 8 and 9, and four assessments at 4 to 8 d intervals during trials 10, 11 and 12.
[c] Values from trials 7, 8 and 9 or trials 10, 11 and 12, each with five replicates per treatment, are combined when statistically significant differences (P > 0.05; F tests with and degrees of freedom (df) indicated.
[d] Means each column accompanied by the same letter are not different (P ≤ 0.05; Tukey's Test). Each mean is accompanied by its standard error (± SE).

(22 to 42% efficacy). The greatest and most consistent *P. capsici* control was from *Fusarium solani* FUS25, which reduced proportions of dead plants by 61 to 65%. Both of the tested experimental *Pseudomonas* treatments (PB 26 and the mixture of FC 7B, FC 8B and FC 9B) showed similar disease control trends, with 45 to 51% disease reduction, compared to the untreated controls. *Trichoderma* sp. TW2, applied to the growing media every 7 d, provided a consistent disease reduction of 40–41%.

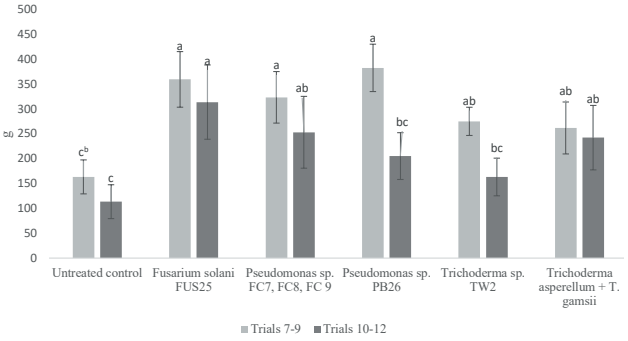

Figure 1. Mean fresh weight biomass (g)[a] of healthy sweet peppers 'Corno di Toro' plants treated according to Protocol III at the end of trials 7, 8 and 9 (31 to 34 d after inoculation), and trials 10, 11 and 12 (21 to 23 d after inoculation). [a] Mean fresh weight of plants per treatment from trials 7, 8 and 9 (df = 5; F = 30.446; P < 0.0001) or trials 10, 11 and 12 (df = 5; F = 34.384; P < 0.0001), each with five replicates per treatment, are combined because significant differences were not observed for trials 7, 8 and 9 (df = 2; F = 2.684 P = 0.055) or trials 10, 11 and 12 (df = 2; F = 1.701 P = 0.190), as indicated by F tests. [b]Means accompanied by the same letter do not differ (P ≤ 0.05; Tukey's Test). Each mean is accompanied by associated with its standard error (± SE).

Disease reductions were observed for all the tested BCAs, and a similar trend was observed for the different disease amounts in trials 7, 8 and 9 (df = 5, F = 27.655, P < 0.0001) and trials 10, 11 and 12 (df = 5, F = 33.733, P < 0.0001). The least AUDPC values, compared to the non-treated controls, were from *Fusarium solani* FUS25, followed by the tested *Pseudomonas* strains and *Trichoderma* TW2 (Table 6).

Applications of the BCAs to the growing media generally increased fresh plant biomass at the end of both sets of trials, compared to the untreated controls, although inconsistent results were observed for *Pseudomonas* PB26 and *Trichoderma* TW2 (Figure 1).

DISCUSSION

Phytophthora capsici is a broad host range pathogen (Granke *et al*., 2012), important in most sweet pepper growing areas. There are few chemical options for management of the diseases caused by this pathogen, due to the lack of effective soil fumigants, its resistance to some effective fungicides (Bower and Coffey, 1985; Hwang *et al*., 1996; Lamour and Hausbeck, 2001; Parra and

Ristaino, 2001; Tamietti and Valentino, 2001; Kousik *et al*., 2008; Miao *et al*., 2016; Barchenger *et al*., 2018; Hunter *et al*., 2018), and the complexity for host breeding to select cultivars resistant to local pathogen isolates (Acquadro *et al*., 2020).

Soilless crop cultivation is expanding throughout the world, but by itself this approach cannot solve the problems of managing soil-borne pathogens (Jenkins and Averre, 1983), since many of them, including *P. capsici*, may be introduced through infected planting material (Granke *et al*., 2012) or irrigation water (Ristaino *et al*., 1993; Hong and Moorman, 2005; Gevens *et al*., 2007). Growth and spread of zoosporic pathogens are particularly severe problems in soilless systems (Stanghellini and Rasmussen, 1994). Management strategies that minimize inoculum dispersal have, therefore, considerable potential for disease reduction. Increased understanding of the impacts of crop management measures in soilless systems is needed for the sweet pepper-*P. capsici* pathosystem.

The present study examined the efficacy of resistance inducers, based on K-phosphite and K-silicate, used alone or in combinations, and of experimental biocontrol agents under conditions of high disease pressure, in a closed soilless system. K-silicate only partially reduced the incidence of *P. capsici* (20–23% efficacy) and its development, also when combined with K-phosphite, at the tested standard or reduced dosages. However, phosphite combinations could possibly reduce the risks of selection of *Phytophthora* isolates resistant to phosphite (Hunter *et al*., 2018), and address control of more than one pathogen in integrated pest management. Addition of 75 or 100 mg L^{-1} of silicon to the hydroponic nutrient solution reduced the severity of anthracnose caused by *Colletotrichum capsici* or *C. gloeosporioides* in *Capsicum annuum* (Jayawardana *et al*., 2015).

The mode of action of silicates and their functioning in several pathosystems are not yet fully understood. French-Monar *et al*., (2010) reported that bell pepper plants treated with calcium silicate had reduced root lesions and crown and stem necrosis caused by *P. capsici*, although at lower levels of reduction than found in other hosts. Together with possible formation of physical barriers to pathogens, from silicon accumulation in plants with differences depending on species, this element can influence plant defense responses and interact with key components of plant stress signalling systems, thus leading to induced resistance to pathogens (Liang *et al*., 2006; Wang *et al*., 2017).

Of the products tested in the present study, potassium phosphite provided the best control of *P. capsici*, when applied to pepper plants by adding soluble forms to nutrient solution of the closed hydroponic system, and when added to the growing medium. No effects on pepper development were detected after addition of this compound. However, the possible phytotoxic effects of phosphite, applied in soilless systems via a nutrient solution, should be considered. These compounds may precipitate and accumulate, as has been described for several fertilizers (Sambo *et al*., 2019). For example, tomato and pepper plants treated with either commercial or technical formulations of phosphite in a soilless system exhibited reduced growth (Forster *et al*., 1998).

The results obtained in the present study are similar to those of Förster *et al*. (1998), who observed reduced symptoms caused by *P. capsici* on tomato and pepper plants grown in a greenhouse hydroponic system treated with phosphite. Several factors are associated with the inhibition of pathogen growth as a result of phosphite treatments. These include phosphite concentration, the nature of the salts, the acidification of the plant growth medium and the pathogen life cycle (Guest and Bompeix, 1990; Smillie *et al*., 1989; Khalil *et al*., 2009; Khalil and Alsanius, 2011; Sambo *et al*., 2019). The results obtained in the present study show that the concentration of applied K-phosphite affected control of Phytophthora root and crown rot of sweet pepper, with greatest control provided by the standard dosages here tested.

Phosphite may act directly on pathogens, by inhibiting their growth (Fenn and Coffey, 1984, Smillie *et al*., 1989; Grant *et al*., 1990; Smillie *et al*., 1989), and possibly by priming the host defense in several pathosystems during pre-infection or post-inoculation stages of the pathogens. Liu *et al*. (2016) reported that phosphite, at >5 μg mL^{-1}, had a direct effect on mycelium growth and zoospore production in the sweet pepper-*P. capsici* pathosystem. Moreover, this compound increased transcription of antioxidant enzyme genes, and those involved in ethylene and abscisic acid biosynthesis, which mediated control of the pathogen at a higher phosphite concentration (1 g L^{-1}) (Liu *et al*., 2016).

Phosphites are receiving a growing interest in horticulture (Gomez-Merino and Trejo-Téllez, 2015). Their application to soilless cultivation should be tested on different host-pathogen combinations, because some host plants are more responsive to phosphite than others (Guest and Bompeix, 1990; Shearer and Crane, 2012). Potassium phosphite reduced the Phytophthora crown rot of soilless grown zucchini grown by 62–94%, when applied directly to growing media, or via a nutrient solution, when the pathogen was inoculated 5–7 d before planting (Gilardi *et al*., 2020). Phosphites are particularly active against oomycetes and have long been used for management of Phytophthora diseases in several

crops (Fenn and Coffey 1984; Smillie *et al*., 1989; Guest and Bompeix, 1990; Förster *et al*., 1998, Dobrowolski *et al*., 2008), and in specific situations, based on greenhouse and field studies of soil-borne pathogens in several pathosystems. These include tomato/*Phytophthora nicotianae* (Gilardi *et al*., 2014); zucchini/*P. capsici* (Gilardi *et al*., 2015); lettuce/*Fusarium oxysporum* f. sp. *lactucae*; rocket/*Fusarium oxysporum* f. sp. *raphani* (Gilardi *et al*., 2016); potato/*Rhizoctonia solani* (Lobato *et al*., 2010), and common bean/*Sclerotinia sclerotiorum* (Fagundes-Nacarath *et al*., 2008).

Biocontrol agents may be worthwhile for disease management in soilless production systems (Paulitz, 1997; Postma, 2009; Vallance *et al*., 2011; Lee and Lee, 2015). In the past 20 years, several studies have demonstrated reduced disease and practical implementation (Lamichhane *et al*., 2017; Villeneuve, 2017; Barratt *et al*., 2018; Raymaekers *et al*., 2020). In the present study, the *Pseudomonas putida* isolate mixture (FC 7B, FC 8B, FC 9B), *Pseudomonas* sp. PB26, *F. solani* FUS25 and *Trichoderma* sp. TW2, introduced into the soilless system 48-72 h before the pathogen inoculation, followed by four applications at 7 d intervals, reduced *P. capsici* on pepper by 45 to 64%. This result indicates further research is warranted. The most consistent results in control of Phytophthora crown rot were provided by *F. solani* FUS25 (60-64%% efficacy). The same biocontrol strain sometimes provided good, but variable results (8-54% efficacy) on zucchini, when applied to growing medium immediately at inoculation with *P. capsici* and 5–6 d before planting (Gilardi *et al*., 2020). Although the mechanism of action of *F. solani* FUS25 is not known, the most likely strategy for its use should be as a protectant or in preventative treatments. Establishment of BCAs in host root systems can also vary according to the host. The root systems of sweet pepper have greater surface areas than root systems of zucchini, which instead develops roots with few branches.

The good results obtained in the present study add evidence for applying BCAs in soilless cultivation systems against diseases caused by oomycetes. *Pseudomonas* sp. is known to be effective in reducing cucumber root colonization by *Pythium aphanidermatum* (Moulin *et al*., 1994; Chatterton *et al*., 2004), and Pythium disease on cucumber grown in a closed rockwool system (Postma *et al*., 2000). *Streptomyces griseoviride* ('Mycostop') is effective against *Pythium ultimum* on cucumber (Wolfhechel and Funck Jensen, 1991), while *Trichoderma virens* ('Soilgard') and *Gliocladium catenulatum* ('Prestop') are active against *Pythium aphanidermatum,* the causes of the damping-off of cucumbers grown in rockwool (Punja and Yip, 2003).

Increased understanding of BCA modes of action is needed to achieve a widespread application of these agents. Disease suppression could be related to different mechanisms: including production of antibiotics, secondary metabolites, lytic enzymes, phytohormones, siderophores, volatiles, and induction of host resistance (Köhl *et al*., 2019). For example, pepper plants inoculated with *Fusarium oxysporum* f. sp. *lycopersici* developed local and systemic resistance against *P. capsici* (Silvar *et al*., 2009), and the foliar pathogen *Botrytis cinerea* (Dı´az *et al*., 2005). Endophytic *Trichoderma* isolates induced resistance in hot pepper to *P. capsici* (Bae *et al*., 2011). *Pseudomonas* induced motility inhibition of *P. capsici* zoospores (Zohara *et al*., 2016), which are the only mobile propagules found in recirculating nutrient solutions (Stanghellini *et al*., 1996). Iron competition was important in the antagonistic activity of *Trichoderma asperellum* against *F. oxysporum* f. sp. *lycopersici* of tomato grown in a soilless medium based on perlite (Segarra *et al*., 2010).

Little is known about the capability of biocontrol agents to suppress Phytophthora blight on peppers grown in soilless systems.

Selected strains of the *Pseudomonas*, *Bacillus*, and *Trichoderma* have long been known for ability to improve plant growth and induce host systemic resistance against diseases and pests in different ecosystems, including soilless systems (Paulitz, 1997; Domenech *et al*., 2006; Gravel *et al*., 2007; Berg, 2009; Lee and Lee, 2015.; Sambo *et al*., 2019). Several biocontrol agents introduced into hydroponically grown fruit and vegetables have provided positive effects on yields and quality of horticultural products. In the present study, significant reduction in Phytophthora crown rot observed after treatment with *Fusarium solani* FUS25 was confirmed, by increased biomass fresh weight, with similar or greater increases than those from the commercial mixture of *Trichoderma asperellum* + *T. gamsii*.

In general, if a biocontrol agent is given time to become well-established in plant growth media, before pathogens are introduced (often through planting material), it can prevent infections or can interfere with pathogen inoculum production that may spread throughout the systems (Fry, 1982). *Pseudomonas chlororaphis*, *Bacillus cereus*, and *B. gladioli* strains, applied in small-scale hydroponic units, suppressed root colonization of chrysanthemum by *Pythium aphanidermatum* when applied 14-7 d before pathogen inoculation, rather than at the same time as inoculation (Liu *et al*., 2007). Selected antagonistic *Pseudomonas*, *Fusarium* or *Trichoderma* strains, previously tested in pot trials in peat medium against Fusarium wilt agents of lettuce and wild rocket

(Gilardi *et al*., 2019; Srinivasan *et al*., 2009), or in naturally infested soil in a zucchini-*P. capsici* pathosystem (Cucu *et al*., 2020), were here used in preventative treatments in a closed soilless system, before inoculation of peat substrate with *P. capsici*. Optimizing the conditions in the soilless environment to which biocontrol agents were introduced, resulted in improved disease management consistency.

The results obtained in this study provide evidence for using phosphite-based products and biocontrol agents against Phytophthora crown and root rot of pepper, grown in soilless systems. They also show that there is not one solution for the management of these diseases. Different options should be considered and adapted to the different situations, relying on good extension services. Soilless cultivation provides good opportunities for exploitation and practical application of new disease management tools, such as resistance inducers and biocontrol agents. These have been intensively studied in recent years, expanding the integrated disease management options for intensive vegetable production (Paulitz, 1997; Lamichhane *et al*., 2017; Messelink *et al*., 2020).

ACKNOWLEDGEMENTS

This research was funded from Fondazione Cassa Risparmio Cuneo, Agroalimentare 4.0, SFIDA Project 'Low environmental impact management strategies for the horticultural sector'. The authors thank Marguerite Jones for language revision of the paper manuscript, and Dr. Massimo Pugliese and AgriNewTech s.r.l for providing the *Pseudomona*s sp. PB26, *Fusarium solani* FUS25 and *Trichoderm*a sp. TW2 microorganisms. The authors thank the anonymous referees and Prof. Richard Falloon for the helpful suggestions and manuscript improvement.

LITERATURE CITED

Acquadro A., Barchi L., Portis E., Nourdine M., Carli C., … Lanteri S., 2020. Whole genome resequencing of four Italian sweet pepper landraces provides insights on sequence variation in genes of agronomic value. *Scientific Reports* 10: 9189.

Bae H., Roberts D. P., Lim H.-S., Strem M. D., Park S.-C., … Bailey, B. A., 2011. Endophytic *Trichoderma* isolates from tropical environments delay disease onset and induce resistance against *Phytophthora capsici* in hot pepper using multiple mechanisms. *Molecular Plant Microbe Interactioms* 24: 336–351.

Barchenger D.W., Lamour K.H., Bosland P.W., 2018. Challenges and strategies for breeding resistance in *Capsicum annuum* to the multifarious pathogen, *Phytophthora capsici*. *Frontiers Plant Science* 9*:* 628.

Barratt B.I.P., Moran V.C., Bigler F., van Lenteren J.C., 2018. The status of biological control and recommendations for improving uptake for the future. *BioControl* 63: 155–167.

Berg G., 2009. Plant-microbe interactions promoting plant growth and health: perspective for controlled use of microorganisms in agriculture. *Applied Microbiology and Biotechnology* 84: 11–18.

Bi Y., Hu J., Cui X., Shao J., Lu X., … Liu X., 2014. Sexual reproduction increases the possibility that *Phytophthora capsici* will develop resistance to dimethomorph in China. *Plant Pathology* 63: 1365–1373.

Bower L. A., Coffey M.D., 1985. Development of laboratory tolerance to phosphorous acid, fosetyl-Al, and metalaxyl in *Phytophthora capsici*. *Canadian Journal of Plant Pathology* 7:1–6.

Calvo-Bado L. A., Petch G. M., Parsons N., Morgan J. A. W., Pettitt T. R., Whipps J. M., 2006. Microbial community responses associated with the development of oomycete plant pathogens on tomato roots in soilless growing systems. *Journal of Applied Microbiology* 100: 1194–1207.

Chatterton S., Sutton J., Boland G., 2004. Timing *Pseudomonas chlororaphis* applications to control *Pythium aphanidermatum*, *Pythium dissotocum*, and root rot in hydroponic peppers. *Biological Control* 30: 360–373.

Cherif M., Asselin A. Belanger R. R., 1994. Defense responses induced by soluble silicon in cucumber roots infected by *Pythium* spp. *Phytopathology* 84: 236–242.

Clematis F., Minuto A., Gullino M.L., Garibaldi A. 2009. Suppressiveness to *Fusarium oxysporum* f. sp. *radicislycopersici* in re-used perlite and perlite–peat substrates in soilless tomatoes. *Biological Control* 48: 108–114.

Cucu M. A., Gilardi G., Pugliese M., Ferrocino I., Gullino M. L., 2020. Effects of biocontrol agents and compost against the *Phytophthora capsici* of zucchini and their impact on the rhizosphere microbiota. *Applied Soil Ecology* 154: 103659.

Dı´az J., Silvar C., Varela M.M., Bernal A., Merino F., 2005. *Fusarium* confers protection against several pathogenic fungi in pepper. *Plant Pathology* 54: 773–780.

Dobrowolski M. P., Shearer B. L., Colquhoun I. J., O'Brien P. A., Hardy G. E. S. J., 2008. Selection for decreased sensitivity to phosphite in *Phytophthora*

cinnamomi with prolonged use of fungicide. *Plant Pathology* 57: 928–936.

Domenech J., Reddy M.S., Kloepper J.W., Ramos B., Gutierrez-Mañero J., 2006. Combined application of the biological product LS213 with *Bacillus*, *Pseudomonas* or *Chryseobacterium* for growth promotion and biological control of soil-borne diseases in pepper and tomato. *Biocontrol* 51: 245–258.

Fagundes-Nacarath I.R.F., Debona D., Brás V.V., Silveira P.R., Rodrigues F.A., 2018. Phosphites attenuate *Sclerotinia sclerotiorum*-induced physiological impairments in common bean. *Acta Physiologiae Plantarum* 40: 198.

FAOSTAT 2019. *Crop Production Data*. Rome: Food and Agriculture Organization of the United Nations. Available at http://www.fao.org/faostat/en/#data. Accessed March 13, 2019.

Fenn M.E., Coffey M.D., 1984. Studies on the *in vitro* and *in vivo* antifungal activity of fosetyl-Al and phosphorous acid. *Phytopathology* 74: 606- 611.

Förster H., Adaskaveg J. E., Kim D. H., Stanghellini M. E., 1998. Effect of phosphite on tomato and pepper plants and on susceptibility of pepper to *Phytophthora* root and crown rot in hydroponic culture. *Plant Disease* 82: 1165–1170.

Foster J.M., Hausbeck M.K., 2010. Resistance of pepper to Phytophthora crown, root, and fruit rot is affected by isolate virulence. *Plant Disease* 94: 24–30.

French-Monar R., Rodrigues F. A., Korndöfer G. H., Datnoff L. E., 2010. Silicon suppresses Phytophthora blight development on bell pepper. *Journal of Phytopathology* 158: 554–560.

Fry W.E., 1982. *Principles of Plant Disease Management*. Academic Press, New York, USA, 378 pp.

Garibaldi A., Gilardi G., Gullino M.L., 2014. Critical aspects in disease management as a consequence of the evolutionof soil-borne pathogens. *Acta Horticolturae* 1044: 43–52.

Gevens A. J., Donahoo R. S., Lamour K. H., Hausbeck M. K., 2007. Characterization of *Phytophthora capsici* from Michigan surface irrigation water. *Phytopathology* 97: 421–428.

Gilardi G., Demarchi S., Martano G., Gullino M.L., Garibaldi A., 2014. Success and failures of grafting pepper against soil-borne pathogens. *Acta Horticulturae* 1044: 67–71.

Gilardi G., Demarchi S., Gullino M.L., Garibaldi A., 2015. Nursery treatments with non-conventional products against crown and root rot, caused by *Phytophthora capsici*, on zucchini. *Phytoparasitica* 43: 501–508.

Gilardi G., Demarchi S., Gullino M.L., Garibaldi A., 2016. Evaluation of the short term effect of nursery treatments with phosphite-based products, acibenzolar-S-methyl, pelleted *Brassica carinata* and biocontrol agents, against lettuce and cultivated rocket fusarium wilt under artificial inoculation and greenhouse conditions. *Crop Protection* 85: 23–32.

Gilardi G., Pugliese M., Gullino M.L., Garibaldi A., 2019. Nursery treatments with resistant inducers, soil amendments and biocontrol agents for the management of the Fusarium wilt of lettuce under glasshouse and field conditions. *Journal of Phytopathology* 167: 98–110.

Gilardi G., Pugliese M., Gullino M.L., Garibaldi A., 2020. Effect of biocontrol agents and potassium phosphite against Phytophthora crown rot, caused by *Phytophthora capsici*, on zucchini in a closed soilless system. *Scientia Horticolturae* 265: 109207.

Gomez-Merino F.C. and Trejo-Téllez L.I.T., 2015. Biostimulant activity of phosphite in horticulture. *Scientia Horticolturae* 196: 82–90.

Granke L. L., Quesada-Ocampo L., Lamour K., Hausbeck M. K., 2012. Advances in research on *Phytophthora capsici* on vegetable crops in the United States. *Plant Disease* 96: 1588–1600.

Gravel V., Antoun H., Tweddell R.J., 2007. Growth stimulation and fruit yield improvement of greenhouse tomato plants by inoculation with *Pseudomonas putida* or *Trichoderma atroviride*: possible role of indole acetic acid (IAA). *Soil Biology and Biochemistry* 39: 1968–1977.

Guest D.I., Bompeix G., 1990. The complex mode of action of phosphonates. *Australasian Plant Pathology* 19: 113–115.

Gullino M.L., Pugliese M., 2011. New strain of *Fusarium solani* and its uses. *Patent number* IT2011TO01016.

Grant B.R., Dunstan R.H., Griffith J.M., Niere J.O., Smillie R.H., 1990. The mechanism of phosphonic (phosphorous) acid action in Phytophthora. *Australasian Plant Pathology* 19: 115–121.

Hausbeck M.K., Lamour K. H., 2004. *Phytophthora capsici* on vegetable crops: research progress and management challengers. *Plant Disease* 88: 1292–1303.

Hong C.X., Moorman G.W., 2005. Plant pathogens in irrigation water: challenges and opportunities. *Critical Reviews in Plant Sciences* 24: 189–208.

Hunter S., Williams N., McDougal R., Scott P., Garbelotto M., 2018. Evidence for rapid adaptive evolution of tolerance to chemical treatments in *Phytophthora* species and its practical implications. *PLOS ONE* 13(12): e0208961.

Hwang B.K., Kim Y.J., Kim C.H., 1996. Differential interactions of *Phytophthora capsici* isolates with pepper genotypes at various growth stages. *European Journal of Plant Pathology* 102: 311–316.

Jayawardana H., Weerahewa, H.L.D., Saparamadu M., 2015. Enhanced resistance to anthracnose disease in chili pepper (*Capsicum annuum* L.) by amendment of the nutrient solution with silicon. *The Journal of Horticultural Science and Biotechnology* 90: 557–562.

Jenkins S.F., Averre C.W., 1983. Root diseases of vegetables in hydroponic culture systems. *Plant Disease* 67: 968–970.

Khalil S., Alsanius, W.B., Hultberg M., 2009. Effect of growing media on the interaction between biocontrol agents and root pathogens in a closed hydroponic system. *Journal of Horticultural Science and Biotechnology* 84: 489–494.

Khalil S., Alsanius W.B., 2011. Effect of growing medium water content on the biological control of root pathogens in a closed soilless system. *Journal of Horticultural Science and Biotechnology* 86: 298–304.

Kim K. D., Nemec S., Musson G. 1997. Effects of composts and soil amendments on soil microflora
and Phytophthora root and crown rot of bell pepper. *Crop Protection* 16: 165–172.

Köhl J., Kolnaar R., Ravensberg W.J., 2019. Mode of action of microbial biological control agents against plant diseases: relevance beyond efficacy. *Frontiers Plant Science* 10: 845.

Köhl J., Postma J., Nicot P., Ruocco M., Blum B., 2011. Stepwise screening of microorganisms for commercial use in biological control of plant-pathogenic fungi and bacteria. *Biological Control* 57: 1–12.

Kousik C. S., Keinath A. P., 2008. First report of insensitivity to cyazofamid among isolates of Phytophthora *capsici* from the southeastern United States. *Plant Disease* 92: 979.

Lamichhane J.R., Bischoff-Schaefer M., Bluemel S., Dachbrodt-Saaydeh S., Dreux L. K., … Villeneuve F., 2017. Identifying obstacles and ranking common biological control research priorities for Europe to manage most economically important pests in arable, vegetable and perennial crops. *Pest Management Science* 73: 14–21.

Lamour K. H., Hausbeck M. K., 2001. The dynamics of mefenoxam insensitivity in a recombining population of *Phytophthora capsici* characterized with amplified fragment length polymorphism markers. *Phytopathology* 91: 533–557.

Lee B.K., Kim B.S., Chang S.W., Hwang B. K., 2001. Aggressiveness to pumpkin cultivars of *isolates* of *Phytophthora capsici* from pumpkin and pepper. *Plant Disease* 85: 497–500.

Lee S., Lee J., 2015. Beneficial bacteria and fungi in hydroponic systems: types and characteristics of *hydroponic* food production methods. *Scientia Horticolturae* 195: 206–215.

Liang Y., Hua H., Zhu Y., Zhang J., Cheng C., Romheld V. 2006. Importance of plant species and external silicon concentration to active silicon uptake and transport. *New Phytology* 172: 63–72.

Liu P., Li B., Lin M., Chen G., Ding X., Weng Q., 2016. Phosphite induced reactive oxygen species production *and* ethylene and ABA biosynthesis mediate the control of *Phytophthora capsici* in pepper (*Capsicum annuum*). *Functional Plant Biology* 43: 563–574.

Liu W., Sutton J.C., Grodzinski B., Kloepper J., 2007. Biological control of *Pythium* root rot of chrysanthemum in small-scale hydroponic units. *Phytoparasitica* 35: 159–178.

Lobato M.C., Olivieri F.P., Daleo G.R., Andreu A.B., 2010. Antimicrobial activity of phosphites against different potato pathogens. *Journal Plant Disease Protection* 117: 102–109.

Masago H., Yoshikawa M., Fukada M., Nakanishi N., 1977. Selective inhibition of *Pythium* spp. On a medium for direct isolation of *Phytophthora* spp. From soils and plants. *Phytopathology* 67: 425–428.

Matta A., Garibaldi A., 1981. Malattie delle piante ortensi, Edagricole Bologna, Italy, 232 pp.

Mercier J., Manker D.C., 2005. Biocontrol of soil-borne diseases and plant growth enhancement in greenhouse soilless mix by the volatile producing fungus *Muscodor albus*. *Crop Protection* 24: 355–362.

Messelink G.J., Labbé R., Marchand G., Tavella L., 2020. Sweet pepper: Main Pest and Diseases Problems. In: *Integrated Pest and Disease Management in Greenhouse Crops* (M.L. Gullino, R. Albajes, P. Nicot, J.C. Van Lenteren, eds.), Springer, Dordrecht, The Netherlands, 513–535.

Miao J., Cai M., Dong X., Liu L., Lin D., ... Liu, Xiii, 2016. Resistance assessment for oxathiapoprolin in *Phytophthora capsici* and the detection of a point mutation (G769W) in PcORP1 that confers resistance. *Frontiers in Microbiology* 7: 615.

Moulin F., Lemaceau P., Alabouvette C., 1994. Pathogenicity of Pythium species on cucumbers in peat-sand, rockwool and hydroponics. *European Journal of Plant Pathology* 100: 3– 17.

Nielsen C.J., Ferrin D.M., Stanghellini M.E., 2006a. Efficacy of biosurfactants in the management of Phytophthora *capsici* on pepper in recirculating hydroponic systems. *Canadian Journal of Plant Pathology* 28: 450–460.

Nielsen C.J., Ferrin D.M., Stanghellini M.E., 2006b. Cyclic production of sporangia and zoospores by *Phytophthora capsici* on pepper roots in hydroponic culture. *Canadian Journal of Plant Pathology* 28: 461–466.

Owen-Going T.N., Sutton J.C., Grodzinski B., 2003. Relationships of *Pythium* isolates and pepper plants in single-plant hydroponic units. *Canadian Journal of Plant Pathology* 25: 155–167.

Parra G., Ristaino J.B., 2001. Resistance to mefenoxam and metalaxyl among field isolates of *Phytophthora capsici* causing Phytophthora blight of bell pepper. *Plant Disease* 85: 1069–1075.

Paulitz T.C., 1997. Biological control of root pathogens in soilless and hydroponic systems. *Horticultural Science* 32: 193–196.

Punja Z.K., Yip R., 2003. Biological control of damping-off and root rot caused by *Pythium aphanidermatum* on greenhouse cucumbers. *Canadian Journal of Plant Pathology* 25: 411–417.

Pernezny K. L., Roberts P. D., Murphy J. F., Goldberg N. P., 2003. *Compendium of Pepper Diseases*. 1th ed.American Phytopathological Society Press, St Paul, USA, 63 pp.

Postma J., Willemsen-de Klein M.J.E.I.M., Van Elsas J.D., 2000. Effect of the indigenous microflora on the development of root and crown rot caused by *Pythium aphanidermatum* in cucumber grown on rockwool. *Phytopathology* 90: 125–133.

Postma J. 2009. The Status of Biological Control of Plant Diseases in Soilless Cultivation. In: *Recent Developments in Management of Plant Diseases* (U. Gisi, I. Chet, M.L. Gullino, eds.) Springer, Dordrecht, The Netherlands, 133–146.

Pugliese M., Liu B.P., Gullino M.L., Garibaldi A., 2008. Selection of antagonists from compost to control soil-borne pathogens. *Journal of Plant Disease and Protection* 115: 220–228.

Rankin L., Paulitz T.C., 1994. Evaluation of rhizosphere bacteria for biological control of Pythium root rot of greenhouse cucumbers in hydroponic culture. *Plant Disease* 78: 447–451.

Raymaekers K., Ponet L., Holtappels D., Berckmans B., Cammue P.A.B., 2020. Screening for novel biocontrol agents applicable in plant disease management – a review. *Biological Control* 144: 104240.

Ristaino J.B., Johnston S.A., 1999. Ecologically based approached to management of Phytophthora blight on bell pepper. *Plant Disease* 83: 1080–1089.

Ristaino J. B., Larkin R. P., Campbell C. L., 1993. Spatial and temporal dynamics of Phytophthora epidemics in commercial bell pepper fields. *Phytopathology* 83: 1312–1320.

Sambo P., Nicoletto C., Giro A., Pii Y., Valentinuzzi F.,… Cesco S., 2019. Hydroponic Solutions for Soilless Production Systems: Issues and Opportunities in a Smart Agriculture Perspective. *Frontiers in Plant Science* 10: 923.

Segarra G., Casanova E., Avilés M., Trillas I., 2010. *Trichoderma asperellum* strain T34 controls Fusarium wilt disease in tomato plants in soilless culture through competition for iron. *Microbial Ecology* 59: 141–149.

Shaner G., Finney R.E., 1977. The effect of nitrogen fertilization on the expression of slow-mildewing resistance in Knox wheat. *Phytopathology* 67: 1051–1056.

Shearer B.L., Crane C.E., 2012. Variation within the genus *Lambertia* in efficacy of low-volume aerial phosphite spray for control of *Phytophthora cinnamomi*. *Australasian Plant Pathology* 4: 147–57.

Sibilia C., 1952. Review of the most important phytopathological records observed in 1949 on *Capsicum annuum*, Italy. *Stazione di Patologia Vegetale Bollettino*, Roma, Sor III, 8, 285.

Silvar C., Merino F., Dı´az J., 2009. Resistance in pepper plants induced by *Fusarium oxysporum* f. sp. *lycopersici* involve different defence-related genes. *Plant Biology* 11: 68–74.

Smillie R., Grant B.R., Guest D., 1989. The mode of action of phosphite: evidence of both direct and indirect modes of action on three Phytophthora spp. in plants. *Phytopathology* 79: 921–926.

Song A., Xue G., Cui P., Fan F., Liu H., … Liang Y., 2016. The role of silicon in *enhancing* resistance to bacterial blight of hydroponic-and soil-cultured rice *Scientific Reports* 6: 24640.

Srinivasan K., Gilardi G., Garibaldi A., Gullino M.L., 2009. Bacterial antagonists from used rockwool soilless substrates suppress Fusarium wilt of tomato. *Journal of Plant Pathology* 91: 147–154.

Stanghellini M.E. Tomlinson A. 1987. Inhibitory and lytic effects of nonionic surfactant on various asexual stages in the life cycle of *Pythium* and *Phytophthora* species. *Phytopathology* 77: 112–114.

Stanghellini M.E., Miller R.M., 1997. Biosurfactants: their identity and potential efficacy in the biological control of zoosporic plant pathogens. *Plant Disease* 81: 4–12.

Stanghellini M.E., Kim D.H., Rasmussen S.L., Rorabaugh P.A., 1996. Control of root rot of peppers caused by *Phytophthora capsici* with a non-ionic surfactant. *Plant Disease* 80: 1113–1116.

Stanghellini M.E., Rasmussen S., 1994. Hydroponics: a solution for zoosporic pathogens. *Plant Disease* 74: 173–178.

Tamietti G., Valentino D., 2001. Physiological characterization of a population of *Phytophthora* capsici Leon. from northern Italy. *Journal of Plant Pathology* 83: 199–205.

Vallance D., Guérin-Dubrana F., Blancard D., Rey P., 2011. Pathogenic and beneficial microorganisms in

soilless cultures. *Agronomy for Sustainable Development* 31: 191–203.

Van Der Gaag D. J., Wever G., 2005. Conduciveness of different soilless growing media to *Pythium* root and crown rot of cucumber under near-commercial conditions. *European Journal of Plant Pathology* 112: 31–41.

Wang M., Gao L., Dong S., Sun Y., Shen Q., Guo S., 2017. Role of Silicon on Plant–Pathogen Interactions. *Annunci Frontiers in Plant Science* 8: 701.

Wolfhechel H., Funck Jensen D., 1991. Influence of the water potential of peat on the ability of *Trichoderma harzianum* and *Gliocladium virens* to control *Pythium ultimum*. In: *Biotic interactions and soil-borne diseases* (A.B.R. Beemster, G.J. Bollen, M. Gerlagh, M.A. Ruissen, B. Schippers, A. Tempel ed.), Elsevier, Amsterdam, The Netherlands, 392–397.

Zheng J., Sutton J.C., Yu H., 2000. Interactions among *Pythium aphanidermatum*, roots, root mucilage, and microbial agents in hydroponic cucumbers. *Canadian Journal of Plant Pathology* 22: 368–379.

Phytopathologia Mediterranea
The international journal of the
Mediterranean Phytopathological Union

Firenze University Press
www.fupress.com/pm

Short Notes

Detection and phylogeny of viruses in native Albanian olive varieties

Toufic ELBEAINO[1,*], Magdalena CARA[2], Shpend SHAHINI[2], Pasko PANDELI[1]

[1] *Istituto Agronomico Mediterraneo di Bari, Via Ceglie 9, 70010 Valenzano (BA), Italy*
[2] *Agricultural University of Tirana, Department of Plant Protection, Albania*
*Corresponding author. E-mail: elbeaino@iamb.it

Summary. Forty samples representing 14 native Albanian and two foreign olive varieties were collected from an olive varietal collection plot in the Valias region (Tirana, Albania). The samples were assayed by RT-PCR for presence of olive-infecting viruses, including arabis mosaic virus (ArMV), cherry leaf roll virus (CLRV), cucumber mosaic virus (CMV), olive latent ringspot virus (OLRSV), olive latent virus 1 (OLV-1), olive leaf yellowing-associated virus (OLYaV), strawberry latent ringspot virus (SLRSV) and by PCR for the bacterium *Xylella fastidiosa* (Xf). Ninety-eight percent of the samples were infected with at least one virus. OLYaV was the most prevalent (85% of samples), followed by OLV-1 (50%), OLRSV (48%), CMV (28%), SLRSV (3%) and CLRV (5%), whereas ArMV and Xf were absent. Fifty-five percent of the samples were infected with one virus, 13% with two viruses, 20% with three, and 5% with four. Analyses of the nucleotide sequences of the Albanian virus isolates generally showed low genetic variability, and that most were phylogenetically related to Mediterranean isolates, in particular to those from Greece and Italy. Five olive trees, representing three native cultivars ('Managiel', 'Kalinjot' and 'Kushan-Preze') and one foreign ('Leccino'), were found to be plants of the *Conformitas Agraria Communitatis* ("*CAC*") category i.e. free of ArMV, CLRV, SLRSV and OLYaV. Only one tree of the native cultivar 'Ulliri i kuq' was free of all tested viruses, so this is plant material of the "Virus-tested" category. Olives derived from both categories could be used for propagation of standard quality plant materiel in a future certification programme for olive in Albania. This is the first report of CLRV, OLRSV, CMV and OLV-1 in Albania. The study also reveals the precarious health status of native olive varieties in the Valias varietal collection plot. However, the discovery of six plants representing two certifiable categories is a first step in a future olive tree certification program in the country.

Keywords. RT-PCR, sequence and phylogenetic analyses, certification programme.

Citation: T. Elbeaino, M. Cara, S. Shahini, P. Pandeli (2021) Detection and phylogeny of viruses in native Albanian olive varieties. *Phytopathologia Mediterranea* 60(1): 165-174. doi: 10.36253/phyto-11985

Accepted: January 30, 2021

Published: May 15, 2021

Data Availability Statement: All relevant data are within the paper and its Supporting Information files.

Competing Interests: The Author(s) declare(s) no conflict of interest.

Editor: Nihal Buzkan, Kahramanmaraş Sütçü Imam University, Turkey.

INTRODUCTION

Olive (*Olea europaea*) is one of the oldest and most important fruit tree crops in Albania (Belaj *et al*., 2003). Currently, there are 54,000 ha of olive groves containing approx. 10 million trees in Albania, of which thousands are secular (Ismaili, 2009). The olive growing area in this country extends

from the northern border of Shkoder to Konispol in the south, penetrating the mainland towards the east, through river valleys, creating a continuum of olive groves (Velo and Topi, 2017). Until 2009, the olive groves were distributed as follows: 10% on flat land, 83% on hillsides and 7% in steep areas (MAFCP, 2009); however, this situation has changed in favour of flat land and hilly areas making olive cultivation a dominant feature of the landscapes (Kolaj *et al*., 2017).

Most olive production in Albania is concentrated in the coastal and mountainous areas (Fier, Berat, Elbasan and Vlora regions) with Mediterranean climatic conditions. In 2018, almost 100,000 tons of olives were produced, an increase of 3.2% compared to previous years, and the olive oil industry produced 6,000 tons of product (Lazemetaj, 2018).

The genetic resources of Albanian olive groves are varied, with many ancient native varieties (approx. 50 varieties), but only six ('Kalinjot', 'Krypsi Beratit', 'Bardhi Tiranë', 'Krypsi Elbasanit', 'Mixan' and 'Himara') make up 85% of the national production (MoA, 2017). Olive tree propagation is mainly by grafted or self-rooted cuttings, which undergo a *Conformitas Agraria Communitatis* ("*CAC*") certification. This is based on visual assessment of the health status of the olive tree and is managed by the "National Seed and Plant Institute" of the Ministry of Agriculture (MoA). To preserve Albanian olive germplasm, the MoA with the collaboration of the Agricultural University of Tirana has established a varietal collection plot in the Valias region of Albania. This plot contains the most important native varieties (Genetic Bank of the University of Tirana, Albania). Initially, these "mother" plants of different varieties were selected based on visual inspections, regardless of their phytosanitary status.

Although this approach can be valid for excluding some diseases, it is not appropriate for virus infections which can be masked in plants in latent forms and\or at low concentrations, thus leading to the selection of false virus-free olive trees. As with other crops, propagation of olive by vegetative means favours virus spread. Olive is affected by 15 viruses (Martelli, 2013), some of which are agents of identified diseases, while most cause latent infections, the effects of which have yet to be determined.

Three surveys of virus diseases (Saponari *et al*., 2002; Çakalli *et al*., 2006; Luigi *et al*., 2009), carried out on, respectively, 38, 37 and 50 trees, have summarized knowledge on olive viruses present in Albania. Only strawberry latent ringspot virus (SLRSV) and olive leaf yellowing-associated virus (OLYaV) were identified. Following the growing interest of farmers in the use of high-quality nursery plants, identification of healthy plants that can be used as a sources of propagation material for growers has become a necessity to improve the national olive industry. Albania has therefore started a certification programme for the multiplication of olive plant material. As part of this programme, a survey was conducted in the varietal collection plot of "mother" plants (in the Valias region) to assess the virus phytosanitary status of native varieties that could be used in the future. Furthermore, the recent outbreak of the olive quick decline syndrome, caused by *Xylella fastidiosa* (Xf) in Italy (Saponari *et al*., 2013), and its identification in other European countries (France, Spain, Germany) made it necessary to extend this investigation to survey for this bacterium, for which the results of both studies are reported in the present paper.

MATERIALS AND METHODS

Field survey and source of plant material

In March 2018, a survey was conducted in a plot for the varietal collection of olive (Valias, Tirana, Albania) which was established by the Albanian Ministry of Agriculture to include the most important olive varieties in the country. The olive germplasm in this plot has been periodically subjected to phenotypic and pomological evaluations in order to identify trees that could be used as propagation material in the Albanian certification programme.

Forty olive trees with no apparent symptoms were each sampled. Leaves and cuttings (approx. 25-30 cm long) aged between 1 and 2 years, were taken from each tree canopy. In total, 16 cultivars were sampled, of which 14 were native and two were foreign (Table 1).

Three clones of each cultivar were sampled, and the samples were labelled, stored in plastic bags at 4°C and brought to the laboratory for analysis. Cuttings from olive seedlings kept in screenhouses at the Mediterranean Agronomic Institute of Bari, which were healthy as indicated by RT-PCR assays were used as negative control samples, and different plants infected (also indicated by RT-PCR) with arabis mosaic virus (ArMV), cherry leaf roll virus (CLRV), cucumber mosaic virus (CMV), olive latent ringspot virus (OLRSV), olive latent virus 1 (OLV-1), OLYaV and SLRSV, were used as positive control samples.

Extraction of total nucleic acids

For virus detection, total nucleic acids (TNAs) were extracted from 0.2 g of phloem tissues of each sample

Table 1. Olive samples collected from the varietal collection plot of Valias region (Tirana, Albania), assayed by RT-PCR for the presence of seven olive-infecting viruses. * indicates *CAC* category plants; ** indicates *Virus-tested* category plant.

Cv. N°	Cultivar	Sample N°.	ArMV	SLRSV	CLRV	OLYaV	OLRSV	CMV	OLV-1
1	Boç	1	-	-	-	+	+	-	-
		2	-	-	-	+	+	-	-
		3	-	-	-	+	+	-	-
2	Managjel	1*	-	-	-	-	+	-	+
		2	-	-	-	+	+	-	+
3	Frangu	1	-	-	-	+	-	-	+
		2	-	-	-	+	-	-	+
		3	-	-	-	+	-	-	+
4	Kushan	1	-	-	-	+	-	-	+
		2	-	-	-	+	+	-	+
		3	-	-	-	+	-	-	+
5	I bardhi i Tiranes	1	-	-	-	+	+	-	+
		2	-	-	-	+	+	-	+
		3	-	+	-	+	+	-	+
6	Kalinjot	1*	-	-	-	-	+	+	-
		2*	-	-	-	-	-	+	-
		3	-	-	-	+	-	+	-
7	Krypsi i Krujes	1	-	-	-	+	+	+	-
		2	-	-	+	+	+	+	-
		3	-	-	-	+	+	-	-
8	Kokermadhi i Beratit	1	-	-	+	+	-	+	-
		2	-	-	-	+	-	+	+
		3	-	-	-	+	-	+	+
9	I holli i Himares	1	-	-	-	+	+	-	-
		2	-	-	-	+	+	-	-
		3	-	-	-	+	+	-	-
10	Mixan	1	-	-	-	+	-	+	-
		2	-	-	-	+	-	-	+
		3	-	-	-	+	-	+	-
11	Lecino Valias	1	-	-	-	+	+	-	-
		2	-	-	-	+	-	-	-
		3*	-	-	-	-	-	-	+
12	Frantoio-Valias	1	-	-	-	+	+	-	-
		2	-	-	-	+	+	+	+
13	Kushan-Preze	1*	-	-	-	-	-	-	+
		2	-	-	-	+	-	-	+
14	I bardhi i Tiranes-Preze	1	-	-	-	+	-	-	-
		2	-	-	-	+	-	-	+
15	Mixan-Preze	1	-	-	-	+	-	-	+
16	Ulliri i kuq-Preze	1**	-	-	-	-	-	-	-
	Number of infected trees		**0**	**1**	**2**	**34**	**19**	**11**	**20**
	% infected trees		**0**	**2.5**	**5**	**85**	**47.5**	**27.5**	**50**

(cortical scrapings). Each sample was homogenized in 1 mL of grinding buffer (0.4 M guanidine thiocyanate, 0.2 M NaOAc (pH 5.2), 25 mM EDTA, 1.0 M KOAc (pH 5.0), and 2.5% w/v PVP-40). Nucleic acids were then purified with silica particles (Foissac *et al*., 2001).

For Xf detection, DNA was extracted following the CTAB protocol (2% hexadecyl trimethyl-ammonium bromide, 0.1 M Tris-HCl (pH 8), 20 mM EDTA, and 1.4 M NaCl) (Hendson *et al*., 2001). For each sample, 0.3 g of fresh leaf midrib and petiole was homogenized with 2 mL of CTAB buffer, using an automated hammer. Extracted sap was incubated at 65°C and then chloroform treated. TNA was precipitated with 0.6 volume of cold 2-isopropanol and resuspended in 120 µL of sterile water for PCR assays.

Reverse transcription (RT) and polymerase chain reaction (PCR)

Samples were assayed by RT-PCR for the presence of seven olive viruses, including ArMV, CLRV, CMV, OLRSV, OLV-1, OLYaV and SLRSV. Virus RNAs were reverse transcribed using 200 U of *Moloney Murine Leukaemia virus* reverse transcriptase enzyme (Invitrogen Corporation), 4 µL of 5XFS M-MLV buffer, 2 µL of DTT (0.1 M), and 0.5 µL of dNTPs (10 mM). The mixture was incubated at 39°C for 1 h and then at 70°C for 10 min. PCR was performed using 2.5 µL of cDNA, together with 2.5 µL of 10× Taq polymerase buffer (Promega Corporation), 1 µL of 25 mM $MgCl_2$, 0.5 µL of 10 mM dNTPs, 0.5 µL of 10 µM of sense and antisense primers (Table 2) and 1 unit of Taq DNA polymerase (5U μL^{-1}) in a final volume of 25 µL. Amplifications were carried out in a thermocycler (Biometra) after a preliminary denaturation at 94°C for 4 min, followed by 35 cycles at 94°C for 35 s, annealing at 55°C for 35 s (58°C for OLYaV) and 72°C for 35 s, and a final extension step at 72°C for 7 min. Amplified products were electrophoresed in 5% TBE polyacrylamide gel (PAGE) and visualized by silver nitrate staining.

DNA was extracted from olive samples following the CTAB protocol and assayed by PCR using primers RST31/33, which are widely used in the detection of different Xf subspecies (Minsavage *et al.,* 1994). Reactions consisted of a 1× amplification buffer in a final volume of 25 µL, containing 2.5 µL of TNA, 1 µL of dNTPs (10 mM), 0.5 µL of each sense and antisense primers (10 µM), and 1.25 U of Taq DNA polymerase. PCR cycles consisted of 94°C for 1 min followed by 40 cycles of 94°C for 30 s, 55°C for 30 s, and 72°C for 45 s, and a final step of 72°C for 5 min. PCR reactions were electrophoresed in 1.2% TAE agarose gels.

Cloning, sequencing and bioinformatic analyses

Based on the occurrence of each virus in the tested samples, amplified RT-PCR products yielded from different infected olive trees were transformed in StrataClone^{TM} PCR Cloning vector pSC-A (Stratagene), subcloned into *Escherichia coli* DH5α cells, and three DNA clones from each sample were custom sequenced bidirectionally (Eurofins Genomics). Nucleotide sequences were analyzed with the DNA Strider 1.1 program (Marck, 1988). Multiple alignments of nucleotide sequences were performed using the default options of CLUSTALX 1.8 (Thompson *et al*., 1997). The BLASTn program was used to search for nucleotide homology in GenBank (Altschul *et al*., 1990). Tentative phylogenetic trees were constructed with the MEGA 6 version software, using the Neighbor-joining method, with 1000 bootstrap replicates (Tamura *et al*., 2013).

RESULTS AND DISCUSSION

Detection of olive viruses and Xylella fastidiosa

RT-PCR detection of olive viruses showed that almost all the native Albanian olive cultivars tested were infected with a least with one virus (97.5% of infection). Only one tree was virus-free. OLYaV was the most prevalent virus (in 85% of samples), followed by OLV-1 in 50% of samples (Table 1). The high incidence of OLYaV in the sampled Albanian olive trees was similar to that reported in other countries, including Lebanon (24%), Syria (15%), Tunisia (49%), Italy (42%), and the United States of America (93%) (Saponari *et al*., 2002; Albanese *et al*., 2003; Al Abdullah *et al*., 2005; Fadel *et al*., 2005; Faggioli *et al*., 2005; Al Rwahnih *et al*., 2011; El Air *et al*., 2011). The transmission of this virus occurs through the exchange of infected plant propagation material; however, it is strongly suspected that the olive psyllid (*Euphyllura olivinae*), which has been repeatedly found to host OLYaV, is the vector of this virus in nature, although this has not been demonstrated with experimental transmission tests (Sabanadzovic *et al*., 1999). For this reason, it is difficult to establish which path OLYaV has taken in the varietal collection plot to reach such high incidence.

OLV-1 is a polyphagous soilborne virus capable of infecting crops without being transmitted by vectors. These two characteristics make this virus very transmissible. OLV-1 has also been shown to be present in blossoms (Lobão *et al*., 2002), pollen (Saponari *et al*., 2002), and fruit pulp (Félix, unpublished) of infected trees, as well as in high proportions (> 80%) of seedlings originating from infected olive trees (Saponari *et al*., 2002)

Table 2. List of primers used in RT-PCR assays for detecting the olive-infecting viruses. CP, Coat protein; RdRP, RNA-dependent RNA Polymerase; HSP70-like protein, Heat shock protein 70 kDa-like protein.

Virus	Genus	Amplified region	Primer sequence (5' to 3')	Amplicon length (bp)	Reference
ArMV	Nepovirus	CP gene	TTGGTTAGTGAATGGAACGG TCAACTCACCCTCCAAATCCC	504	Grieco *et al*., 2000
CLRV	Nepovirus	CP gene	TTGGCGACCGTGTAACGGCA GTCGGAAAGATTACGTAAAAGG	416	Faggioli *et al*., 2005
OLRSV	Nepovirus	3'terminal	TTGCAAAACTAGTGCCAGAGG TGCATAAGGCTCACAGGAG	480	Grieco *et al*., 2000
CMV	Cucumovirus	RdRP gene	TAACCTCCCAGTTCTCACCGT CCATCACCTTAGCTTCCATGT	513	Grieco *et al*., 2000
OLV-1	Alphanecrovirus	3'terminal	ACACAGAAATCATAAGTGCC CCATAGCACCATCATACC	299	Faggioli *et al*., 2005
OLYaV	Closterovirus	HSP70 gene	CGAAGAGAGCGGCTGAAGGCTC GGGACGGTTACGGTCGAGAGG	383	Sabanadzovic *et al*., 1999
SLRSV	Sadwavirus	CP gene	CCCTTGGTTACTTTTACCTCCTCATTGTCC AGGCTCAAGAAAACACAC	293	Faggioli *et al*., 2005

indication transmission through seeds. By means of ovule fertilization with infected pollen and\or by grafting of cultivar plants that are 'recalcitrant' to rooting onto seedlings originated from infected seeds, all these approaches make again OLV-1 a very infectious virus. Factors favouring the high OLV-1 incidence in the olive trees of Valias field merits future investigation.

The OLRSV incidence particularly high (48%) compared with olive orchards in other Mediterranean countries, i.e., Tunisia (17%), Lebanon (14%), and Syria 12% (El Air *et al*., 2011; Al Abdullah *et al*., 2005; Fadel *et al*., 2005). No vector for OLRSV is known; however, as a nepovirus, its natural transmission could occur through nematodes. These pests have not been reported from the Valias collection plot, suggesting that the transmission of OLRSV may have occurred through infected self-rooted olive tree cuttings.

Among the viruses tested, CMV was the third most commonly found (28% of the samples). This incidence is similar to reports from other countries, i.e., Syria (23%) and Tunisia (26%) (Al Abdullah *et al*., 2005; El Air *et al*., 2011). Although CMV is transmitted through many different aphid vectors (*Myzus* spp.), the presence in Albanian olive cultivars may not be attributed to these, because their association with olive has not been demonstrated.

SLRSV and CLRV were found at low incidence, i.e., 1% for SLRV and 3% for CLRV, and ArMV was not detected. The rare presence\absence of these three polyphagous neopoviruses in Albanian olives is satisfactory.

Excluding the OLYaV infections, whose investigation on olive plants is regulated on the basis of a simple visual inspection for the presence of leaf yellowing symptoms (EU Directives n°. 2016/97 for "*CAC*" [*Conformitas Agraria Communitatis*] category), and not on laboratory tests as conducted in the present study, the phytosanitary status of the 14 native Albanian cultivars tested here can be considered as acceptable.

A high proportion (93%) of the tested olive plants material was free of ArMV, CLRV, SLRSV, and symptoms of yellowing of the leaves. It is therefore legitimate to classify the plants as "*CAC*" category. The presence of OLYaV found in the samples based on laboratory tests is worrying, because the latent period of this virus in the infected plant material is unpredictable. For phytosanitary safety, therefore, this material should be excluded from the "*CAC*" category in the future Albanian certification programme. Consequently, five trees of three 3 native varieties and one foreign cultivar ('Leccino') were eligible for the "*CAC*" category. Only one plant of the native cultivar 'Ulliri i kuq' was found free of all the viruses tested, so this plant can be designated in the "*Virus-tested*" plant material category. For the remaining olive cultivars, for which no virus-free plants were detected, sanitation measures (thermotherapy and\or *in vitro* shoot tip culture), or sanitary selections for a greater number of olive plants, are recommended for the future certification programme in Albania. It is notable that attempts to correlate the presence of any single virus or group of viruses with specific host symptoms in Valias plot were unsuccessful. This agrees with other reports on the symptomatology of these viruses (Martelli, 2013).

PCR results showed that Xf was not present in any of the tested samples, confirming previous reports of absence of this pathogen in Albania (Cara *et al*., 2016).

Sequence variability

All of the virus sequences obtained in this study were deposited in the GenBank under different accession numbers (acc.n°), and are shown in the phylogenetic trees (Figure 1). The sequence of SLRSV found only in one Albanian olive tree of cultivar 'I Bardhi i Tiranes' (isolate *I Bardhi3*) had 80.5% to 93.5% similarity with those in GenBank; whereas two isolates *Gr\Ts* and *Gr\Ms* (acc.n°, respectively, MK936233 and 706532), were recently identified in olive trees in Greece (Manthoudiakis *et al*., 2020), and these were the most related isolates (93.5% similarity). The SLRSV isolates present in the Genbank database showed 22% of variability, in the coat protein homologue region investigated here.

The sequence analyses of CLRV isolates found in two Albanian olive cultivars, i.e., 'Krypsi' and 'Kokermadhi', showed, respectively, 86% and 87% to 98% similarity with homologue isolates in the database. Both SLRSV isolates (*Krypsi 2* and *Kokermadhi 4*) shared 98.2% similarity with the *Adilcevaz* isolate from Turkey (acc.n° FJ785323), and *Gr\Gd* (acc.n° MK936236) and *Gr\Tr* (acc. n° MK936235) from Greece, whereas the sequence similarity between the two SLRSV isolates was 96%.

The incidence of OLV-1 was greater than that of SLRSV and CLRV; thus, 11 isolates, i.e., one from each OLV1-infected cultivar (Table 1), were chosen for sequencing. The comparison of their sequences showed three different representative sequence-types of all 11 OLV-1 isolates that were present as single infections in cultivars 'Kokermadhi', 'Kushan' and 'Mixan', and in mixed virus infections. Albanian OLV-1 isolates shared 88% to 98.3% similarity with those of the GenBank. Whereas isolate *Kushan3* had similarity of 98.3% with isolate *V10* from Portugal (acc.n° KF804063), isolate *Kokermadhi3* had 96% similarity with *P33* (acc.n° MN586597, from Tunisia), and *Mixan2* had 97% similarity with *G1A* (acc.n° KF804056, from Portugal).The Albanian OLV-1 isolates showed 93.3% and 98% similarity.

In the case of OLYaV, one isolate from each of the 15 OLYaV-infected cultivars was sequenced. After the sequence analysis, seven different sequence-types were

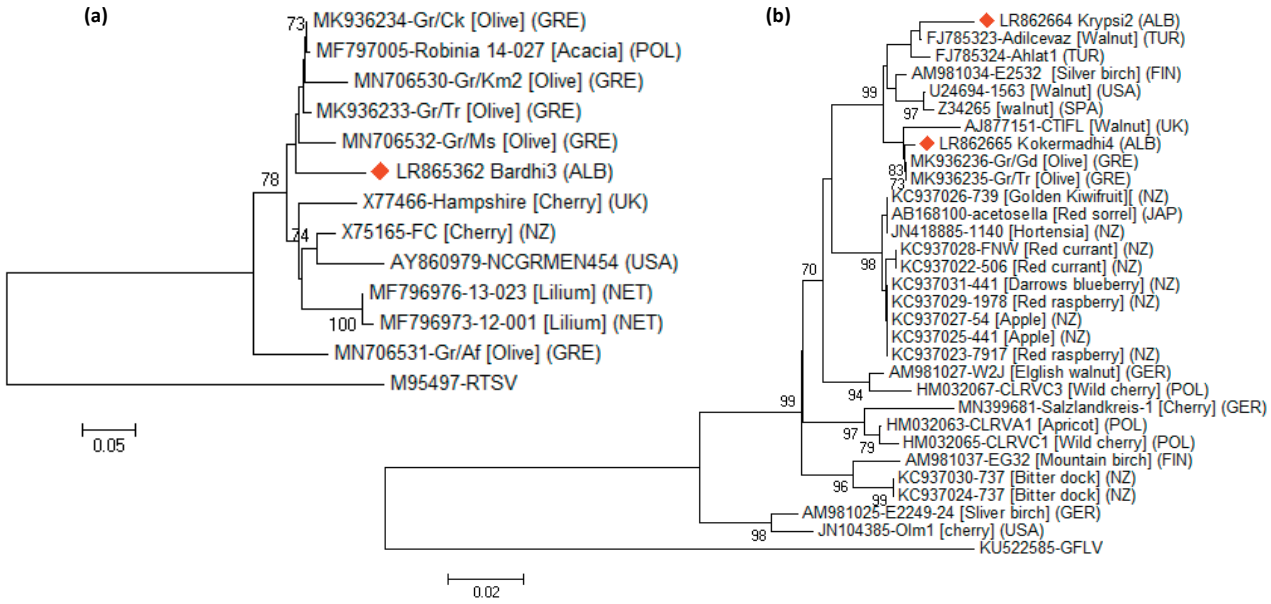

Figure 1. Phylogenetic trees based on nucleotide sequences of different partial genes\domains of SLRSV (a), CLRV (b), OLV-1 (c), CMV (d) and OLYaV (e). Alignments were obtained using Clustal X 1.8, and analyzed by the Neighbor-Joining method with 1000 bootstrap replicates. The percentage of replicate trees (when >70%) in which the virus isolates clustered together is shown next to each branch. GenBank accession number, name, isolation sources and countries of origin of each corresponding virus isolate used in the analysis are reported in the phylogenetic tree. *Rice tungro spherical virus* (RTSV) of the genus *Waikavirus*, *Grapevine fanleaf virus* (GFLV) of the genus *Nepovirus*, *Olive mild mosaic virus* (OMMV) of the genus *Alphanecrovirus*, *Fig mosaic virus* (FMV) of the genus *Emaravirus* and *Daucus carota* HSP70 gene, were used as outgroup species. The abbreviations used for countries of origin of the isolates are: Albania (ALB); Australia (AUS); Chile (CHI); Croatia (CROA); Egypt (EGY); Finland (FIN); France (FRA); Germany (GER); Greece (GRE); India (IND); Israel (ISR); Italy (ITA); Japan (JAP); Malaysia (MAL); Netherlands (NET); New Zealand (NZ); Palestine (PAL); Poland (POL), Portugal (PORT); South Korea (S-KOR); Spain (SPA); Tunisia (TUN); Turkey (TK); Uganda (UGA); United Kingdom (UK); and United States of America (USA). Albanian virus isolates are indicated in red.

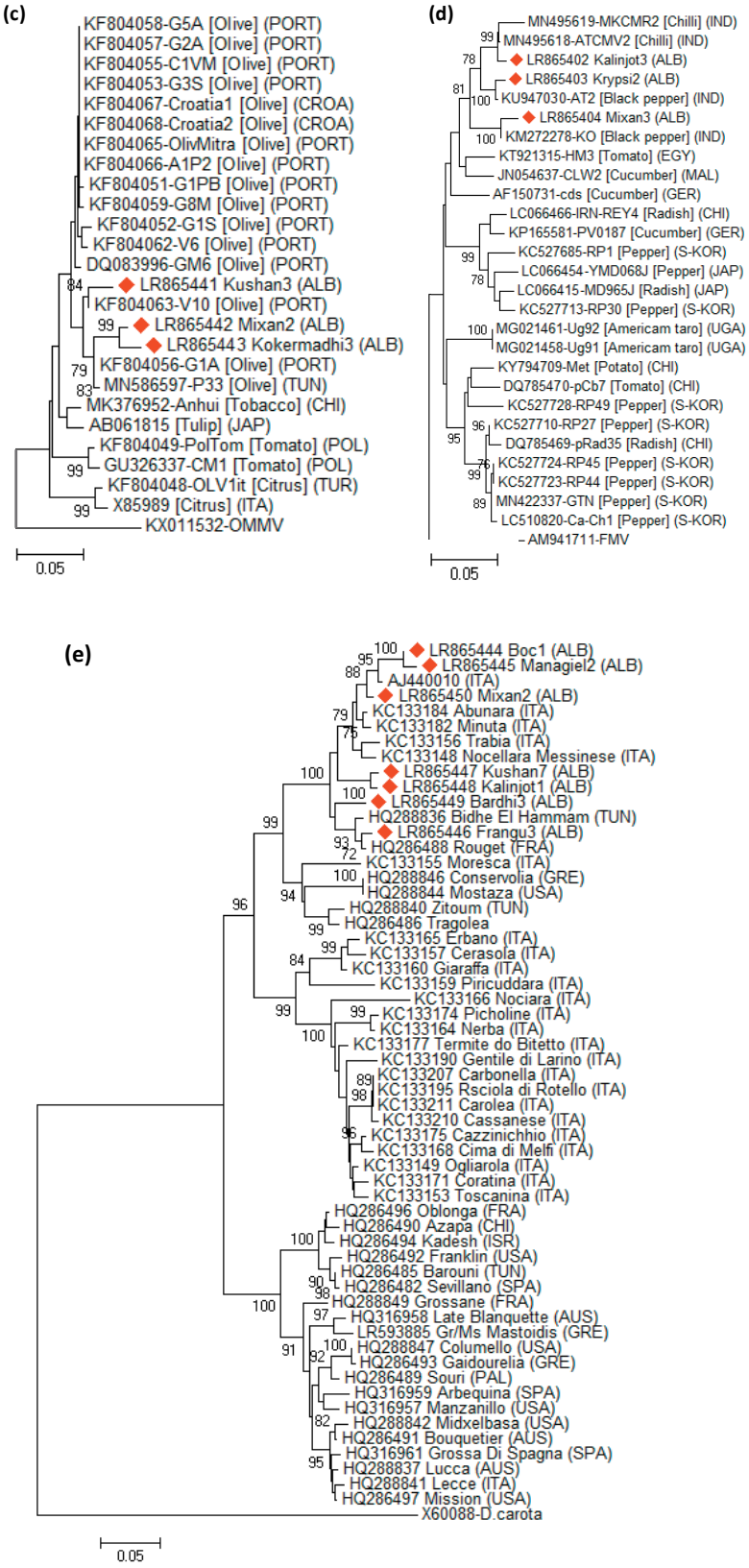

Figure 1. Continued.

identified, sharing 88.2% to 98.6% similarity. BLASTn sequence analysis showed that isolate *Mangiel2* was the most variable among the Albanian isolates and with those of the GenBank, with sequence similarity of 69.9%. Opposite to this, greatest similarity was found with *Frangu3* isolate that showed 98.9% similarity with GenBank isolates. In general, the similarity margin, comparing the sequences of the seven Albanian isolates with those in Genbank, ranged from 90.3% (*Bardhi3*) to 98.9% (*Frangu3*). In particular, isolates *Boç1* and *Mangiel2* had the greatest similarity (respectively, 97.1% and 96%) with the Italian isolate *AJ* (acc.n° AJ440010). *Mixan2* shared 97.9% similarity with isolate *Abunara* from Tunisia (acc.n° KC133184). Of the three OLYaV isolates, *Kushan7* had 93.7% similarity with isolate *Rouget* (acc.n° HQ286488, from France), *Kalinjot1* had 92.4% similarity with *Bidhel Hammam* (acc.n° HQ288836, from Tunisia), and *Frangu3* had 98.9% similarity with *Nocellara messinese* (acc.n° KC133148, from Italy).

Nine Albanian olive cultivars were shown to be infected with OLRSV, so their RT-PCR amplicons were sequenced. BLASTn analyses of obtained sequences (acc.n° LR865438, isolate *Kalinjot3*; LR865403, isolate *Krypsi2*; and LR865404, *Mixan3*) showed that these isolates shared 99.1% to 99.3% similarity with the unique OLRSV isolate in the GenBank (acc.n° NC_038863); whereas the intraspecies variability ranged from 0.9% to 1.5%.

Five Albanian cultivars were infected with CMV (Table 1), so their RT-PCR amplicons were sequenced. Nucleotides sequence comparison for these isolates showed three different sequence types, found as single infections in the olive cultivars 'Kalinjot', 'Krypsi' and 'Mixan'. The sequence from 'Kalinjot' shared 89.8% to 99.4% similarity with the homologue from the GenBank, that from 'Krypsi' was 89.0% to 99.2% similar, and the sequence from 'Mixan' was 87.8% to 98.8%. The Albanian isolates were 93.3% to 96.1% similar to each other. The CMV sequences of the other two infected cultivars ('Kokermadhi' and 'Frantoio Valias') were identical to that of the isolate from 'Kalinjot'.

Phylogenetic analyses

The phylogenetic analyses conducted in this study aimed to determine relationships between viruses found in the Albanian olive cultivars and their homologues of international origins. In the case of SLRSV, the analysis was conducted on the few sequences of isolates from olive reported in the GenBank, together with those from other crops. In the phylogenetic tree, the Albanian isolate of SLRSV (*Bardhi3*) clustered in one clade together with Greek isolates from olive (*Gr\Tr*, *Gr\Ms* and *Gr\km2*) (Figure 1a). A similar clustering was found for CLRV isolates from Albania, i.e., *Kokermadhi4,* that grouped together with olive isolates from Greece (*Gr\Gd*, *Gr\Tr*). In contrast, *Krypsi2* clustered closely to *Adilcevaz* and *Ahlat1* isolates, both reported from walnuts in Turkey (Figure 1b).

The OLV-1 phylogenetic tree had four differentiated clusters based on infected hosts rather than geographic origins. The largest cluster was composed of isolates from olive from Portugal, for which the Albanian isolates *Kokermadhi2*, *Kushan3* and *Mixan2* were part of in a distinct clade (Figure 1c).

Analogous to SLRSV, the lack of CMV sequences from olive in GenBank conditioned the phylogenetic analysis that was based on isolates from different crops rather than on those from olive. The phylogenetic tree for CMV isolates did not show any distribution, based on host species and\or geographic origin. However, the Albanian isolates from olive formed one clade with those from chili and black pepper from India (Figure 1d). It is likely that this indistinct distribution of CMV isolates in the phylogenetic tree was conditioned by the polyphagous nature of this virus, exposing it to sequence recombination that has generated a quasi-species which is difficult to be differentiated by phylogenetic analysis.

The presence of a single for OLRSV sequence in GenBank has limited the design of a phylogenetic scenario for this virus. The present analysis was therefore limited, only reporting the genetic variability found among the three isolates that were sequenced.

The phylogenetic tree of OLYaV showed two clusters, one which was diversified with isolates from different origins, i.e., the United States of America, Australia, Chile, France, Greece, Italy, Israel, Palestine, Spain, and Tunisia, while the second was composed of Mediterranean isolates, i.e., from France, Greece, Italy, and Tunisia. The exception was isolate from the United States of America, which has a Spanish denomination (cultivar 'Morteza'). The Albanian isolates all grouped together in a clade close to Italian isolates.

CONCLUSIONS

This study was carried out to identify a "*Virus-free*", or at least "*Virus-tested*", plant material that could be part of primary resources for a future certification programme for olive in Albania. This research is not unique, because two decades ago, two similar investigations were conducted in this country to identify possible virus infections in native olive trees, using double-

stranded RNA analyses (Çakalli *et al*., 2006; Saponari *et al*., 2002). Both investigations reported a virus incidence of 22 to 24%; but did not specify the identity of the viruses in the Albanian olive cultivars. Eight years later, a third investigation was undertaken on 50 olive trees, and this reported the presence of only two viruses i.e., SLRSV and OLYaV in a few olive cultivars (Luigi *et al*., 2009). Excluding these three investigations, little is known of the occurrence and distribution of other viruses that may be present in Albanian olive cultivars.

The present study reports for the first time the presence of four viruses (CLRV, OLRSV, OLV-1 and CMV) in the most important Albanian olive cultivars. Although the number of samples tested was limited and does not allow a comprehensive definition of the incidence of these viruses as only the Valias collection plot was assayed, discovery of these viruses in most of the 14 cultivars is of great concern. This is particularly because these native cultivars are pomologically and phenotypically important and are likely to be part of the future olive certification programme in Albania.

This study identified five olive trees of three native cultivars ('Managiel', 'Kalinjot' and 'Kushan-Preze') and one foreign cultivar ('Leccino') that were found free of ArMV, SLRSV, CLRV and OLYaV, and one olive tree of cultivar 'Uliri i Kuq-Preze' that was free of all the tested viruses. Based on EU directives (EU nº. 2016/97 for the category "*CAC*" [*Conformitas Agraria Communitatis*]), the plant material of these Albanian cultivars, found in the phytosanitary categories "*CAC*" and "*Virus-tested*", are valuable candidate clones that can be used in the propagation of high quality material in the future olive certification programme. At the genome level, all the viruses found in the Albanian cultivars presented low genetic variability, compared to that reported from other Mediterranean countries (Mathioudakis *et al*., 2020; Al Rwahnih *et al*., 2011; El Air *et al*., 2011; Essakhi *et al*., 2006; Al Abdullah *et al*., 2005). The limited exchange of olive plant material in the Balkan area, in particular of Albanian native olives, has preserved the phytosanitary status of this material from the introduction of international viruses isolates. Further laboratory analyses should be carried out on more olive clones, and on cultivars not tested in this study, to identify healthy candidates that could be part of a future olive certification programme in Albania.

ACKNOWLEDGMENT

This research was conducted in the framework of the project "Sustainable development of the olive sector in Albania – ASDO", as part of the "Program for the modernization of the agricultural sector – PROMAS" funded by the Albanian Ministry of Agriculture and Rural Development and by the Italian Agency for Development Cooperation (AICS) of the Ministry of Foreign Affairs and International Cooperation.

LITERATURE CITED

Al Abdullah A, Elbeaino T, Saponari M, Hallakand M., 2005. Preliminary evaluation of the status of olive-infecting viruses in Syria. *EPPO Bulletin* 35: 249–252.

Albanese G., Faggioli F., Ferretti L., Sciarroni R., La Rosa R., Barba M., 2003. Sanitary status evaluation of olive cultivars in Calabria and Sicily. *Journal of Plant Pathology* 85: 304.

Al Rwahnih M., Guo Y., Daubert S., Golino D., Rowhani A., 2011. Characterization of latent viral infection of olive trees in the national clonal germplasm repository in California. *Journal of Plant Pathology* 93: 227–231.

Altschul S.F., Stephen F., Gish W., Miller W., Myers E.W., Lipman D.J., 1990. Basic local alignment search tool. *Journal of Molecular Biology* 215: 403–410.

Belaj A., Satovic Z., Ismaili H., Panajoti D., Dallo L., Trujillo I., 2003. RAPD genetic diversity of Albanian olive germplasm and its relationships with other Mediterranean countries. *Euphytica* 130: 387–395.

Çakalli A., Myrta A., Savino V., Kullaj E., Shahini S… Ruci, T., 2006. Applying of dsRNA isolation test for identification of viruses on the main Albanian olive native varieties. *Yearbook of Plant Protection Society of the Republic of Macedonia*, Vol. XVII, p. 63.

Cara M., Merkuri J., Koka E., Bacaj M., Cara O., 2016. Xylella fastidiosa does not occur in Albania: Preliminary results. *Journal of Multidisciplinary Engineering Science and Technology* 3(10): 5701–5705.

El Air M., Mahfoudhi N., Digiaro M., Najjar A., Elbeaino T., 2011. Detection of olive-infecting viruses in Tunisia. *Journal of Phytopathology* 159: 283–286.

Essakhi S., Elbeaino T., Digiaro M., Saponari M., Martelli G.P., 2006. Nucleotide sequence variations in the HSP70 gene of Olive leaf yellowing-associated virus. *Journal of Plant Pathology* 88: 285–291.

Fadel C., Digiaro M., Choueiri E., Elbeaino T., Saponari M…Martelli G.P., 2005. On the presence and distribution of olive viruses in Lebanon. *EPPO Bulletin* 35: 33–36.

Faggioli F., Ferretti L., Albanese G., Sciarroni R., Pasquini G.,… Barba M., 2005. Distribution of olive tree viruses in Italy as revealed by one-step RT-PCR. *Journal of Plant Pathology* 87: 45–51.

Foissac X., Svanella-Dumas L., Gentit P., Dulucq M.J., Candresse T., 2001. Polyvalent detection of fruit tree tricho-, capillo- and foveaviruses by nested RT-PCR using degenerate and inosine containing primers (DOP RT-PCR). *Acta Horticulturae* 550: 37–43.

Grieco F., Alkowni R., Saponari M., Savino V., Martelli G.P., 2000. Molecular detection of olive viruses. *EPPO Bulletin* 30: 469–473.

Hendson M., Purcell A.H., Chen D., Smart C., Guilhabert M., Kirkpatrick B., 2001. Genetic diversity of Pierce's disease strain and other pathotypes of *Xylella fastidiosa*. *Applied Environmental Microbiology* 67: 895–903.

Ismaili H., 2009. Study on the condition and production of olive plant material in Albania. Conference: MBUMK: "Olive development project in Albania" *National Conference*. July 2009.

Kolaj R., Ozuni E., Skunca D., Zahoalia D., 2017. The challenges of collective action for olive growers in Albania. *European Journal of Interdisciplinary Studies* 7: 93–98.

Lazemetaj L., 2018. The sector of olive oil production in Albania, achievements and challenges in future. *International Journal of Advanced Research and Innovative Ideas in Education* I (4)*:* 2395-4396.

Lobão D.L., Félix M.R., Clara M.I.E., Oliveira S., Leitão F.A., Serrano J.F., 2002. Detection of Olive latent virus 1 in Olea europaea L. tissues by reverse transcription-polymerase chain reaction. *XIII Congresso Nacional de Bioquimíca, Lisboa*, Portugal, p 102.

Luigi M., Manglli A., Thomaj F., Buonaurio R., Barba M., Faggioli F., 2009. Phytosanitary evaluation of olive germplasm in Albania. *Phytopathologia Mediterranea* 48: 280–284.

MAFCP., 2009. Study on the actual situation of olive orchards and the perspectives of its development. Ministry of Agriculture, Food and Consumer Protection. Tirana, Albania. (In Albanian).

Mathioudakis M.M., Saponari M., Hasiów-Jaroszewska B., Elbeaino T., Koubouris G., 2020. Detection of viruses in the major olive tree cultivars of Greece using a rapid and effective RNA extraction method toward the certification of virus-tested propagation material. *Phytopathologia Mediterranea* 59: 203–211.

Marck, C., 1988. DNA Strider: a C program for the fast analysis of DNA and protein sequences on the Apple Macintosh family computers. *Nucleic Acids Research* 16: 1829–1836.

Martelli G.P., 2013. A brief outline of infectious diseases of olive. *Palestine Technical University Research Journal* 1(1): 1–9

Ministry of Agriculture - Statistical Yearbook, 2017. Statistical Processing: INSTAT.

Minsavage G.V., Thompson C.M., Hopkins D.L., Leite M.V.B.C., Stall R.E., 1994. Development of a polymerase chain reaction protocol for detection of *Xylella fastidiosa* in plant tissue. *Phytopathology* 84: 456–461.

Sabanadzovic S., Abou-Ghanem N., La Notte P., Savino V., Scarito G., Martelli G.P., 1999. Partial molecular characterization and RT-PCR detection of a putative closterovirus associated with leaf yellowing. *Journal of Plant Pathology* 81: 37–45.

Saponari M., Alkowni R., Grieco F., Driouech N., Hassan M., Di Terlizzi B., 2002. Detection of Olive-infecting virus in the Mediterranean basin. *Acta Horticulturae* 586: 787–790.

Saponari M., Boscia D., Nigro F., Martelli G.P., 2013. Identification of DNA sequences related to *Xylella fastidiosa* in oleander, almond and olive trees exhibiting leaf scorch symptoms in Apulia (Southern Italy). *Journal of Plant Pathology* 95: 668.

Tamura K., Stecher G., Peterson D., Filipski A., Kumar S., 2013. MEGA6: Molecular Evolutionary Genetics Analysis version 6.0. *Molecular Biology and Evolution* 30: 2725–2729.

Thompson J.D., Gibson T.J., Plewniak F., Jeanmougin F., Higgins D.G., 1997. The CLUSTAL X windows interface: flexible strategies for multiple sequence alignment aided by quality analysis tools. *Nucleic Acids Research* 25: 4876–4882.

Velo S., Topi D., 2017. The production potential of the olive oil from native cultivars in Albania. *International Journal of Engineering Research & Science* 3: 38–43.

Finito di stampare da
Logo s.r.l. – Borgoricco (PD) – Italia

Mediterranean Phytopathological Union

Founded by Antonio Ciccarone

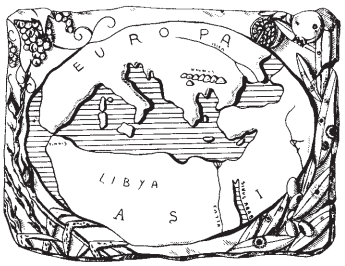

The Mediterranean Phytopathological Union (MPU) is a non-profit society open to organizations and individuals involved in plant pathology with a specific interest in the aspects related to the Mediterranean area considered as an ecological region. The MPU was created with the aim of stimulating contacts among plant pathologists and facilitating the spread of information, news and scientific material on plant diseases occurring in the area. MPU also intends to facilitate and promote studies and research on diseases of Mediterranean crops and their control.
The MPU is affiliated to the International Society for Plant Pathology.

MPU Governing Board

Affiliated Societies

Arab Society for Plant Protection (ASPP), http://www.asplantprotection.org/
French Society for Phytopathology (FSP), http://www.sfp-asso.org/
Hellenic Phytopathological Society (HPS), http://efe.aua.gr/
Israeli Phytopathological Society (IPS), http://www.phytopathology.org.il/
Italian Phytopathological Society (SIPAV), http://www.sipav.org/
Portuguese Phytopathological Society (PPS), http://www.spfitopatologia.org/
Spanish Society for Plant Pathology (SEF), http://www.sef.es/sef/

2021 MPU Membership Dues

Institutional MPU Membership: : € 200.00 (college and university departments, libraries and other facilities or organizations). Beside the open-access on-line version of *Phytopathologia Mediterranea*, the print version can be received with a € 50 contribution to mail charges (total € 250,00 to receive the print version). Researchers belonging to an Institution which is a member of the Union are entitled to publish with a reduced page contribution, as the Individual Regular members.
Individual Regular MPU Membership*: € 50.00 (free access to the open-access on-line version of Phytopathologia Mediterranea and can get the print version with a contribution to mail charges of € 50 (total € 100,00 to receive the print version).

*Students can join the MPU as a Student member on the recommendation of a Regular member. Student MPU members are entitled to a 50% reduction of the membership dues (proof of student status must be provided).

Payment information and online membership renewal and subscription at www.mpunion.com

For subscriptions and other information visit the MPU web site:
www.mpunion.com
or contact us at: Phone +39 39 055 2755861/862 – E-mail: phymed@unifi.it

Phytopathologia Mediterranea

Volume 60, April, 2021

Contents

Direttore responsabile: Giuseppe Surico • Autorizzazione del Tribunale di Firenze n. 4923 del 5-1-2000 • *Printed by* Logo S.r.l. - Padova, Maggio 2021
€ 70,00